

# Recent Developments in the Synthesis and Structure of Organosilanols†

Vadapalli Chandrasekhar,\* Ramamoorthy Boomishankar, and Selvarajan Nagendran

Department of Chemistry, Indian Institute of Technology—Kanpur, Kanpur-208 016, India

Received June 2, 2003

## Contents

1. Introduction	5847
2. General	5847
2.1. Preparative Aspects	5847
2.2. Acidity and Basicity	5849
3. Monosilanols	5850
3.1. Synthesis of Monosilanols	5851
3.2. <sup>29</sup> Si NMR	5855
3.3. X-ray Crystal Structures of Monosilanols	5857
4. Silanols Containing More than One Si–OH Unit	5862
4.1. Synthesis	5862
4.2. <sup>29</sup> Si NMR	5866
4.3. X-ray Crystal Structures of Compounds Containing More than One Si–OH Group	5867
5. Silanols Based on Silsesquioxane Frameworks	5875
5.1. Synthesis of Silsesquioxane Silanols	5876
5.2. <sup>29</sup> Si NMR	5879
5.3. X-ray Structures of Silsesquioxane Silanols	5879
5.4. Silanols at the Silica Surfaces	5881
6. Silanediols and Other Compounds Containing Si(OH) <sub>2</sub> Units	5883
6.1. Synthesis of Silanediols Containing One or Two Si(OH) <sub>2</sub> Groups	5884
6.2. <sup>29</sup> Si NMR	5888
6.3. X-ray Crystal Structures of Silanediols and Related Compounds	5888
7. Silanetriols and Bis(silanetriols) Containing One or Two Si(OH) <sub>3</sub> Units	5894
7.1. Synthesis	5894
7.2. <sup>29</sup> Si NMR	5898
7.3. X-ray Crystal Structures of Silanetriols	5898
8. Emerging Applications of Silanols	5901
8.1. Metallasiloxanes	5901
8.2. Ceramic Applications	5901
8.3. Cross-Coupling Reactions	5905
8.4. Protease Inhibitors	5906
9. Summary and Outlook	5907
10. Acknowledgment	5908
11. References	5908

## 1. Introduction

Silanols are compounds containing Si–OH bonds and are silicon analogues of alcohols.<sup>1</sup> Si–OH-containing compounds are ubiquitous in nature. Thus, the total content of undissociated orthosilicic acid, Si(OH)<sub>4</sub>, in the world's oceans is estimated to

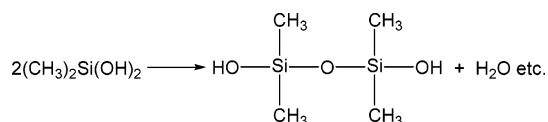
be 10<sup>7</sup> mol with an average concentration of 70 μM.<sup>2,3</sup> Among the organosilanols that can be prepared in the laboratory there is an enormous amount of diversity depending on the number of hydroxyl functionalities attached to silicon (and other substituents present). Broadly, we would like to classify these organosilanols into three major groups. Thus, the first group of compounds contains one or more Si–OH units. Compounds containing one or more Si(OH)<sub>2</sub> units are classified in the second group. Finally the third group of compounds is those that contain one or more Si(OH)<sub>3</sub> units. The terms such as silanetriols and silanediols are used to denote compounds that possess three and two hydroxyl groups on the *same* silicon center. Mono-, di-, and trisilanols are used to denote compounds containing one, two and three –Si(OH) groups, respectively. Other trivial names are also used such as siloxane diols, silsesquioxane silanols, etc. A pictorial representation of the prominent Si–OH-containing compounds is given in Chart 1.

The last comprehensive review on silanols appeared in 1995.<sup>4</sup> Recently, a more specialized review on polysilanols has appeared.<sup>5</sup> This current review will focus on the recent developments in this area and will cover the preparative and structural aspects of various types of silanols that have been reported since 1994. Emerging applications of silanols will also be reviewed.

## 2. General

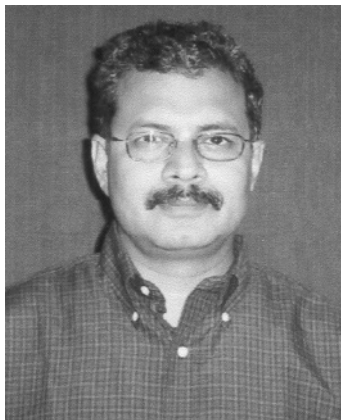
### 2.1. Preparative Aspects

The tendency of compounds containing Si–OH groups is to involve in an intermolecular condensation reaction to afford stable siloxane frameworks by the elimination of water. This is summarized by the observation of Rochow.<sup>6</sup>

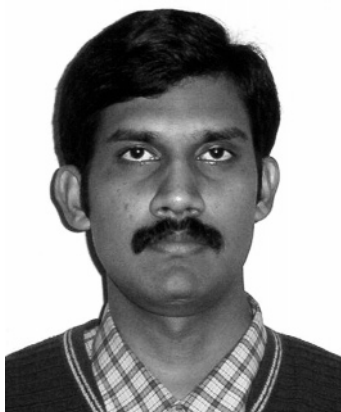


*The methyl silicols undergo partial condensation immediately to form the viscous intermediate products. This goes on until sticky liquid products result. On warming condensation proceeds further, spitting off more water (which evaporates in part or stays behind in globules). The end result is a clear resinous body, which I believe to be methyl silicone.<sup>6</sup>*

† Dedicated to Prof. H. W. Roesky and Prof. C. N. R. Rao.



Vadapalli Chandrasekhar was born at Calcutta (now Kolkata), India, in November 1958. He obtained his M.Sc. degree from Osmania University, Hyderabad, India, in 1977. He received his Ph.D. degree in 1982 from the Indian Institute of Science, Bangalore, under the supervision of Professor S. S. Krishnamurthy. He worked as a postdoctoral research associate with Professor R. R. Holmes at the University of Massachusetts, Amherst (1983–1986), and then as a senior research officer in the Indian Petrochemicals Corporation at Vadodara for 1 year. He then joined the Department of Chemistry at the Indian Institute of Technology—Kanpur in 1987 as an assistant professor. He became an associate professor in 1991 and has been working as a full professor since 1995. His research interests are in the area of inorganic rings and main-group organometallic Chemistry. He has been a recipient of several national and international awards and fellowships.



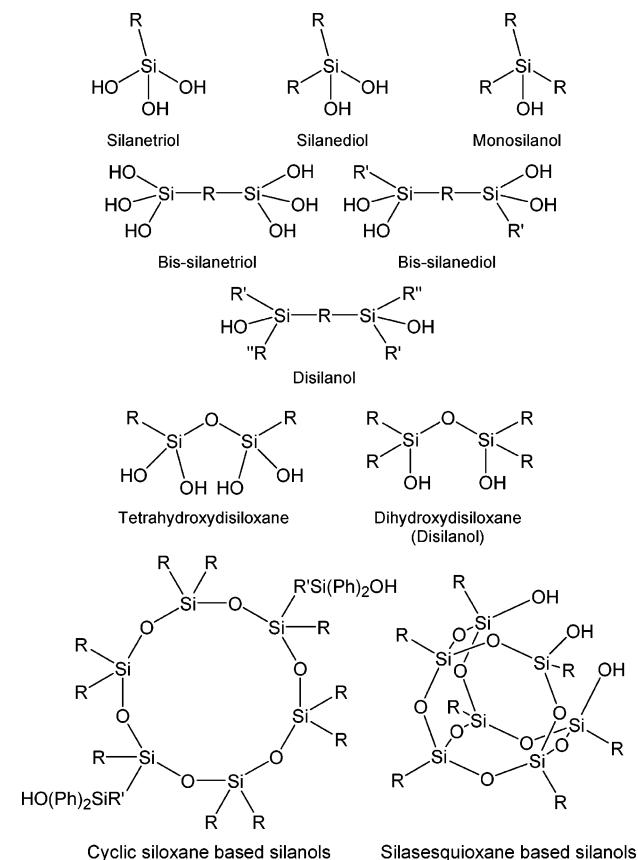
Ramamoorthy Boomishankar was born at Madurai, India, in 1976. He received his B.Sc. (1996) and M.Sc. (1998) degrees in Chemistry from Madura College, affiliated with Madurai Kamaraj University, Madurai. He received his Ph.D. (2004) degree from the Indian Institute of Technology—Kanpur under the supervision of Professor V. Chandrasekhar. A major part of his doctoral work involved the synthesis of cages and supramolecules based on organosilicon and organotin motifs and their application in catalysis. Since February 2004 he has been working as a postdoctoral researcher at the University of Illinois at Urbana—Champaign. His current research interests are in the area of hybrid main-group-metal—transition-metal cages, clusters, and supramolecules and studying their materials aspects.

The formation of stable siloxanes can be potentially difficult for isolation of silanols. This tendency to a large extent also affects the shelf lives of the silanols. However, the condensation reaction is slower at lower temperatures. Also, since the condensation is an intermolecular process, higher dilution reduces the probability of such reactions. Many preparations of silanols take into consideration these above factors. Further, kinetic stabilization of silanols is possible.<sup>7</sup> Intermolecular condensation reaction is prevented by the presence of sterically encumbered substituents



Selvarajan Nagendran was born at Virudhunagar, India, in 1974. He received his B.Sc. (1994) and M.Sc. (1996) degrees in Chemistry from V. H. N. S. N. College, Virudhunagar, affiliated with Madurai Kamaraj University, Madurai. He obtained his Ph.D. (2002) degree in main-group organometallic chemistry at the Department of Chemistry, Indian Institute of Technology—Kanpur, under the supervision of Professor V. Chandrasekhar. He was awarded the Senior Research Fellowship (SRF) of the Council of Scientific and Industrial Research (CSIR), New Delhi, India, and the "Honorable Mention for the 2003 IUPAC prize for Young Chemists" by the International Union of Pure and Applied Chemists (IUPAC). He was also awarded the "FY2003 JSPS Postdoctoral Fellowship for Foreign Researchers" by the Japan Society for promotion of Sciences (JSPS), Japan. He is currently working as a JSPS postdoctoral research fellow in the research group of Professor Mitsuo Kira at the Department of Chemistry, Tohoku University, Sendai, Japan. His main research interest is in the area of organosilicon chemistry, and he is presently engaged in the synthesis of novel unsaturated compounds of silicon.

### Chart 1. Various Types of Silanols



on silicon. Thus, for example, N-bonded silanetriols  $\text{ArN}(\text{SiMe}_3)\text{Si}(\text{OH})_3$  ( $\text{Ar} = 2,6\text{-Me}_2\text{-C}_6\text{H}_3$ ,  $2,6\text{-}i\text{-Pr}_2\text{-C}_6\text{H}_3$ ,  $2\text{-}i\text{-Pr-6-Me-C}_6\text{H}_3$ ,  $2,4,6\text{-Me}_3\text{C}_6\text{H}_2$ ) and  $2,6\text{-}i\text{-Pr}_2\text{-}$

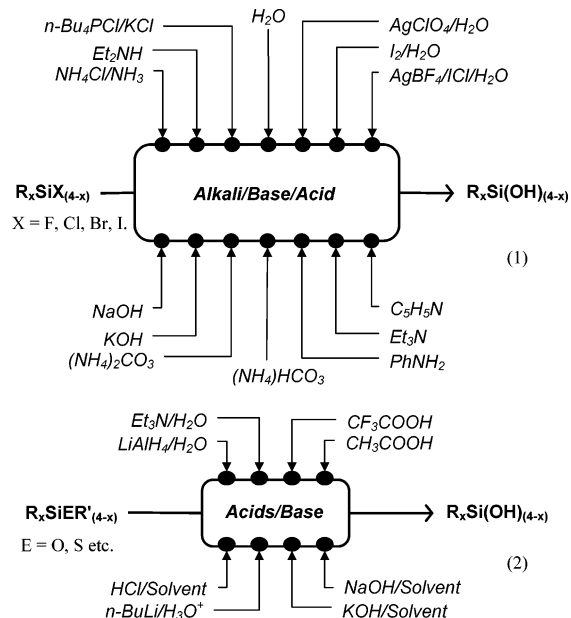
$C_6H_5N(SiMe_2Pr-i)Si(OH)_3$  that contain three hydroxyl groups on a *single* silicon center are quite stable and remain unchanged for long periods of time.<sup>8</sup> This surprising stability is attributed to the steric encumbrance of the bulky aromatic amino substituent on the silicon atom. The condensation of the Si–OH groups can also be minimized by scavenging acidic and basic impurities that catalyze such reactions. For example, acidic impurities that remain after the hydrolysis of a Si–Cl moiety can be deleterious to the stability of the Si–OH-containing compound. The use of mild bases such as triethylamine or aniline has been found to be quite effective to remove the hydrogen chloride formed in the reaction.

Although the synthesis of many silanols requires mild reaction conditions, certain triorganosilicon compounds require harsh reaction conditions for conversion to the corresponding silanols. Thus, while  $Ph_3SiH$  or  $(Me_3Si)_3CSiMe_2H$  can be easily oxidized to the corresponding silanols  $Ph_3SiOH$ <sup>9</sup> or  $(Me_3Si)_3CSiMe_2OH$ ,<sup>4</sup> the compound containing two *tert*-butyl substituents, viz.,  $t-Bu_2SiH_2$ , affords a mixture of  $t-Bu_2SiH(OH)$  and  $t-Bu_2Si(OH)_2$  under similar reaction conditions.<sup>4</sup> Further, the silane containing even bulkier substituents  $(Me_3Si)_3CSiPh_2H$  is not converted to the silanol at all under the reaction conditions employed above. In an example that illustrates the reverse situation, although N-bonded silanols  $ArN(SiMe_3)Si(OH)_3$  containing sterically hindered aromatic amine substituents are readily prepared and quite stable, attempts to prepare their analogues containing unsubstituted aniline moiety ( $Ar = C_6H_5$ ) completely failed.<sup>10</sup> Thus, it is evident that while compounds containing Si–OH group can be prepared, sufficient care should be exercised in choosing appropriate silicon substrates and reaction conditions.

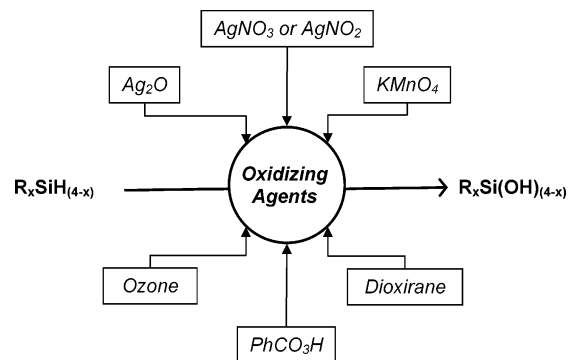
In general, there are two main methods of synthesis of silanols. (1) Hydrolysis of compounds containing a Si–X (X = F, Cl, Br, I, H, carboxylate, perchlorate, sulfate, cyanates, alkoxy) group is a very convenient way of preparing silanols (Scheme 1). Compounds containing bulkier substituents on silicon are more readily hydrolyzed if they possess a carboxylate, perchlorate, or triflate moiety. Chlorides are the preferred starting materials in many instances. In most situations hydrolysis can be accomplished with the aid of a convenient hydrogen chloride acceptor such as aniline or triethylamine. It has been observed that the shelf lives of silanols prepared by using triethylamine as the base are better than those prepared by the use of aniline, particularly because of the difficulty of separating trace amounts of residual aniline from the product.

The second general method of preparing the monosilanols is by oxidation of the corresponding Si–H-containing compound. Several different types of oxidizing agents have been utilized. These include perbenzoic acid,  $KMnO_4$ ,  $AgNO_2$ ,  $AgNO_3$ ,  $Ag_2O$ ,  $O_3$ , and dioxiranes (Scheme 2). The choice of oxidizing agent is dependent on the reactivity of the Si–H-containing compound.<sup>11a</sup> In recent years the dioxiranes  $C(CF_3)(CH_3)(O_2)$  or  $C(CH_3)_2(O_2)$  have proved to be excellent reagents for the oxidation of Si–H

### Scheme 1



### Scheme 2

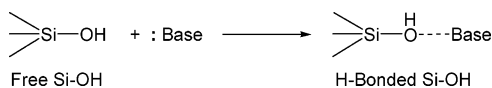


compounds. This reaction is mild and can be carried out even at low temperatures. The byproduct formed in this reaction is a ketone, viz.  $(CF_3)(CH_3)CO$  or  $(CH_3)_2CO$  which is noninterfering and volatile. This reaction involves the insertion of electrophilic oxygen in a Si–H bond and has been particularly effective for compounds containing organometallic groups attached to silicon as well as those that contain direct Si–M bonds. *N*-Hydroxyphthalimide is similarly a mild oxidizing agent which effects a free-radical aerobic oxidation of silanes to silanols in the presence of Co(II) ions.<sup>11b</sup> Recently, a heterogeneous oxidation of silanes to silanols using hydroxyapatite ruthenium complexes was also described.<sup>11c</sup>

## 2.2. Acidity and Basicity

The nature of the Si–OH group in terms of its behavior as a proton donor (Brønsted acid) has been a subject of intense investigation.<sup>12</sup> Apart from academic curiosity, this is also of importance from the point of view of understanding the nature of the reaction sites on silica surfaces. The acidity of silanols has been probed by various techniques. These include direct titration with a suitable base,<sup>13</sup> NMR studies,<sup>14–16</sup> as well as infrared spectroscopic studies. The most convenient method that appears to be applicable to most silanols is the infrared spectroscopic technique.

In this method the *free* Si–OH stretching frequency of a silanol is measured. This is followed by measurement of the Si–OH stretching upon hydrogen-bonding interaction of the silanol with a suitable proton acceptor.<sup>12</sup> The frequency shift is correlated with the proton-donor strength or the acidity of the silanol.



Although the stretching frequency values of silanols do change depending on the conditions of the experiment (Nujol, KBr pellet, type of solvent, etc.), the variation is not substantial. Further, the Si–OH stretching for various types of silanols remains invariant. For example, the IR stretching frequencies of some diverse silanols reflect the constancy of the *free* Si–OH frequency: Ph<sub>3</sub>SiOH (CHCl<sub>3</sub>, 3667 cm<sup>-1</sup>),<sup>17</sup> Et<sub>3</sub>SiOH (CHCl<sub>3</sub>, 3672 cm<sup>-1</sup>),<sup>17</sup> *n*-Bu<sub>3</sub>SiOH (CHCl<sub>3</sub>, 3671 cm<sup>-1</sup>),<sup>17</sup> HO(SiPh<sub>2</sub>O<sub>4</sub>)H (CHCl<sub>3</sub>, 3680 cm<sup>-1</sup>),<sup>18</sup> (*t*-BuO)<sub>3</sub>SiOH (CHCl<sub>3</sub>, 3695 cm<sup>-1</sup>),<sup>19</sup> (PhO)<sub>3</sub>SiOH (CHCl<sub>3</sub>, 3685 cm<sup>-1</sup>),<sup>20</sup> Et<sub>2</sub>Si(OH)<sub>2</sub> (CCl<sub>4</sub>, 3682 cm<sup>-1</sup>),<sup>21</sup> Ph<sub>2</sub>Si(OH)<sub>2</sub> (CCl<sub>4</sub>, 3670, 3681 cm<sup>-1</sup>),<sup>21</sup> 2,6-Me<sub>2</sub>-C<sub>6</sub>H<sub>3</sub>-N(SiMe<sub>3</sub>)SiMe(OH)<sub>2</sub> (CCl<sub>4</sub>, 3620 cm<sup>-1</sup>),<sup>22</sup> Co<sub>3</sub>(CO)<sub>9</sub>-CSi(OH)<sub>3</sub> (Nujol, 3640 cm<sup>-1</sup>).<sup>23</sup> In hydrogen-bonded situations the Si–OH stretching frequency shifts to lower wavenumbers. For example, the IR spectra of the N-bonded silanediols ArN(SiMe<sub>3</sub>)SiMe(OH)<sub>2</sub> (Ar = 2,6-Me<sub>2</sub>-C<sub>6</sub>H<sub>3</sub>, 2,6-*i*-Pr<sub>2</sub>-C<sub>6</sub>H<sub>3</sub>) in the solid state (recorded either as a KBr pellet or in Nujol) show a broad peak at about 3350 cm<sup>-1</sup>. In solution, apart from the broad peak mentioned above, a new sharp peak at 3620 cm<sup>-1</sup> begins to predominate (Figure 1).<sup>22</sup>

The extent of the shift of the Si–OH stretching frequency to lower wavenumbers upon hydrogen bonding depends on the type of proton acceptor. A number of proton acceptors in combination with a variety of silanols have been studied. The details of these investigations are found elsewhere.<sup>24</sup> From these studies the following broad conclusions can be drawn.

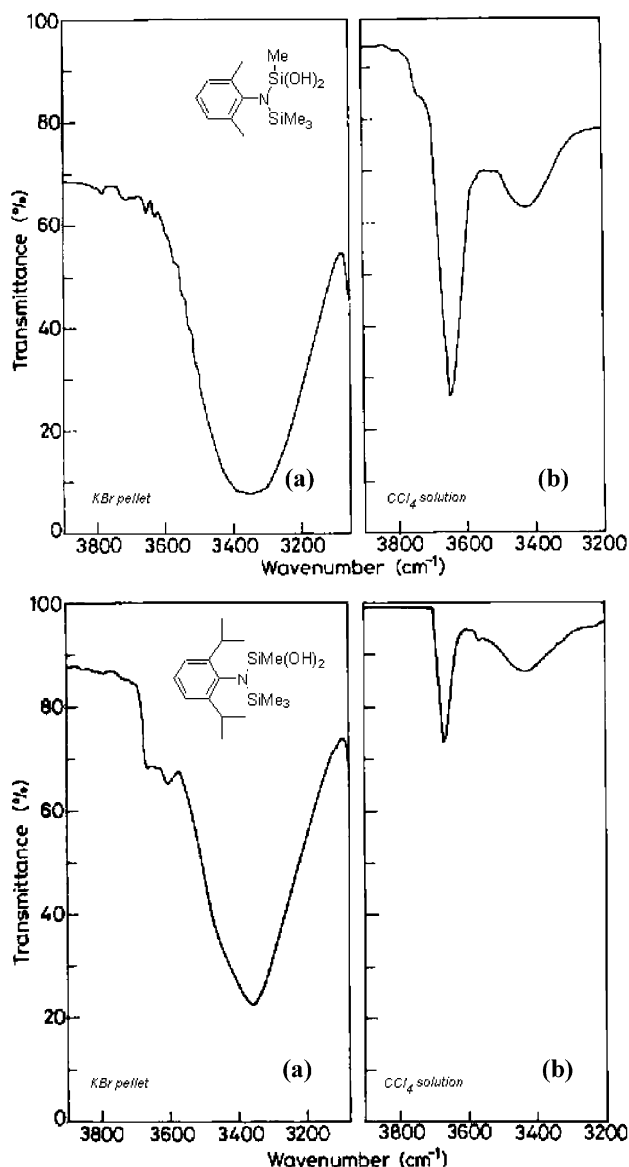
(1) Silanols are always more acidic than the corresponding carbinols: R<sub>3</sub>SiOH > R<sub>3</sub>COH.

(2) The general order of acidity can be given as aryl silanols > alkyl silanols > aryl carbinols > alkyl carbinols.<sup>25</sup>

(3) Within a given series of silanols the Brønsted acidity depends on the substituents on the silicon. More electronegative substituents lead to greater acidity. For example, in the series Me<sub>3</sub>SiOH, (MeO)<sub>3</sub>SiOH, Cl<sub>3</sub>SiOH, the acidity order is Cl<sub>3</sub>SiOH > (MeO)<sub>3</sub>SiOH > Me<sub>3</sub>SiOH.

(4) Gas-phase acidity studies also reveal that the solution trends are extended to the gas phase as well. For example, H<sub>3</sub>SiOH has a higher acidity than CH<sub>3</sub>OH.

Although silanols are quite acidic, as is evident from the above discussion, they are also quite basic. In this regard, they are completely different from carbinols. In the latter there is an inverse relationship between the acidity and basicity for a given compound.<sup>25</sup> Because of the high acidity as well as high basicity of silanols, they are found to possess extensive hydrogen bonding among themselves as



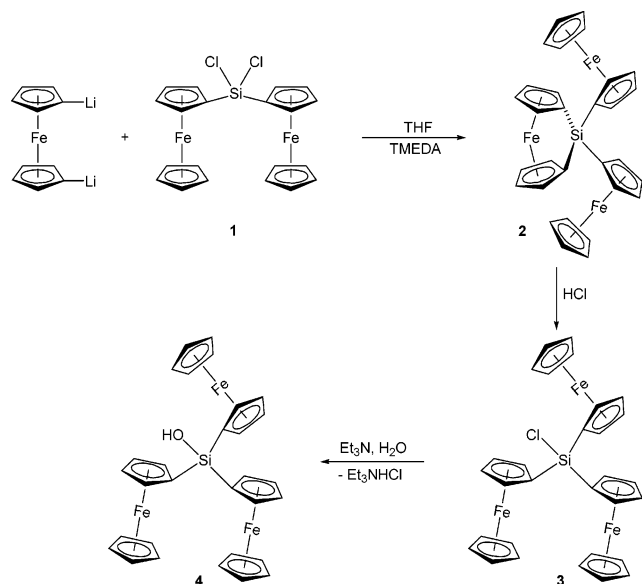
**Figure 1.** IR spectra of 2,6-Me<sub>2</sub>-C<sub>6</sub>H<sub>3</sub>-N(SiMe<sub>3</sub>)SiMe(OH)<sub>2</sub> and 2,6-*i*-Pr<sub>2</sub>-C<sub>6</sub>H<sub>3</sub>-N(SiMe<sub>3</sub>)SiMe(OH)<sub>2</sub> (a) as a KBr pellet and (b) in CCl<sub>4</sub> solution.

well as other types of compounds that can act as either proton donors or proton acceptors.

### 3. Monosilanols

Monosilanols are the largest family of silanols. These are of three types: (a) R<sub>3</sub>SiOH [e.g., Me<sub>3</sub>SiOH,<sup>26–28</sup> Et<sub>3</sub>SiOH,<sup>9,29,30</sup> *n*-Bu<sub>3</sub>SiOH,<sup>32,33</sup> *t*-Bu<sub>3</sub>SiOH, *s*-Bu<sub>3</sub>SiOH,<sup>34</sup> (*c*-C<sub>6</sub>H<sub>11</sub>)<sub>3</sub>SiOH,<sup>35,36</sup> Ph<sub>3</sub>SiOH,<sup>9,37,38</sup> (1-naphthyl)<sub>3</sub>SiOH,<sup>39</sup> (*t*-BuO)<sub>3</sub>SiOH,<sup>19,40–43</sup> (Me<sub>3</sub>SiO)<sub>3</sub>SiOH,<sup>44</sup> (PhMe<sub>2</sub>SiO)<sub>3</sub>SiOH,<sup>44</sup> (*neo*-C<sub>5</sub>H<sub>12</sub>O)<sub>3</sub>SiOH<sup>45</sup>]; (b) R<sub>2</sub>R'SiOH [e.g., Me<sub>2</sub>EtSiOH,<sup>46</sup> *t*-Bu<sub>2</sub>MeSiOH,<sup>47</sup> (*n*-C<sub>6</sub>H<sub>11</sub>)Me<sub>2</sub>SiOH,<sup>46</sup> (SiMe<sub>3</sub>)<sub>3</sub>C(Me)<sub>2</sub>SiOH,<sup>48,49</sup> (SiMe<sub>3</sub>)<sub>3</sub>-C(Et)<sub>2</sub>SiOH,<sup>50</sup> *t*-Bu<sub>2</sub>SiClOH,<sup>51</sup> *t*-Bu<sub>2</sub>SiBrOH,<sup>51</sup> *t*-Bu<sub>2</sub>-Si(NH<sub>2</sub>)OH,<sup>52</sup> (PhCHCl)Me<sub>2</sub>SiOH,<sup>53</sup> (PhCHBr)Me<sub>2</sub>-SiOH,<sup>53</sup> (*t*-Bu<sub>2</sub>MeSiO)<sub>2</sub>SiFOH,<sup>47,54</sup> (Me<sub>3</sub>SiO)<sub>2</sub>(PhMe<sub>2</sub>-SiO)SiOH,<sup>44</sup> (Me<sub>3</sub>SiO)(PhMe<sub>2</sub>SiO)<sub>2</sub>SiOH,<sup>44</sup> [MeO(CH<sub>2</sub>)<sub>2</sub>O(CH<sub>2</sub>)<sub>4</sub>]Me<sub>2</sub>SiOH,<sup>46</sup> (PhMe<sub>2</sub>Si)<sub>3</sub>CSiMe<sub>2</sub>OH,<sup>46</sup> [(Me<sub>3</sub>SiO)(Me<sub>2</sub>SiO)<sub>2</sub>SiMeOH,<sup>55</sup> [(SiMe<sub>3</sub>)<sub>2</sub>C(SiMe<sub>2</sub>Br)]-SiMe<sub>2</sub>OH,<sup>56</sup> (*neo*-C<sub>5</sub>H<sub>11</sub>O)Me<sub>2</sub>SiOH<sup>57</sup>]; (c) RR'R''SiOH [e.g., PhMe(1-naphthyl)SiOH,<sup>58</sup> (SiMe<sub>3</sub>)<sub>3</sub>CSi(Ph)-

Scheme 3



(OMe)OH,<sup>59</sup> (PhMe<sub>2</sub>Si)<sub>3</sub>CSi(Me)(HOH),<sup>60</sup> (Cp\*(CO)<sub>2</sub>Fe)-Si(*p*-tolyl)(H)OH,<sup>61</sup> (Cp(CO)<sub>2</sub>Fe)Si(*i*-Pr)(H)OH,<sup>61</sup> (Cp\*-CO)<sub>2</sub>(PMe<sub>3</sub>)Fe)SiMe(H)OH<sup>61</sup> etc. Examination of all of these silanols reveals that the Si–OH group is reasonably robust and present in various types of compounds which contain many types of bonds such as Si–C, Si–H, Si–M, Si–O, Si–F, Si–Cl, Si–I or Si–Br. Some of the recent examples of monosilanols are discussed below.

### 3.1. Synthesis of Monosilanols

Ferrocenyl-substituted silicon compounds have attracted interest from various points of view.<sup>62</sup> Although Fc<sub>3</sub>Si(OH) and Fc<sub>2</sub>Si(OH)<sub>2</sub> were known earlier,<sup>63</sup> improved synthesis of these compounds was recently reported. Thus, Manners and co-workers have shown that silicon-bridged ferrocenophanes are convenient starting materials for the preparation of hybrid polymers that contain alternately silicon and ferrocene units linked in a chain.<sup>64</sup> It has also been

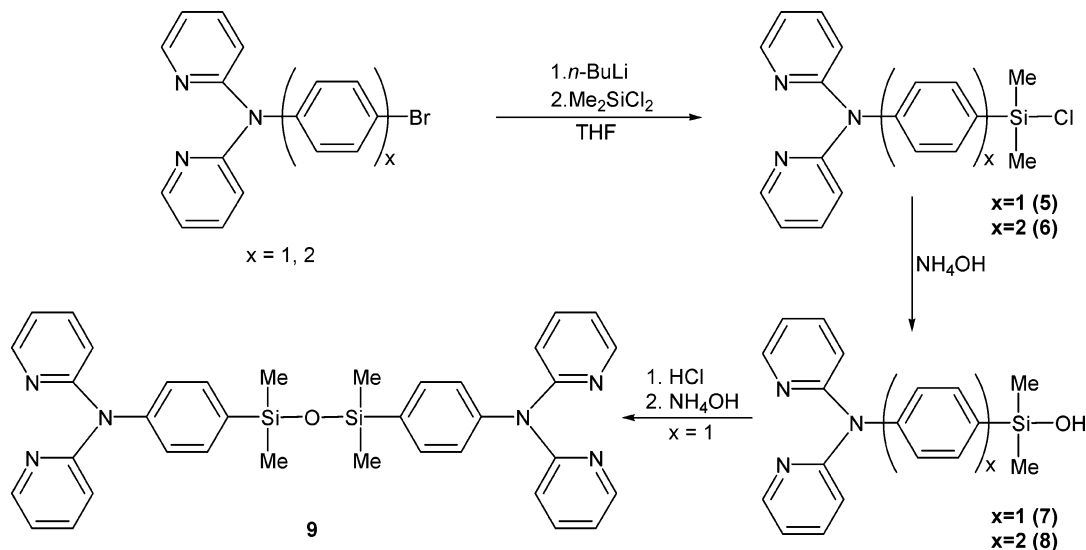
shown from this group that a similar highly strained trimetallic [1] silaferrocenophane (2) containing Fc<sub>2</sub>Si (Fc = ferrocenyl) group can be prepared by reaction of Fc<sub>2</sub>SiCl<sub>2</sub> (1) with 1,1'-dilithioferrocene. Reaction of 2 with hydrogen chloride affords the triferrocenyl-silicon chloride Fc<sub>3</sub>SiCl (3). The driving force for the formation of 3 is the relief in ring strain in the ferrocenophane (2). Hydrolysis of Fc<sub>3</sub>SiCl (2) using triethylamine as the base leads to the formation of the silanol Fc<sub>3</sub>SiOH (4) in excellent yields (Scheme 3).<sup>65</sup>

Interest in organosilicon compounds as electroluminescent materials prompted the synthesis of the blue luminescent silanols containing chromophores 2,2'-dipyridylaminophenyl and 2,2'-dipyridylaminobiphenyl. This is accomplished by a stepwise procedure. Thus, lithiation of (2-Py)<sub>2</sub>N-C<sub>6</sub>H<sub>4</sub>-*p*-Br or (2-Py)<sub>2</sub>N-C<sub>6</sub>H<sub>4</sub>-*p*-C<sub>6</sub>H<sub>4</sub>-*p*-Br (Py = pyridyl) with *n*-butyllithium followed by reaction with Me<sub>2</sub>SiCl<sub>2</sub> afforded the monochloro derivatives (2-Py)<sub>2</sub>N-C<sub>6</sub>H<sub>4</sub>-*p*-SiMe<sub>2</sub>-Cl (5) and (2-Py)<sub>2</sub>N-C<sub>6</sub>H<sub>4</sub>-*p*-C<sub>6</sub>H<sub>4</sub>-*p*-Si(Me)<sub>2</sub>-Cl (6). It has been noted that if the lithium reagent is added to the dimethyldichlorosilane (rather than the other way), the predominant product formed is Me<sub>2</sub>Si[C<sub>6</sub>H<sub>4</sub>-*p*-N(2-Py)<sub>2</sub>]<sub>2</sub> or Me<sub>2</sub>Si[C<sub>6</sub>H<sub>4</sub>-*p*-C<sub>6</sub>H<sub>4</sub>-*p*-N(2-Py)<sub>2</sub>]<sub>2</sub>. Hydrolysis of the chloro derivatives 5 and 6 in the presence of ammonium hydroxide leads to the formation of the monosilanols (2-Py)<sub>2</sub>N-C<sub>6</sub>H<sub>4</sub>-*p*-Si(Me)<sub>2</sub>-OH (7) and (2-Py)<sub>2</sub>N-C<sub>6</sub>H<sub>4</sub>-*p*-C<sub>6</sub>H<sub>4</sub>-*p*-Si(Me)<sub>2</sub>-OH (8), respectively.<sup>66</sup> In the presence of an acid, self-condensation of the silanol (7) occurs to afford the disiloxane (9) (Scheme 4).

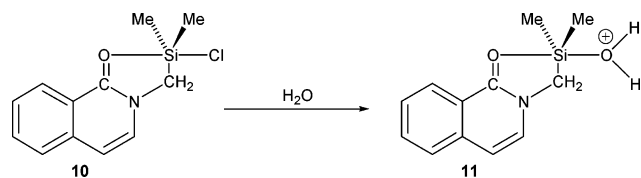
At 77 K the silicon derivatives 7–9 showed new longer wavelength emission bands (408 and 426 nm for 7; 487 and 518 nm for 8; 407 and 430 nm for 9) in addition to the normal fluorescence bands (379, 394, and 384 nm for 7; 382, 398, and 391 nm for 8; 379 and 381 nm for 9) observed at room temperature. From the decay lifetimes of the long-wavelength emission bands it was possible to attribute them as due to phosphorescence.

A protonated hypervalent silanol 11 has been prepared recently by a base-free hydrolysis of the

Scheme 4



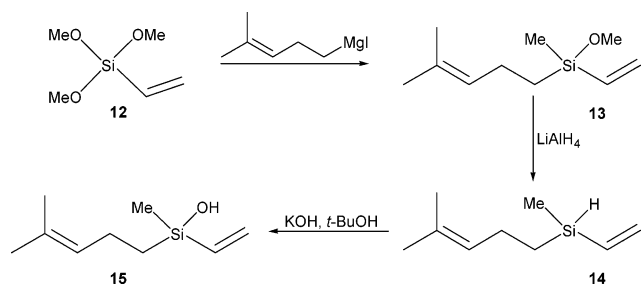
## Scheme 5



corresponding chloride **10** (Scheme 5).<sup>67</sup> Compound **11** has been proposed to serve as a model for the intermediates involved in the nucleophilic substitution reactions, in general, and hydrolytic reactions, in particular, at Si(IV) centers.

Compounds containing Si–H groups can also be hydrolyzed to afford the corresponding silanols. Silalinalool, a pheromone analogue, has been recently synthesized by a three-step synthetic procedure starting from the vinyl trimethoxysilane **12**, which is converted to **13** by action of the Grignard reagent. Reduction of **13** with lithium aluminum hydride leads to the triorganosilane **14**. The latter is hydrolyzed using alcoholic potassium hydroxide to afford the silanol **15** (Scheme 6).<sup>68</sup> Compound **15** is the silicon

## Scheme 6



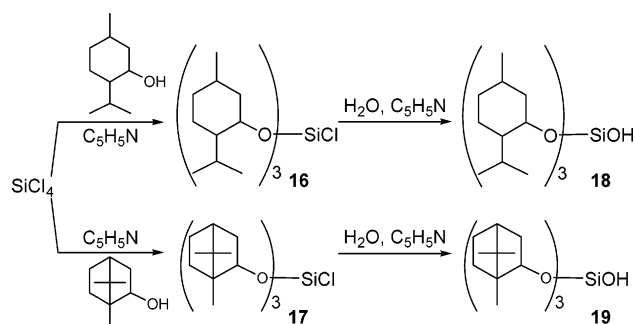
analogue of the pheromone linalool. It may be noted that the hydrolysis reaction does not affect the two different olefin functionalities present in **14**, which remain intact in the final silanol **15**.

Silanols of the type (OR)<sub>3</sub>Si(OH) are of considerable interest. First, in these compounds the silicon center has an immediate coordination environment of four oxygens, which is similar to the situation found in many naturally occurring silicate minerals.<sup>69</sup> Second, Tilley and co-workers very elegantly demonstrated the usefulness of (*t*-BuO)<sub>3</sub>SiOH for the preparation of a variety of metallasiloxanes. These metallasiloxanes have been found to be useful as excellent low-temperature precursors for the preparation of metal silicates.<sup>70</sup> Alkoxy silanols have also been recently viewed as model compounds for the intermediates in the sol–gel processes involving silicon alkoxides, Si(OR)<sub>4</sub>.<sup>71</sup>

Reaction of silicon tetrachloride with (–)-menthol or [(1*S*)-endo]-(–)-borneol in the presence of pyridine affords the trialkoxy silicon chlorides **16** and **17** as a colorless oil and solid, respectively. Mild hydrolysis of these silicon chlorides with pyridine and an excess of water affords the silanols **18** and **19**. While **18** is a colorless oil, **19** is a crystalline solid (Scheme 7).<sup>72</sup>

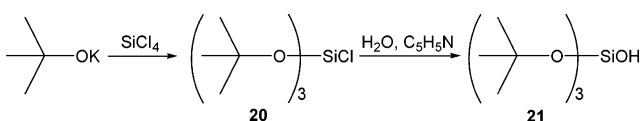
Although the synthesis of (*t*-BuO)<sub>3</sub>SiOH was known previously,<sup>40–43</sup> recently an improved synthesis of this compound was reported. This involves reaction the

## Scheme 7



*t*-BuOK with SiCl<sub>4</sub> to afford the chloride (*t*-BuO)<sub>3</sub>SiCl, **20**. Hydrolysis of **20** with a large excess of water in the presence of a slight excess of pyridine afforded the silanol (*t*-BuO)<sub>3</sub>SiOH, **21**, as a solid substance (Scheme 8).<sup>19</sup>

## Scheme 8



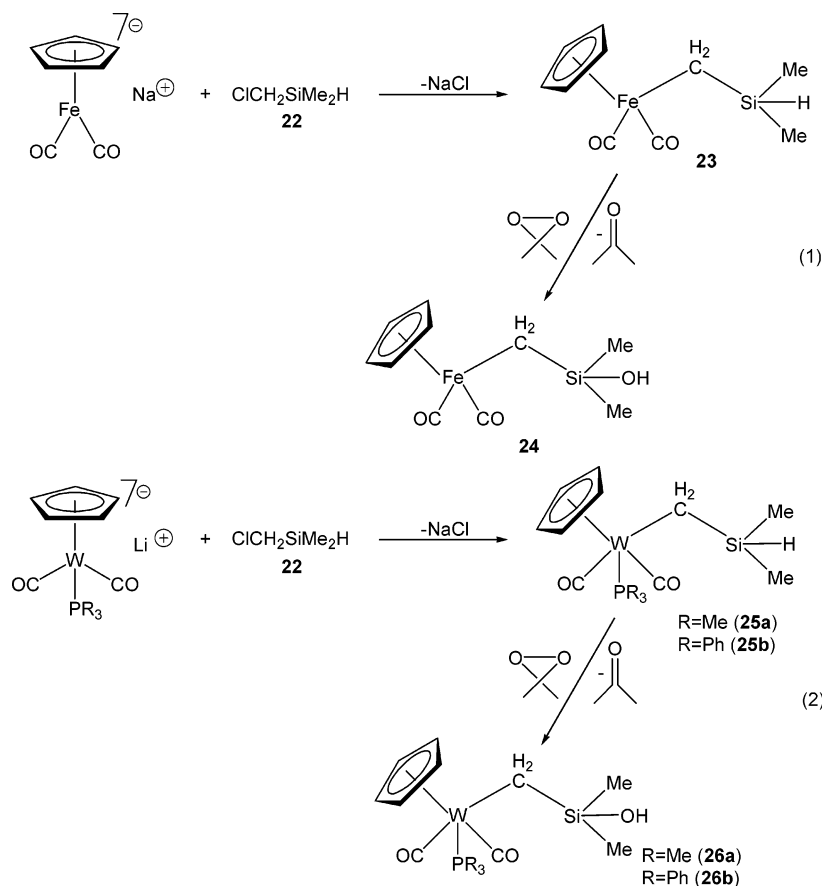
Apart from Fe<sub>3</sub>SiOH (**4**), whose synthesis has been discussed *vide supra*, other organometallic-moiety-containing silanols can also be prepared. It has also been found possible to link half-sandwich organometallic moieties to silanols. This can be accomplished either through a –CH<sub>2</sub> spacer group or directly. The latter contain a Si–M bond. Scheme 9 shows examples of CpFe(CO)<sub>2</sub>CH<sub>2</sub>–, CpW(CO)<sub>2</sub>(PMe<sub>3</sub>)–CH<sub>2</sub>–linked silanols. Reaction of [(η<sup>5</sup>-Cp)Fe(CO)<sub>2</sub>]<sup>–</sup>Na<sup>+</sup> or [(η<sup>5</sup>-Cp)W(CO)<sub>2</sub>(PR<sub>3</sub>)]<sup>–</sup>Li<sup>+</sup> with Si(Me)<sub>2</sub>(H)(CH<sub>2</sub>Cl) (**22**) leads to formation of the transition-metal–organometallic-linked silyl hydrides [(η<sup>5</sup>-Cp)Fe(CO)<sub>2</sub>–CH<sub>2</sub>Si(Me)<sub>2</sub>H] (**23**), [(η<sup>5</sup>-Cp)W(CO)<sub>2</sub>(PMe<sub>3</sub>)CH<sub>2</sub>Si(Me)<sub>2</sub>–H] (**25a**), and [(η<sup>5</sup>-Cp)W(CO)<sub>2</sub>(PPh<sub>3</sub>)CH<sub>2</sub>Si(Me)<sub>2</sub>H] (**25b**), respectively. Reaction of these silyl hydrides with dimethyldioxirane leads to assembly of the corresponding silanols [(η<sup>5</sup>-Cp)Fe(CO)<sub>2</sub>CH<sub>2</sub>Si(Me)<sub>2</sub>OH] (**24**),<sup>73a</sup> [(η<sup>5</sup>-Cp)W(CO)<sub>2</sub>(PMe<sub>3</sub>)CH<sub>2</sub>Si(Me)<sub>2</sub>OH] (**26a**),<sup>74</sup> and [(η<sup>5</sup>-Cp)W(CO)<sub>2</sub>(PPh<sub>3</sub>)CH<sub>2</sub>Si(Me)<sub>2</sub>OH] (**26b**),<sup>73b</sup> respectively (Scheme 9). It has also been reported that the silanols **26a** and **26b** as well as other derivatives [(η<sup>5</sup>-Cp<sup>\*</sup>)Fe(CO)<sub>2</sub>CH<sub>2</sub>SiMe<sub>2</sub>OH] (**27**)<sup>73a</sup> and [(η<sup>5</sup>-Cp)Fe(CO)<sub>2</sub>CH<sub>2</sub>SiMePhOH] (**28**)<sup>73a</sup> can also be prepared by a triethylamine-assisted hydrolysis of the corresponding chlorides.

The preparation of silanols where a direct Si–M bond is present is shown in Scheme 10. The first step involves synthesis of the metal-bound silanes **29a**, **29b**, **31a**, and **31b** by reaction of R<sub>2</sub>Si(H)Cl with the metal salt of the corresponding organometallic anion. The ruthenium-bound silanols **30a** and **30b** can be prepared readily by the oxygen insertion reaction of the silanes (**29a** and **29b**) with dimethyloxirane.<sup>74</sup>

A variation of this method involves the catalytic conversion of the tungsten analogues (**31a** and **31b**) to the corresponding silanols (**32a** and **32b**) assisted by urea–hydrogen peroxide and MeReO<sub>3</sub> (Scheme 10).<sup>75</sup>

Silanols containing two Si–M bonds have also been prepared (Scheme 11). The electron-rich metal cen-

## Scheme 9



ters are believed to decrease the acidity of the Si–OH units and prevent self-condensation. An interesting variation in synthetic methodology in the above preparations leads to the isolation of a silanol containing either a Si–Cl or a Si–H bond. Thus,  $[\{\eta^5\text{-Cp}\}\text{Fe}(\text{CO})_2\}_2\text{Si}(\text{H})\text{OH}]$  (**34**), which contains a Si–H bond, can be prepared by hydrolysis of the corresponding chloride  $[\{\eta^5\text{-Cp}\}\text{Fe}(\text{CO})_2\}_2\text{Si}(\text{H})\text{Cl}]$  (**33**) (eq 1, Scheme 11). On the other hand,  $[\{\eta^5\text{-Cp}\}\text{Fe}(\text{CO})_2\}_2\text{Si}(\text{Cl})\text{OH}]$  (**35**), which contains a Si–Cl bond, is prepared by dioxirane-assisted oxygen insertion into the corresponding silane  $[\{\eta^5\text{-Cp}\}\text{Fe}(\text{CO})_2\}_2\text{Si}(\text{H})\text{Cl}]$  (**33**) (eq 2, Scheme 11).<sup>76</sup>

Another important feature of the oxygen insertion reaction is that this is highly regiospecific. Thus,  $[\{\eta^5\text{-Cp}\}\text{Fe}(\text{CO})_2\}_2\text{Si}(\text{H})(\text{OSiMe}_2\text{H})]$  (**36**) contains two different types of Si–H bonds: (1) a Si–H where the silicon is attached to two iron centers and an oxygen and (2) a Si–H where the silicon is attached to two carbons and an oxygen. Reaction of **36** with dimethyldioxirane leads to activation of only the metal-bound Si–H (eq 3, Scheme 11). Thus, oxygen insertion preferentially occurs in this Si–H bond, leading to formation of the silanol  $[\{\eta^5\text{-Cp}\}\text{Fe}(\text{CO})_2\}_2\text{Si}(\text{OH})(\text{OSiMe}_2\text{H})]$  (**37**).<sup>76</sup> The regiospecificity observed in this reaction has been attributed to electronic activation of the Si–H moiety by the electron-releasing metal fragment.

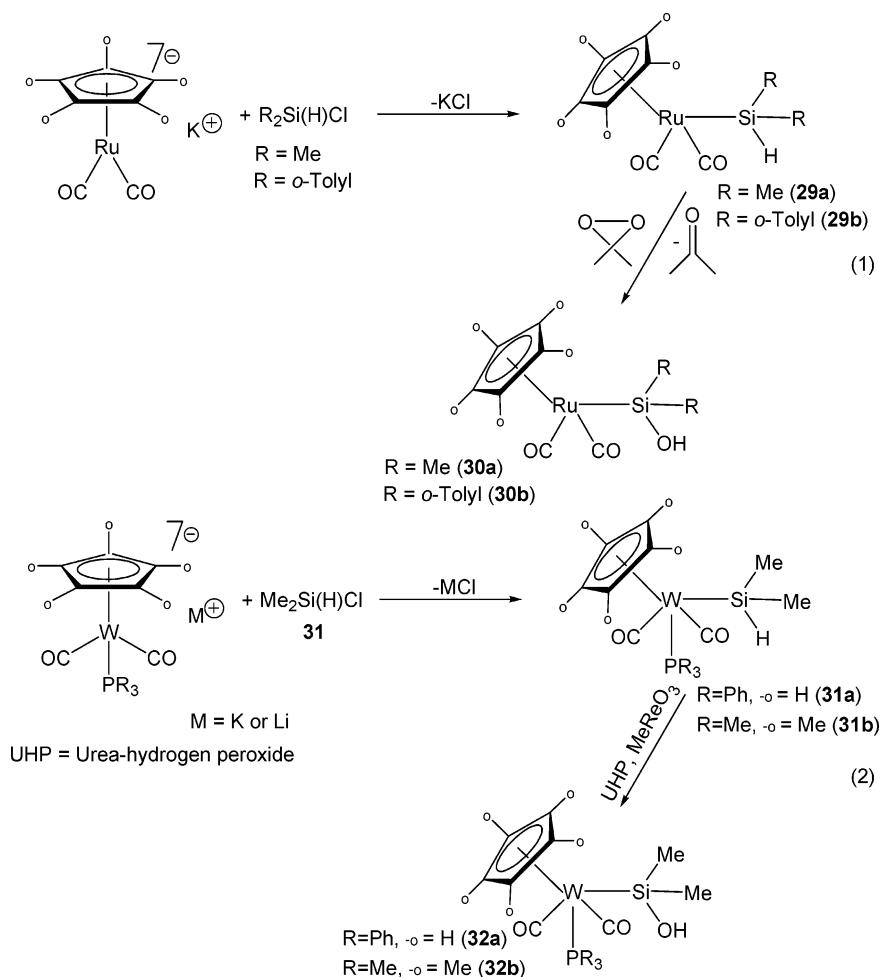
Metallasilanols containing rhodium and iridium have been prepared by direct oxidative addition of secondary silanols.<sup>77</sup> Treatment of an orange solution of *trans*-( $\text{PPh}_3$ )<sub>2</sub>Ir-(C<sub>2</sub>H<sub>4</sub>)Cl with a stoichiometric

amount of R<sub>2</sub>SiH(OH) leads to the formation of the metallasilanols (**38a**, **38b**) (eq 1, Scheme 12). While the formation of **38a** is rapid, **38b** is formed quite slowly due to the presence of the bulky *tert*-butyl groups.<sup>77a</sup> Treatment of the coordinatively unsaturated triphenylphosphine complexes of iridium with silanols has resulted in formation of the coordinatively saturated iridium–silanols.<sup>77b</sup> Thus, the stoichiometric reaction of (PPh<sub>3</sub>)<sub>3</sub>Ir(CO)H with *i*-Pr<sub>2</sub>SiH(OH) (**39**) resulted in the partial conversion (60%) of the latter to the silanol **40a**. On the other hand, if an excess of **39** is used, the silanol **40a** is formed in quantitative (97%) yields (eq 2, Scheme 12).<sup>77b</sup> Similarly, reaction of the more reactive (PPh<sub>3</sub>)<sub>2</sub>Ir(CO)Me with an excess of R<sub>2</sub>SiH(OH) results in formation of the corresponding metallasilanols **40a** and **40b**.<sup>77b</sup> The formation of these products (**40a** and **40b**) are facilitated by the Si–H oxidative addition followed by Me–Si reductive elimination. Similarly, the coordinatively unsaturated rhodium complex (PEt<sub>3</sub>)<sub>3</sub>RhCl reacts with the secondary silanol **39** forming the rhodium-containing silanol **43**.<sup>77b</sup>

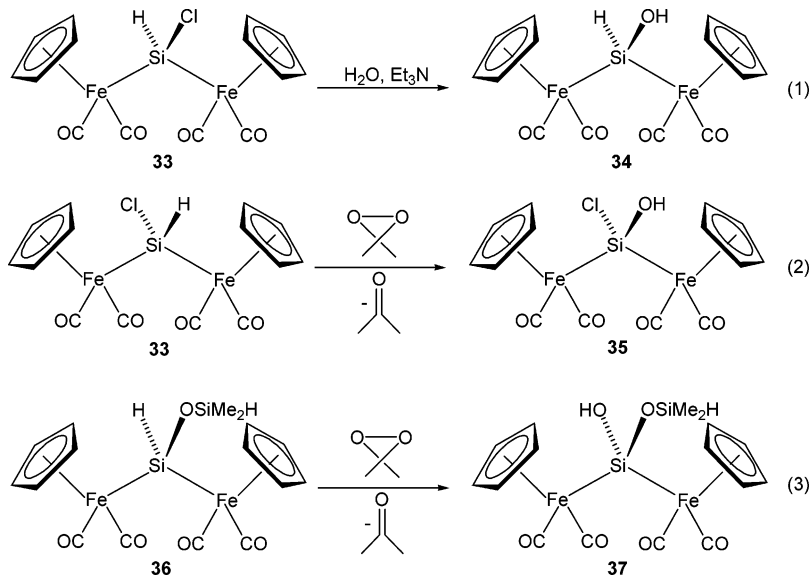
A cyclic phosphine-substituted platinum-containing silanol (**41b**) has been isolated in a reaction involving the native phosphine complex with the secondary silanols (eq 4, Scheme 12). The silanol intermediate **41a** generates an unstable silanone **42**.<sup>77c</sup>

Other methods for synthesis of monosilanols involve reactions of silanediols or disilanols. Thus, displacement of the hydroxyl group from the osmium precursor [Os<sub>3</sub>(CO)<sub>10</sub>(μ-H)(μ-OH)] with the silanediol Ph<sub>2</sub>Si(OH)<sub>2</sub> (**44**) or disilanol HOSiPh<sub>2</sub>OSiPh<sub>2</sub>OH (**45**)

Scheme 10



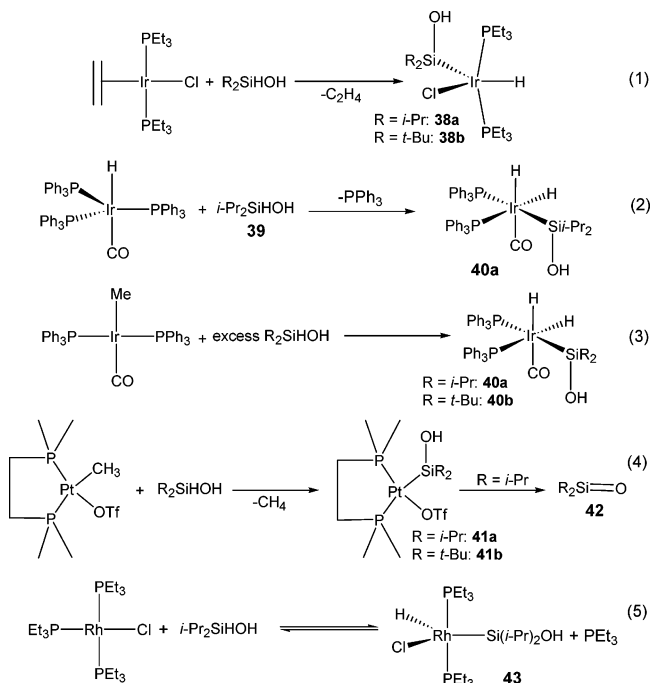
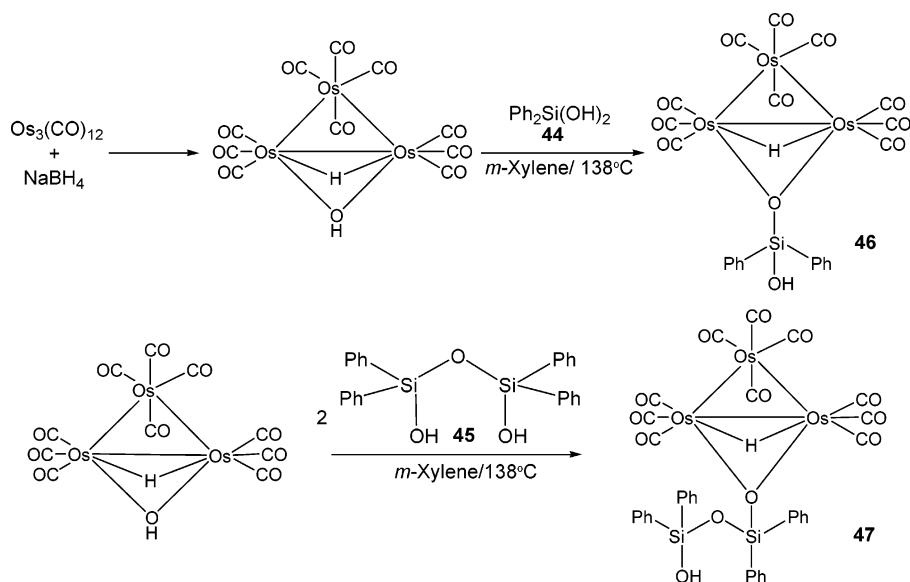
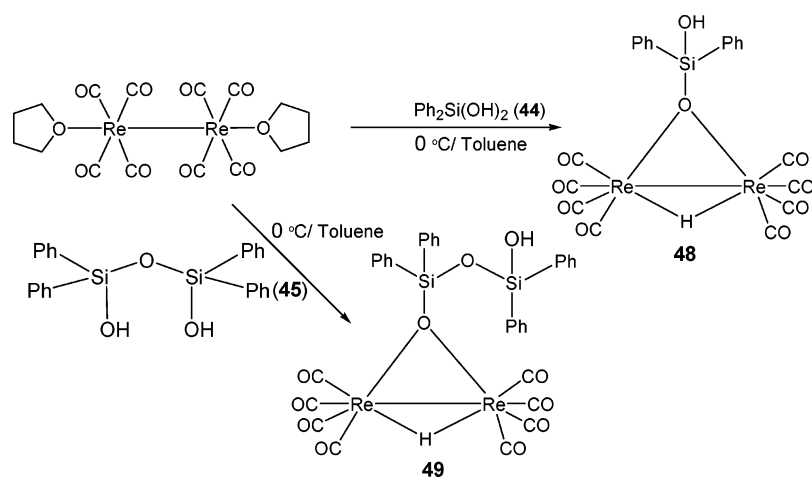
Scheme 11



leads to formation of the monosilanols  $[\text{Os}_3(\text{CO})_{10}(\mu\text{-H})(\mu\text{-OSiPh}_2\text{OH})]$  (**46**) and  $[\text{Os}_3(\text{CO})_{10}(\mu\text{-H})(\mu\text{-OSiPh}_2\text{-O-SiPh}_2\text{OH})]$  (**47**).<sup>78a</sup> In these compounds the silicon atom is connected to the osmium cluster by means of a  $\mu\text{-O}$  bridge (Scheme 13). Displacement of the hydroxyl group from the osmium cluster is favored by the increased acidity of the Si-OH group.

Recently, the rhenium-containing monosilanols have also been synthesized. Thus, reaction of the rhenium precursor  $\text{Re}_2(\text{CO})_8(\text{thf})_2$  with silanediol **44** or siloxanediol **45** leads to formation of the corresponding monosilanols  $[\text{Re}_2(\text{CO})_8(\mu\text{-H})(\mu\text{-OSiPh}_2\text{OH})]$  (**47**) and  $[\text{Re}_2(\text{CO})_8(\mu\text{-H})(\mu\text{-OSiPh}_2\text{-O-SiPh}_2\text{OH})]$  (**48**).<sup>78b</sup> These reactions occur at 0 °C (Scheme 14),



**Scheme 12**

**Scheme 13**

**Scheme 14**


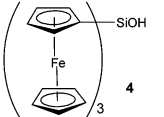
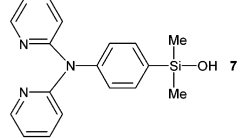
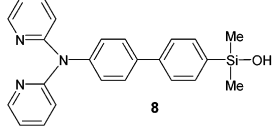
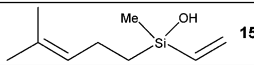
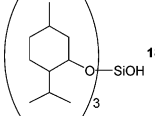
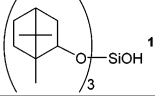
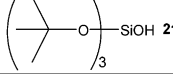
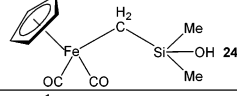
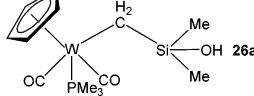
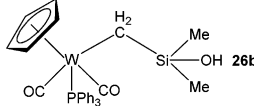
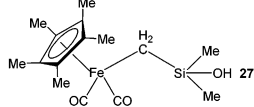
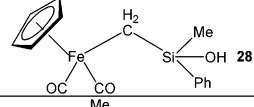
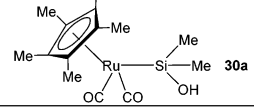
in contrast to those involving the osmium derivatives.

### 3.2. $^{29}\text{Si}$ NMR

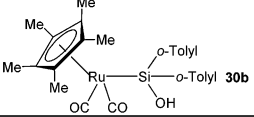
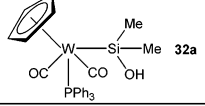
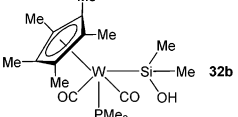
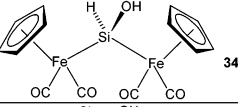

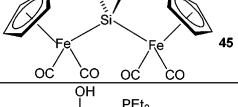
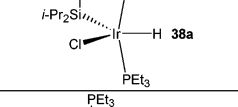
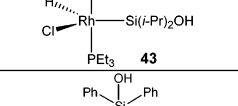
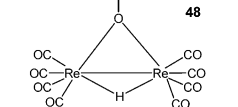
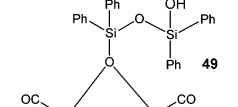
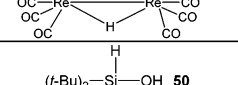
The  $^{29}\text{Si}$  NMR data for various monosilanols that have been recently prepared are summarized in Table 1. The  $^{29}\text{Si}$  chemical shift for the  $\text{Si}-\text{OH}$  moiety shows a large variation. It can be seen from the values given in Table 1 that the variation is between  $-90.4$  and  $+120.5$  ppm. Since the coordination number around silicon is four and is invariant, in these compounds the chemical shift variation may be traced to the influence of the other substituents that are attached to silicon.

The most shielded silicon centers are those that contain a coordination environment of four oxygen atoms. The  $^{29}\text{Si}$  chemical shifts for these compounds have the lowest  $\delta$  values. Thus, compounds **18**, **19**, and **21** (entries 5, 6, and 7, Table 1) have chemical shifts of  $-82.2$ ,  $-79.8$ , and  $-90.4$  ppm, respectively. Compounds with a  $\text{C}_3\text{O}$  coordination around silicon show some interesting trends. While in compounds **7**, **8**, and **15** the  $^{29}\text{Si}$  signals are seen at 6.2, 7.2, and 6.3 ppm, respectively (entries 2–4, Table 1), the

Table 1.  $^{29}\text{Si}$  NMR Data for Various Monosilanols

S.No.	Compound	Coordination Environment around Silicon	$^{29}\text{Si}$ NMR (ppm)	Ref
1		$\text{C}_3\text{O}$	-2.4	65
2		$\text{C}_3\text{O}$	6.2	66
3		$\text{C}_3\text{O}$	7.2	66
4		$\text{C}_3\text{O}$	6.3	68
5		$\text{O}_4$	-82.2	72
6		$\text{O}_4$	-79.8	72
7		$\text{O}_4$	-90.4	19
8		$\text{C}_3\text{O}$	21.8	73a
9		$\text{C}_3\text{O}$	23.8	73a
10		$\text{C}_3\text{O}$	23.4	73a
11		$\text{C}_3\text{O}$	21.1	73a
12		$\text{C}_3\text{O}$	11.7	73a
13		$\text{C}_2\text{RuO}$	52.4	74

influence of a remote electron-rich organometallic unit separated from the silicon by the methylene unit is to push the chemical shifts downfield (entries 8–12, Table 1). In contrast, in  $\text{Fc}_3\text{SiOH}$  (**4**) the observed signal is at  $-2.4$  ppm (entry 1, Table 1). The most deshielded silicon centers are seen where the electron-rich metal centers are directly attached to the silicon. Thus, in compounds **30a**, **30b**, **32a**, and **32b**, which contain one Si–M bond, the corresponding  $^{29}\text{Si}$  chemical shifts are 52.4, 48.2, 49.6, and 51.5 ppm, respectively (entries 13–16, Table 1). The

S.No.	Compound	Coordination Environment around Silicon	$^{29}\text{Si}$ NMR (ppm)	Ref
14		$\text{C}_2\text{RuO}$	48.2	74
15		$\text{C}_2\text{WO}$	49.6	75
16		$\text{C}_2\text{WO}$	51.5	75
17		$\text{HF}_2\text{O}$	97.2	76
18		$\text{ClF}_2\text{O}$	120.5	76
19		$\text{Fe}_2\text{O}_2$ $\text{C}_2\text{HO}$	92.4 -10.6	76
20		$\text{IrC}_2\text{O}$	19.6	77a
21		$\text{RhC}_2\text{O}$	58.1	77b
22		$\text{C}_2\text{O}_2$	-22.5	78b
23		$\text{C}_2\text{O}_2(\text{OH})$ $\text{C}_2\text{O}_2(\text{Re})$	-37.3 -28.8	78b
24		$\text{C}_2\text{HO}$	12.7	79

presence of two Si–M bonds moves the chemical shift to even higher frequency. Thus, in silanols **34**, **35**, and **37** the  $^{29}\text{Si}$  chemical shifts are 97.2, 120.5, and 92.4 ppm, respectively (entries 17–19, Table 1). The influence of directly attached hydrogen appears to be similar to that of the remotely attached electron-rich organometallic center. Thus, in  $(t\text{-Bu})_2\text{Si}(\text{H})(\text{OH})$  (**20**)<sup>79</sup> the  $^{29}\text{Si}$  signal is seen at 12.7 ppm (entry 24, Table 1). In the transition-metal series, when we move from the first to second row there is not much difference in the chemical shift. Hence, the rhodium-

containing silanol **43** shows a chemical shift value of 58.1 ppm.<sup>77b</sup> However, introduction of the third-row transition metal leads to an enhancement of shielding. Thus, the iridium-containing silanol **38a** shows a peak at 19.6 ppm (entry 20, Table 1).<sup>77a</sup> In the case of silanols attached to rhenium clusters, the presence of the remote metal atom has little effect on the chemical shift value. The observed signals at -22.5 (**48**) and -37.3 (**49**) (entries 22 and 23, Table 1) are typical of a C<sub>2</sub>O<sub>2</sub> environment around silicon.<sup>78b</sup>

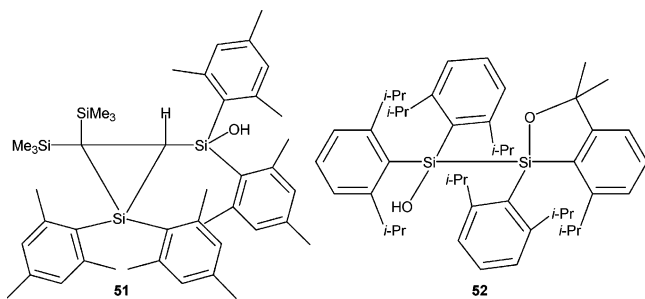
### 3.3. X-ray Crystal Structures of Monosilanols

Although some monosilanols are oils, many of them are solids and can be crystallized. X-ray crystal structural analysis of a number of monosilanols has been carried out. A summary of the structural details is presented in Table 2. In the case of the protonated silanol **11** (entry 4, Table 2), the Si–OH<sub>2</sub> distance is considerably long [1.911(14) Å].<sup>67</sup> This represents an unusual situation where the Si–O bond is weakened by protonation. The Si–OH bond length in other monosilanols varies between 1.610(3) [found in (*t*-BuO)<sub>3</sub>SiOH (**21**)]<sup>19</sup> and 1.683(3) Å [found in (*t*-BuO)<sub>3</sub>Si(H)(OH) (**34**)].<sup>76</sup> The average Si–OH distance in silanols as noted by Lickiss<sup>4</sup> is about 1.64 Å. This value is considerably shorter than the *normal* Si–O bond distance of 1.76 Å estimated from the sum of the covalent radii of silicon and oxygen. The shortening of the Si–O bond distance in silanols is attributed to the polarity of the Si–O bond. It is also possible that negative hyperconjugation effects may be important. It does appear, however, that d-orbital involvement at silicon is minimal.

The X-ray crystal structures of monosilanols (as in all silanols containing the Si–OH bonds) are dominated by hydrogen-bonding effects. Three situations are recognized in monosilanols.

(1) The silanols are totally monomeric without any hydrogen bonding. Relatively few examples of this type are known.<sup>4</sup> Apart from the two compounds **51** and **52** known previously (Chart 2), recent examples

Chart 2

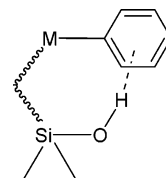


of this type include compounds **46–48** (entries 14–16, Table 2). The steric hindrance of the substituents on silicon is believed to be responsible for this situation.

(2) The second situation pertains to compounds where although conventional hydrogen-bonding effects are absent, the hydrogen atom of the Si–O–H unit is involved in an O–H⋯π-type interaction with an aryl substituent on silicon. In this type the loss of conventional hydrogen bonding is made up to some

extent by the hydroxyl hydrogen interacting with the edge of an aryl moiety (Chart 3). Silanols that show

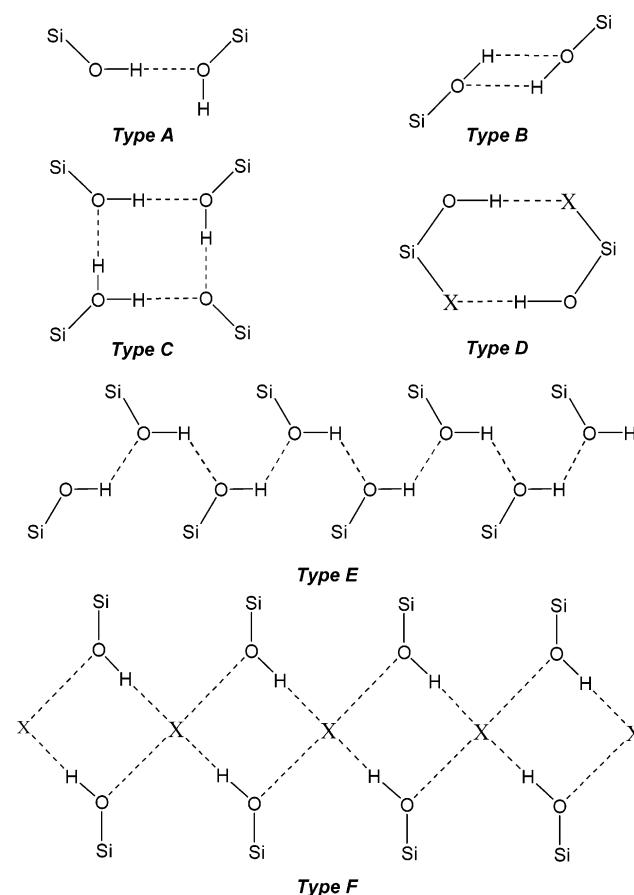
Chart 3



this type of interaction in the solid state have been discussed earlier by Lickiss.<sup>4</sup>

(3) The third type of situation is where the silanols are involved in intermolecular hydrogen bonding. This is the most prevalent type of intermolecular interaction, and several types of structures are formed in the solid state as a result of this type of hydrogen bonding. At least six types of structural patterns seem to be formed as a result of this predominant O–H⋯O hydrogen bonding. These are summarized in Chart 4.

Chart 4. Most Common Types of Hydrogen-Bonding-Aided Structures of Monosilanols



The simplest of these is where two silanols interact with each other to afford a dimer. Two types of dimers appear to be possible. In the first one a linear dimer (Type A, Chart 4) is formed as a result of one of the silanols acting as a proton donor while the other acts as a proton acceptor. This type of a situation has been found in the crystal structure of Fc<sub>3</sub>SiOH (**4**) (Figure 2).<sup>65</sup> The intermolecular H⋯O

Table 2. X-ray Structural Data for Monosilanols

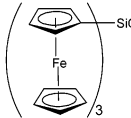
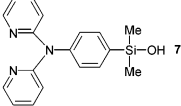
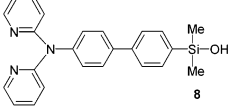
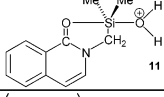
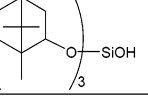
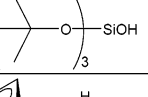
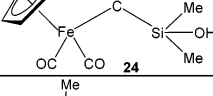
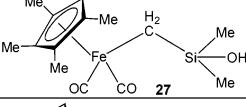
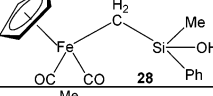
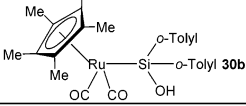
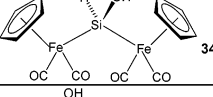
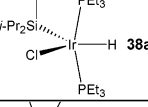
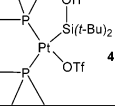
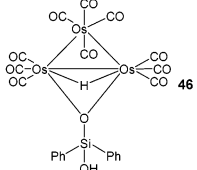
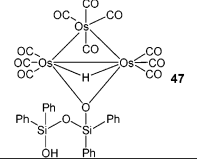
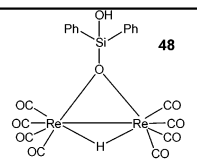
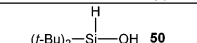
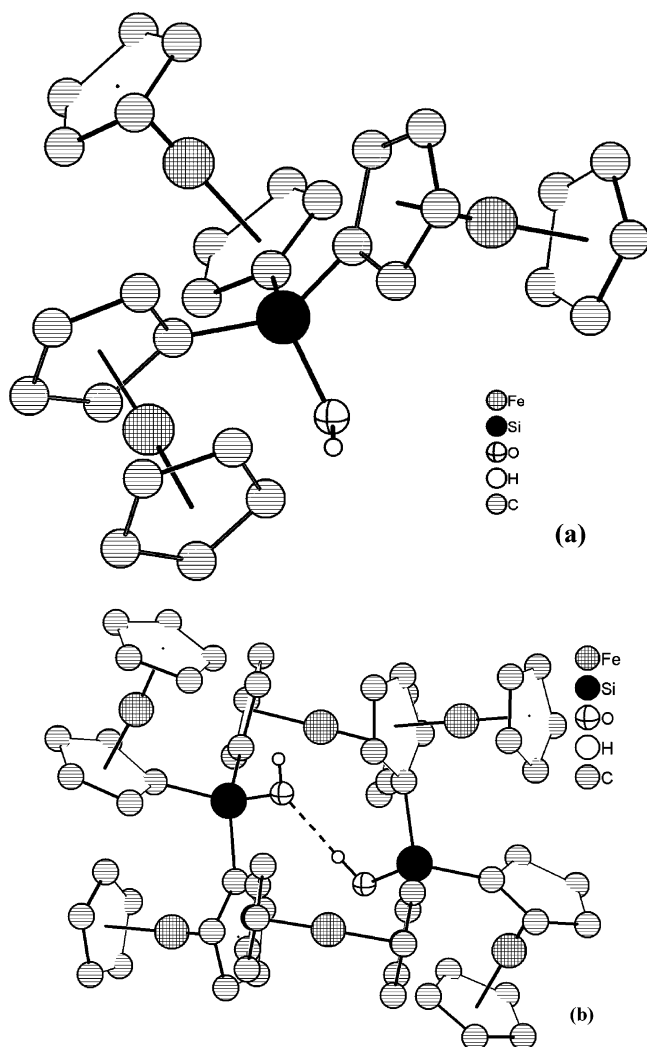
S.No.	Compound	Hydrogen bonding parameters				Structural Summary	Ref.
		Si-OH (Å)	OH...O (Å)	O...O (Å)	O-H...O (°)		
1	 4	1.638(3), 1.651(3)	1.887(2)	2.726(4)	177.7(17)	linear dimer (Type A, Chart 4)	65
2	 7	1.634(1)	2.089(1) (OH...N)	2.875(4) (O...N)	169.33(1) (OH...N)	An anti-parallel head to tail cyclic dimeric structure (Type D, Chart 4)	66
3	 8	1.631(3)	2.019(7), 2.063(7) (OH...O) ---	2.809(9) (O...O) 2.733(8) (O...N)	161.92(2)	One dimensional zig-zag polymer (Type E, Chart 4)	66
4	 11	1.911(14)	1.751(4) (OH...O) 2.179(3) (OH...C)	2.596(2) 2.997(1) (O...C)	173.24(3) 171.91(2) (OH...C)	Ladders consisting of puckered, fused 10- membered rings (Type F, Chart 4)	67
5	 19	1.610(7)	1.696(1), 1.857(1)	2.748(1), 2.784(2)	167.58(3), 171.68(4)	Dimeric structure with a eight-membered Si <sub>2</sub> O <sub>4</sub> ring (Type D, Chart 4)	72
6	 21	1.610(3)	1.826(2)	2.808(4)	172.86(2)	Dimeric structure with a eight-membered Si <sub>2</sub> O <sub>4</sub> ring (Type D, Chart 4)	19
7	 24	1.659(13)	1.963(15), 1.972(16)	2.732(4), 2.741(4)	172.46(1), 169.67(1)	Tetrameric O <sub>4</sub> H <sub>4</sub> rings (Type C, Chart 4)	73a
8	 27	1.658(12)	1.942(2)	2.751(2)	163.69(9)	Zig-Zag chains through disordered Si-OH protons (Type E, Chart 4)	73a
9	 28	1.664(13)	1.919(1)	2.696(2)	167.57(1)	Tetrameric O <sub>4</sub> H <sub>4</sub> rings (Type C, Chart 4)	73a
10	 30b	1.645(18)	2.172(27)	2.809(32)	134.57(2)	Cyclic dimer (O <sub>2</sub> H <sub>2</sub> ) (Type B, Chart 4)	74
11	 34	1.683(3)	2.197	2.991	157.95	Cyclic dimer (O <sub>2</sub> H <sub>2</sub> ) (Type B, Chart 4)	76
12	 38a	1.660(2)	2.684(1)	3.281(1)	128.43(1)	One dimensional zig-zag polymer (Type E, Chart 4)	77a
13	 41b	1.661(8)	1.80(3)	-	-	Monomeric structure (H-bonding with solvated triflate group)	77c
14	 46	1.645(3)	-	-	-	Monomeric	78a
15	 47	1.632(4)	-	-	-	Monomeric	78a

Table 2 (Continued)

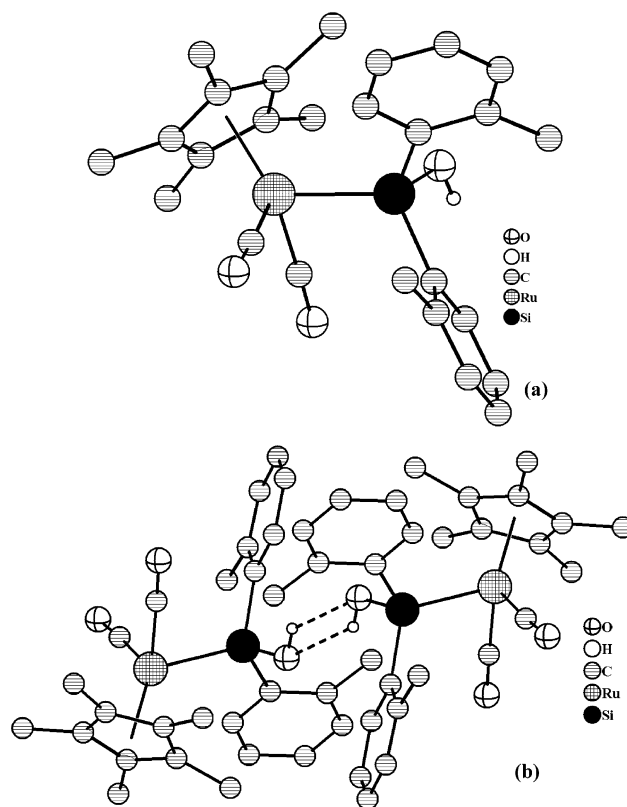
S.No.	Compound	Hydrogen bonding parameters				Structural Summary	Ref.
		Si-OH (Å)	OH...O (Å)	O...O (Å)	O-H...O (°)		
16	 48	1.635(1)	-	-	-	Monomeric	78b
17	 50	1.651(3)	2.001(3)	2.701(4)	142.9	Tetrameric O <sub>2</sub> H <sub>4</sub> rings (Type C, Chart 3)	79



**Figure 2.** X-ray crystal structure of Fc<sub>3</sub>SiOH (4). (a) View of the discrete molecule of Fc<sub>3</sub>SiOH. (b) View of the O-H...O-bonded dimer of 4. The hydrogens present on the ferrocenyl moieties are omitted for clarity.

distance is 1.887(2) Å, while the O...O distance is 2.726(4) Å. The O-H...O bond angle is 177.7(17)°. These parameters, in particular the linearity of the O-H...O bond, are indicative of a strong hydrogen bond. Consistent with this structure, two intense peaks were observed in the IR spectrum of 4: a sharp band at 3635 cm<sup>-1</sup> corresponding to the free Si-OH and a broad band at 3382 cm<sup>-1</sup> corresponding to the hydrogen-bonded Si-OH.<sup>65</sup>

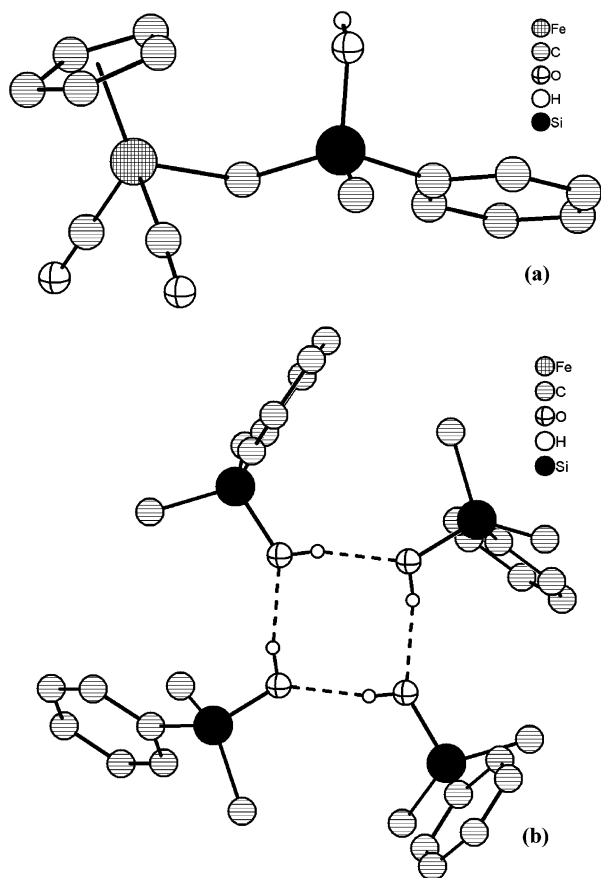
The second type of dimer results when the two interacting silanol moieties act both as proton donors as well as proton acceptors (Type B, Chart 4). Interaction of this type leads to formation of a four-



**Figure 3.** X-ray crystal structure of Cp\*<sub>2</sub>Ru(CO)<sub>2</sub>Si(o-Tolyl)<sub>2</sub>OH (30b). (a) View of the discrete molecule of Cp\*<sub>2</sub>Ru(CO)<sub>2</sub>Si(o-Tolyl)<sub>2</sub>OH. (b) Hydrogen-bonded cyclic dimer of 30b. All other hydrogen atoms are omitted for clarity.

membered O<sub>2</sub>H<sub>2</sub> ring. Because of the steric constraints involved in the four-membered ring, the H...O as well as O...O distances are expected to be longer than the situation found for 4. Thus, for {(η<sup>5</sup>-Cp\*)Ru(CO)<sub>2</sub>}Si(o-Tolyl)<sub>2</sub>(OH) (30b) (entry 10, Table 2; Figure 3)<sup>74</sup> the intermolecular H...O bond length is 2.172 (27) Å while the O...O distance is 2.809(32) Å. Also noticeable is the acute O-H...O bond angle, 134.57(2)°. Similarly, in [(η<sup>5</sup>-Cp)Fe(CO)<sub>2</sub>]<sub>2</sub>Si(H)(OH) (34), which also forms the Type B structure, the H...O and O...O bond distances are 2.197 and 2.991 Å while the O-H...O bond angle is 157.95° (entry 11, Table 2).<sup>76</sup> In the iridium-containing metallasilanol 38a, the presence of the Ir-Cl bond has led to the formation of a one-dimensional polymeric chain due to slightly weak H...Cl interactions.<sup>77a</sup> While the H...Cl distance is 2.684(1) Å, the OH...Cl angle is 128.43(1)° (entry 12, Table 2).

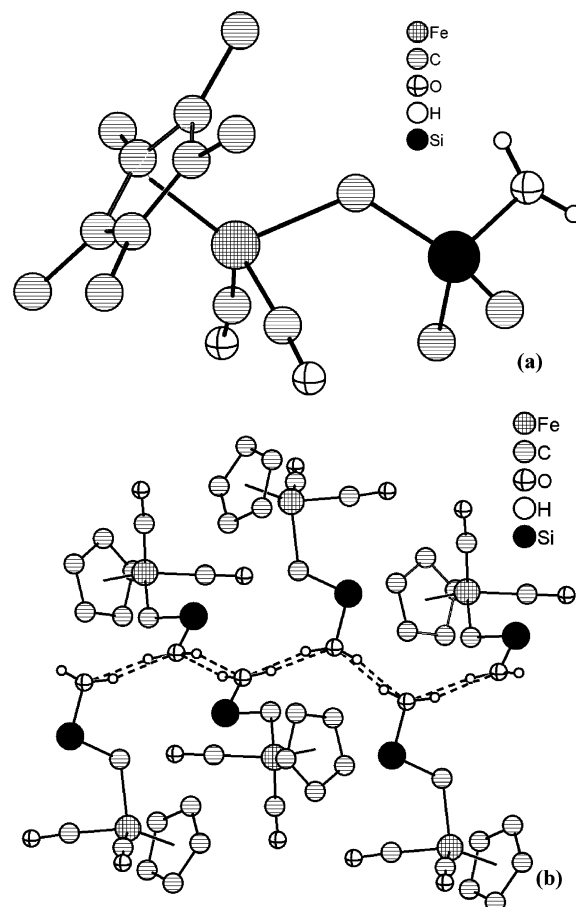
Intermolecular hydrogen bonding also assists in larger sized ring formation in monosilanols. Thus, tetrameric structures (Type C, Chart 4) leading to an



**Figure 4.** (a) Diamond view of CpFe(CO)<sub>2</sub>CH<sub>2</sub>Si(Me)(Ph)OH (**28**). The hydrogens present on the carbon atoms are omitted for clarity. (b) View of the tetrameric agglomerate of **28** formed in the solid state by intermolecular O–H···O hydrogen bonding. The Cp rings, methyl groups, carbonyl groups, and all the other hydrogen atoms are omitted.

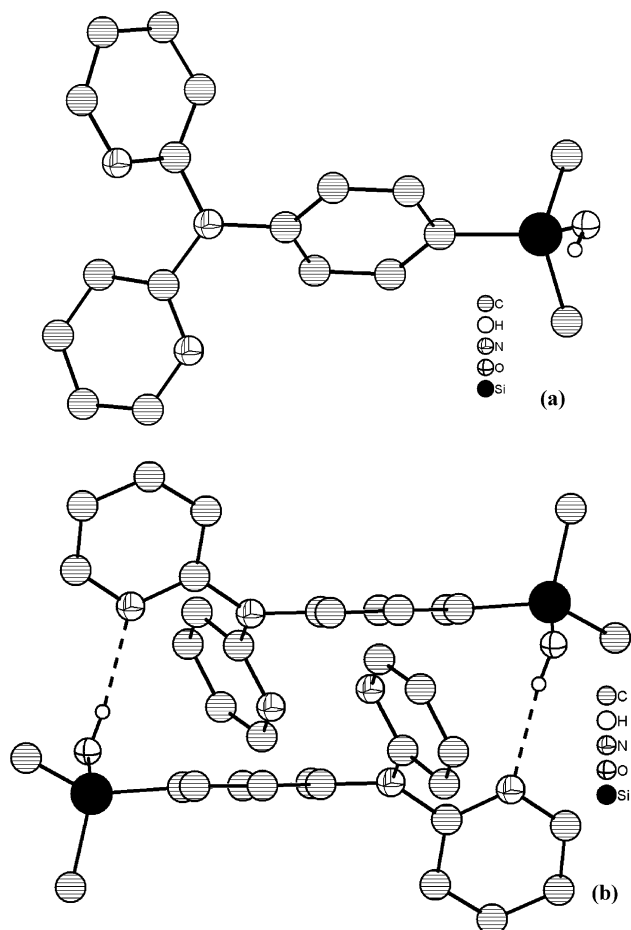
eight-membered O<sub>4</sub>H<sub>4</sub> ring are found for {(η<sup>5</sup>-Cp)Fe(CO)<sub>2</sub>}CH<sub>2</sub>SiMe<sub>2</sub>OH (**24**),<sup>73a</sup> {(η<sup>5</sup>-Cp)Fe(CO)<sub>2</sub>}CH<sub>2</sub>Si(Me)(Ph)OH (**28**),<sup>73a</sup> and *t*-Bu<sub>2</sub>SiHOH(**50**).<sup>79</sup> The Si–O bond distances observed in these compounds are 1.659(13), 1.664(13), and 1.651(3) Å, respectively, while the O···O contacts within the O–H···O hydrogen bonds are 2.732(4) and 2.741(4) (24), 2.696(2) (28), and 2.701(4) Å (50). The near linear O–H···O bond angles of 172.46(1)° in **24** and 167.57(1)° in **28**, in contrast to the shorter angle 142.9° in **50**, is noted (entries 7, 9, and 17, Table 2). It has been suggested that tetrameric units formed in **24** are further connected to each other in a ladder-type fashion by weak C–H···O–C interactions involving the proton of a cyclopentadienyl ring and the oxygen of the carbon monoxide ligand.<sup>73a</sup> The IR spectrum of **24** in pentane shows a sharp peak at 3698 cm<sup>-1</sup> corresponding to the free Si–OH group. The X-ray crystal structure of **28** which shows the formation of the eight-membered O<sub>4</sub>H<sub>4</sub> ring is given in Figure 4.

Intermolecular O–H···O hydrogen bonding in monosilanols also leads to the formation of polymeric chain structures (Type E, Chart 4). In this mode the silanols also function as both proton acceptors and proton donors. A one-dimensional polymeric zigzag chain-type of structure is found for {(η<sup>5</sup>-Cp\*)Fe(CO)<sub>2</sub>}CH<sub>2</sub>SiMe<sub>2</sub>OH (**27**)<sup>73a</sup> (Figure 5) and (2-Py)<sub>2</sub>N-C<sub>6</sub>H<sub>4</sub>-*p*-C<sub>6</sub>H<sub>4</sub>-*p*-Si(Me<sub>2</sub>)OH (**8**).<sup>66</sup> In **27** the molecules



**Figure 5.** (a) Diamond view of Cp\*Fe(CO)<sub>2</sub>CH<sub>2</sub>Si(Me)<sub>2</sub>OH (**27**). (b) The zigzag polymeric chain of **27**. The hydrogens on the Si–OH are positionally disordered. The methyl groups and all other hydrogen atoms are omitted.

are connected to each other by O–H···O contacts to afford a linear polymeric structure. Disorder in the position of the hydrogen gives the impression of O<sub>2</sub>H<sub>2</sub> ring formation. The H···O bond distance in **29** is 1.942(2) Å, while the O···O contact is 2.751(2) Å. The O–H···O bond angle in this compound is 163.69(9)°. The presence of additional heteroatoms (such as nitrogen) or other oxygen-containing groups (such as alkoxy) in the monosilanol structural motif leads to the possibility of the heteroatom or alkoxy oxygen atom interacting as a base with the Si–OH proton (Type D, Chart 4). In such situations it is the subtle balance between the relative basicities of the silanol oxygen vis-à-vis the other interacting atoms as well as the most favorable geometric needs of the interaction that seem to govern the eventual structure that is formed. Thus, in the dipyridylamino-linked silanols (2-Py)<sub>2</sub>N-C<sub>6</sub>H<sub>4</sub>-*p*-Si(Me<sub>2</sub>)OH (**7**) and (2-Py)<sub>2</sub>N-C<sub>6</sub>H<sub>4</sub>-*p*-C<sub>6</sub>H<sub>4</sub>-*p*-Si(Me<sub>2</sub>)OH (**8**) the presence of the additional heteroatoms in the form of nitrogen atoms allows other hydrogen-bonding possibilities.<sup>66</sup> Accordingly, in **7** each Si–O–H proton of one silanol molecule interacts with the pyridine nitrogen of another molecule, leading to formation of an antiparallel head-to-tail cyclic dimer (Figure 6). In this compound the H···N distance is 2.089(1) Å while the O···N contact is 2.875(4) Å. The O–H···N angle is quite linear, 169.33(1)° (entry 2, Table 2), indicating that a fairly strong hydrogen bond is formed. In contrast

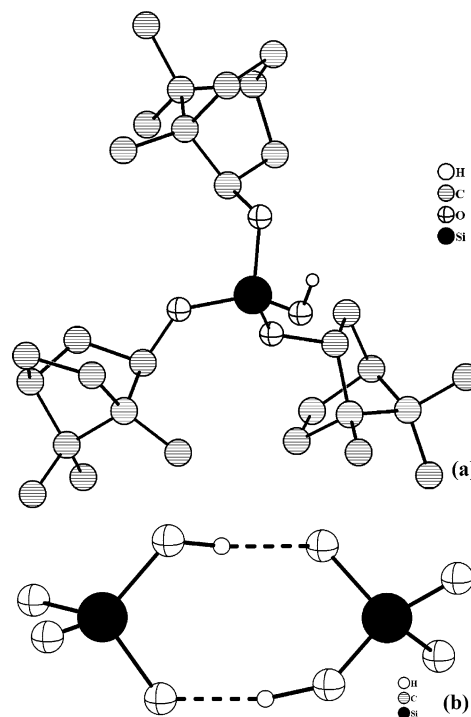


**Figure 6.** (a) View of the discrete molecule of **7**. (b) The hydrogen-bonded dimer of **7** formed as a result of two O–H···N interactions.

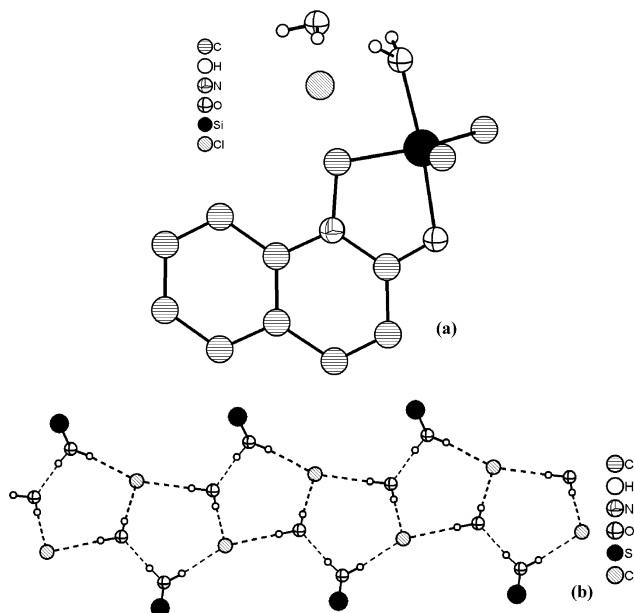
to the situation found for **7**, the related silanol **8** displays two types of hydrogen bonds. The first type is similar to what is observed for **7**, viz., a O–H···N hydrogen bond between two neighboring molecules [O···N, 2.759(8) Å]. The second hydrogen bond occurs between the two oxygen atoms of the hydroxyl groups from two independent molecules (O···O, 2.785(7) Å) (entry 3, Table 2).<sup>66</sup> The latter mode of interaction causes the formation of a one-dimensional hydrogen-bonded polymer structure (Type E, Chart 4).

In the case of trialkoxysilanols **19** and **21**, the oxygen of the OR group attached to silicon acts as a base and is involved in hydrogen bonding to the Si–O–H moiety. Such a pairwise interaction leads to formation of eight-membered Si<sub>2</sub>O<sub>4</sub>H<sub>2</sub> dimers (Figure 7). In these compounds the Si–OH distance is 1.610 Å. The H···O contacts are quite short; while in **19** two contacts of 1.696(1) and 1.857(1) Å are observed, for **21** one contact with a distance of 1.826(2) Å is observed. As anticipated, the formation of a strain-free dimeric structure ensures good O–H···O bond angles (167.58(3)° and 171.68(4)° for **19** and 172.86–(2)° for **21**). The effect of hydrogen bonding is also seen in the infrared spectrum; the IR spectrum of **19** as a KBr pellet shows the presence of a broad band at 3380 cm<sup>-1</sup> corresponding to the O–H stretching frequency.<sup>72</sup>

In the protonated monosilanol **11**, the presence of a water of crystallization along with a chloride anion



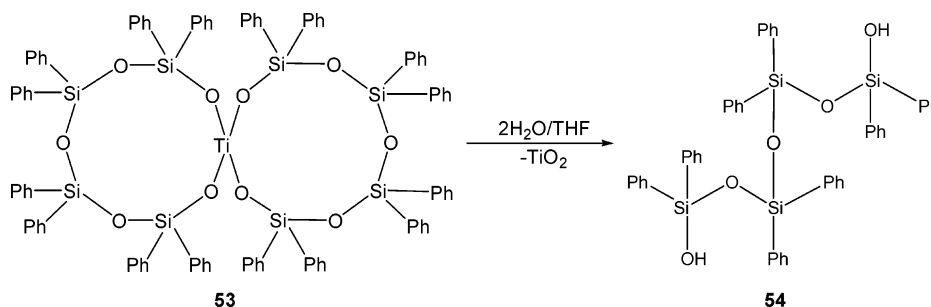
**Figure 7.** (a) DIAMOND view of the discrete molecule of **19**. (b) Framework of the hydrogen-bonded dimer of **19**. The Si–OH is hydrogen bonded to the oxygen of the alkoxy group.



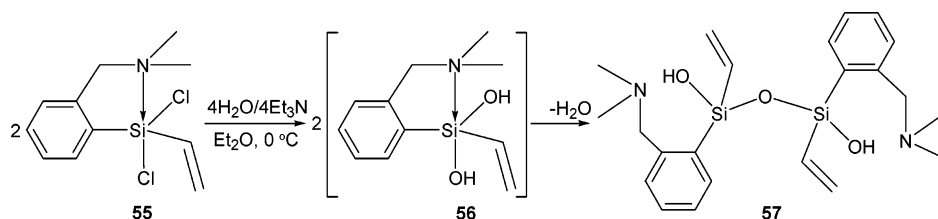
**Figure 8.** (a) DIAMOND view of the discrete molecule of **11**. (b) The hydrogen-bonded framework of **11** showing the formation of a polymeric network.

leads to the formation of a *polymeric ladder* (Type F, Chart 4). Each chloride ion is tricoordinate, being involved in a trifurcated hydrogen (O–H···Cl) bonding to two *free* water molecules as well as with one Si–OH<sub>2</sub> unit. This leads to formation of a chain of edge-sharing fused five-membered rings (Figure 8).<sup>67</sup> In the case of **41b**, the hydroxyl groups are intramolecularly hydrogen bonded to the triflate group, and hence, the structure of the molecule remains monomeric.

## Scheme 15



## Scheme 16



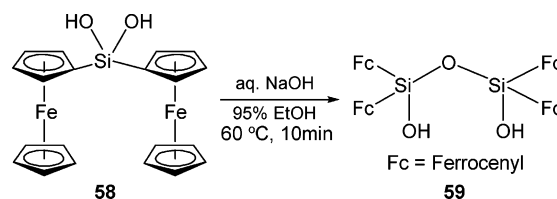
## 4. Silanols Containing More than One Si–OH Unit

Silanols containing more than one Si–OH unit are well known. These compounds are also similar to monosilanols in that only *one* hydroxyl group is present on a given silicon center. However, more than one such silicon center may be present in the molecule. Thus, if two Si–OH centers are present, such a compound is known as a disilanol, and if three Si–OH centers are present it is known as trisilanol and so on. The most prominent example of a disilanol is  $\text{Ph}_2\text{Si}(\text{OH})\text{O}(\text{OSi}(\text{OH})\text{Ph}_2)_2$ ,<sup>80</sup> where two monosilanol units are linked by a bridging oxygen. This compound has a very rich chemistry and has been used in the synthesis of several types of metallasiloxanes. This aspect has been reviewed recently.<sup>81</sup> Several other types of disilanols are known and have been discussed previously [e.g.,  $(\text{Me}_2\text{SiOH})_2\text{O}$ ,<sup>80,82</sup>  $(\text{Et}_2\text{SiOH})_2\text{O}$ ,<sup>83</sup>  $(n\text{-Pr}_2\text{SiOH})_2\text{O}$ ,<sup>84</sup>  $(i\text{-Pr}_2\text{SiOH})_2\text{O}$ ,<sup>85</sup>  $(t\text{-Bu}_2\text{SiOH})_2\text{O}$ ,<sup>86</sup>  $(\text{Me}(\text{thienyl})\text{SiOH})_2\text{O}$ ,<sup>87</sup>  $[(\text{C}_{10}\text{H}_{13})\text{MeSiOH}]_2\text{O}$ ,<sup>88</sup>  $(t\text{-Bu}_2\text{Si}(\text{OH})\text{O})_2\text{SiMe}_2$ ,<sup>89</sup>  $(\text{Ph}_2\text{Si}(\text{OH})\text{O})_2\text{SiPh}_2$ ,<sup>90</sup>  $(\text{Ph}_2\text{Si}(\text{OH})\text{N})\text{Me}_2\text{Si}(\text{Ph}_2\text{Si}(\text{OH})\text{N})\text{SiPh}_2$ ,<sup>91</sup>  $\text{HO}(\text{SiPh}_2)_4\text{OH}$ ,<sup>92,93</sup>  $\text{HO}(\text{SiPh}_2)_5\text{OH}$ ,<sup>93</sup>  $(\text{Me}_3\text{Si})_2\text{C}(\text{SiMe}_2\text{OH})_2$ ,<sup>94</sup>  $\text{CH}_2(\text{SiMe}_2\text{OH})_2$ ,<sup>95</sup>  $\text{Zn}[\text{C}(\text{SiMe}_3)_2(\text{SiMe}_2\text{OH})]_2$ ,<sup>96</sup> and  $p\text{-}(\text{SiMe}_2\text{OH})_2\text{C}_6\text{H}_4$ .<sup>97</sup>] In addition to disilanols, compounds containing more than two Si–OH units have also been studied. Some of the examples that have been covered in earlier reviews include  $[(\text{Ph}_2\text{SiOH})_2\text{O}]_3$ <sup>98</sup> and  $(\text{SiMe}_2\text{OH})_4\text{C}$ .<sup>80,99</sup> Feher and co-workers observed that a partially condensed silsesquioxane  $(\text{C-C}_6\text{H}_{11})_7\text{Si}_7\text{O}_9(\text{OH})_3$  containing three Si–OH functional groups can be used as an excellent precursor for the construction of a wide range of metallasiloxanes. These aspects have also been covered in some critical recent reviews.<sup>100,101</sup> The newer developments in the synthesis of silsesquioxane type of silanols are treated separately in the next section.

## 4.1. Synthesis

Among compounds that can be called di- and multisilanols, compounds containing up to sixteen Si–OH units have been synthesized. However, X-ray structural characterization is limited to compounds

## Scheme 17



containing a maximum of six Si–OH groups. The synthetic methods involved in the preparation of these compounds are extremely diverse and will be discussed below.

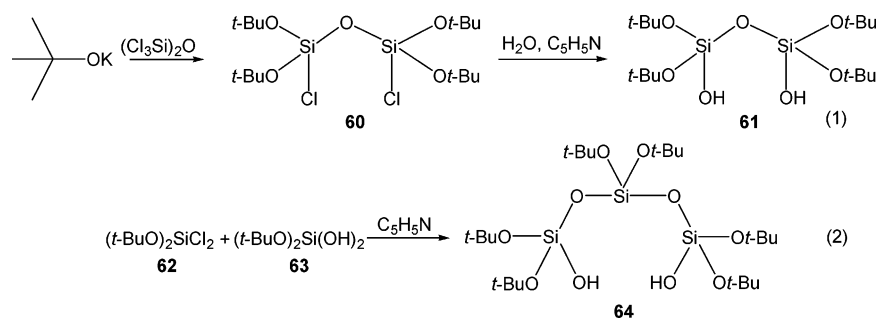
Hydrolysis of the titanosiloxane *spiro*- $\text{Ti}[(\text{OSiPh}_2)_4\text{O}]_2$ , **53**, has been reported to afford the disilanol, (octaphenyltetrasiloxanediol) **54**, where the two terminal Si–OH units are separated by the  $[-\text{O}-\text{Si}-\text{O}-\text{Si}-\text{O}-]$  linker (Scheme 15).<sup>102</sup> This reaction is driven by the formation and elimination of  $\text{TiO}_2$ . The precursor spirocyclic titanosiloxane **53** is itself synthesized in an interesting reaction involving  $\text{Ph}_2\text{Si}(\text{OH})_2$  with  $\text{Ti}(i\text{-PrO})_4$ .<sup>103</sup>

Dehydration of monosilanols can be used as an effective means to generate disilanols. A silicon dichloride (**55**) that is intramolecularly stabilized by the coordination of a pendant donor nitrogen center has been found to generate an oxygen-bridged disilanol **57**. The formation of **57** is believed to occur through the intermediacy of the silanediol **56**. It has been suggested that condensation of two molecules of **56** by elimination of water leads to **57** (Scheme 16).<sup>104</sup> An interesting aspect of **57** is that it is a diastereomeric mixture of the meso and racemic isomers. These two isomers could be separated manually and characterized. It has also been observed that the individual diastereomers could be isomerized by the action of water under neutral conditions.

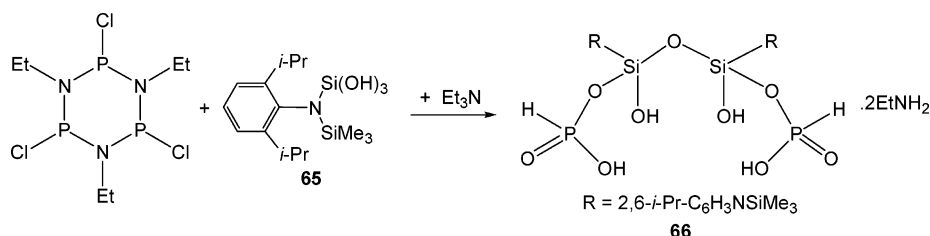
The tetraferrocenylsiloxanediol **59** is obtained by dehydration of the corresponding silanediol (**58**) under vigorous basic conditions (Scheme 17).<sup>105</sup> Unlike the situation with compound **56**, in this instance the diferrocenylsilanediol could be isolated and converted to the disilanol **59**.



## Scheme 18



## Scheme 19



In contrast to the dehydration methods discussed above, a direct method of obtaining the disilanol is also possible. Thus, reaction of *t*-BuOK with hexachlorodisiloxane (Cl<sub>3</sub>Si)<sub>2</sub>O affords 1,1,3,3-tetrakis(*tert*-butoxy)1,3-dichloro-1,3-disiloxane, [(*t*-BuO)<sub>2</sub>SiCl]<sub>2</sub>O, **60**, as a distillable colorless oil. The hydrolysis of **60** using a large excess of water (with a slight excess of pyridine) afforded the disilanol **61** in nearly quantitative yields. Interestingly, the disilanol **61** is quite stable and does not undergo self-condensation reaction in the presence of pyridine (eq 1, Scheme 18).<sup>19</sup> A (RO)<sub>2</sub>SiO<sub>2</sub>-bridged disilanol [{(*t*-BuO)<sub>2</sub>Si(OH)]<sub>2</sub>(*t*-BuO)<sub>2</sub>SiO<sub>2</sub>] (**64**) can be synthesized by a *direct* reaction of (*t*-BuO)<sub>2</sub>Si(OH)<sub>2</sub> (**63**) with (*t*-BuO)<sub>2</sub>SiCl<sub>2</sub> (**62**) (eq 2, Scheme 18).<sup>19</sup>

An interesting example of a lipophilic silicophosphate [RSi(OH){OP(O)(H)(OH)}<sub>2</sub>O·2EtNH<sub>2</sub>] [R = (2,6-*i*-Pr<sub>2</sub>-C<sub>6</sub>H<sub>3</sub>-N(SiMe<sub>3</sub>))] (**66**) was synthesized recently in the reaction of the N-bonded silanetriol RSi(OH)<sub>3</sub> (**65**) with the λ<sup>3</sup>-cyclotriphosphazane [EtNPCI]<sub>3</sub> (Scheme 19).<sup>106</sup> Compound **66** was obtained in about 35% yield by an unprecedented degradation of the cyclophosphazane ring. The mechanism of this unusual reaction remains to be delineated. The interesting aspect of **66** is that it possesses the disilanol unit and also two P(OH) groups. Such compounds are of interest as precursors for metal-containing silicophosphate materials.

A series of cyclic and linear M–O containing silanols **67**–**71** has been reported (Scheme 20). Synthesis of these compounds involves, in most cases, reaction of a N-bonded silanetriol with a suitable metal substrate. Thus, reaction of Cp<sup>\*</sup>MCl<sub>4</sub> (M = Mo, W; eq 1, Scheme 20) with RSi(OH)<sub>3</sub> [R = (2,6-*i*-Pr<sub>2</sub>-C<sub>6</sub>H<sub>3</sub>-N(SiMe<sub>3</sub>))] affords six-membered metallasiloxanes (**67a,b**) containing two Si–OH units.<sup>107</sup> Reaction probably first involves self-condensation of the silanetriol RSi(OH)<sub>3</sub> to a disiloxanediol {RSi(OH)<sub>2</sub>}<sub>2</sub>O. The latter reacts with Cp<sup>\*</sup>MCl<sub>4</sub> by elimination of HCl to afford **67a** and **67b**.

The six-membered cyclometallasiloxanes **67a** and **67b** are readily converted by aerial oxidation to afford

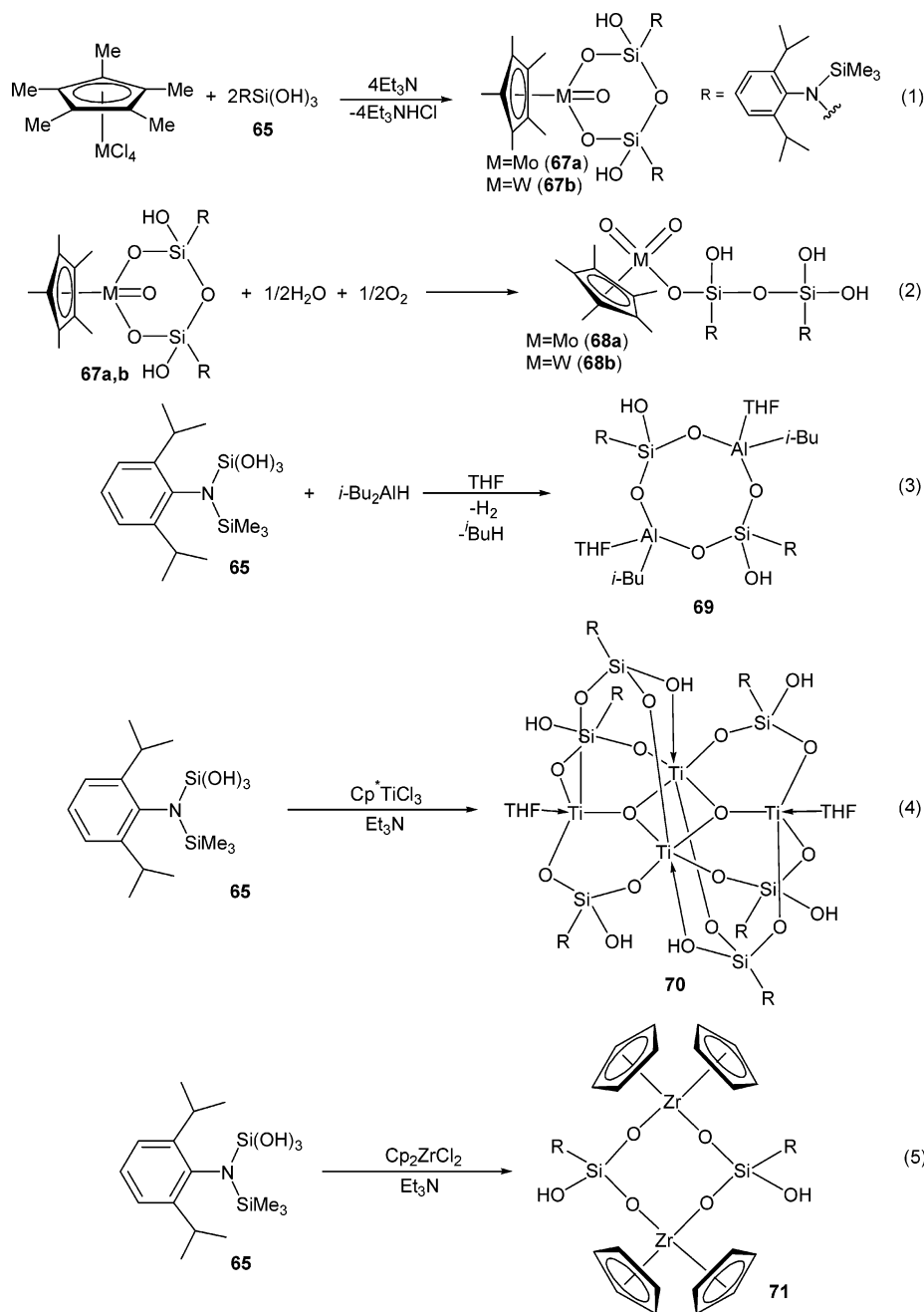
the linear metallasiloxanes **68a** and **68b**, which contain Si–OH and Si(OH)<sub>2</sub> groups (eq 2, Scheme 20).<sup>107</sup> Reaction of RSi(OH)<sub>3</sub> with other organometallic substrates leads to different Si–OH-containing products. Thus, reaction with *i*-Bu<sub>2</sub>AlH affords a cyclic eight-membered aluminosiloxane **69** (eq 3, Scheme 20).<sup>108</sup> Each silicon center in the molecule carries a hydroxyl group. Reaction of RSi(OH)<sub>3</sub> with Cp<sup>\*</sup>TiCl<sub>3</sub> in the presence of triethylamine leads to a titanosiloxane cage **70** containing a Ti<sub>4</sub>Si<sub>6</sub> framework (eq 4, Scheme 20).<sup>109</sup> The structure of this complex cage is built from a central Ti<sub>4</sub>O<sub>2</sub> core which is linked by a periphery of six RSiO<sub>2</sub>OH units. In contrast to the complex cage obtained in reaction of RSi(OH)<sub>3</sub> with Cp<sup>\*</sup>TiCl<sub>3</sub>, the corresponding reaction with Cp<sub>2</sub>ZrCl<sub>2</sub> affords an eight-membered compound (**71**) containing the Si<sub>2</sub>Zr<sub>2</sub>O<sub>4</sub> framework (eq 5, Scheme 20).<sup>110</sup> Two Si–OH groups are contained in this metallasiloxane.

Tacke and co-workers have shown that reaction of RCH<sub>2</sub>Si(OMe)<sub>3</sub> (R = C<sub>4</sub>H<sub>8</sub>NO; **72**) with [Ph<sub>2</sub>Si(OH)]<sub>2</sub> (**73**) leads to the formation of a 10-membered macrocyclic ring (**74**) which contains two disilane and two disiloxane units (eq 1, Scheme 21).<sup>111</sup> The two antipodal ends of the macrocycle contain the Si–OH units. A similar type of reaction of **72** also occurs with the diphenylsiloxanediol **45** to afford macrocycle **75** (eq 2, Scheme 21).

Trisiloxane- and trisilazane-supported silanols have been reported recently by Roesky and co-workers. Thus, reaction of hexachlorodisilane Cl<sub>3</sub>Si–SiCl<sub>3</sub> with (Me<sub>3</sub>Si)<sub>2</sub>CHLi results in replacement of one chlorine each on the disilane to afford the product [{(Me<sub>3</sub>Si)<sub>2</sub>CH}Cl<sub>2</sub>Si–SiCl<sub>2</sub>{CH(SiMe<sub>3</sub>)<sub>2</sub>}] (**76**). Ammonolysis leads to the formation of [{(Me<sub>3</sub>Si)<sub>2</sub>CH}(NH<sub>2</sub>)<sub>2</sub>Si–Si(NH<sub>2</sub>)<sub>2</sub>{CH(SiMe<sub>3</sub>)<sub>2</sub>}] (**77**). Hydrolysis of the latter with water/hydrogen peroxide leads to the formation of the trisiloxane [Si(OH){CH(SiMe<sub>3</sub>)<sub>2</sub>}O]<sub>3</sub> (**78**) (eq 1, Scheme 22).<sup>112a</sup>

Interestingly, the stereochemistry of the Si–OH groups in **78** is *cis* with respect to each other and they are found in the axial positions of the chair confor-

## Scheme 20



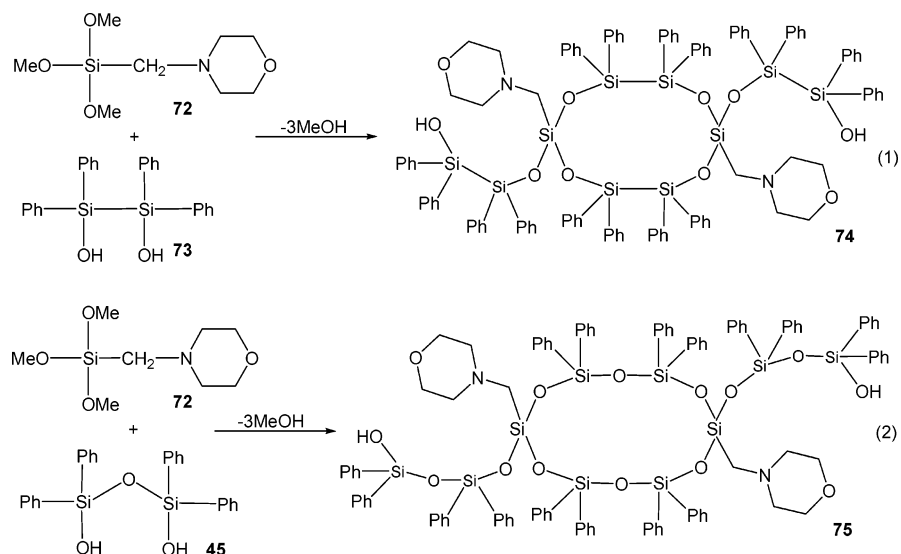
mation of the six-membered  $\text{Si}_3\text{O}_3$  ring. Synthesis of the trisilazane ring containing Si–OH groups is carried out in a different way. Thus, reaction of the silicon trichloride  $\{(\text{SiMe}_3)_2\text{CH}\}\text{SiCl}_3$  (**79**) with Na/NH<sub>3</sub> in the presence of *adventitious amounts* of moisture affords the six-membered  $[(\text{SiMe}_3)_2\text{CHSi}(\text{OH})]\text{NH}_3$  (**80**; eq 2, Scheme 22).<sup>112b</sup>

Interesting examples of sterically hindered *cis*-, *trans*-cyclotrisiloxane triol (**82**) and tetrasiloxane disilanol (**83**) have been synthesized by treating a mixture of the sterically hindered silanetriol (**81**) and siloxane tetrachloride  $(\text{RSiCl}_2)_2\text{O}$ . Unlike in the previous reactions, reaction between **81** and  $(\text{RSiCl}_2)_2\text{O}$  requires reflux conditions and fairly longer reaction times. The tetrasiloxane disilanol **83** has also been exclusively obtained by reaction of  $(\text{RSiCl}_2)_2\text{O}$  and the tetrahydroxy disiloxane  $[\text{RSi}(\text{OH})_2]_2\text{O}$  ( $\text{R} = 2,4,6\text{-}i\text{-Pr}_3\text{-C}_6\text{H}_2$ ).<sup>113</sup>

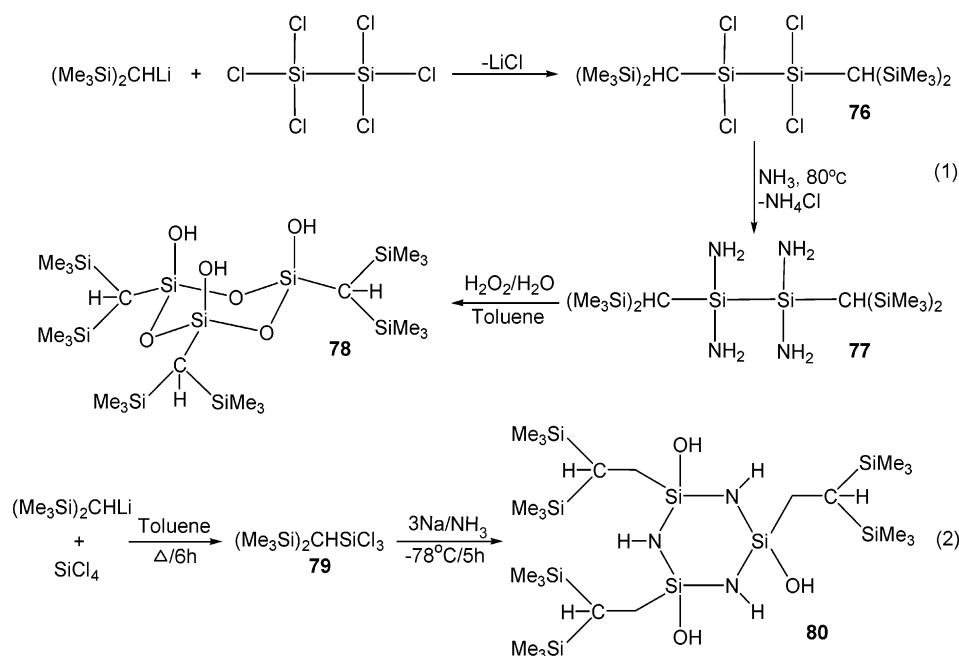
A furan-bridged bis-silanol has been prepared by hydrolysis of the corresponding difluorosilane (**84**) (Scheme 24) in strong basic conditions using KOH.<sup>114</sup> The disilanol thus obtained (**85**) forms adducts with various species such as KF (**85a**), H<sub>2</sub>O (**85b**), NH<sub>3</sub> (**85c**), and MeNH<sub>2</sub> (**85d**).

In an interesting reaction the trisilaallene **88** was prepared in a two-step reaction by treatment of the silylene **86** with  $\text{SiCl}_4$  and subsequent treatment of the trichloride **87** with  $\text{KC}_8$  at  $-40^\circ\text{C}$  for 1 day. Compound **88** is the stable silicon analogue of an allene and has a formal sp hybridization. Hydrolysis of **88** with water results in the formation of 1,3-dihydroxydisilane **89**.<sup>115</sup> The trisilaallene **88** and its silanol derivative **89** have bent structures. This is in contrast with the carbon allenes where the carbon atoms are linearly arranged.

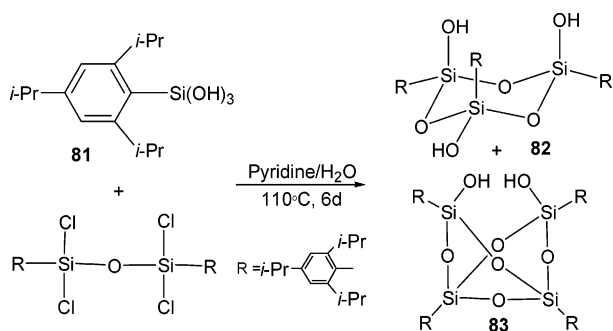
## Scheme 21



## Scheme 22



## Scheme 23



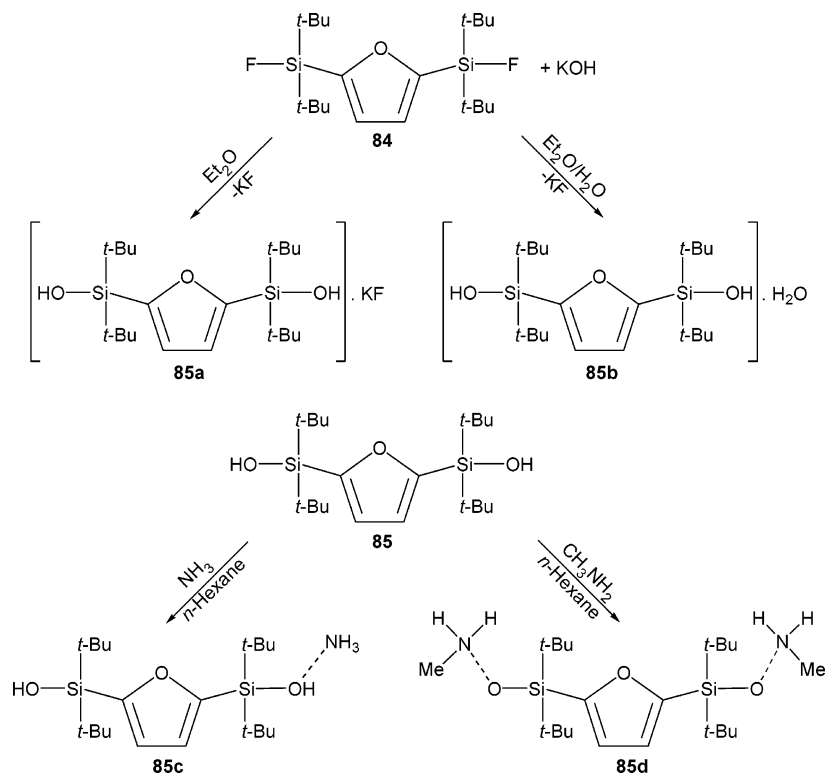
Several dendrimeric compounds (**90–95**) containing peripheral Si–OH groups varying from 3 to 16 have been prepared (Chart 5).<sup>116a</sup>

Typically the syntheses of these dendrimeric silanols are accomplished by a divergent methodology.<sup>116a,116b</sup> Schemes 26 and 27 illustrate the prin-

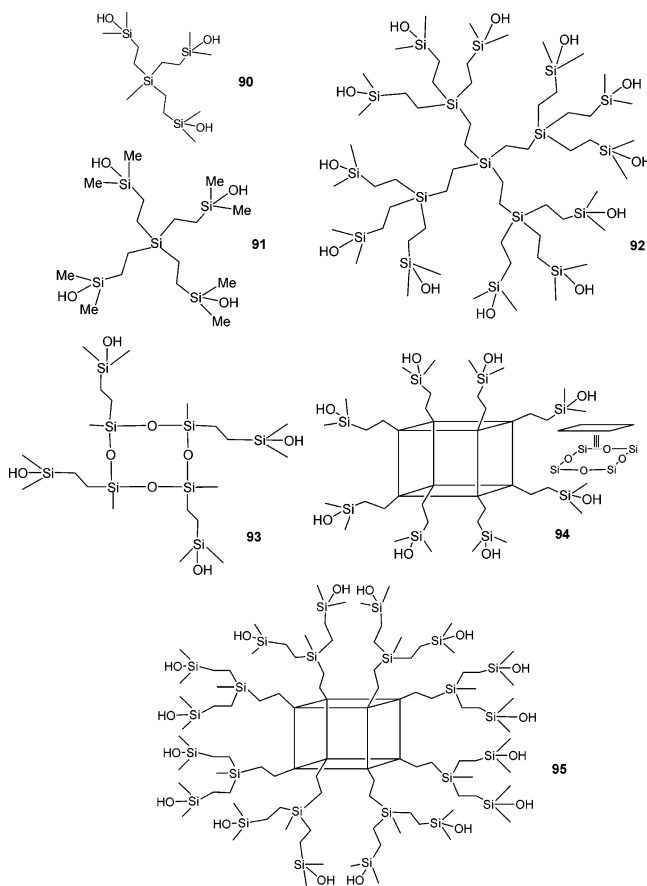
ciples involved in this synthetic strategy. For example, the dendrimeric tetrasilanol **91** is prepared in the following manner. Tetravinylsilane, Si(CH=CH<sub>2</sub>)<sub>4</sub> (**96**), is hydrosilylated with Me<sub>2</sub>SiHCl in the presence of Speier's catalyst to afford the pentasilane **97**, which can be directly hydrolyzed to the tetrasilanol **91** using water/aniline. However, a cleaner synthetic route involves the reduction of **97** to **98**. The latter contains four peripheral Si–H moieties. These are converted to the corresponding Si–OH-containing compound **91** by the action of Pd/C and water at room temperature (Scheme 26).<sup>116a</sup>

Similarly, synthesis of the dendrimeric multisilanol **95** is accomplished by a divergent synthetic strategy (Scheme 27).<sup>116a</sup> Thus, the octavinylsilsequioxane **99** is hydrosilylated with HSiMeCl<sub>2</sub> to afford **100**, which contains eight SiCl<sub>2</sub> units in the periphery. Reaction of **100** with vinylmagnesium bromide converts it into **101**, which has 16 peripheral vinyl groups. Hydro-

## Scheme 24

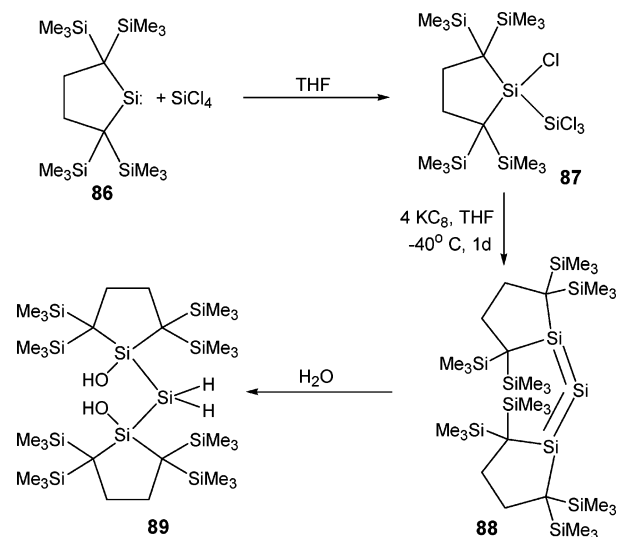


## Chart 5. Various Dendrimeric Silanols



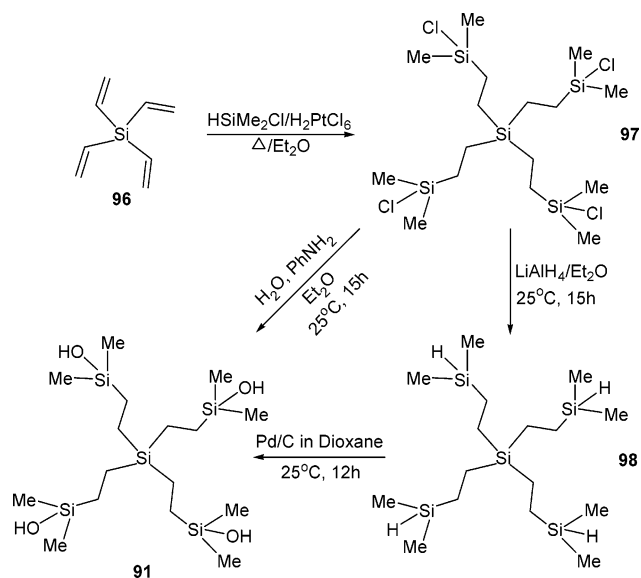
silylation of **101** followed by Pd/C treatment affords the dendrimeric silanol **95**, which contains 16 Si–OH groups in the periphery of the dendrimeric assembly.

## Scheme 25

4.2. <sup>29</sup>Si NMR

Available <sup>29</sup>Si NMR data for various compounds containing more than one Si–OH group are summarized in Table 3. The trends observed in these compounds are similar to those found in monosilanols (vide supra). Thus, in disilanols **61** and **64** where the silicon contains an O<sub>4</sub> coordination environment, the <sup>29</sup>Si chemical shifts are significantly upfield shifted (–94.1 and –93.5 ppm, entries 3 and 4, Table 3) reflecting the enhanced shielding experienced by the <sup>29</sup>Si nucleus. Similarly, in compounds **66**, **68a**, **68b**, **69**, and **71** where the silicon has a NO<sub>3</sub> coordination environment, the chemical shifts are slightly downfield shifted in comparison to **61** and **64** (entries 5–9, Table 3). In compounds **74** and **75** where the silicon has a CO<sub>3</sub> coordination environment, the observed

## Scheme 26



chemical shifts are  $-73.3$  and  $-77.3$  ppm, respectively (entries 10 and 11, Table 3). However, anomalous

chemical shifts of  $-21.8$  and  $-25.1$  ppm are observed for the trisiloxane- and trisilazanetriols **78** and **80**, respectively (entries 12 and 13, Table 3). The reason for the decreased shielding in these compounds is not clear. The trisiloxane trisilanol **82** shows two resonances at  $-60.0$  and  $-60.8$  ppm in the ratio 2:1. This clearly indicates that **82** is present as a mixture of its *cis* and *trans* isomers.<sup>113</sup> In compounds **54** and **59** the observed chemical shifts are at  $-39.9$  and  $-25.6$  ppm reflecting the decreased shielding (entries 1 and 2, Table 3). In **85** where the silicon has a  $C_3O$  coordination environment, the largest deshielding effect is felt with the chemical shift being  $+1.0$  ppm (entry 15, Table 3). The 1,3-dihydroxytrisilane **89** shows resonances at  $-90.0$  ( $SiH_2$ ),  $1.7$  and  $3.7$  ( $SiMe_3$ ), and  $39.6$  ppm ( $Si-OH$ ).<sup>115</sup>

## 4.3. X-ray Crystal Structures of Compounds Containing More than One Si-OH Group

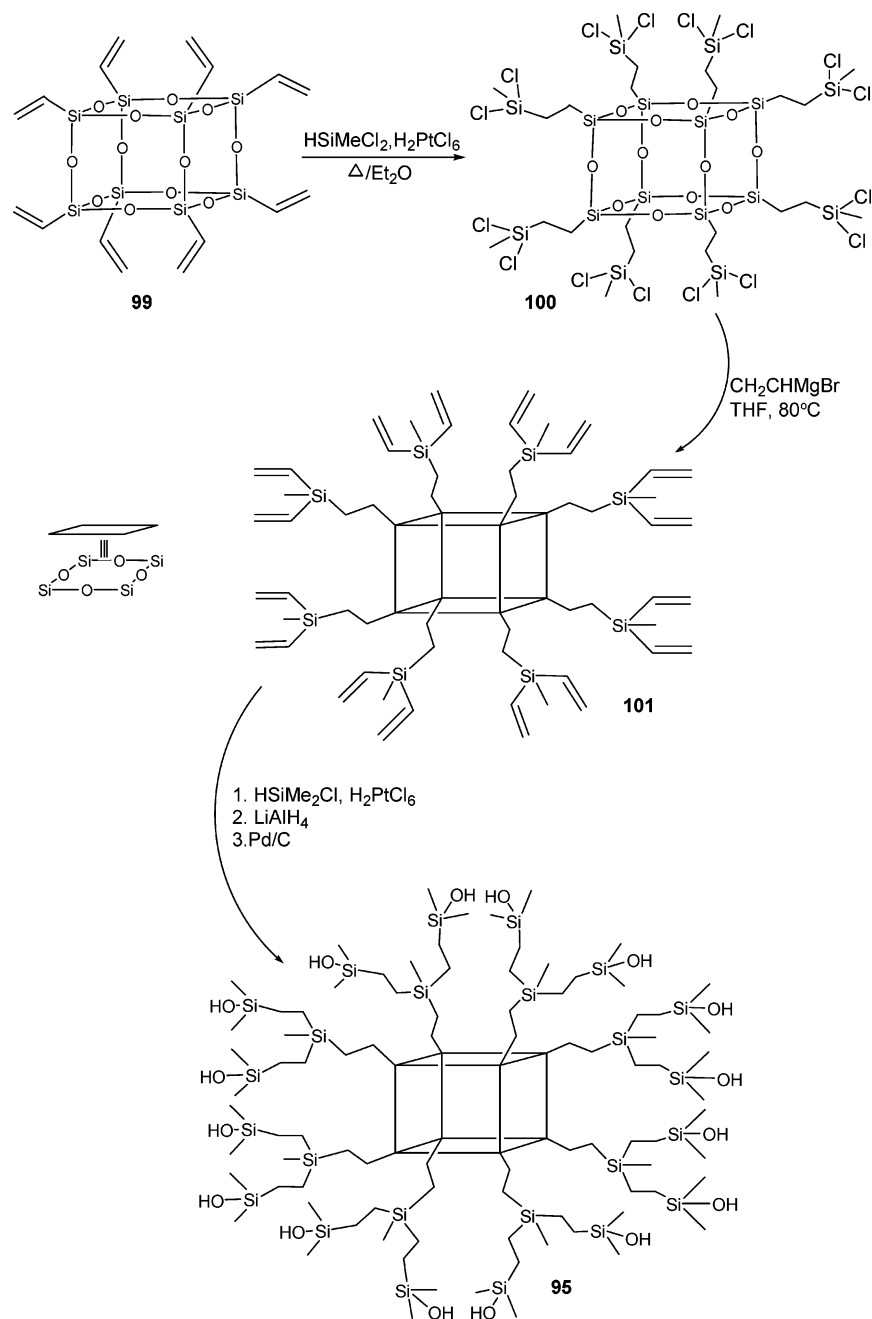
X-ray structural data for compounds containing more than one Si-OH group are listed in Table 4. Among these, disiloxane diols form the majority. An analysis of the X-ray crystal structures carried out

Table 3.  $^{29}Si$  NMR Data for Compounds Containing More than One Si-OH Group

S.No.	Compound	Coordination Environment around Silicon	$^{29}Si$ NMR (ppm)	Ref.
1		$C_2O_2(Si-OH)$ $C_2O_2$	-39.9 -47.8	102
2		$C_2O_2$	-25.6	105
3		$O_4$	-94.1	19
4		$O_4(Si-OH)$ $O_4$	-93.5 -104.4	19
5		$NO_3$ $NC_3$	-82.9 8.1	106
6		$NO_3(Si-OH)$ $NO_3$ $NC_3$	-72.8 -74.1 7.3, 7.2	107
7		$NO_3(Si-OH)$ $NO_3$ $NC_3$	-73.1 -74.0 7.8, 7.3	107
8		$NO_3$ $NC_3$	-77.0 1.2	108
9		$NO_3$ $NC_3$	-79.4 3.7	110

S.No.	Compound	Coordination Environment around Silicon	$^{29}Si$ NMR (ppm)	Ref.
10		$CO_3$ $C_2OSi$	-73.3 -17.1, -16.1, -15.3	111
11		$CO_3$ $C_2OSi$	-77.3 -47.0, -44.4, -37.2	111
12		$CO_3$ $C_4$	-21.8 -0.2	112a
13		$N_2CO$ $C_4$	-25.1 -1.5	112b
14		$CO_3$	-60.0 -60.8	113
15		$C_3O$	1.0	114
16		$Si_2H_2$ $C_4$ $C_4$ $SiC_2O$	-90.0 1.7 3.7 39.6	115

## Scheme 27



earlier<sup>4</sup> has found that four major types of intermolecular hydrogen-bonding interactions are present among disilanol. These are summarized in Chart 6.

Type G represents a situation where two disilanol units are hydrogen bonded to each other in a head-head manner. Interaction among such dimers leads to the formation of polymeric sheets or polymeric tapes. In this structural formation  $\text{Si}_4\text{O}_6$  rings alternate with  $\text{O}_4$  rings (intervening hydrogens are not shown in the chart). The disiloxanediol  $[\text{Me}(\text{3-thienyl})\text{Si}(\text{OH})_2\text{O}]$  shows a Type G type of a structure in its solid state.<sup>87</sup> Type H represents a situation where one of the disilanol moieties in the dimeric unit of Type G undergoes a translational shift so that perfect head-to-head dimerization does not occur. This results in a zigzag polymeric network containing the propagation of dimers of  $\text{Si}_2\text{O}_3$  rings. Examples that show Type H structure are  $[\text{R}_2\text{Si}(\text{OH})_2\text{O}]$  ( $\text{R} = i\text{-Pr}$ ,<sup>87</sup>

$c\text{-C}_5\text{H}_9$ ). In Type I the translational shift of one of the disilanol moieties occurs even further. This form consists of alternate  $\text{Si}_2\text{O}_5$  rings that are fused to each other. Examples of disiloxanediols showing Type I structure are  $[\text{R}_2\text{Si}(\text{OH})_2\text{O}]$  ( $\text{R} = \text{Me}$ ,<sup>82</sup> Et,<sup>83</sup>  $n\text{-Pr}$ ,<sup>84</sup> Ph<sup>117</sup>). Type J represents a more complex two-dimensional network formation. The disiloxanediol  $\{\mu\text{-(CH}_2)_3[\text{MeSi}(\text{OH})_2\text{O}]\}$  shows such a polymeric network formation.<sup>118</sup>

Several other structural types have been found to occur in this family of compounds in addition to those shown in Chart 6. These are discussed below.

Compounds **54**, **57**(meso), **57**(rac), **70**, **74**, **75**, and **89** are monomeric compounds. Although **66** is dimeric as a result of intermolecular P–OH interactions, the Si–OH units contained in this molecule do not participate in intermolecular hydrogen bonding.<sup>106</sup>

Table 4. X-ray Structural Data for Compounds Containing More than One Si–OH Group

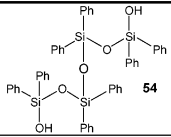
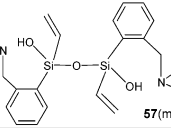
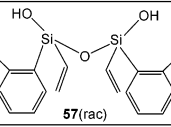
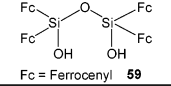
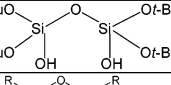
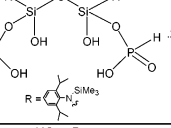
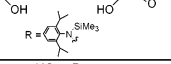
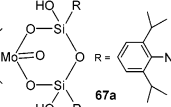
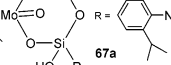
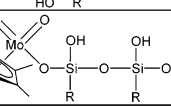
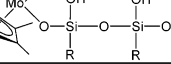
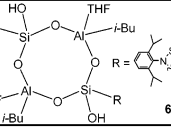
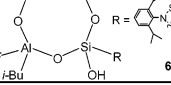
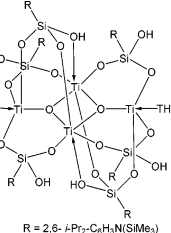
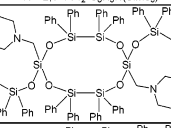
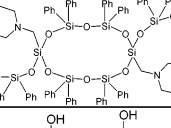
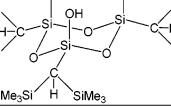
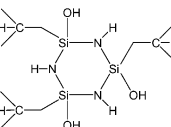
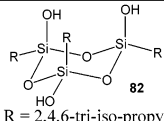
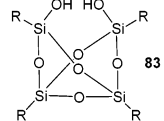
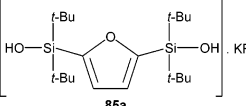
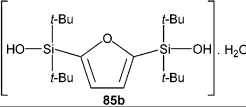
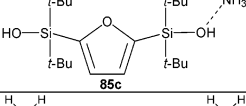
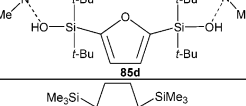
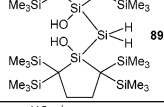
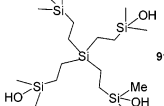
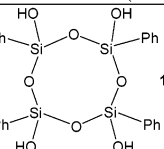
S.No.	Compound	Hydrogen Bonding Parameters				Structural Summary	Ref.
		Si–OH (Å)	OH...O (Å)	O...O (Å)	O–H...O (°)		
1	 <b>54</b>	1.626(3)	-	-	-	Monomeric structure	102
2	 <b>57(meso)</b>	1.605(8)	1.857(2) (OH...N) (intra)	2.620(3) (O...N)	170.80(4) (OH...N)	Monomeric structure	104
3	 <b>57(rac)</b>	1.619(2)	1.943(3) (OH...N) (intra)	2.706(3) (O...N)	165.16(2) (OH...N)	Monomeric structure	104
4	 <b>59</b> Fc = Ferrocenyl	1.634(3), 1.644(7)	-	2.920(1), 2.931(5)	-	Double-Chain structure	105
5	 <b>61</b>	1.604(1)	1.916(4)	2.779(5)	173.99(2)	Polymeric chain structure	19
6	 <b>66</b> R = 	1.595(3), 1.604(2)	1.830(2), 1.889(1) (OH...O) 1.566(3) (OH...OP)	2.679(4), 2.735(1)	173.27(2), 176.93(3)	Dimeric structure through P-OH...OP interactions	106
7	 <b>67a</b> R = 	1.626(1), 1.631(1)	2.154(3) OH...O=Mo	2.932(9)	147.18(2)	Dimeric structure	107
8	 <b>68a</b> R = 	1.602(3)- 1.631(3)	1.936(2)- 2.070(2) OH...O=Mo	2.758(4)- 2.889(4)	148.45(2)- 171.32(2)	Dimeric structure forming a tubular box	107
9	 <b>69</b> R = 	1.813(5)	-	-	-	Monomeric structure	108
10	 <b>70</b> R = 2,6- <i>i</i> -Pr <sub>2</sub> -C <sub>5</sub> H <sub>3</sub> N(SiMe <sub>3</sub> )	1.628(6)- 1.664(1)	1.966(8)- 2.353(6)	2.662(2)- 3.090(2)	140.14(5)- 149.96(5)	Monomeric cage structure	109
11	 <b>74</b>	1.638(1)	1.932(3) (OH...N) intra	2.737(4) (O...N)	166.75(1) (OH...N)	Monomeric structure	111
12	 <b>75</b>	1.621(1)	2.016(6) (OH...N) intra	2.787(3) (O...N)	171.98(6) (OH...N)	Monomeric structure	111
13	 <b>78</b>	1.639(2)	1.903(2)	2.714(2)	1.67.80(2)	Dimeric structure	112a
14	 <b>79</b>	1.673(3)	1.955(2)	2.833(3)	173.79(2)	Dimeric structure	112b

Table 4 (Continued)

S.No.	Compound	Hydrogen Bonding Parameters				Structural Summary	Ref.
		Si-OH (Å)	OH...O (Å)	O...O (Å)	O-H...O (°)		
15	 82 R = 2,4,6-tri-iso-propyl	1.622(1) 1.648(4)	1.714(8) 2.412(7)	2.788(1) 2.805(11)	124.71(1) 177.92(2)	Polymeric Chain	113
16	 83 R = 2,4,6-tri-isopropyl phenyl	1.634(8), 1.636(5)	1.894(5), 2.416(5)	2.975(7), 2.801(6)	161.37(1), 168.32(1)	Dimeric four membered ring	113
17	 85a	1.619(4), 1.623(3)	1.867(5), 1.901(5) (OH...O) 1.803(3), 1.900(4) (OH...F)	2.594(3) 2.632(2), 2.724(1)	141.96(4), 146.8(2) 170.06(2), 172.06(5)	Dimeric structure	114
18	 85b	1.653(2)	1.998(2)- 2.016(2)	2.759(3)- 2.863(3)	159.84(1)- 175.11(2)	Polymeric chain	114
19	 85c	1.630(2), 1.635(4)	1.931(2)- 2.484(2)	2.693(1)- 3.323(1)	153.06(1)- 166.00(2)	Dimeric structure	114
20	 85d	1.625(2), 1.635(4)	1.845(3)- 2.365(4)	2.667(2)- 3.265(4)	164.86(1)- 169.88(3)	Polymeric ladders	114
21	 89	1.674(8), 1.688(1)	1.903(2) (Intra)	2.803(9)	159.51(8)	Monomeric	115
22	 91	1.658(6)- 1.668(3)	-	2.698(7)	-	One-dimensional polymer	116a
23	 102	1.609(1)- 1.629(9)	1.786(9)- 1.969(1)	2.621(1)- 2.787(1)	158.96(1)- 175.10(1)	Dimeric tubular structure	119

The molecular structure of 1,3,5,7-tetrasiloxane-1,7-diol,  $\text{Ph}_2(\text{OH})\text{Si}(\text{OSiPh}_2\text{O})_2\text{Si}(\text{OH})\text{Ph}_2$  (**54**), is shown in Figure 9. The notable features of the molecular structure of **54** is the linearity of the central Si-O-Si bond angle and the absence of any intermolecular O-H...O hydrogen bonding. A weak hydrogen-bonding interaction between the Si-O-H and phenyl group has been indicated. The IR spectrum of this compound shows a band at  $3591\text{ cm}^{-1}$ . The slight shift in frequency observed in this case in comparison to other free Si-OH stretching frequencies is consistent with the O-H... $\pi$  interaction in the solid state.<sup>102</sup>

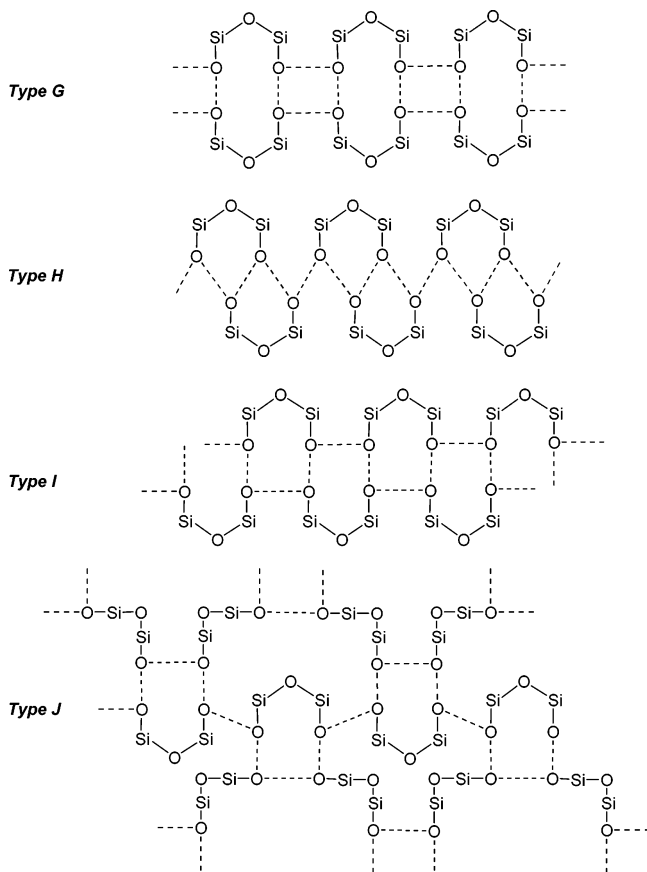
The X-ray crystal structures of **57(meso)** and **57(rac)** are shown in Figure 10. While in **57(meso)** a perfectly linear Si-O-Si bond is seen, in **57(rac)** the Si-O-Si angle is  $161.50(18)^\circ$ . It may be noted that in some disiloxanes of the type  $\text{R}_3\text{Si-O-SiR}_3$  (R = vinyl, phenyl, benzyl) the Si-O-Si bond is also quite linear. However, in many siloxane diols  $(\text{SiR}_2\text{OH})_2\text{O}$

(R = Me, Et, *i*-Pr,  $\text{C}_6\text{H}_5$ ) the observed Si-O-Si bond angles are in the range of  $141\text{--}163^\circ$ . The Si-OH bond distances in **57(meso)** and **57(rac)** are 1.605(8) and 1.619(2) Å, respectively. The monomeric nature of **57(meso)** and **57(rac)** is readily traced to the strong intramolecular hydrogen bonding of the Si-OH with the nitrogen of the amino substituent on the aromatic group. The nitrogen atom of the amino group and the Si-O-H unit are suitably oriented for the formation of a six-membered cyclic ring (Figure 10).<sup>104</sup> The observed O-H...N bond angles and N...H and N...O distances (Table 4) indicate that the hydrogen bonds are quite strong. For example, the N...O distance observed in normal hydrogen-bonding situations is found to vary between 2.62 and 2.93 Å. In **57(meso)** this distance is 2.620(3) Å, while in **57(rac)** it is 2.706(3) Å.

The eight-membered aluminosiloxane **69** containing two Si-OH groups is also monomeric and does not show intermolecular hydrogen-bonding interac-

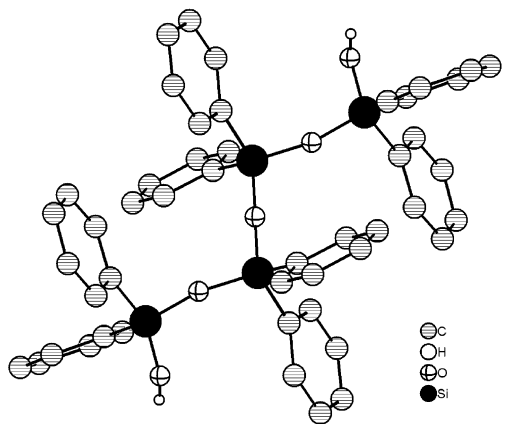


### Chart 6. The Four Major Types of Intermolecular Hydrogen-Bonding Interactions Present among Disilanols

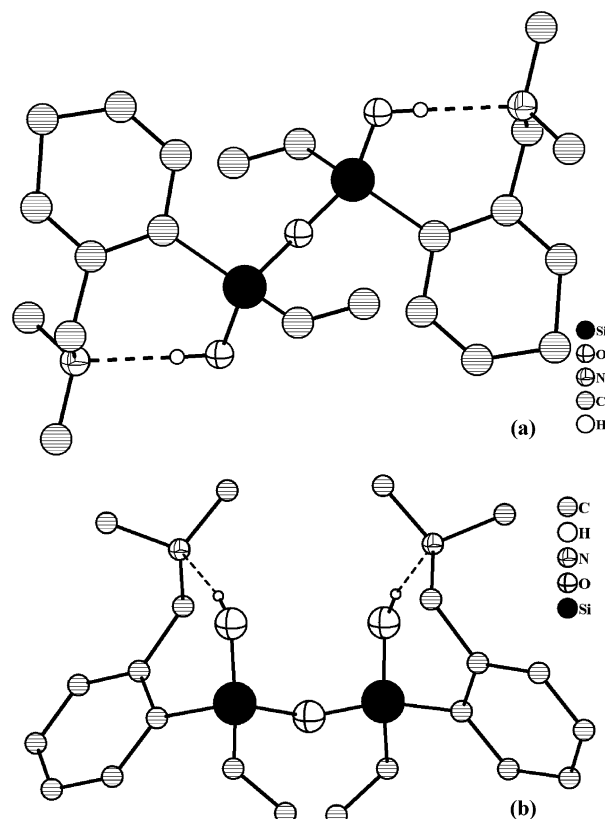


tions. Compound **69** contains an  $\text{Al}_2\text{Si}_2\text{O}_4$  ring (Figure 11). The ring has an approximate chair conformation with two antipodal oxygens being out of the plane formed by the remaining six atoms. It has been suggested that the basic framework found in **69** is analogous to that present in the mineral gismondine,  $(\text{CaAl}_2\text{Si}_2\text{O}_8(\text{H}_2\text{O})_4)_n$ .<sup>108</sup> The average Si–O (endocyclic) distance is 1.59 Å, while the exocyclic Si–O distance is considerably longer, 1.813(5) Å.

The cage compound  $[\text{RSi}(\text{OH})(\text{O})_2]_6\text{Ti}_4(\mu_3\text{-O})_2$  ( $\text{R} = (2,6\text{-}i\text{-Pr}_2\text{C}_6\text{H}_3)\text{NSiMe}_3$ ) (**70**) contains four titanium centers which are surrounded by  $\text{RSi}(\text{OH})(\text{O})_2$  silanolate ligands, two  $\mu_3\text{-O}$  atoms, and two coordinated



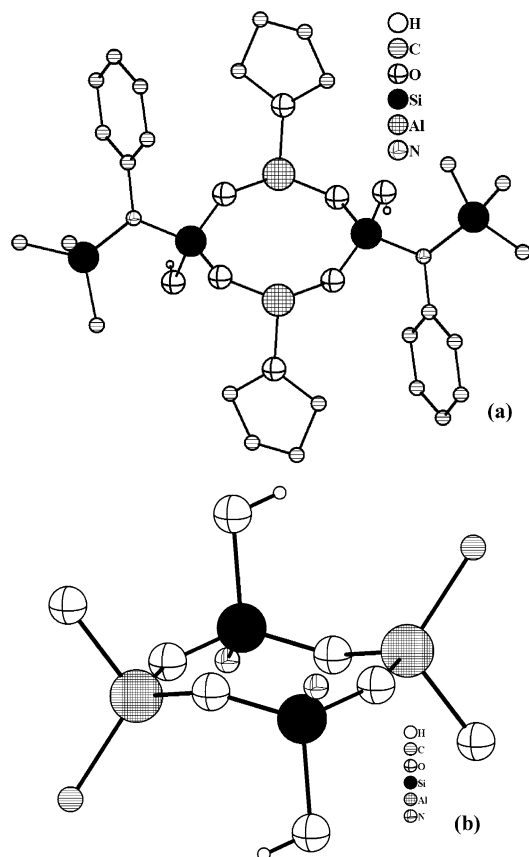
**Figure 9.** Molecular structure of octaphenyl tetrasiloxane diol **54**.



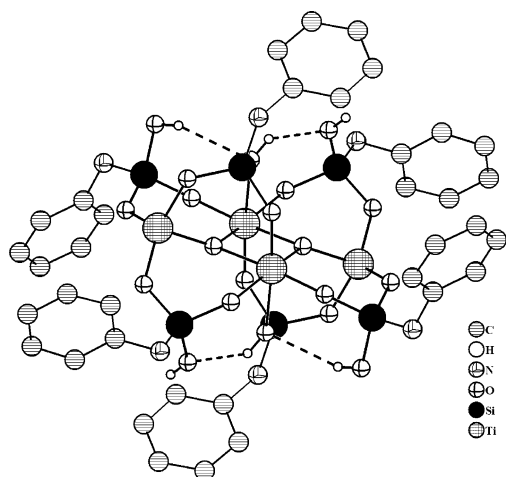
**Figure 10.** (a) Meso isomer of the vinyl-substituted disiloxane diol **57**. (b) The racemic form of **57**. Both isomers show intramolecular hydrogen bonding with the nitrogen atom of the dimethylamino group. The hydrogens present on the carbon atoms are omitted.

THF molecules (Figure 12). The core of the molecule comprises of a planar four-membered  $\text{Ti}_2\text{O}_2$  ring. The four Ti–O edges of this core unit are also a part of the six-membered  $\text{Ti}_2\text{SiO}_3$  rings. Two  $\text{RSi}(\text{OH})\text{O}_2$  ligands cap the overall titanasiloxane framework. The cage structure is not proliferated by intermolecular hydrogen bonding because of the strong intramolecular interactions between the Si–OH units.<sup>109</sup>

The 10- and 12-membered macrocycles **74** and **75** have two Si–OH units located in the opposite ends of the molecule. These macrocycles adopt chair conformations with respect to the position of their silicon atoms. The two morpholinomethyl substituents occupy axial positions, while the two  $\text{OPh}_2\text{Si-SiPh}_2\text{OH}$  or  $\text{OPh}_2\text{Si-O-SiPh}_2\text{OH}$  groups are in equatorial positions. The two exocyclic functional groups (the silanol and amino moieties) form intramolecular O–H $\cdots$ N hydrogen bonds ( $\text{N}\cdots\text{O}$  in **74** = 2.737(4) Å and in **75** = 2.787(3) Å while the O–H $\cdots$ N angles are 166.75(1)° and 171.98(6)°, respectively) (Figure 13). Clearly these intramolecular O–H $\cdots$ N hydrogen bonds are responsible for effectively blocking the possibility of other intermolecular hydrogen bonding in these two molecules, which leads to the formation of monomeric structures.<sup>111</sup> In the crystal structure of the 1,3-dihydroxytrisilane **89**, the two Si–OH groups interact with each other in an intramolecular hydrogen bonding. Moreover, the presence of the bulky  $\text{SiMe}_3$  groups prevents further propagation of the molecule.<sup>115</sup>

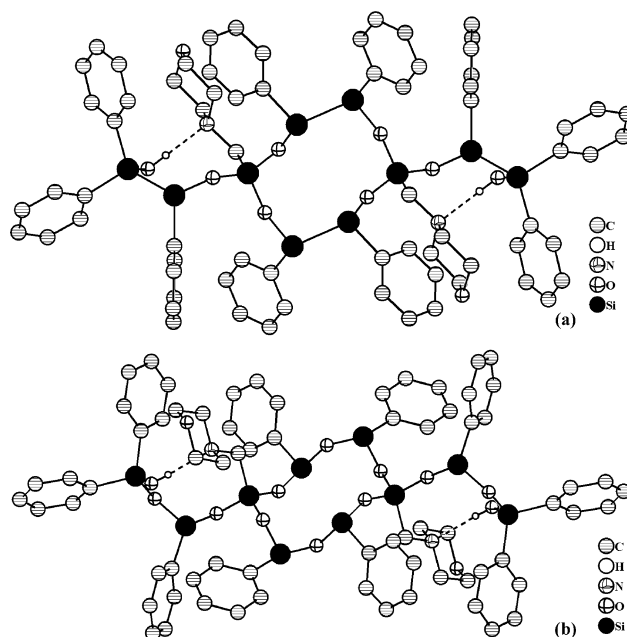


**Figure 11.** (a) DIAMOND-generated picture of the molecular structure of the eight-membered aluminosiloxane **69**. (b) View of the aluminosiloxane core showing an approximate chairlike conformation. (In both a and b isobutyl groups on aluminum have been omitted for clarity).

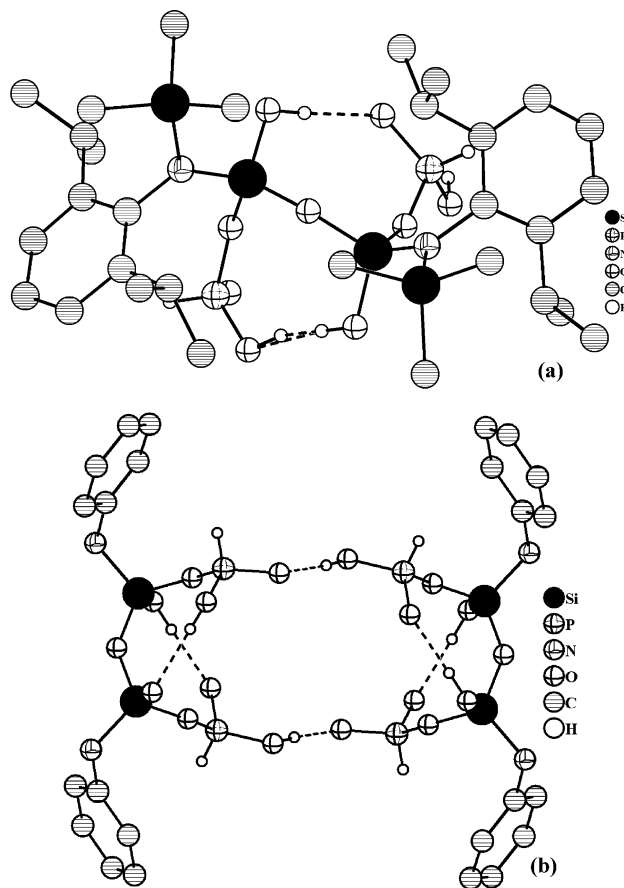


**Figure 12.** Molecular structure of the titanasiloxane cage **70** ( $-\text{SiMe}_3$  groups on nitrogen have been omitted). Intramolecular hydrogen bonding present among the Si-OH units are shown by the dotted lines.

The silicophosphonate  $[\text{RSi}(\text{OH})\{\text{OP}(\text{O})\text{H}(\text{OH})\}]_2$  ( $\text{R} = 2,6\text{-}i\text{-Pr}_2\text{-C}_6\text{H}_3\text{-NSiMe}_3$ ), **66**, adopts a dimeric structure as a result of the  $\text{P}=\text{O}-\text{H}\cdots\text{O}=\text{P}$  interactions between two molecules. The Si-OH groups participate in intramolecular hydrogen bonding with  $\text{P}=\text{O}-\text{H}$  as well as  $\text{P}=\text{O}$  groups. However, the interactions of the Si-OH units do not extend the dimeric structure further (Figure 14).<sup>106</sup>

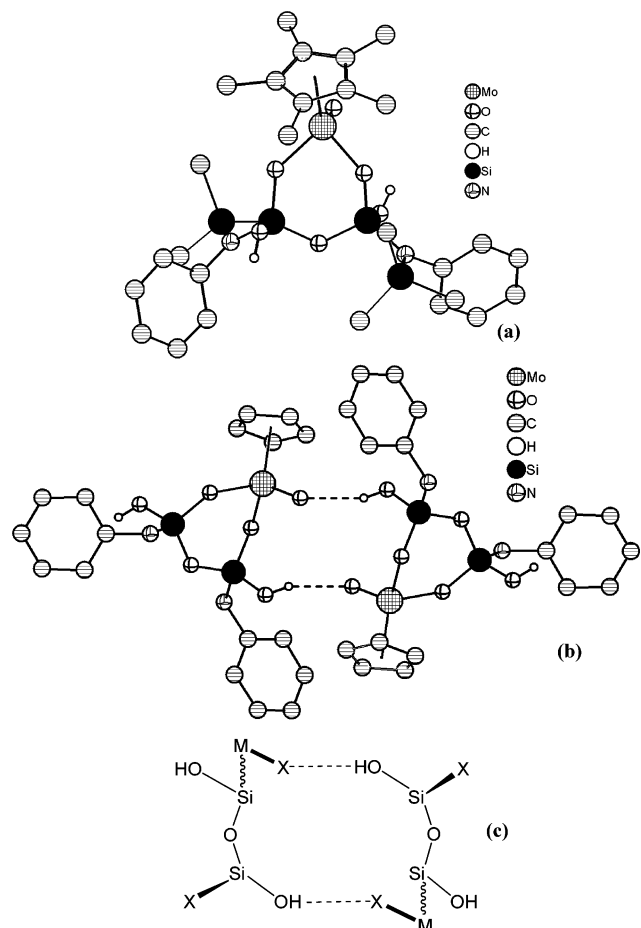


**Figure 13.** (a) Disilanol **74** anchored to a 10-membered macrocycle. (b) Disilanol **75** anchored to a 12-membered macrocycle. The Si-OH moieties are intramolecularly hydrogen bonded to the nitrogen of the morpholino group.



**Figure 14.** (a) Molecular structure of the silicophosphonate **66**. The Si-OH's are intramolecularly hydrogen bonded to the P-OH or P=O group. (b) View of the dimeric cage-like structure obtained due to the  $\text{P}=\text{O}\cdots\text{HO}-\text{P}$  interactions. The *i*-Pr and  $\text{SiMe}_3$  groups are omitted for clarity.

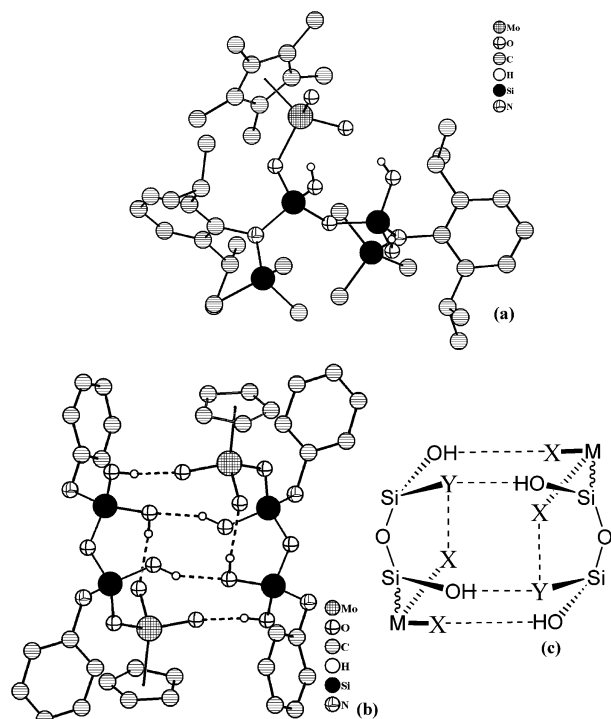
Other disilanol that form dimeric structures are **67a**, **67b**, **78**, **80**, **83**, **85a**, **85c**, and **102**. As discussed



**Figure 15.** (a) Discrete molecule of the cyclic metallasiloxane **67a**. (b) Formation of the dimeric structure through intermolecular Si–OH...O=Mo hydrogen bonds. (c) Schematic showing the connectivity between the two molecules of **67a** (M = Mo and X = O).

vide supra, reactions of Cp\**M*Cl<sub>4</sub> (M = Mo, W) with RSi(OH)<sub>3</sub> (R = 2,6-*i*-Pr<sub>2</sub>-C<sub>6</sub>H<sub>3</sub>-NSiMe<sub>3</sub>) lead to isolation of six-membered metallasiloxanes Cp\*Mo-[2,6-*i*-Pr<sub>2</sub>-C<sub>6</sub>H<sub>3</sub>-NSiMe<sub>3</sub>]<sub>2</sub>Si<sub>2</sub>O<sub>3</sub>(OH)<sub>2</sub> containing the Si<sub>2</sub>MO<sub>3</sub> framework [**67a** (M = Mo), **67b** (M = W)] or acyclic derivatives Cp\*MO<sub>2</sub>[2,6-*i*-Pr<sub>2</sub>-C<sub>6</sub>H<sub>3</sub>-NSiMe<sub>3</sub>]<sub>2</sub>-Si<sub>2</sub>O<sub>2</sub>(OH)<sub>3</sub> [**68a** (M = Mo); **68b** (M = W)]. The X-ray crystal structures of **67a** and **68a** are shown in Figures 15 and 16, respectively. **67a** comprises of a six-membered ring containing one molybdenum and two silicon atoms bridged by oxygen atoms. The six-membered ring has a boat conformation. Two such molecules are linked in the solid state via Mo–O...H–O–Si hydrogen bonding, which leaves one *free* Si–OH on each molecule (Figure 15). The acyclic derivative **68a** also forms a dimeric structure in the solid state (Figure 16). In contrast to the situation in the six-membered ring **67a**, in **68a** all the Si–OH groups participate in O–H...O hydrogen bonding. Thus, four inter- and two intramolecular hydrogen bonds are formed leading to a tubular architecture.<sup>107</sup>

The six-membered rings trihydroxycyclotrisiloxane **78** and the trihydroxycyclotrisilazane **80** also form dimeric structures in the solid state. The Si<sub>3</sub>O<sub>3</sub> ring in **78** is in a chair conformation. All three OH groups are oriented in the same direction with respect to the ring plane. The endocyclic and exocyclic Si–O distances are nearly the same: 1.642 and 1.639(2) Å.

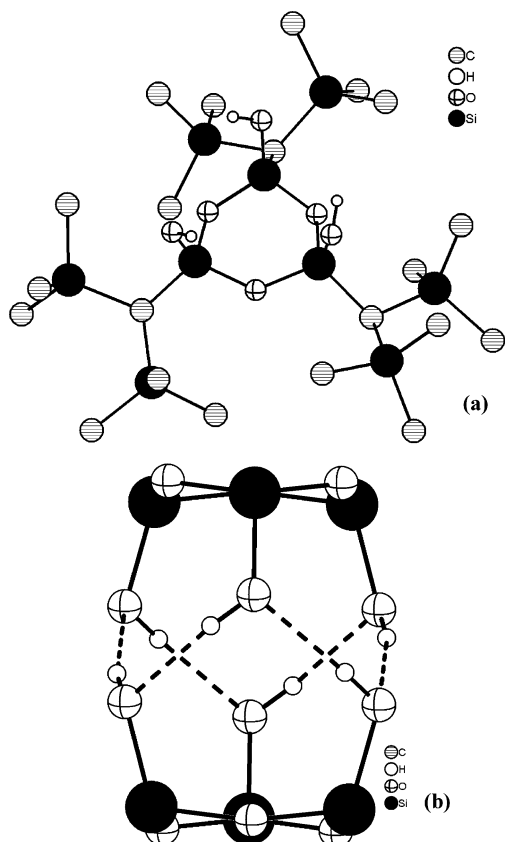


**Figure 16.** (a) View of the discrete molecule of the acyclic metallasiloxane **68a**. (b) Formation of a dimeric structure due to four intermolecular hydrogen bonds. Two intramolecular hydrogen bonds are also seen. (c) Schematic showing the formation of a tubular box (M = Mo, X = O, Y = OH).

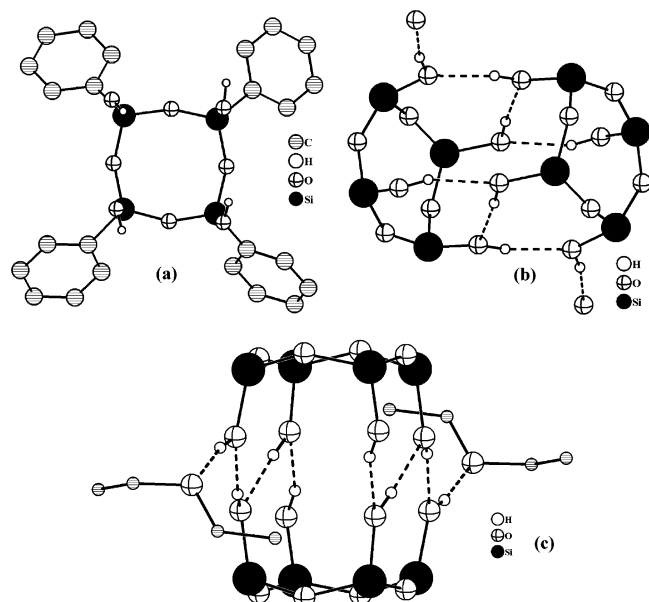
The Si–O–Si angle in the trisiloxane ring is considerably acute and is 130.46(9)°. The intermolecular hydrogen bonding between the two molecules of **78** leads to the formation of a barrel type of structure with the two faces of the barrel being made up of the six-membered trisiloxane rings.<sup>112a</sup> The central rim of the barrel is stitched by the intermolecular hydrogen bonds between the three *cis*-hydroxyl groups of one molecule with their corresponding counterparts from the other molecule (Figure 17). Each oxygen is involved in a bifurcated hydrogen-bonding pattern similar to that of Type H (Chart 6) found for other siloxanediols. The other six-membered ring trihydroxycyclotrisilazane **80** also adopts a similar structure as that of **78**.<sup>112b</sup> The molecular structure of the 1,4-dihydroxy tetrasiloxane **83** shows that the two hydroxyl groups are separated quite far away. Due to the presence of the solvated methanol a dimeric structure is obtained, leading to the formation of the four-membered O<sub>4</sub> ring.<sup>113</sup>

The tetrahydroxy cyclotetrasiloxane [Si(Ph)(O–H)O]<sub>4</sub> (**102**) also forms a dimeric structure. Two molecules of **102** approach each other in a face-to-face manner to form a tubular cage as a result of intermolecular O–H...O hydrogen bonds (Figure 18).<sup>119</sup>

Although the X-ray crystal structures of the native furan-bridged disilanol 2,5-bis(*di-tert*-butylhydroxysilyl)furan has not been reported, four crystal structures are known of this compound in the form of various adducts. Thus, the KF adduct **85a** and the NH<sub>3</sub> adduct **85c** form dimeric structures in the solid state. In both of these molecules the disilanol units

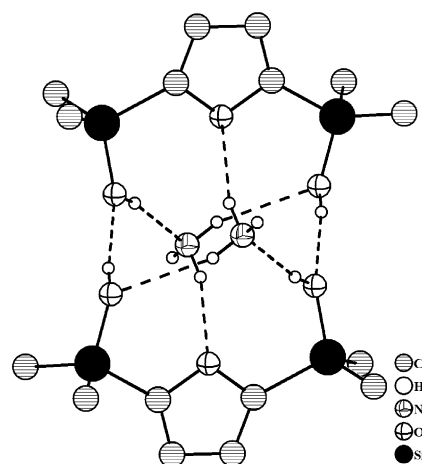


**Figure 17.** (a) DIAMOND view of the trihydroxycyclotrisiloxane **78**. (b) The orientation of the three hydroxyl groups is cis to each other. The zigzag arrangement of the hydrogen bonding leads to the formation of a dimeric barrel-type structure. The  $\text{CH}(\text{SiMe}_3)_2$  groups are omitted for clarity.

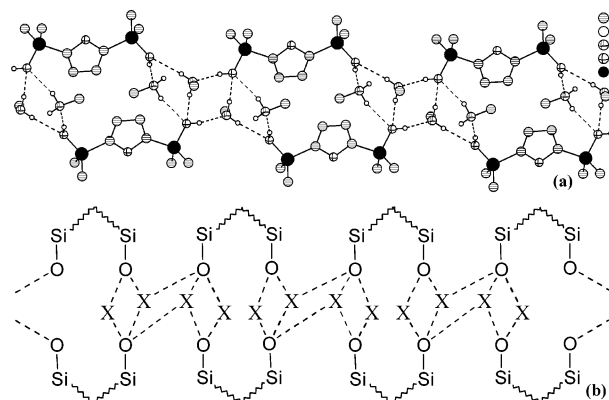


**Figure 18.** (a) View of the discrete molecule of tetrahydroxycyclotetrasiloxane **102**. (b) Formation of a dimeric cage-like structure. (c) All four  $\text{Si}-\text{OH}$  groups are arranged in a cis fashion. Further proliferation of the hydrogen bonding is terminated by solvent molecules in the form of diethyl ether.

are bridged to each other by  $\text{O}-\text{H}\cdots\text{O}$  hydrogen bonds. In **85c** two ammonia molecules further strengthen the interactions by acting as bridges with



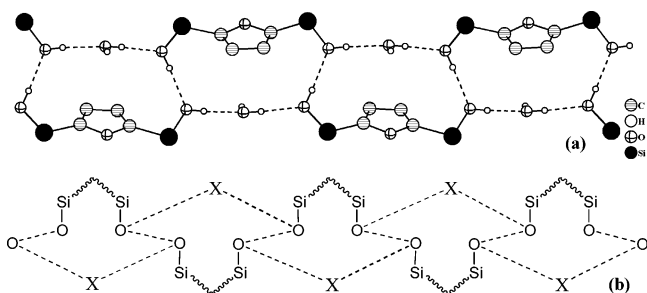
**Figure 19.** Ammonia adduct of the furan-bridged disilanol **85c**. A dimeric structure is obtained due to the  $\text{O}-\text{H}\cdots\text{O}$  hydrogen bonds. Two molecules of  $\text{NH}_3$  are held inside the cavity due to  $\text{OH}\cdots\text{N}$  and  $\text{NH}\cdots\text{O}$  hydrogen bonds.



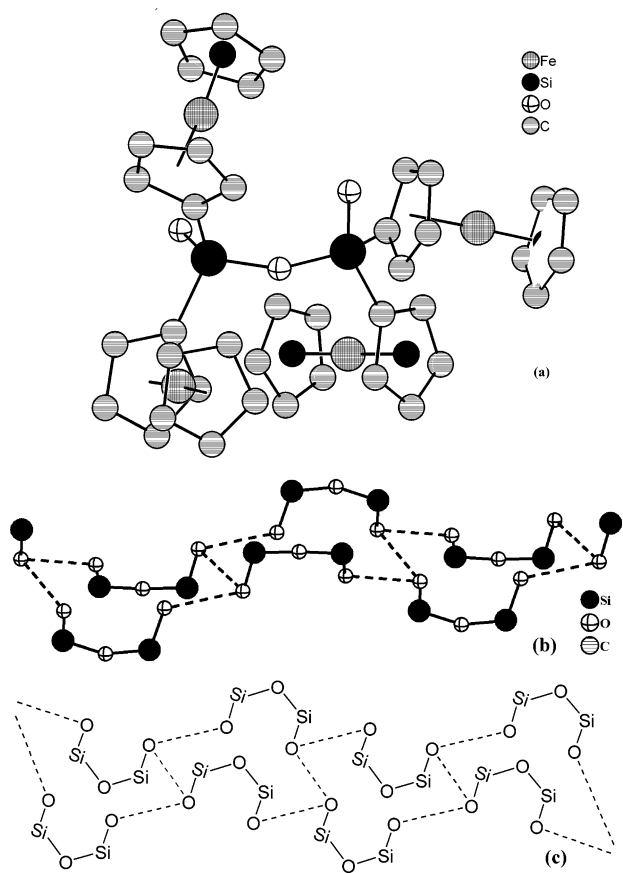
**Figure 20.** (a) Methylamine adduct of the furan-bridged disilanol **85d**. Two nearly-parallel polymeric sheets are connected through  $\text{OH}\cdots\text{N}$  hydrogen bonds with the methylamine molecules. (b) Schematic showing the polymeric ladder-type arrangement of  $\text{Si}-\text{OH}$  and  $\text{CH}_3\text{NH}_2$  groups ( $\text{X} = \text{CH}_3\text{NH}_2$ ).

the oxygen atom of the furan as well as the oxygen and  $\text{O}-\text{H}$  of the silanol moieties (Figure 19). In **85a** the role of ammonia is taken up by potassium, which lies in the center of the dimeric structure. The immediate coordination environment of the potassium atom is comprised of four oxygens of the  $\text{Si}-\text{OH}$  units, two furan oxygen atoms, as well as the fluoride ion.<sup>114</sup>

Replacement of ammonia by methylamine leads to a polymeric ladder type of architecture in the furan-bridged disilanol **85d**. In this structure two nearly parallel interlinked polymeric sheets are formed as a result of the two  $\text{Si}-\text{OH}$  units on each disilanol interacting with the methylamine to form  $\text{O}-\text{H}\cdots\text{N}$  hydrogen bonds (Figure 20). A slight variation of the polymeric structural motif occurs in the water adduct **85b**. Each disilanol moiety interacts with two anti-parallel molecules in a proton-acceptor and proton-donor manner. The water of crystallization completes the cyclic loop by hydrogen bonding with two adjacent  $\text{Si}-\text{OH}$  units derived from two different disilanol molecules. This leads to the formation of a polymeric sheet structure (Figure 21).<sup>114</sup>



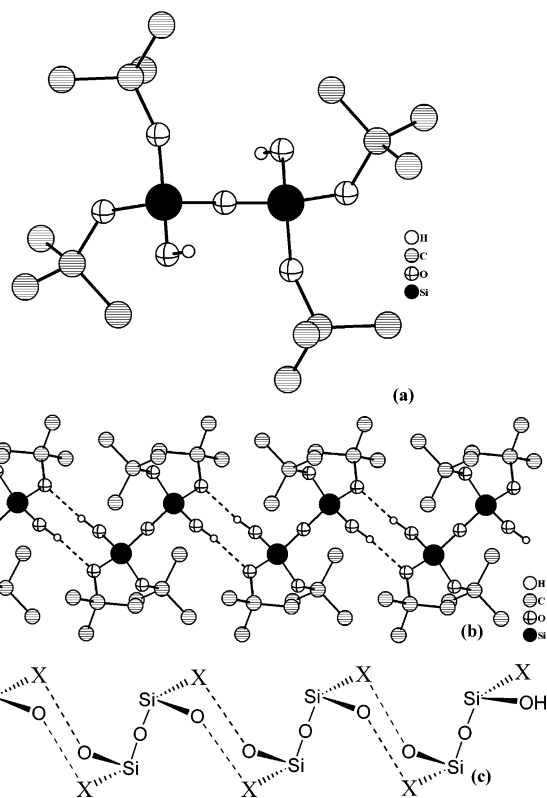
**Figure 21.** (a) Water adduct of the furan-bridged disilanol **85b**. Proliferation of the  $\text{Si}_2\text{C}_4\text{O}_5\text{H}_4$  15-membered rings in a polymeric network. (b) Schematic showing the hydrogen bonds between the disilanol and the water molecules ( $\text{X} = \text{H}_2\text{O}$ ).



**Figure 22.** (a) Molecular structure of the tetraferrocenyl disiloxane diol **59**. (b) Formation of the double-chain structure due to intermolecular hydrogen bonding. (c) Schematic showing the nearly parallel orientation of the two chains that form the double chain.

The tetraferrocenyl disiloxanediol  $\text{Fc}_2\text{Si}(\text{OH})-\text{O}-\text{Si}(\text{OH})\text{Fc}_2$  (**59**) forms a hydrogen-bonded double-chain structure.<sup>105</sup> Each chain contains end-to-end-connected disiloxanediol units which alternately flip their orientation as shown in Figure 22. Two such chains, where every disiloxanediol of one chain that is nearly parallel to its counterpart from the other chain, are linked to each other to form the double-chain structure.<sup>105</sup>

The X-ray crystal structure of  $(t\text{-BuO})_2\text{Si}(\text{OH})-\text{O}-\text{Si}(\text{OH})(\text{O}-\text{Bu}-t)_2$  (**61**) shows that the  $\text{Si}-\text{O}-\text{Si}$  angle is nearly linear  $178(1)^\circ$ . Intermolecular aggregation in the solid state is facilitated by the interaction of centrosymmetrically related molecules. Two hydrogen-



**Figure 23.** (a) Molecular structure of the disilanol  $[(t\text{-BuO})_2\text{Si}(\text{OH})]_2\text{O}$  (**61**). (b) Formation of a chain structure due to the  $\text{Si}-\text{OH}$  interacting with the oxygens of the *tert*-butoxy group. (c) Schematic showing the relative orientation of the  $\text{Si}-\text{OH}$ 's forming the  $\text{Si}_2\text{O}_4$  rings.

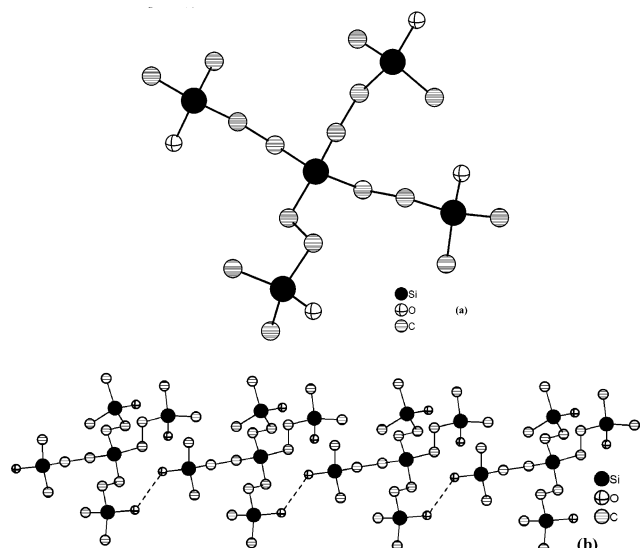
bonding interactions are formed by each molecule, and this leads to formation of a chain structure containing interlinked six-membered chair-shaped  $\text{Si}_2\text{O}_4$  rings (Figure 23). It should be noted that analogous to the monosilanol  $(t\text{-BuO})_3\text{SiOH}$  (**21**), in the case of **61** the *tert*-butoxy oxygen also participates in  $\text{O}-\text{H}\cdots\text{O}$  hydrogen bonding.<sup>19</sup>

Unlike the other cyclic trisilanol **78** and **80** where the three  $\text{Si}-\text{OH}$  groups are in an *all-cis* configuration, the cyclotrisiloxane **82** exists in a *cis-trans-cis* configuration. One of the  $\text{Si}-\text{OH}$  groups interact with the solvated methanol molecule to form a hydrogen-bonded one-dimensional polymeric chain.<sup>113</sup>

The dendrimeric tetrasilanol **91** associates in the solid state through involvement of two  $\text{Si}-\text{OH}$  units, one as a proton donor and the other as a proton acceptor. This leads to generation of a one-dimensional polymeric network (Figure 24).<sup>116a</sup> The  $\text{Si}-\text{OH}$  bond distances observed in this compound, viz., 1.658(6) and 1.668(3) Å, are slightly longer than the distances normally seen in other silanols.

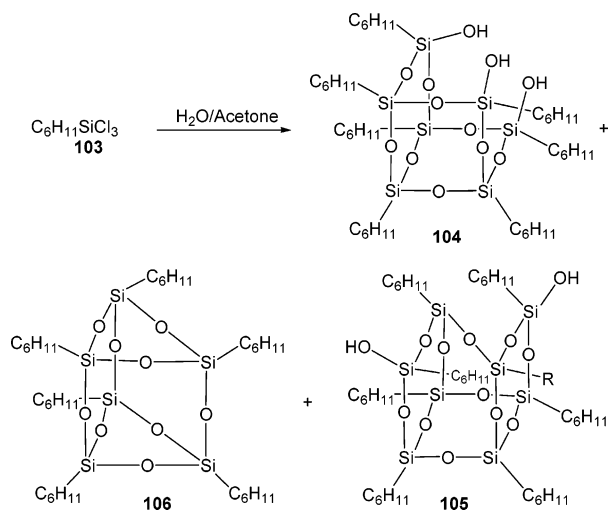
## 5. Silanols Based on Silsesquioxane Frameworks

Incompletely condensed silsesquioxanes containing  $\text{Si}-\text{OH}$  groups have gained considerable prominence in recent years.<sup>100,120,121</sup> These compounds have been shown to be effective homogeneous mimics for zeolites as well as amorphous and mesoporous silica which contain surface silanol sites.<sup>122-124</sup> Also, many of these have been shown to be excellent starting materials for the preparation of a number of metal-



**Figure 24.** (a) View of the dendrimeric tetrasilanol **91**. (b) Proliferation into the polymeric network due to OH...O hydrogen bonds.

### Scheme 28



lasiloxanes,<sup>100</sup> some of which have also found applications in catalysis such as in olefin polymerization. These aspects have been reviewed recently<sup>125,126</sup> and will not be repeated here. The modification of silsesquioxanes and silsesquioxane-based silanols to other silanols will be dealt with here.

### 5.1. Synthesis of Silsesquioxane Silanols

Fehér and co-workers pioneered research efforts to assemble a number of silsesquioxane-based compounds.<sup>100,127,128</sup> A common procedure is the direct hydrolytic condensation of  $C_6H_{11}SiCl_3$  ( $C_6H_{11}$  = cyclohexyl) in acetone (Scheme 28).<sup>127</sup> From here on in this section, unless otherwise stated,  $C_6H_{11}$  will imply a cyclohexyl group and  $C_5H_9$  will imply a cyclopentyl group. Although this method is useful in producing multigram quantities of the silsesquioxanes, it takes a considerable amount of time: the original procedure by Fehér as applied for the hydrolytic condensation of  $C_6H_{11}SiCl_3$  involves a time period of 2–36 months. During this prolonged reaction time it is possible to isolate three main products,  $[(C_6H_{11})_7-$

$Si_7O_9(OH)_3]$  (**104**),  $[(C_6H_{11})_8Si_8O_{11}(OH)_2]$  (**105**) and  $[(C_6H_{11})_6Si_6O_9]$  (**106**). The most important product in this reaction is the silsesquioxane trisilanol **104** containing three favorably placed Si–OH groups. A number of *corner-capping* reactions of this trisilanol are now known with a variety of metal substrates.<sup>100,129,130</sup>

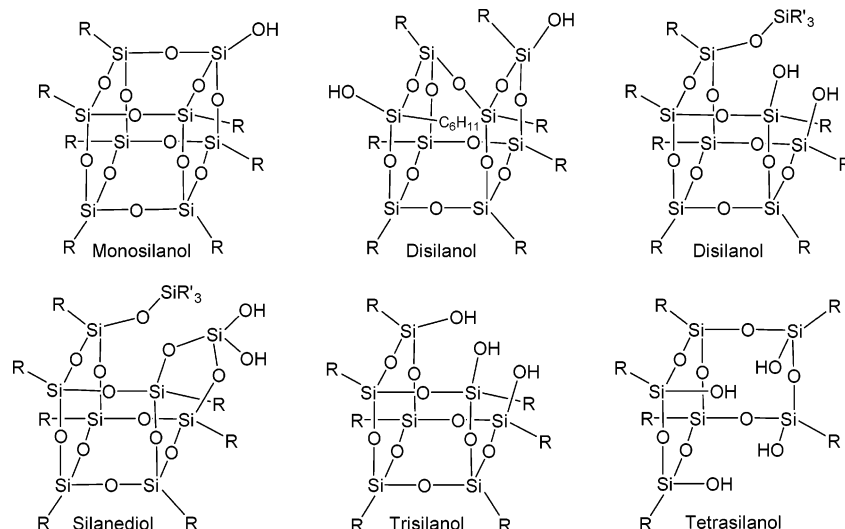
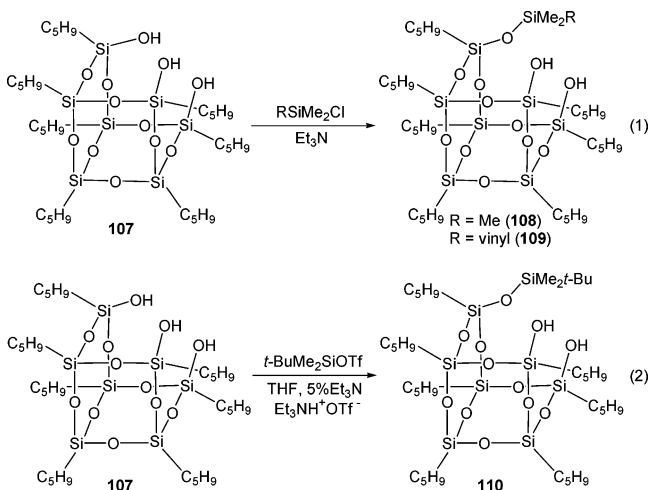
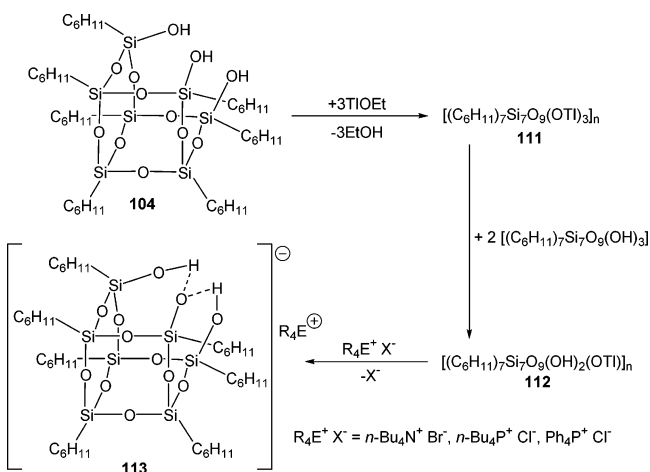
Recently, an alternate method has been developed for the synthesis of silsesquioxane frameworks that contain Si–OH groups. This is accomplished by the selective and controlled cleavage of the more readily available completely condensed silsesquioxanes. Fehér and co-workers successfully demonstrated this strategy by use of an acid<sup>131,132</sup> or a base<sup>133</sup> to produce incompletely condensed silsesquioxanes with inversion or retention of stereochemistry at the silicon center. Typical examples of silanols supported on incompletely condensed silsesquioxanes are listed in Chart 7.

Among various silsesquioxanes, the trisilanols of the type  $R_7Si_7O_9(OH)_3$  [ $R = C_6H_{11}$  (**104**),  $C_5H_9$  (**107**)] are the most studied compounds. One or more –OH groups of the trisilanol can be selectively protected by the silyl-protecting functions such as  $SiMe_3$ ,  $SiMe_2t-Bu$ , or  $SiMe_2Ph$ .<sup>134</sup> In general, these silylation reactions are sluggish in the absence of a base. When the trisilanol  $(C_5H_9)_7Si_7O_9(OH)_3$  (**107**) is treated with trimethyl chlorosilane<sup>135</sup> or vinyltrimethyl chlorosilane<sup>136</sup> in the presence of an excess of  $Et_3N$ , the corresponding disilanols  $(C_5H_9)_7Si_7O_9(OSiMe_3)(OH)_2$  (**108**) and  $(C_5H_9)_7Si_7O_9(OSiMe_2CH=CH_2)(OH)_2$  (**109**) are produced. The TBDMS (*tert*-butyldimethylsilyl) derivative of the disilanol  $(C_5H_9)_7Si_7O_9(OSiMe_2t-Bu)(OH)_2$  (**110**)<sup>137</sup> is obtained by reaction of **107** with TBDMS triflate (Scheme 29). Thus, such procedures are useful in conversion of trisilanols to disilanols as well as to monosilanols. All three types of derivatives can be further used to prepare metal-containing oligosilsesquioxanes.

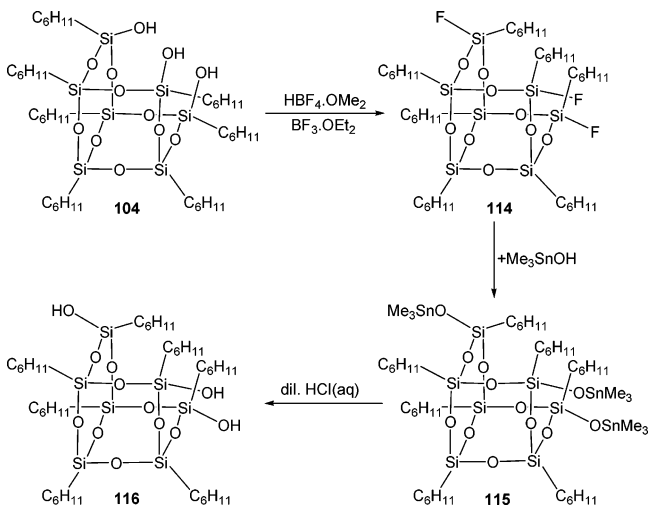
An interesting example of an incompletely condensed anionic silsesquioxane has been obtained by reaction of the trisilanol **104** with thallium(I) ethoxide. This reaction initially produces a thallium ester  $[(C_5H_9)_7Si_7O_9(OTl)_3]_n$  (**111**), which on subsequent reaction with two more equivalents of the trisilanol **104** gives the comproportionation product  $[(C_5H_9)_7Si_7O_9(OH)_2(OTl)]_n$  (**112**). The final monoanionic silsesquioxane **113** is obtained by addition of  $[Ph_4P]Cl$ ,  $[n-Bu_4P]Cl$ , or  $[n-Bu_4N]Br$  (Scheme 30).<sup>138</sup>

An inversion of stereochemistry at the silicon can be observed on reaction of a strong acid such as  $HF_4$  with the trisilanol  $(C_6H_{11})_7Si_7O_9(OH)_3$ . Thus, reaction of **104** with  $HF_4 \cdot OMe_2$  leads to formation of the corresponding trifluoro derivative **114**. Interestingly, acid treatment of the trisilanol does not lead to dehydration or formation of a salt. The trifluoride **114** is found to be resistant to direct hydrolysis with water and pyridine. An interesting strategy has been devised to overcome this problem.

Thus, reaction of **114** with  $Me_3SnOH$  affords the trimethylstannoxy derivative,  $(C_6H_{11})_7Si_7O_9(OSnMe_3)_3$  (**115**). Hydrolysis of **115** with aqueous hydrochloric acid leads to the trisilanol **116** (Scheme 31).<sup>131</sup> The only difference between trisilanols **104** and **116** is the

**Chart 7. Various Types of Silsesquioxane-Based Silanols**

**Scheme 29**

**Scheme 30**


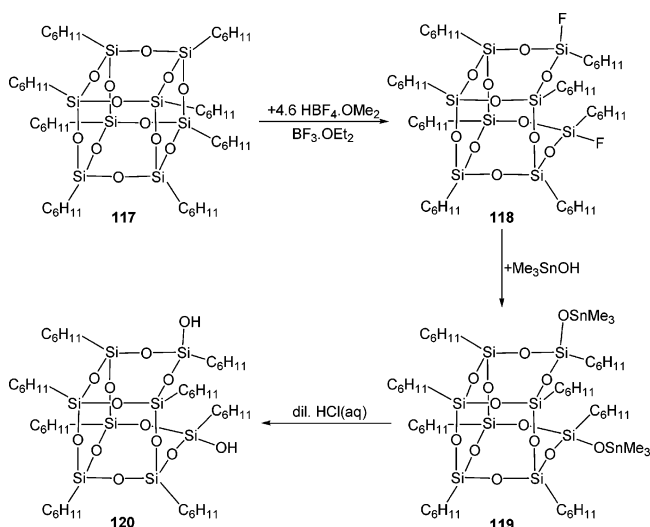
relative orientation of the three  $\text{-OH}$  groups. It is believed that the initial attack of the protic acid  $\text{HBF}_4$  causes an inversion of stereochemistry at the silicon centers. Subsequent reactions including hydrolysis proceed with the retention pathway. This leads to the final trisilanol **116** having an opposite orientation of the three  $\text{Si-OH}$  groups in comparison to the starting compound **104**.

**Scheme 31**


Selective *framework cleavage* reactions can also be performed with  $\text{HBF}_4$ . The fully condensed octameric silsesquioxane **117** can be selectively cleaved by  $\text{HBF}_4 \cdot \text{OMe}_2$  in the presence of  $\text{BF}_3 \cdot \text{OEt}_2$  to give the corresponding difluoro derivative **118**. This on further treatment with  $\text{Me}_3\text{SnOH}$  leads to the formation of bis(trimethylstannoxy) derivative **119** which upon hydrolysis with aqueous  $\text{HCl}$  gives the corresponding octameric disilanol  $(\text{C}_6\text{H}_{11})_8\text{Si}_8\text{O}_{11}(\text{OH})_2$  **120** (Scheme 32).<sup>139</sup>

Triflic acid can also influence the *framework cleavage* reactions. Thus, the fully condensed octameric silsesquioxane **117** reacts with an excess of triflic acid to give the open-framework ditriflate compound possessing either structure **121** or **122**. The ditriflate readily undergoes hydrolysis in the presence of triethylamine to afford the disilanol  $(\text{C}_6\text{H}_{11})_8\text{Si}_8\text{O}_{11}(\text{OH})_2$  **123** (Scheme 33).<sup>139</sup> A stereochemical inversion has also been observed in this reaction. Generally, inversion at silicon center is observed when good leaving groups are replaced by poor nucleophiles while retention is favored when poor leaving groups are replaced by hard nucleophiles.<sup>140</sup> Since the triflate moiety ( $\text{CF}_3\text{SO}_3^-$ ) is a better leaving group and water is a poor nucleophile both the steps viz., attack of the triflate ion as well as hydrolysis by water are believed

## Scheme 32



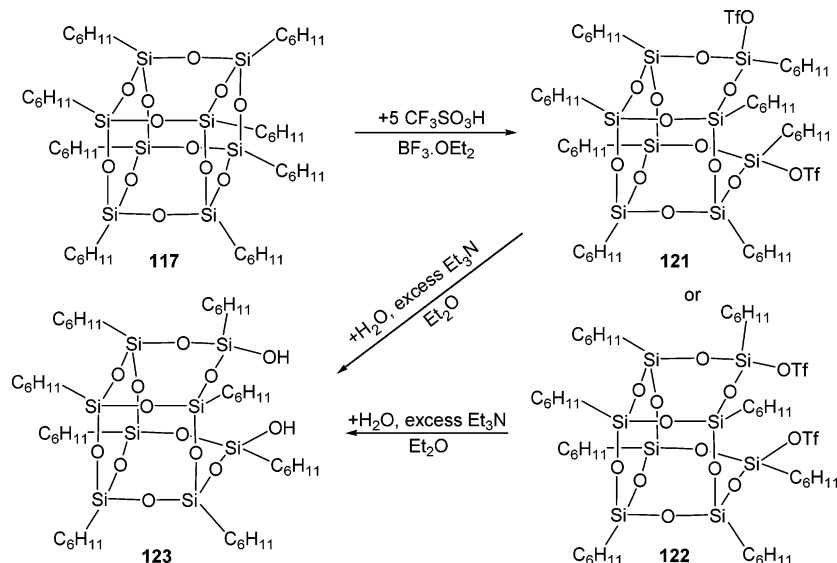
to proceed with complete inversion of stereochemistry at silicon. A triflic-acid-mediated double-cleavage reaction of the fully condensed silsesquioxane **117** has also been observed to afford disilanol of the type **105**.<sup>141</sup>

A double-framework cleavage reaction has also been performed with the fully condensed hexameric silsesquioxane framework ( $c\text{-C}_6\text{H}_{11}$ )<sub>6</sub>Si<sub>6</sub>O<sub>9</sub> **106** with triflic acid. Here, upon cleaving one of the Si–O–Si edges of the silsesquioxane polyhedron, a monotriflate **124** is formed. The latter is converted through the intermediacy of **125** and **126** into the ditriflate **127**. Hydrolysis of **127** affords the disilanol **128** (Scheme 34).<sup>142</sup>

Base-mediated cleavage of the fully condensed octameric silsesquioxanes **117**, **129**, **130**, and **131** leads to assembly of the trisilanols **104** and **132**. Intermediate products containing two (**133**) and three (**134**) Si–OH groups are also isolated in this reaction. However, with time these are also finally converted to the trisilanols **104** and **132** (Scheme 35).<sup>133</sup>

Hexameric silsesquioxane ( $\text{C}_6\text{H}_{11}$ )<sub>6</sub>Si<sub>6</sub>O<sub>9</sub> (**68**) undergoes a homologation and is converted to the

## Scheme 33



heptameric trisilanol **104** upon base-mediated partial hydrolysis (Scheme 36). The tetrasilanol **135** is implicated as an intermediate in this process.<sup>143</sup>

Homologation of **106** also occurs by reaction with vinyltrimethoxysilane followed by treatment with tetraethylammonium hydroxide and hydrochloric acid to afford the vinyl-group-attached trisilanol **136** (Scheme 37).<sup>143a</sup>

Reaction of  $\text{Et}_4\text{NOH}$  with the spherosilicate ( $\text{Me}_3\text{-SiO}$ )<sub>8</sub>Si<sub>8</sub>O<sub>9</sub> (**137**) also produces the tetrasilanol **138** (Scheme 38).<sup>143b</sup>

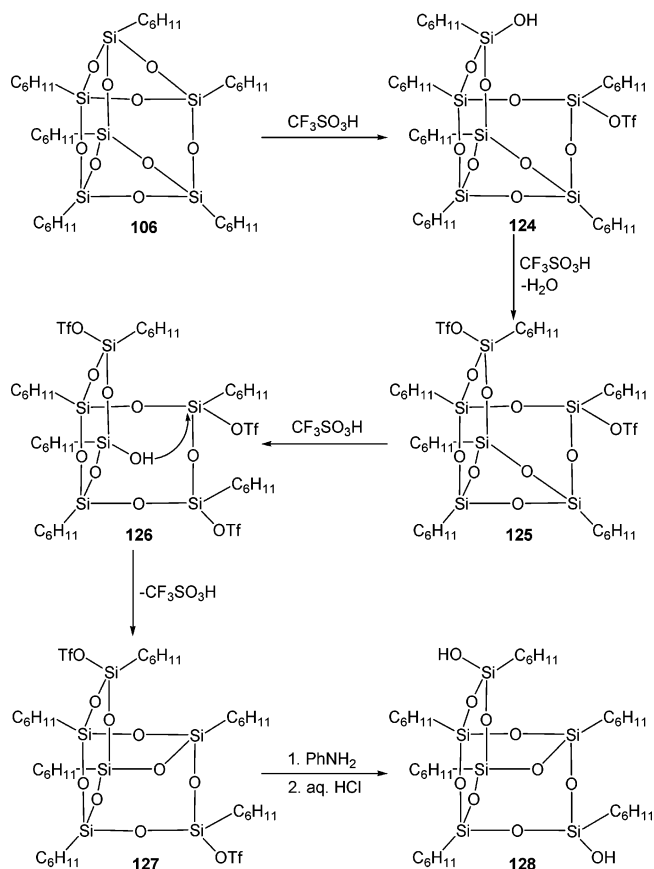
Increasing the steric bulk on the starting silicon compound results in formation of silsesquioxanes containing less silicon atoms. Thus, reaction of the triisopropylphenyl silanetriol **81** with diethylamine in the presence of 2-chloro-1,3-dimethylimidazolium chloride (DMC) as the dehydrating agent leads to formation of the pentameric silsesquioxane-based silanol  $\text{R}_5\text{Si}_5\text{O}_7(\text{OH})$  (**139**).<sup>113</sup>

Interesting examples of silsesquioxane-based silanediols have recently been prepared by a two-step process as illustrated in Scheme 40. Reaction of equimolar amounts of monosilylated trisilanols **108**, **109**, and **140** with  $\text{SiCl}_4$  in the presence of triethylamine affords the geminal dichloro compounds **141**, **142**, and **143**. These chlorides readily undergo hydrolysis by addition of water to give the corresponding geminal silanediols **144**, **145**, and **146**. Both the geminal dichlorides and the geminal disilanol exist as exo and endo isomers with respect to silyl ether ( $\text{OSiR}_2\text{R}'$ ) group.<sup>144</sup>

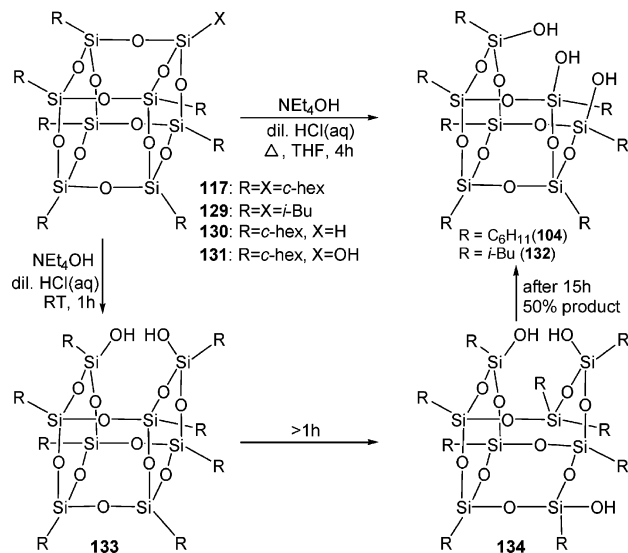
The geminal silanediol **146**, although stable in the solid state, undergoes a self-condensation reaction in *n*-heptane at room temperature to afford the siloxane-linked bis-oligosilsesquioxane **147**. On the other hand, compounds **144** and **145** are converted to the closed ring monosilanol **148** (Scheme 41).<sup>144</sup> The temperatures used for these condensations of the geminal silanols (**144** and **145**) are much lower than those observed for the dehydroxylation of vicinal silanols  $\text{R}_7\text{Si}_7\text{O}_9(\text{OH})_2\text{OR}'$  ( $\text{R} = \text{C}_5\text{H}_9$ ,  $\text{C}_6\text{H}_{11}$ ;  $\text{R}' = \text{H}$ ,  $\text{SiMe}_3$ ,  $\text{SbMe}_4$ ) to yield the condensed compound  $\text{R}_7\text{-Si}_7\text{O}_{10}(\text{OR}')$ . In addition to higher temperatures, the



## Scheme 34



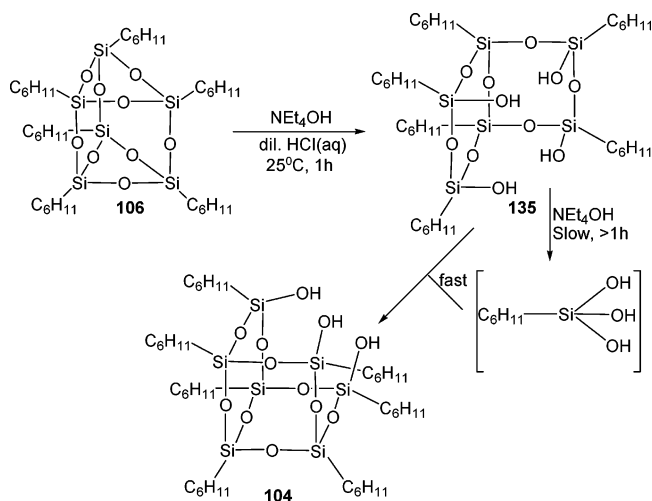
## Scheme 35



vicinal silanols require dehydrating agents as well in order for the condensation to proceed.<sup>127,129</sup> It is interesting to note that siliceous materials used for supporting transition metals need a calcinating temperature as high as 500 °C to form isolated surface silanols.<sup>145</sup>

Synthesis of aluminosilsesquioxanes **149** and **150** that model Brønsted-acidic aluminum sites in aluminosilicates and zeolites is shown in Scheme 42.<sup>146a,b</sup> Reaction of the monosilylated disilanols  $(\text{C}_5\text{H}_9)_7\text{Si}_7\text{O}_9(\text{OSiR}_2\text{R}')(\text{OH})_2$  (**108** and **140**) with trimethyl aluminum in a 2:1 ratio yields the aluminosilsesquioxanes **149** and **150**.

## Scheme 36



These compounds contain a free Si–OH group that forms intramolecular hydrogen bonds with the neighboring silyl ether moiety. Although the presence of hydrogen bonding reduces the Brønsted acidity of **149** and **150**, they are more acidic than the aluminum-free silsesquioxanes. Hence, the former undergo a rapid deprotonation compared to their tri- and disilanol precursors  $(\text{C}_5\text{H}_9)_7\text{Si}_7\text{O}_9(\text{OH})_3$  (**107**) and  $(\text{C}_5\text{H}_9)_7\text{Si}_7\text{O}_9(\text{OSiR}_2\text{R}')(\text{OH})_2$  (**108**, **140**).<sup>146a</sup>

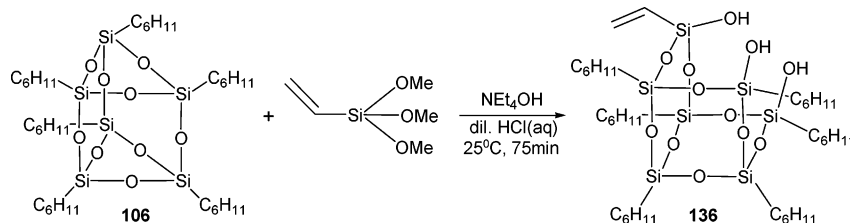
5.2. <sup>29</sup>Si NMR

<sup>29</sup>Si NMR has been extremely valuable in monitoring the course of the reactions of oligosilsesquioxanes and for structural determination of the products as well. In general, the number of <sup>29</sup>Si NMR signals and their relative intensities has been used as a major guide line in addition to the chemical shift differences. For example, in  $(\text{C}_6\text{H}_{11})_7\text{Si}_7\text{O}_9(\text{OH})_3$  (**104**) every silicon center has a  $\text{CO}_3$  environment and hence the chemical shift differences are not expected to be considerable. However, it is noticed that the terminal Si–OH resonate at –60.1 ppm, which is about 9 ppm downfield in comparison to their three neighboring silicon centers (–69.5 ppm).<sup>127</sup> The corner and unique silicon resonates at –67.9 ppm (entry 1, Table 5). This trend is also noticed in the tetrasilanol **135** (entry 11, Table 5). Modification of the terminal silicons leads to appropriate diagnostic changes in their <sup>29</sup>Si NMR values as well as changes in the number of resonances observed. For example, in vinyl trisilanol **136** one can readily see the presence of five resonances in the anticipated ratio of 2:1:2:1:1. In this example the most downfield signals are due to the Si–OH centers connected to the cyclohexyl groups. On the other hand, the Si–OH containing the vinyl group moves upfield to –71.9 ppm.<sup>143a</sup> Data for other silsesquioxane silanols are given in Table 5.

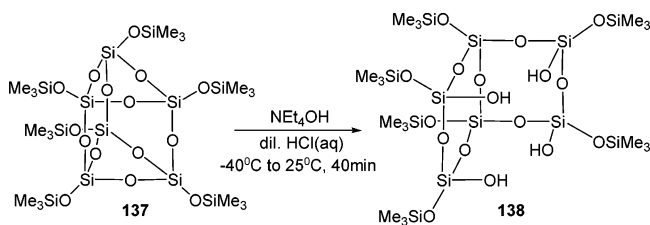
## 5.3. X-ray Structures of Silsesquioxane Silanols

X-ray structural data of silsesquioxane silanols are summarized in Table 6. Although a large number of silsesquioxane-based silanols are known, the number of X-ray crystal structures in this family is rather limited. It has been reported that in many instances

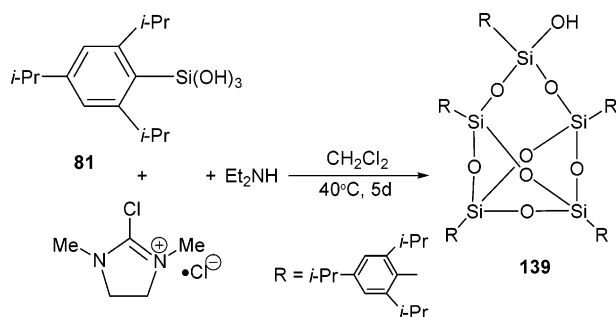
## Scheme 37



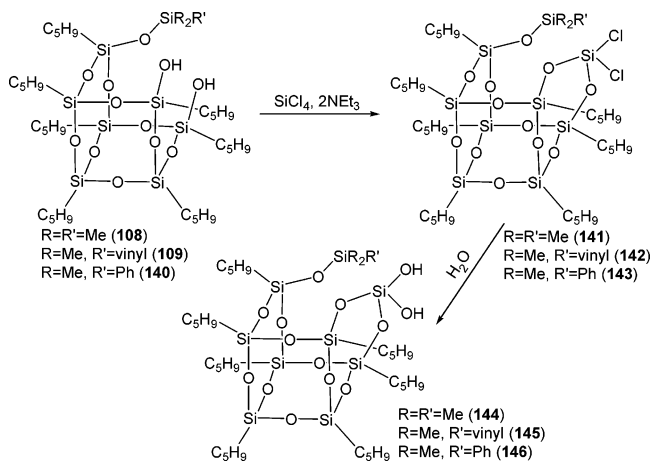
## Scheme 38



## Scheme 39



## Scheme 40

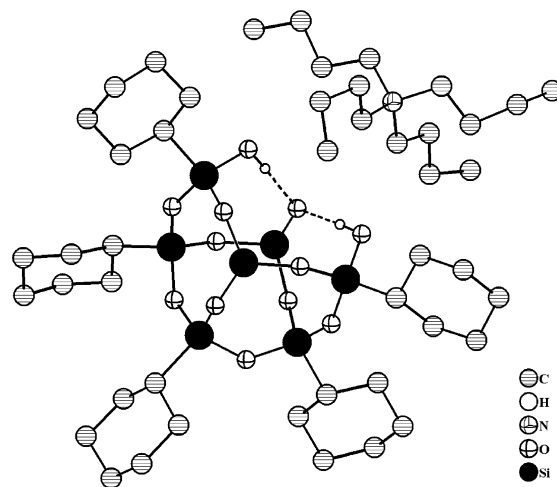


crystals of the compounds of this family diffract poorly and hence good-quality X-ray structures are limited. In addition, many members of this family are sensitive toward moisture. Among the various compounds listed in Table 6, it is noted that for compound **132** (entry 5, Table 6) the X-ray data is not of a good quality for detailed analysis. Hence, no discussion is attempted of this structure except to note that the Si–O bond distances are in the normal range observed for other silanols.<sup>133</sup>

Compound **113** is a formally deprotonated derivative of the trisilanol (*c*-C<sub>6</sub>H<sub>11</sub>)<sub>7</sub>Si<sub>7</sub>O<sub>9</sub>(OH)<sub>3</sub>. Its X-ray structure shown in Figure 25 reveals strong intramolecular hydrogen bonding between the two Si–OH moieties and the deprotonated Si–O unit.<sup>138</sup> The Si–

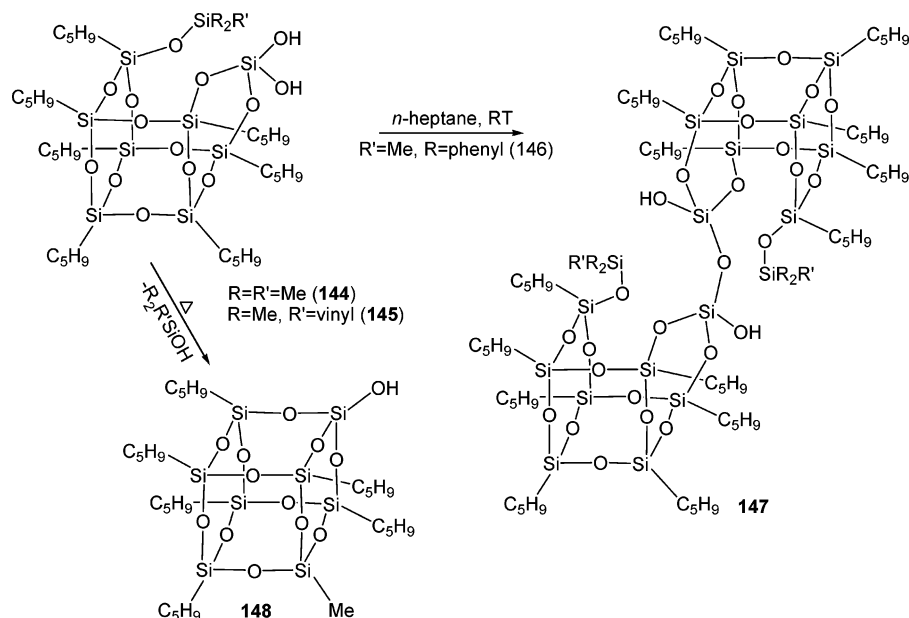
OH distances are 1.587(4) and 1.619(5) Å, respectively, while the Si–O<sup>−</sup> distance is 1.588(3) Å. The hydrogen bonding present in this compound is quite linear but unsymmetrical with one short (0.88–0.89 Å) and one long (1.68–1.79 Å) distance. The inter O···O contacts for the hydrogen-bonded oxygen atoms are 2.571(8) and 2.577(1) Å, respectively. Overall the structure of **113** is monomeric, and this is in contrast to the parent trisilanol **104** where a dimeric structure is found in the solid state.<sup>127</sup> The disiloxane-linked bis(silsesquioxane) **147** is also monomeric. Surprisingly, this compound does not show any intra- or intermolecular hydrogen-bonding interactions. In this compound the Si–O–Si angle corresponding to the bridging disiloxane motif is very nearly linear (171.4(2)°) (Figure 26).<sup>144</sup>

The monosilylated silsesquioxane derivatives (*c*-C<sub>5</sub>H<sub>9</sub>)<sub>7</sub>Si<sub>7</sub>O<sub>9</sub>(OH)<sub>2</sub>(OR) (R = SiMe<sub>3</sub>, **108**; R = SiMe<sub>2</sub>*t*-Bu, **110**) are both dimeric in the solid state (Figures 27 and 28). The asymmetric unit of **108** as well as **110** contains two molecules. In **108** the two molecules in the asymmetric unit are hydrogen bonded to their neighbors, while in **110** the two molecules within the asymmetric unit are hydrogen bonded to each other. Further, in **108** two types of dimers are formed: one of them contains two cyclic O<sub>2</sub>H<sub>2</sub> rings while the other contains two linear O–H···O bonds (Figure 27).<sup>135</sup> The metric parameters involved for these interactions are quite strong and similar to the situation found for other silanols. In **110** a four-membered O<sub>4</sub> ring holds two molecules together (Figure 28).<sup>137</sup> Interestingly, in both **108** as

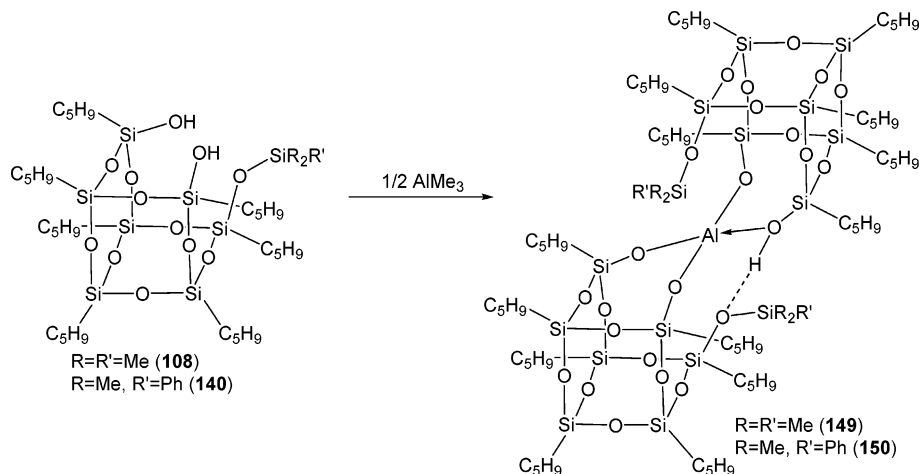


**Figure 25.** Molecular structure of the deprotonated trisilanol **113**. The tetra-*n*-butylammonium cation stabilizes the anionic cage structure. The intramolecular hydrogen bonds are shown as the dotted lines. Two of the seven *c*-C<sub>6</sub>H<sub>11</sub> groups are omitted for clarity.

Scheme 41

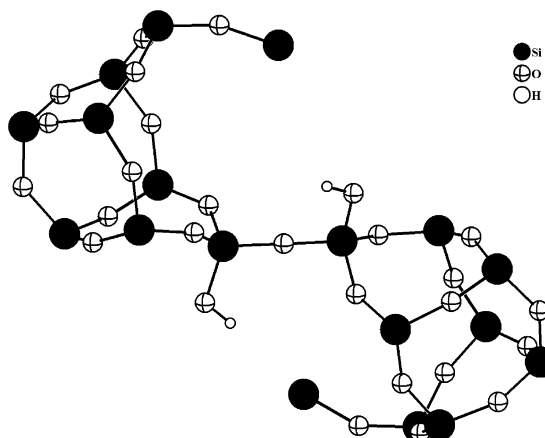


Scheme 42



well as **110** no other oxygen centers are involved in hydrogen-bonding interactions.

The pentameric silsesquioxane silanol **139** also has a similar type of a dimeric structure. The asymmetric unit contains only one molecule, and the hydrogen-



**Figure 26.** Molecular structure of the bis(silsesquioxane silanol) **147**. The *c*-C<sub>5</sub>H<sub>9</sub> and SiMe<sub>2</sub>Ph groups are omitted for clarity.

bonding interaction in this molecule leads to formation of a cyclic four-membered ring similar to that observed in **108** and **110**.<sup>113</sup>

The disilanol **128** has a polymeric-sheet-like structure. The relative orientation of the two Si–OH units makes it difficult for intramolecular hydrogen bonding. Therefore, adjacent molecules interact with each other to generate cyclic O<sub>2</sub>H<sub>2</sub> rings that hold the polymer together (Figure 29).<sup>142</sup>

#### 5.4. Silanols at the Silica Surfaces

Hofmann et al. in 1934 proposed that the unsaturated surface valencies of the silica are satisfied by the chemisorption of water, thereby resulting in the formation of covalently bound hydroxyl groups on silica.<sup>147a</sup> Over the years it has been suggested that a large variety of silanol motifs are present on the silica surfaces.<sup>147b</sup> Depending upon the relative positions of the individual Si–OH groups, they are classified as vicinal silanols, geminal silanols, and isolated silanols (Chart 8).

It has been found that a maximum of 4.9 Si–OH groups are present per square nanometer of silica

Table 5.  $^{29}\text{Si}$  NMR Data for Silsesquioxane-Based Silanols

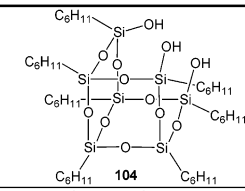
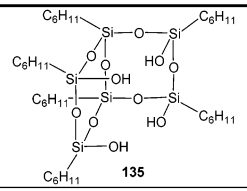
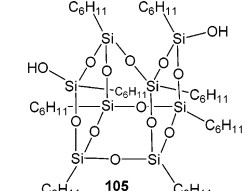
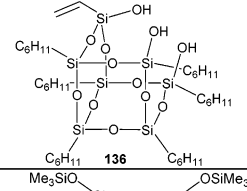
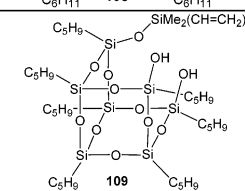
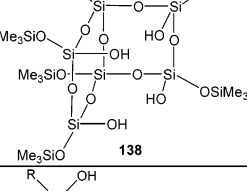
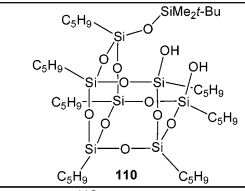
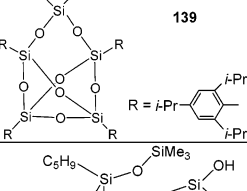
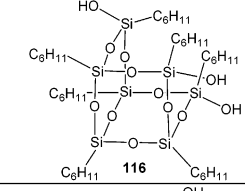
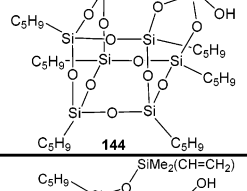
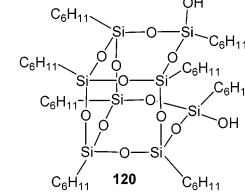
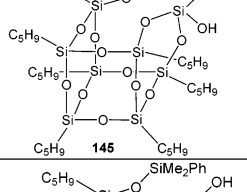
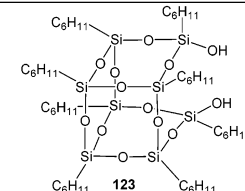
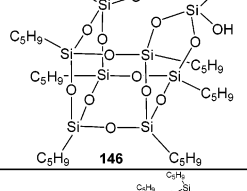
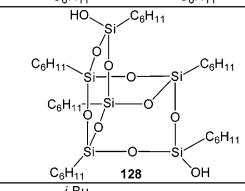
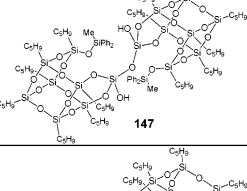
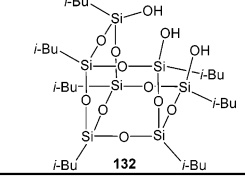
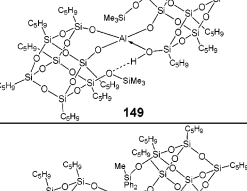
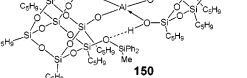
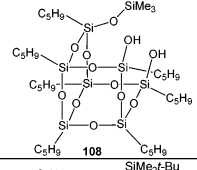
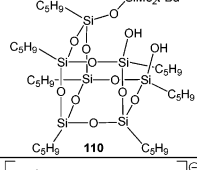
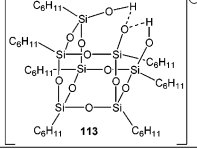
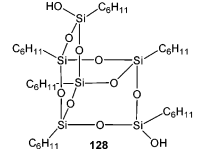
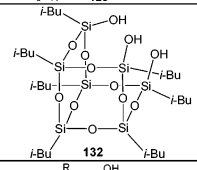
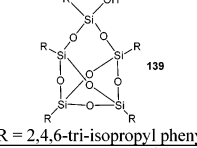
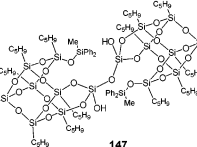
S.No.	Compound	Coordination Environment around Silicon	$^{29}\text{Si}$ NMR (ppm)	Ref.	S.No.	Compound	Coordination Environment around Silicon	$^{29}\text{Si}$ NMR (ppm)	Ref.
1	 104	$\text{CO}_3$	-60.1, -67.9, -69.5 (3:1:3)	127	11	 135	$\text{CO}_3$	-59.4, -68.8 (4:2)	143a
2	 105	$\text{CO}_3$	-58.4, -65.6, -67.5, -68.5 (2:2:2:2)	127	12	 136	$\text{CO}_3$ (Cy-Si-OH) $\text{CO}_3$ $\text{CO}_3$ (Vinyl-Si-OH)	-60.0 -68.1 (s, 1Si), -69.0 (s, 2Si), -69.6 (s, 1Si), -71.9 (2:1:2:1:1)	143a
3	 109	$\text{C}_3\text{O}$ $\text{CO}_3$	-1.0 -56.7, -65.5, -66.4, -67.4 (1:2:2:1:2)	136	13	 138	$\text{CO}_3$	-59.4, -68.8 (4:2)	143b
4	 110	$\text{C}_3\text{O}$ $\text{CO}_3$	-- -53.2, -56.1, -62.9, -63.7, -65.9, -66.8 (1:2:1:1:2:1)	137	14	 139 R = <i>i</i> -Pr	$\text{CO}_3$	-59.34, -67.55, -68.21	113
5	 116	$\text{CO}_3$	-58.8, -67.3, -68.2 (3:1:3)	131	15	 144	$\text{C}_3\text{O}$ $\text{CO}_3$ $\text{O}_4$	11.2 -64.8, -65.1, -65.3, -66.3, -67.3 (1:1:1:2:2) -89.4	144
6	 120	$\text{CO}_3$	-56.8, -67.3, -68.4 (1:1:2)	139	16	 145	$\text{C}_3\text{O}$ $\text{CO}_3$ $\text{O}_4$	-0.7 -64.9, -65.1, -65.3, -66.4, -67.3 (1:1:1:2:2) -89.4	144
7	 123	$\text{CO}_3$	-59.8, -67.58, -6.8 (2:2:4)	139	17	 146	$\text{C}_3\text{O}$ $\text{CO}_3$ $\text{O}_4$	-10.7 -65.0, -65.2, -65.8, -66.3, -67.5 (1:1:1:2:2) -89.4	144
9	 128	$\text{CO}_3$	-55.2, -61.7, -61.9 (2:2:2)	142	18	 147	$\text{C}_3\text{O}$ $\text{CO}_3$ $\text{O}_4$	-10.2 -65.0, -65.0, -65.8, -66.1, -67.8 (1:1:1:2:2) -97.7	144
10	 132	$\text{CO}_3$	-58.5, -66.9, -68.3 (3:1:3)	133	19	 149	$\text{C}_3\text{O}$ $\text{CO}_3$	8.0, 7.9 -58.7, -62.0, -63.4, -64.5, -65.1, -65.1, -65.2, -66.2, -66.4, -67.0, -67.3, -67.5, -68.3, -65.4	146a
					20	 150	$\text{C}_3\text{O}$ $\text{CO}_3$	-9.8 -67.4, -66.9, -64.6, -65.2, -63.5 (1:1:1:2:2)	146b

Table 6. X-ray Structural Data for Silsesquioxane-Based Silanols

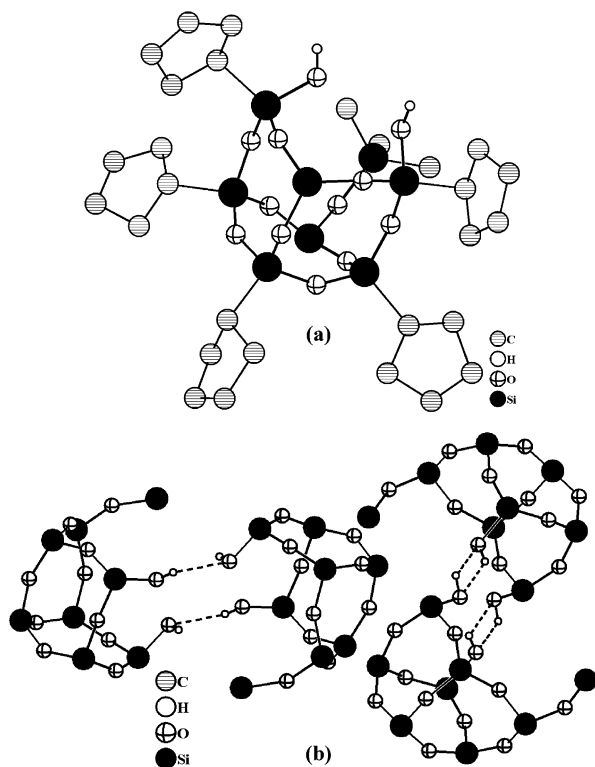
S.No.	Compound	Hydrogen bonding parameters				Structural Summary	Ref.
		Si-OH (Å)	OH...O (Å)	O...O (Å)	O-H...O (°)		
1		1.650(1), 1.652(8)	1.998(1), 2.037(9)	2.659(1), 2.663(1)	131.91(5), 136.21(6)	Dimeric structure	135
2		1.641(7), 1.647(8)	-	2.639(1)- 2.749(9)	-	Dimeric structure	137
3		1.587(4), 1.619(5)	1.680(5)- 1.695(5) (intra)	2.571(8)- 2.577(1)	175.44(5)- 177.53(5)	Monomeric structure	138
4		1.632(5)	1.057(3)	2.787(4)	144.97(2)	polymeric chain	142
5		1.634(8) - 1.641(9)	-	-	-	-	133
6		1.618(4)	2.489(4), 2.546(4)	2.907(3), 3.058(5)	105.60(1), 157.92(1)	Dimeric structure	113
7		1.609(2), 1.620(3)	-	-	-	Monomeric structure	144

surface.<sup>147c</sup> It has also been observed that by raising the temperature the concentration of silanols on these silica surfaces can be altered. Thus, heating a sample of silica in vacuo results in dehydration of Si-OH groups, thereby producing siloxane bridges. Surface silanols of types **A** and **B** are more susceptible to self-condensation upon heating, and hence, it is difficult to differentiate these three types of silanols. Since the isolated silanols **C** tend to withstand the extensive heating of the silica, their properties can be well studied.<sup>148a,b</sup> The surface properties of these porous materials have been studied by various techniques such as FT-IR, Raman, diffuse-IR, total reflectance-IR, photoacoustic-IR, and solid-state NMR spectroscopy. Although both qualitative and quantitative information has been obtained by these spectroscopic methods, they are bulk measurements and provide inaccurate data of the local surface properties.<sup>148a,b</sup> Hence, silsesquioxane model systems have been quite handy in terms of understanding the binding and catalytic properties of the silica surfaces.<sup>126</sup> The types of surface silanols

depicted in Chart 8 can easily be compared with the various silsesquioxane silanols described earlier.

## 6. Silanediols and Other Compounds Containing Si(OH)<sub>2</sub> Units

Silanediols are compounds that contain two hydroxyl groups attached to the same silicon center. Unlike in carbon where ketones are thermodynamically more stable in comparison to the C(OH)<sub>2</sub>-containing geminal diols, in the case of silicon the reverse is true. For example, the silanones R<sub>2</sub>Si=O are unstable<sup>1</sup> in comparison to the cyclic or polymeric derivatives [R<sub>2</sub>SiO]<sub>n</sub> and also with respect to the silanediols R<sub>2</sub>Si(OH)<sub>2</sub>. Consequently, a fairly large number of silanediols are known [e.g., Et<sub>2</sub>Si(OH)<sub>2</sub>,<sup>149</sup> (allyl)<sub>2</sub>Si(OH)<sub>2</sub>,<sup>150</sup> *t*-Bu<sub>2</sub>Si(OH)<sub>2</sub>,<sup>151</sup> *n*-Bu<sub>2</sub>Si(OH)<sub>2</sub>,<sup>21</sup> *i*-Pr<sub>2</sub>Si(OH)<sub>2</sub>,<sup>47,150</sup> *i*-Bu<sub>2</sub>Si(OH)<sub>2</sub>,<sup>47</sup> (*o*-tolyl)<sub>2</sub>Si(OH)<sub>2</sub>,<sup>47</sup> (*c*-C<sub>6</sub>H<sub>11</sub>)<sub>2</sub>Si(OH)<sub>2</sub>,<sup>94</sup> Ph<sub>2</sub>Si(OH)<sub>2</sub>,<sup>152</sup> (*p*-Cl-C<sub>6</sub>H<sub>4</sub>)<sub>2</sub>Si(OH)<sub>2</sub>,<sup>152</sup> (*p*-F-C<sub>6</sub>H<sub>4</sub>)<sub>2</sub>Si(OH)<sub>2</sub>,<sup>152</sup> EtMeSi(OH)<sub>2</sub>,<sup>21</sup> PhMeSi(OH)<sub>2</sub>,<sup>21,153</sup> *t*-BuPhSi(OH)<sub>2</sub>,<sup>4</sup> (C<sub>5</sub>Me<sub>5</sub>)<sub>2</sub>Si(OH)<sub>2</sub>,<sup>154</sup>



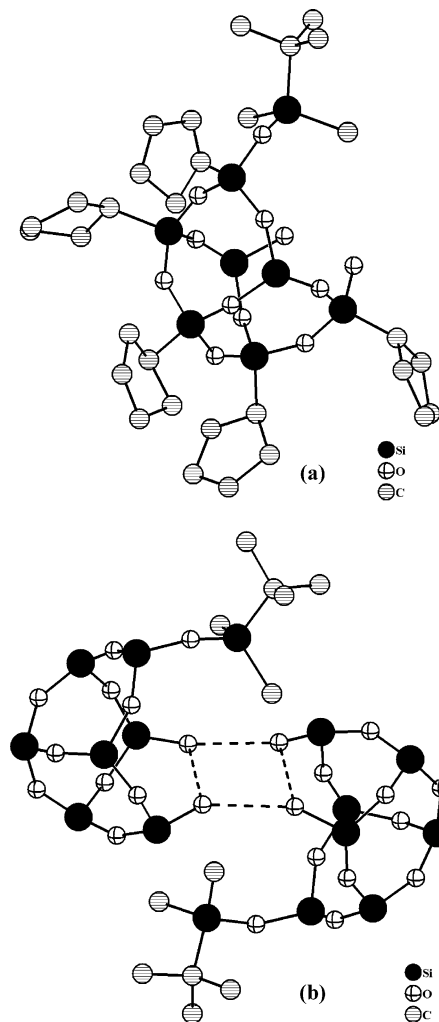
**Figure 27.** (a) DIAMOND picture of the trimethylsilyl derivative **108**. (b) Formation of linear and cyclic dimers as a result of hydrogen bonding in the solid state. The carbon atoms are omitted for clarity.

$(\text{SiMe}_3)_3\text{CSiPh}(\text{OH})_2$ ,<sup>59</sup>  $(\text{SiMe}_3)_3\text{CSi}(\text{O}_2\text{CCF}_3)(\text{OH})_2$ ,<sup>4</sup>  $\text{Cp}^*(\text{CO})_2(\text{PMe}_3)\text{WSi}(\text{OH})_2$ ,<sup>61</sup> etc.].

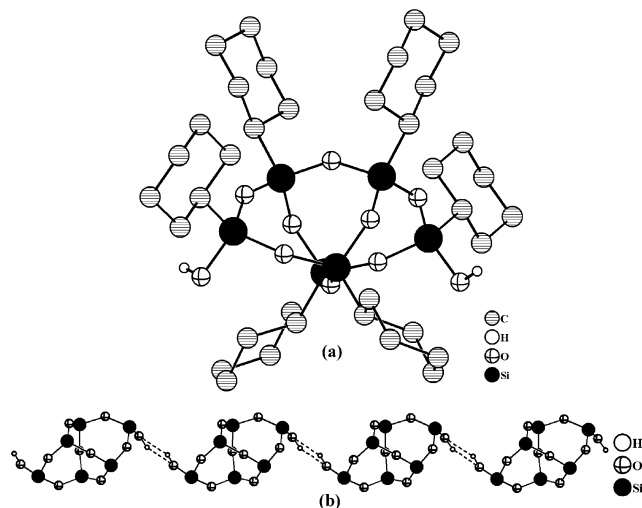
### 6.1. Synthesis of Silanediols Containing One or Two $\text{Si}(\text{OH})_2$ Groups

An aryl-hydrido-silanediol, 2,6-Mes<sub>2</sub>C<sub>6</sub>H<sub>3</sub>(H)Si(OH)<sub>2</sub> **152**, containing the highly sterically encumbered 2,6-dimesitylphenyl substituent has been synthesized from its chloro analogue **151** by hydrolysis. It was found that a base was not required in this reaction (Scheme 43).<sup>155</sup>

A series of ferrocenyl-containing silanediols have been prepared by hydrolysis of the corresponding chlorides (Scheme 44). Reaction of monolithioferrocene with  $\text{RSiCl}_3$  (R = Me, 2-propenyl allyl, *t*-Bu, Ph, *c*-Hex) afforded the mixed substituent containing silicon dichlorides  $(\text{Fc})(\text{R})\text{SiCl}_2$  (**153**–**157**). The dichloride  $(\text{Fc})(n\text{-Bu})\text{SiCl}_2$  (**158**) was prepared by a two-step process. Reaction of the 1,1'-dilithioferrocene with *n*-BuSiCl<sub>3</sub> afforded the ferrocenophane  $[(\eta^5\text{-C}_5\text{H}_4)_2\text{Fe}]\text{-Si}(n\text{-Bu})(\text{Cl})$ . Treatment of this compound with HCl afforded **158**. Hydrolysis of the silcondichlorides in the presence of triethylamine afforded the corresponding silanediols  $(\text{Fc})(\text{R})\text{Si}(\text{OH})_2$  (**159**–**164**) as yellow solids.<sup>156</sup> Diferrocenyl silanediol  $\text{Fc}_2\text{Si}(\text{OH})_2$  (**58**) has been prepared by Manners and co-workers in a multistep synthesis (eq 2, Scheme 44).<sup>157</sup> Reaction of  $\text{SiCl}_4$  with 1,1'-dilithioferrocene affords the highly strained bis-ferrocenophane  $[(\eta^5\text{-C}_5\text{H}_4)_2\text{Fe}]_2\text{Si}$  (**165**). Relief of the ring strain drives the reaction of this ferrocenophane to  $\text{Fc}_2\text{SiCl}_2$  (**1**) upon addition of



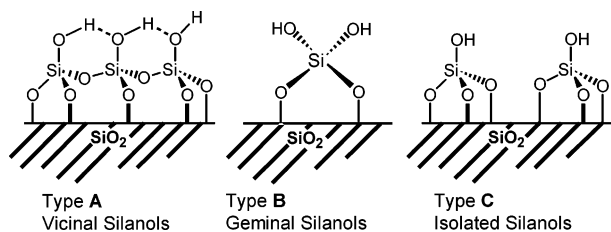
**Figure 28.** (a) DIAMOND picture of the *tert*-butyl dimethyl silyl derivative **110**. (b) Formation of a hydrogen-bonded cyclic four-membered O<sub>4</sub> ring between the two molecules of the asymmetric unit.



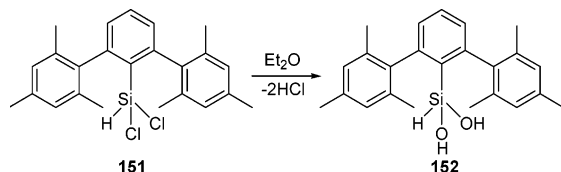
**Figure 29.** (a) X-ray crystal structure of the hexameric silsesquioxane-based disilanol **128**. (b) Propagation of the polymeric cage network due to intermolecular hydrogen bonding between O<sub>2</sub>H<sub>2</sub> units.

hydrogen chloride. Hydrolysis of the  $\text{Fc}_2\text{SiCl}_2$  in the presence of triethylamine affords the silanediol,  $\text{Fc}_2\text{-Si}(\text{OH})_2$  (**58**), as a high-melting orange powder in

## Chart 8



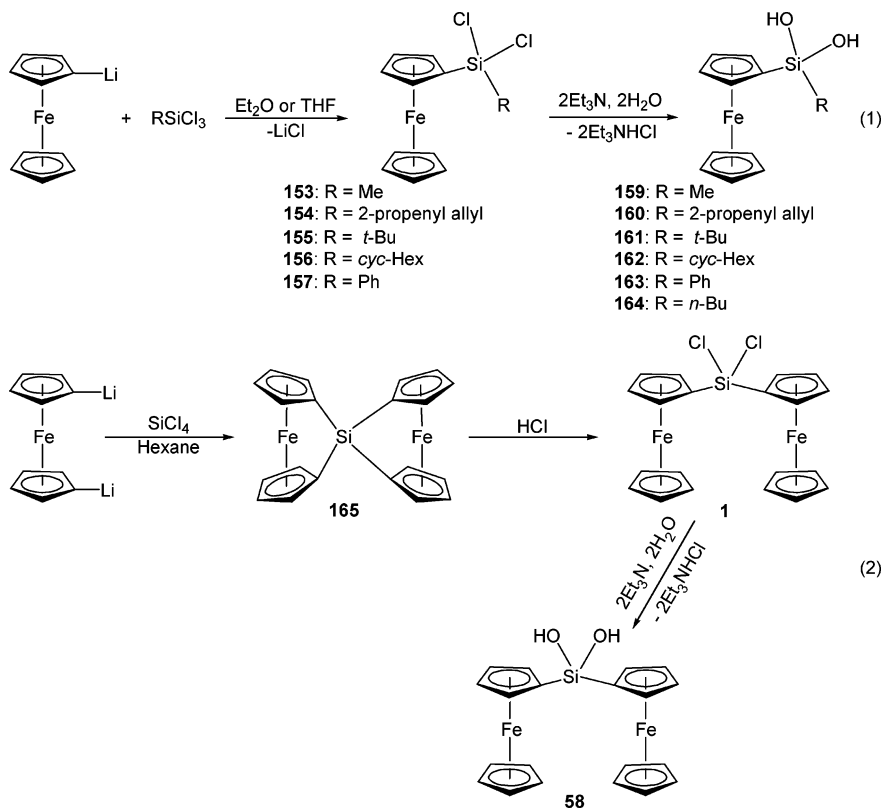
## Scheme 43



about 90% yield. An earlier preparation of this compound involved its isolation in about 4% yield, presumably as a byproduct of the Friedel–Crafts silylation reaction of ferrocene.<sup>63</sup>

Some examples of N-bonded silanediols are known. Sterically hindered amines are required to stabilize the Si(OH)<sub>2</sub> unit. Synthesis of these diols is multistep in nature and begins with a sterically hindered aromatic amine. Lithiation of the aromatic amine followed by reaction with trimethylsilyl chloride affords the silylated amines ArN(SiMe<sub>3</sub>)[Ar = 2,4,6-Me<sub>3</sub>-C<sub>6</sub>H<sub>2</sub> (**166**), 2,6-Me<sub>2</sub>-C<sub>6</sub>H<sub>3</sub> (**167**), 2,6-*i*-Pr<sub>2</sub>-C<sub>6</sub>H<sub>3</sub> (**168**)]. Lithiation of the silylated aromatic amines followed by reaction with organosilyl chlorides affords N-bonded silyl chlorides ArN(SiMe<sub>3</sub>)(Si(Me)Cl<sub>2</sub>) [Ar = 2,4,6-Me<sub>3</sub>-C<sub>6</sub>H<sub>2</sub> (**172**), 2,6-Me<sub>2</sub>-C<sub>6</sub>H<sub>3</sub> (**173**), 2,6-*i*-Pr<sub>2</sub>-C<sub>6</sub>H<sub>3</sub> (**174**)]. These are readily hydrolyzed using

## Scheme 44



a mild base (aniline) to afford the silanediols ArN(SiMe<sub>3</sub>)(Si(Me)(OH)<sub>2</sub>) [Ar = 2,4,6-Me<sub>3</sub>-C<sub>6</sub>H<sub>2</sub> (**175**), 2,6-Me<sub>2</sub>-C<sub>6</sub>H<sub>3</sub> (**176**), 2,6-*i*-Pr<sub>2</sub>-C<sub>6</sub>H<sub>3</sub> (**177**)] in very good yields (Scheme 45).<sup>22</sup> Despite the presence of the Si–N bond, these silanediols are quite stable and are also very lipophilic because of the extensive organic substituents present around them. N-Bonded silanediols can also be prepared by derivatizing the corresponding silanetriols. Thus, one of the hydroxyl groups of the silanetriol can be engaged in reaction of ArN(SiMe<sub>3</sub>)Si(OH)<sub>3</sub> [Ar = 2,4,6-Me<sub>3</sub>-C<sub>6</sub>H<sub>2</sub> (**178**), 2,6-Me<sub>2</sub>-C<sub>6</sub>H<sub>3</sub> (**179**), 2,6-*i*-Pr<sub>2</sub>-C<sub>6</sub>H<sub>3</sub> (**65**)] with trimethylsilyl chloride to afford the corresponding silanediols ArN(SiMe<sub>3</sub>)Si(OH)<sub>2</sub>(OSiMe<sub>3</sub>) [Ar = 2,4,6-Me<sub>3</sub>-C<sub>6</sub>H<sub>2</sub> (**180**), 2,6-Me<sub>2</sub>-C<sub>6</sub>H<sub>3</sub> (**181**), 2,6-*i*-Pr<sub>2</sub>-C<sub>6</sub>H<sub>3</sub> (**182**)] (eq 2, Scheme 45).<sup>158</sup> An unusual rearrangement reaction of the silanetriol 2,4,6-Me<sub>3</sub>-C<sub>6</sub>H<sub>2</sub>-N(SiMe<sub>3</sub>)Si(OH)<sub>3</sub> (**178**) affords the silanediol **183** (Scheme 46).<sup>158</sup>

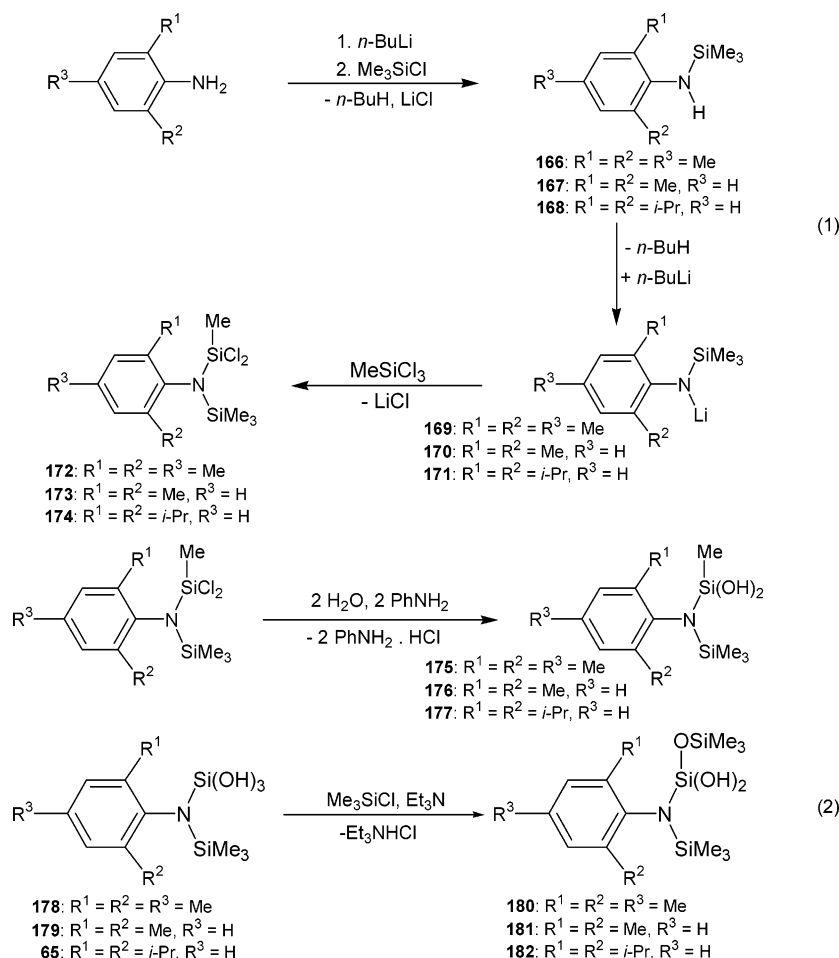
Reaction of the N-bonded silanetriol **65** with ( $\eta^5$ -Cp)<sub>2</sub>TiCl<sub>2</sub> afforded an acyclic silanediol **184** (Scheme 47).<sup>110</sup>

O-Bonded silanediols have also been prepared. Thus, reaction of *t*-BuOK with SiCl<sub>4</sub> afforded the silcondichloride (*t*-BuO)<sub>2</sub>SiCl<sub>2</sub> (**62**), which can be hydrolyzed in the presence of pyridine to afford the silanediol (*t*-BuO)<sub>2</sub>Si(OH)<sub>2</sub> (**63**) (Scheme 48).<sup>19</sup>

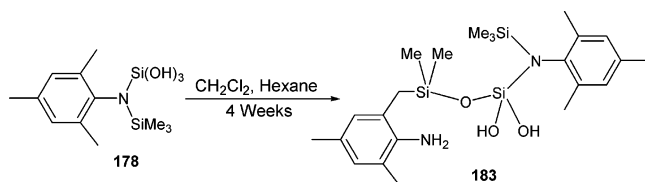
Silanediols containing Si–M bonds (**187a**, **187b**, **190**) are prepared by the electrophilic oxygen insertion reaction into the corresponding Si–H bonds.<sup>159,75</sup> A silanediol containing two Si–M bonds (**192**) can also be prepared by this method (Scheme 49).<sup>77</sup>

Compounds containing two Si(OH)<sub>2</sub> groups are fewer in number in comparison to their Si–OH analogues. One of these tetrahydroxy compounds **193**

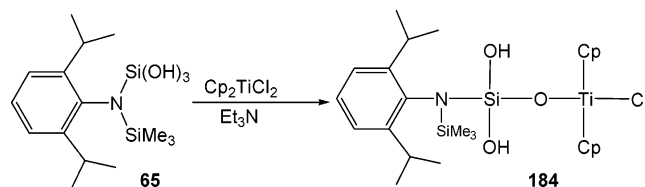
## Scheme 45



## Scheme 46

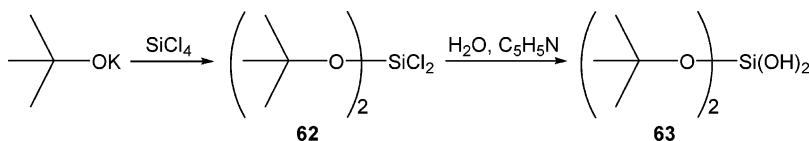


## Scheme 47



contains the Si(OH)<sub>2</sub> units on successive silicon centers and is prepared by hydrolysis of the tetrachlorodisilane **79**, or the tetraaminodisilane **80**. Interestingly, in these reactions the silicon–silicon bond does not degrade and is found to be intact in the final product (Scheme 50).<sup>112</sup>

## Scheme 48

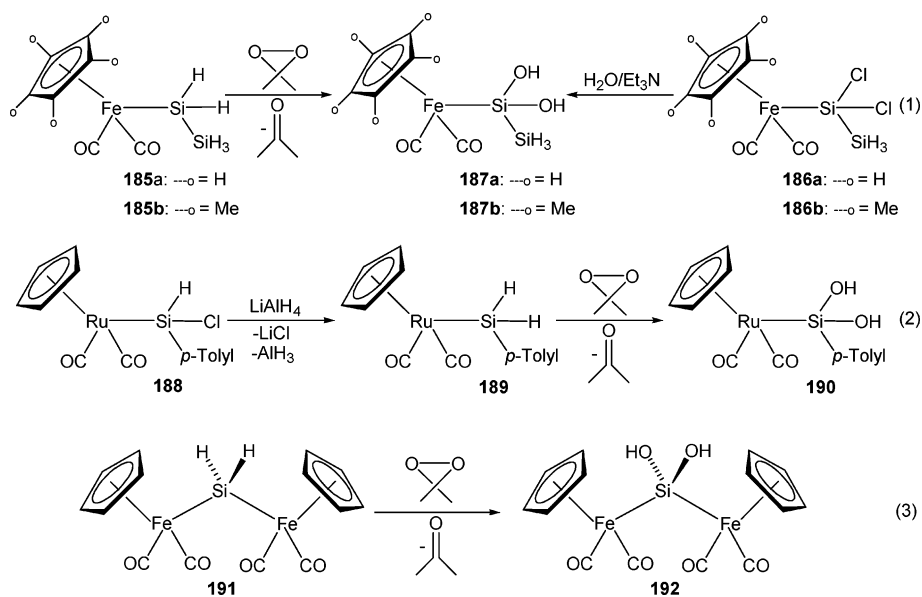


Other compounds of this family contain an oxygen bridge between the two Si(OH)<sub>2</sub> groups. Thus, N-bonded silanetriols **178**, **179**, and **65** can be dehydrated by the action of anhydrous hydrazine to afford the tetrahydroxy compounds **194**, **195**, and **196**, respectively (Scheme 51). These tetrahydroxy products are also accessible by other synthetic procedures. Direct hydrolysis of the N-bonded silanetriols ArN(SiMe<sub>3</sub>)SiCl<sub>3</sub> [Ar = 2,4,6-Me<sub>3</sub>-C<sub>6</sub>H<sub>2</sub> (**197**), 2,6-Me<sub>2</sub>-C<sub>6</sub>H<sub>3</sub> (**198**), 2,6-*i*-Pr<sub>2</sub>-C<sub>6</sub>H<sub>3</sub> (**199**)] in the presence of hydrazine also affords the tetrahydroxy derivatives **194**–**196**. A third preparative route for the tetrahydroxy derivatives consists of a multistep procedure. Thus, reaction of 2,6-*i*-Pr<sub>2</sub>-C<sub>6</sub>H<sub>3</sub>-N(SiMe<sub>3</sub>)-Li (**171**) with hexachlorodisiloxane (Cl<sub>3</sub>Si)<sub>2</sub>O affords the tetrachloro derivative [2,6-*i*-Pr<sub>2</sub>-C<sub>6</sub>H<sub>3</sub>-N(SiMe<sub>3</sub>)-SiCl<sub>2</sub>]<sub>2</sub>O (**200**). The latter on hydrolysis affords the tetrahydroxy derivative **196** (Scheme 51).<sup>160</sup>

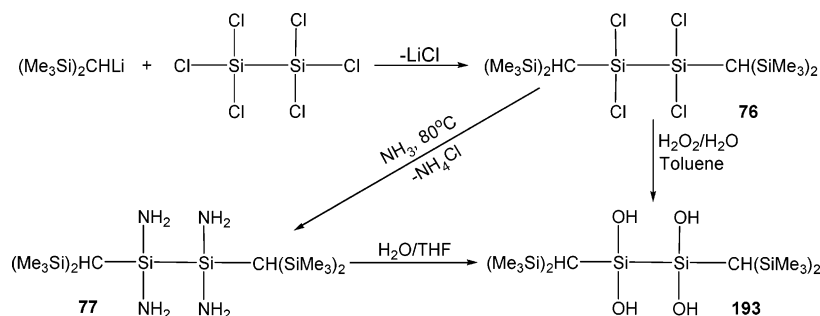
Treatment of the triisopropyl phenyl trichlorosilane **201** with pyridine–water in THF at 0 °C leads to its partial hydrolysis and results in the formation of bis-(2,4,6-triisopropylphenyl)tetrachlorodisiloxane **202**. This on subsequent hydrolysis with aniline–water



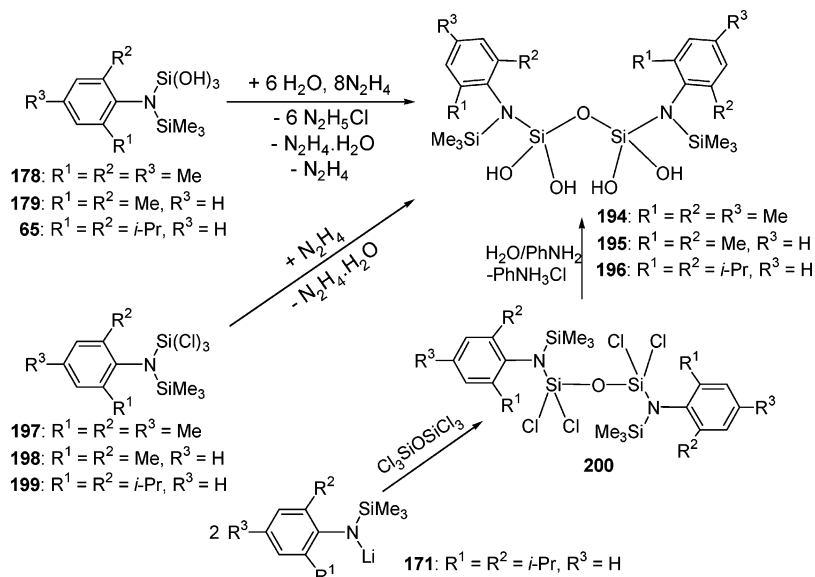
## Scheme 49



## Scheme 50



## Scheme 51

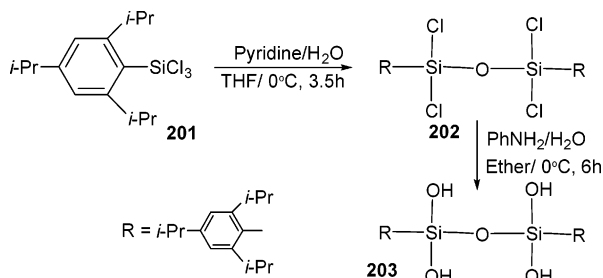


leads to the corresponding tetrasilanol **203** (Scheme 52).<sup>113</sup>

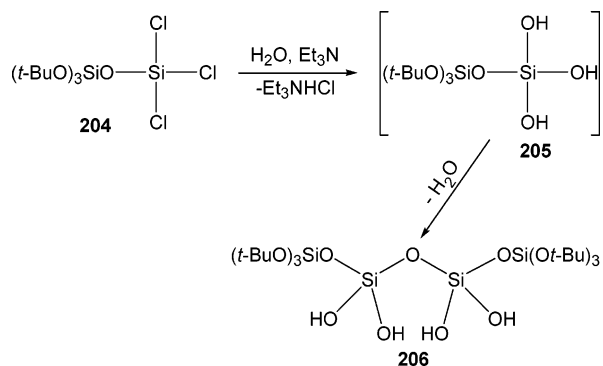
Hydrolysis of  $(t\text{-BuO})_3\text{SiOSiCl}_3$  (**205**) in the presence of triethylamine leads to formation of the tetrahydroxy derivative  $\{[(t\text{-BuO})_3\text{SiO}]\text{Si}(\text{OH})_2\}_2\text{O}$  (**206**), presumably via the intermediary of the corresponding silanetriol  $(t\text{-BuO})_3\text{SiOSi}(\text{OH})_3$  (**205**) (Scheme 53).<sup>161</sup>

Reaction  $2,6\text{-}i\text{-Pr}_2\text{-C}_6\text{H}_3\text{-N}(\text{SiMe}_2\text{Pr-}i)\text{Si}(\text{OH})_3$  (**207**) with  $(\text{Me}_3\text{Si})_3\text{CAI Me}_2$  affords the alumoxane-bridged tetrahydroxy compound **209** (Scheme 54).<sup>162</sup> A rigid phenyl-linked tetrahydroxy derivative  $(\text{OH})_2\text{MeSi-C}_6\text{H}_4\text{-SiMe}(\text{OH})_2$  (**211**) is synthesized by hydrolysis of the corresponding tetramethoxy compound  $(\text{OMe})_2\text{-MeSi-C}_6\text{H}_4\text{-SiMe}(\text{OMe})_2$  (**210**) by acetic acid and water (Scheme 55).<sup>163</sup>

## Scheme 52

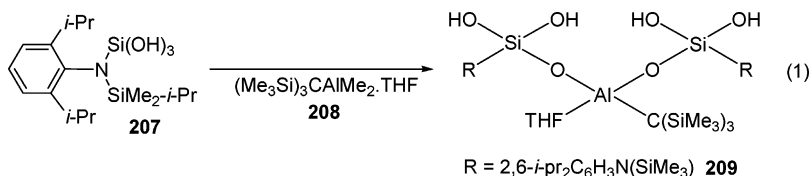


## Scheme 53

6.2. <sup>29</sup>Si NMR

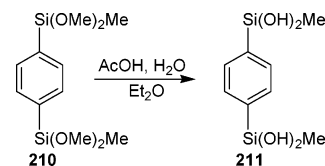
<sup>29</sup>Si NMR data for silanediols and other compounds containing more than one Si(OH)<sub>2</sub> unit are summarized in Table 7. The salient features can be summarized as follows. Silanediols containing a SiO<sub>4</sub> environment show <sup>29</sup>Si NMR chemical shifts that are most upfield corresponding to the largest shielding at silicon. Thus, the chemical shifts for compounds (*t*-BuO)<sub>2</sub>Si(OH)<sub>2</sub> (**63**)<sup>19</sup> and [(*t*-BuO)<sub>3</sub>SiO(OH)<sub>2</sub>]<sub>2</sub>O (**206**)<sup>161</sup> are observed at -81.0 and -90.3 ppm, respectively (entries 2 and 27, Table 7). Replacement of one of the oxygens by a nitrogen has a marginal downfield shift effect. For example, in 2,6-Me<sub>2</sub>-C<sub>6</sub>H<sub>3</sub>-N(SiMe<sub>3</sub>)Si(OH)<sub>2</sub>(OSiMe<sub>3</sub>) (**181**)<sup>158</sup> the chemical shift for the Si(OH)<sub>2</sub> is seen at -72.8 ppm. A similar trend is also noticed for related compounds (entries 12–16, Table 7). Progressive deshielding is seen as oxygen atoms around silicon are replaced by carbons (entries 1, 4–9, 27; Table 7). Among ferrocenyl silanediols<sup>156</sup> the most upfield signal is seen for Fc<sub>2</sub>Si(OH)<sub>2</sub> (**58**) (-25.1 ppm). Replacement of one of the ferrocenyl groups by alkyl or aryl groups results in a deshielding of the silicon center and moves the corresponding chemical shift to a higher frequency (entries 4–9; Table 7).<sup>77</sup> Hydrogens that are directly attached to silicon tend to move the chemical shift upfield. This is noticed in the sterically hindered silanediol **152** (entry 3, Table 7) where the presence of a single Si–H causes the chemical shift to resonate at -31.1 ppm. As observed with monosilanols, at-

## Scheme 54



tachment of electron-rich transition metals directly to silicon causes the chemical shift to move dramatically to the downfield region (entries 18–20, Table 7). The presence of two directly attached electron-rich metal centers causes the chemical shifts of the corresponding silicon centers to move even further downfield; the chemical shift of [(η<sup>5</sup>-Cp)Fe(CO)<sub>2</sub>]<sub>2</sub>Si(OH)<sub>2</sub> (**192**) is observed at 86.8 ppm (entry 21, Table 7). In this regard the SiH<sub>3</sub> group also appears to behave analogously to that of the transition-metal fragment in causing the <sup>29</sup>Si to resonate at higher frequencies. Thus, compounds (η<sup>5</sup>-Cp)Fe(CO)<sub>2</sub>Si(OH)<sub>2</sub>(SiH<sub>3</sub>) (**187a**) (99.8 ppm) and (η<sup>5</sup>-Cp\*)Fe(CO)<sub>2</sub>Si(OH)<sub>2</sub>(SiH<sub>3</sub>) (**187b**) (96.7 ppm) resonate at very high frequencies (entries 18 and 19, Table 7).<sup>159</sup>

## Scheme 55



## 6.3. X-ray Crystal Structures of Silanediols and Related Compounds

X-ray crystal structural data for this family of compounds are given in Table 8. Chart 9 summarizes the most common arrangements in the solid state.

The simplest of the intermolecular arrangements are the cyclic dimer and tetramers (Types K and L, Chart 9). Polymeric structures are possible by various modes of interactions. A linear polymeric chain containing O–H···O interactions is of Type M. More complicated polymeric arrangements are also noticed. Thus, the silanediols can form a head-to-head dimer. Such dimers are connected to each other to form a polymeric sheet (Type N). In this mode alternate Si<sub>2</sub>O<sub>4</sub> and O<sub>4</sub> rings are seen. Notice the similarity of this arrangement with that of the Type G, Chart 6. Translation of one of the molecules that forms a dimer results in the arrangement shown as Type O. This is also similar to the Type H arrangement (Chart 6) seen earlier. Further translation of one of the silanediols molecules in the dimeric unit of Type N results in Type P. If perfect head–head dimers are connected by means of only one O–H···O connection, the result is a Type Q arrangement.

Compounds **183** and **209** are monomeric in the solid state (Figures 30 and 31). Thus, in **183** the aromatic amino group is intramolecularly hydrogen bonded with one of the hydroxyl groups of the Si(OH)<sub>2</sub> unit. The OH···N distance is 1.956(2) Å, while the O–H···N angle is 168.66(2)°. The other hydroxyl in the molecule remains free in the solid state and is not involved in any hydrogen bonding.<sup>158</sup> In the case

R = 2,6-*i*-Pr<sub>2</sub>C<sub>6</sub>H<sub>3</sub>N(SiMe<sub>3</sub>) **209**

Table 7.  $^{29}\text{Si}$  NMR Data for Compounds Containing One or Two  $\text{Si}(\text{OH})_2$  Groups

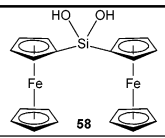
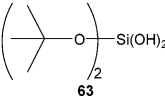
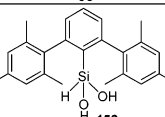
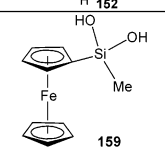
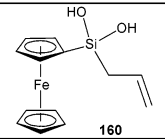
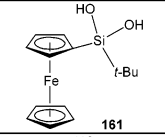
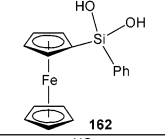
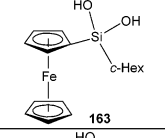
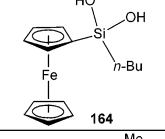
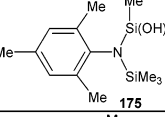


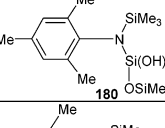
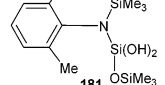
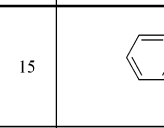
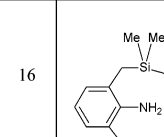
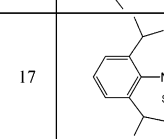
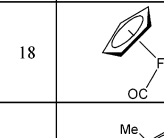
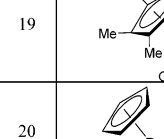
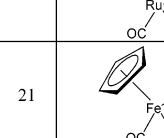
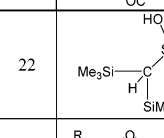
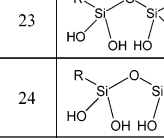
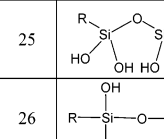
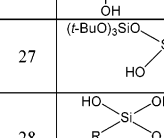
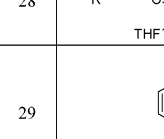
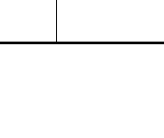


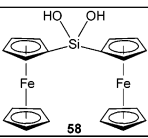
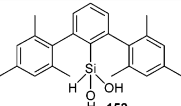
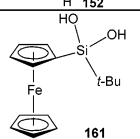
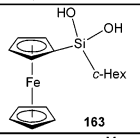
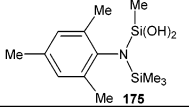
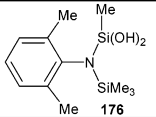
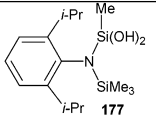
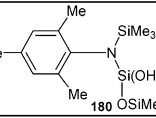
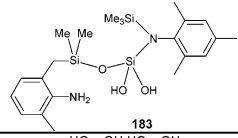
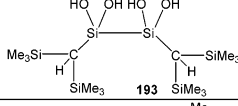
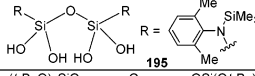
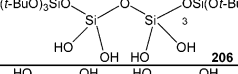
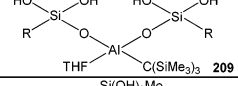
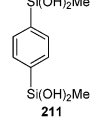
S.No.	Compound	Coordination Environment around Silicon	$^{29}\text{Si}$ NMR (ppm)	Ref.
1		$\text{C}_2\text{O}_2$	-25.1	157
2		$\text{O}_4$	-81.0	19
3		$\text{C}(\text{H})\text{O}_2$	-31.1	155
4		$\text{C}_2\text{O}_2$	-16.5	156
5		$\text{C}_2\text{O}_2$	-14.9	156
6		$\text{C}_2\text{O}_2$	-9.8	156
7		$\text{C}_2\text{O}_2$	-8.1	156
8		$\text{C}_2\text{O}_2$	-11.7	156
9		$\text{C}_2\text{O}_2$	-9.5	156
10		$\text{NCO}_2$ $\text{NC}_3$	-29.2 5.8	22
11		$\text{NCO}_2$ $\text{NC}_3$	-29.4 5.7	22
12		$\text{NCO}_2$ $\text{NC}_3$	-29.9 5.6	22
13		$\text{NO}_3$ $\text{NC}_3$ $\text{OC}_3$	-72.9 6.5 10.3	158
14		$\text{NO}_3$ $\text{NC}_3$ $\text{OC}_3$	-72.8 6.3 10.2	158
15		$\text{NO}_3$ $\text{C}_3\text{O}$ $\text{NC}_3$	-72.9 6.4 10.3	158
16		$\text{NO}_3$ $\text{NC}_3$ $\text{OC}_3$	-72.7 5.2 6.1	158
17		$\text{NO}_3$ $\text{SiC}_3$	-71.8 5.8	110
18		$\text{SiFeO}_2$ $\text{SiH}_3$	99.8 -100.1	159
19		$\text{SiFeO}_2$ $\text{SiH}_3$	96.7 -95.2	159
20		$\text{CRuO}_2$	29.3	75
21		$\text{Fe}_2\text{O}_2$	86.8	77
22		$\text{SiCO}_2$ $\text{C}_4$	-7.4 0.6	112
23		$\text{NO}_3$ $\text{NC}_3$	-73.4 6.9	160
24		$\text{NO}_3$ $\text{NC}_3$	-73.4 7.4	160
25		$\text{NO}_3$ $\text{NC}_3$	-65.3 7.5	160
26		$\text{CO}_3$	-63.0	113
27		$\text{O}_4$ (Si-OH) $\text{O}_4$	-90.3 -103.2	161
28		$\text{NO}_3$ $\text{NC}_3$ $\text{C}_4$	-71.9 8.0 -3.4	162
29		$\text{C}_2\text{O}_2$	-21.3	163

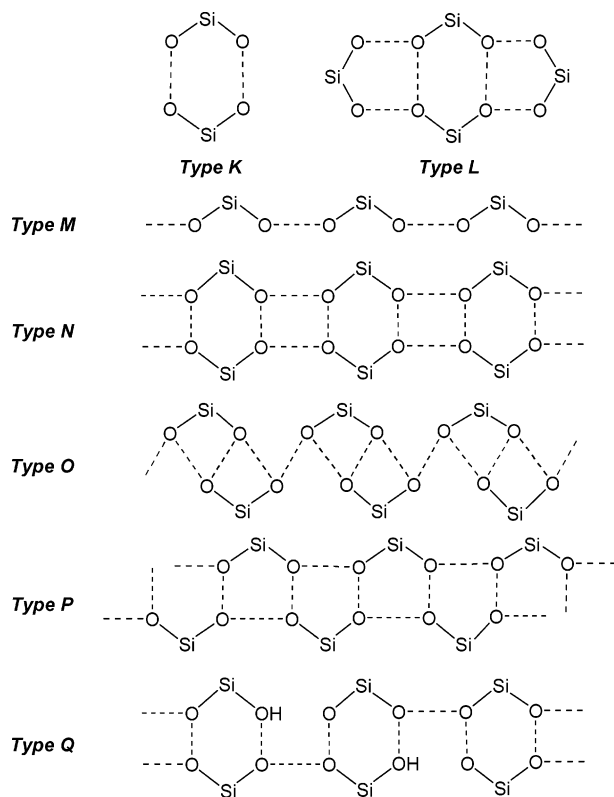
Table 8. X-ray Structural Data for Compounds Containing One or More Si-(OH)<sub>2</sub> Groups

S.No.	Compound	Si-OH (Å)	OH...O (Å)	O...O (Å)	O-H...O (°)	Structural Summary	Ref.
1		1.623(2)- 1.659(2)	2.090(2)- 2.200(2)	2.800(3)- 2.930(3)	143.20(1)- 175.43(1)	Polymeric chains of dimeric units	157
2		1.621(3), 1.649(6)	2.020(4) 2.527(1) (intra OH...π)	2.850(5) 3.248(1)	174.17(6) 149.06(8)	Dimeric structure; also has intramolecular OH...π interaction	155
3		1.618(7)- 1.650(8)	1.778(5)- 1.842(1)	2.735(2)- 2.829(2)	168.87(1)- 176.40(1)	Polymeric chains of dimeric units	156
4		1.635(2)- 1.659(2)	1.721(2)- 2.358(1)	2.823(1)- 3.132(2)	149.37(2)- 162.95(2)	Polymeric chains	156
5		1.635(4)- 1.637(1)	2.123(1)- 2.209(3)	2.769(0)- 2.809(3)	150.84(6)- 171.79(2)	Crinkled ribbon-like structure	22
6		1.630(1)- 1.643(1)	2.012(5)- 2.183(4)	2.761(9)- 2.843(1)	161.54(5)- 171.31(6)	Crinkled ribbon-like structure	164
7		1.608(9)- 1.659(6)	1.982(1)- 2.347(9)	2.713(9)- 2.929(6)	117.78(3)- 167.88(2)	Hexameric structure	164
8		1.599(1), 1.629(2)	2.011(2)- 2.084(4)	2.746(7)- 2.902(1)	144.04(2)- 178.26(4)	Tetrameric structure	158
9		1.623(6), 1.628(3)	1.956(2) (OH...N)	2.780(5)	168.66(2)	Monomeric structure	158
10		1.632(9)- 1.667(6)	1.981(6)- 2.374(4)	2.679(1)- 2.929(1)	148.99(5)- 171.29(6)	Cage structure	112
11		1.609(7)- 1.639(1)	1.818(2)- 2.073(2)	2.610(3)- 2.865(4)	138.53(2)- 162.35(1)	Three-dimensional cage	160
12		1.592(3)- 1.623(3)	1.935(3)- 2.351(4)	2.698(3)- 2.917(4)	170.73(5)- 173.48(2)	One-dimensional chain	161
13		1.617(7)- 1.654(4)	1.843(1)- 2.015(4)	2.679(6)- 2.850(7)	153.17(1)- 174.05(1)	Monomeric structure	162
14		1.634(1)- 1.639(5)	1.869(1)- 1.934(1)	2.676(2)- 2.697(1)	133.77(1)- 165.67(1)	Three-dimensional grid	163

of the alumoxane-bridged silanediol **209** (Figure 31), the two Si(OH)<sub>2</sub> units are intramolecularly hydrogen bonded to each other. Although one Si-OH remains free, the remaining three Si-OH groups are involved in this interaction. Two types of O-H...O distances and angles are seen for this compound: a short distance of 1.843(1) Å and a longer distance of 2.015-

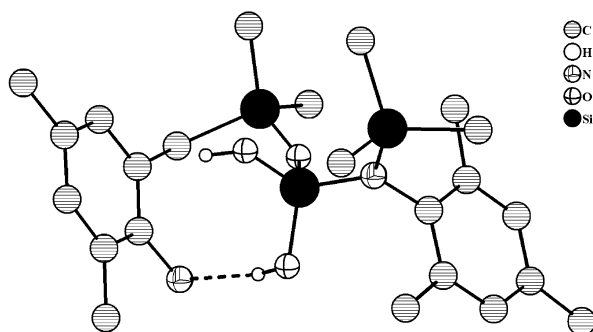
(4) Å. Similarly, a smaller O-H...O angle of 153.17(1)° and a larger angle of 174.05(1)° are seen.<sup>162</sup>

The sterically hindered silanediol **152** forms a dimer in the solid state (Type K, Chart 9). In this mode a six-membered Si<sub>2</sub>O<sub>4</sub> ring is generated. From each Si(OH)<sub>2</sub> group one of the oxygens acts as a proton donor while the other acts as a proton accep-

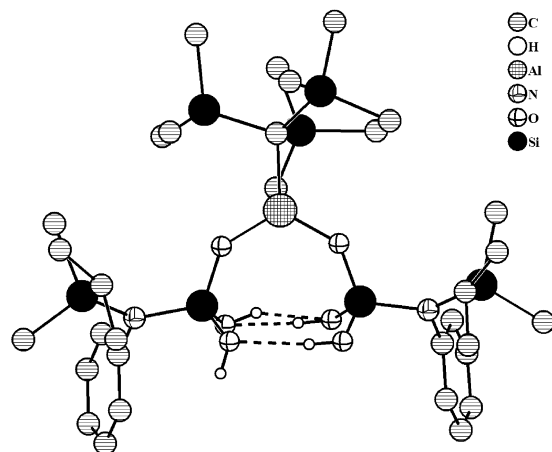
**Chart 9. Most Common Solid-State Structures Formed as a Result of Intermolecular Hydrogen Bonding in Disiloxane Diols**


tor. Two Si–O bond distances are seen. The shorter distance of 1.621(3) Å is associated with the proton-donating Si–OH, while the longer distance of 1.649(6) Å is associated with the proton-accepting Si–O (entry 2, Table 8). The hydrogen of the free Si–OH of each molecule in the dimer points to the centroid of the aromatic substituents presumably because of a O–H··· $\pi$  interaction (O···aromatic centroid distance is 3.248(1) Å) (Figure 32). In the IR spectrum of this compound in the solid state two broad stretching frequencies are observed at 3505 and 3281  $\text{cm}^{-1}$ . The latter is clearly due to the O–H···O hydrogen-bonded Si–OH stretching.<sup>155</sup>

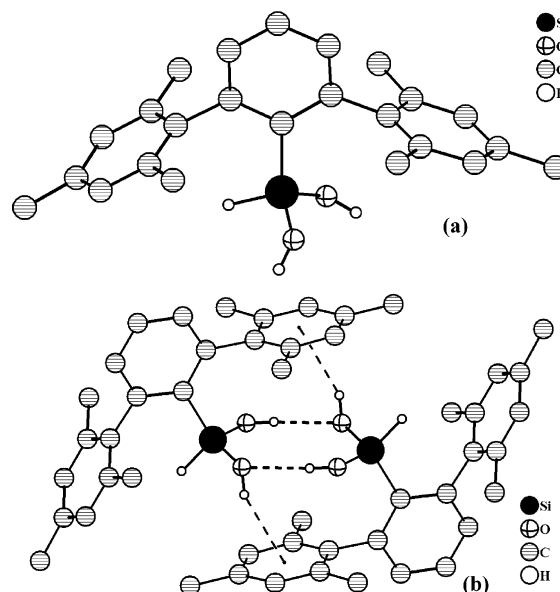
The silanediol 2,4,6-Me<sub>3</sub>-C<sub>6</sub>H<sub>3</sub>-N(SiMe<sub>3</sub>)Si(OSiMe<sub>3</sub>)(OH)<sub>2</sub> (**180**) derived from the corresponding silanetriol shows two types of Si–OH distances, 1.599(1)



**Figure 30.** View of the molecular structure of the silanediol **183** rearranged from a silanetriol. One of the two hydroxyl protons is intramolecularly hydrogen bonded to the amino group while the other remains free. Protons present on the amino group are omitted for clarity.



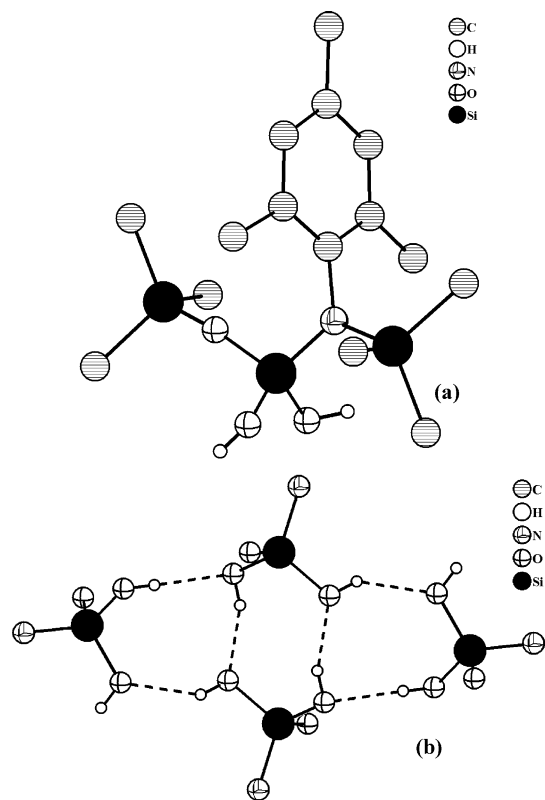
**Figure 31.** View of the alumoxane-bridged bis(silanediol) **209**. The OH groups are intramolecularly hydrogen bonded to each other. The isopropyl groups on the aromatic rings are omitted for clarity.



**Figure 32.** (a) Molecular structure of the sterically hindered hydrido silanediol **152**. (b) Dimeric structure due to intermolecular OH···O and OH··· $\pi$  interactions.

and 1.629(2) Å. This compound forms a tetrameric aggregate in the solid state (Type L, Chart 9). Accordingly, two molecules are connected in a head-to-head manner forming a central Si<sub>2</sub>O<sub>4</sub>H<sub>2</sub> ring. Two more molecules are connected to this central dimer, one on each side (Figure 33). This results in formation of SiO<sub>4</sub>H<sub>3</sub> rings on either side of the central dimer.<sup>158</sup>

The N-bonded silanediol 2,6-*i*-Pr<sub>2</sub>-C<sub>6</sub>H<sub>3</sub>-N(SiMe<sub>3</sub>)-Si(Me)(OH)<sub>2</sub> (**177**) forms two types of hexameric clusters in the solid state (Figure 34). The first hexameric cluster is formed as a result of two symmetrically related trimers being joined to each other by two Si–OH units. This forms a central O<sub>2</sub>H<sub>2</sub> ring reminiscent of the situation found in certain monosilanols (Type B, Chart 4). The O–H···O bond angle in this four-membered ring is quite acute (entry 7, Table 7). Each trimeric unit has a central O–H···O bond that divides the trimer into two segments (Figure 34b). The second hexameric cluster is also formed as a result of two trimeric units being joined

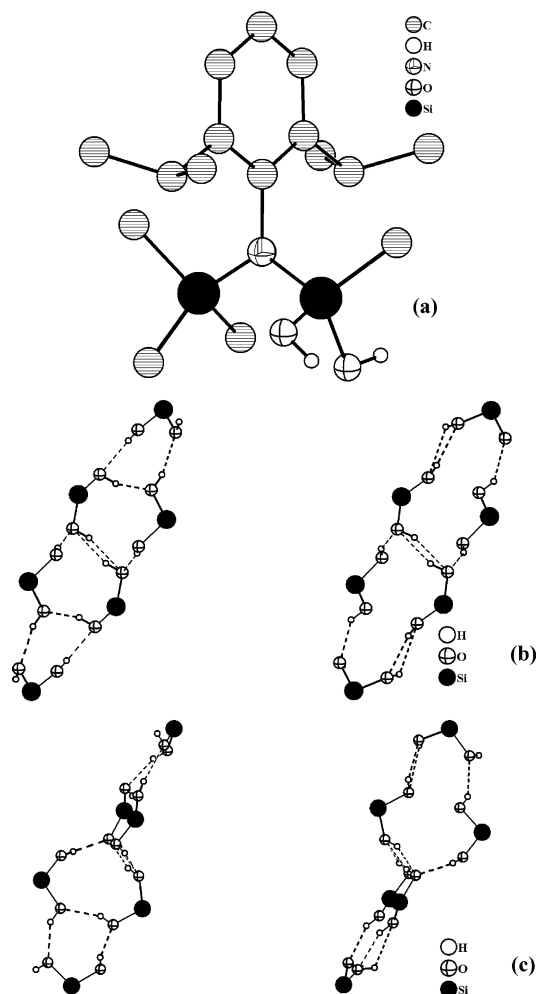


**Figure 33.** (a) DIAMOND picture of the N-bonded silanediol 2,4,6-Me<sub>3</sub>-C<sub>6</sub>H<sub>2</sub>-N(SiMe<sub>3</sub>)Si(OSiMe<sub>3</sub>)(OH)<sub>2</sub> (**180**) derived from the silanetriol (b) Tetrameric agglomerate of **180** in the solid state due to intermolecular hydrogen bonding.

together. However, in this instance *within* the trimer there is an absence of the central O–H···O bond (Figure 34c).<sup>164</sup>

The decrease of steric hindrance in the N-bonded silanediols leads to a change in the solid-state structural pattern. Thus, in compounds 2,4,6-Me<sub>3</sub>-C<sub>6</sub>H<sub>2</sub>-N(SiMe<sub>3</sub>)Si(Me)(OH)<sub>2</sub> (**175**)<sup>22</sup> and 2,6-Me<sub>2</sub>-C<sub>6</sub>H<sub>3</sub>-N(SiMe<sub>3</sub>)Si(Me)(OH)<sub>2</sub> (**176**)<sup>164</sup> a polymeric arrangement is formed in the solid state (Figure 35). Two molecules are involved in the formation of a dimeric unit (Si<sub>2</sub>O<sub>4</sub>H<sub>2</sub>), which is almost perfectly planar. The dimers are interconnected to each other by further hydrogen bonding to afford a polymeric ribbon (Type N, Chart 9; Figure 35c). The dihedral angle between alternate dimeric units is about 20.8°. This results in the dimers being arranged in a crisscross manner with respect to each other (Figure 35b). This gives rise to an overall crinkled ribbon arrangement.

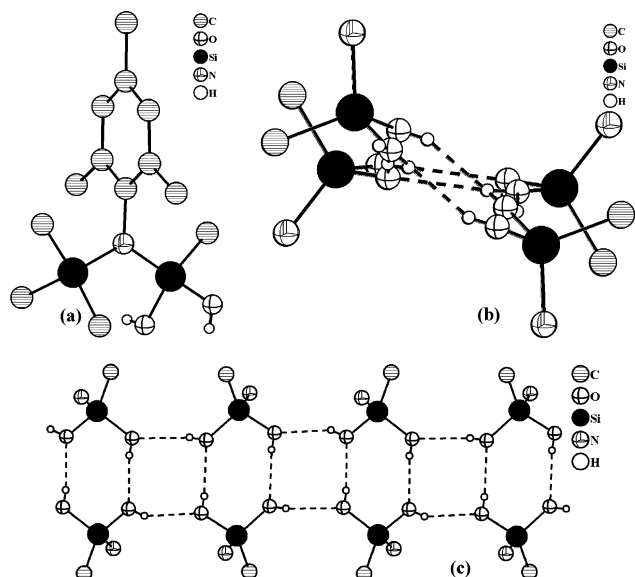
The ferrocenyl-containing silanediol Fc(*c*-Hex)Si(OH)<sub>2</sub> (**163**) has a solid-state structure similar to that of the N-bonded silanediols **175** and **176** discussed above. Two molecules are joined to each other to form a dimer, which are connected to each other further to form a polymeric ribbon.<sup>156</sup> A notable feature of this structure is the parallel arrangement of the ferrocenyl substituents on each side of the polymeric ribbon (Figure 36). In contrast to the X-ray crystal structure of **163**, the other ferrocenyl-containing silanediols Fc<sub>2</sub>Si(OH)<sub>2</sub> (**58**)<sup>157</sup> and Fc(*t*-Bu)Si(OH)<sub>2</sub> (**161**)<sup>156</sup> form slightly different types of polymeric aggregates in comparison to the crinkled-ribbon



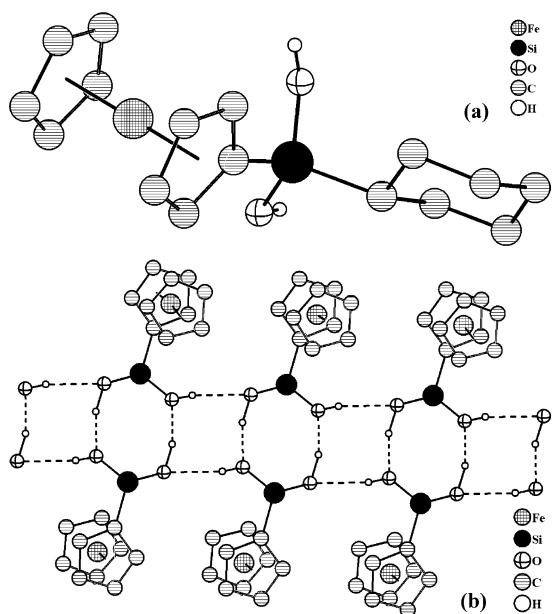
**Figure 34.** (a) Molecular structure of the sterically hindered N-bonded silanediol 2,6-*i*-Pr<sub>2</sub>-C<sub>6</sub>H<sub>3</sub>-N(SiMe<sub>3</sub>)-SiMe(OH)<sub>2</sub> (**177**). (b) Formation of the two discrete hexameric clusters between two symmetry-related trimers. (c) Side view of the hexameric clusters showing the relative orientation of the two trimeric units forming the hexamer.

structures discussed above (Figures 37 and 38). In these compounds two molecules of the diols also interact with each other to form a nonplanar dimeric unit Si<sub>2</sub>O<sub>4</sub>H<sub>2</sub>. Further proliferation of this dimer occurs by a *single* O–H···O hydrogen bond (Figures 37 and 38; Type Q, Chart 9) in contrast to *two* interconnecting O–H···O bonds encountered in the structures of **163**, **175**, and **176**. This results in formation a polymeric tape for compounds **58** and **161**. The distinction between a tape and a ribbon has been made by Whitesides in his classification of hydrogen bonding in amide structures.<sup>165</sup> Thus, in a tape each molecule is hydrogen bonded to two neighboring molecules, while in a ribbon each molecule is hydrogen bonded to *three or more* molecules. It is to be noted that in the polymeric tape structures of **58** and **161** the alternate dimers have two free Si–OH moieties. Also, in contrast to the structure of **163**, the adjacent ferrocenyl units in **161** are not parallel to each other; rather the alternate ferrocenyl substituents have the same stereodisposition.<sup>156</sup>

The tetrasilanol [({*t*-BuO)<sub>3</sub>SiO}Si(OH)<sub>2</sub>]<sub>2</sub> (**206**) also forms a polymeric sheet (Figure 39). This is slightly different from the two types of polymeric sheets

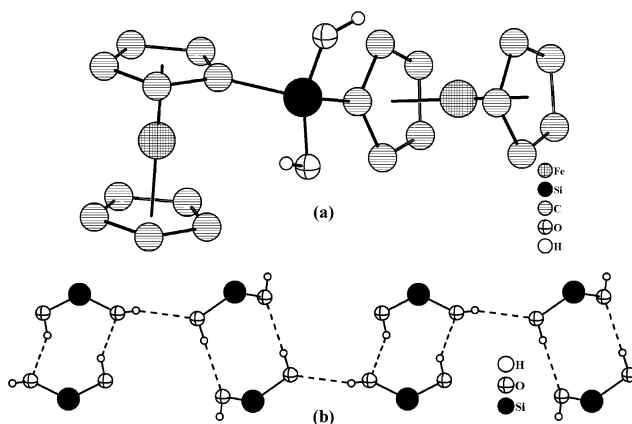


**Figure 35.** (a) Molecular structure of the sterically hindered N-bonded silanediol 2,4,6-Me<sub>3</sub>-C<sub>6</sub>H<sub>3</sub>-N(SiMe<sub>3</sub>)-SiMe(OH)<sub>2</sub> (**175**). (b) Formation of a dimeric motif which proliferates in a crisscross manner. (c) Polymeric ribbon-like network of **175** formed due to intermolecular hydrogen bonding.

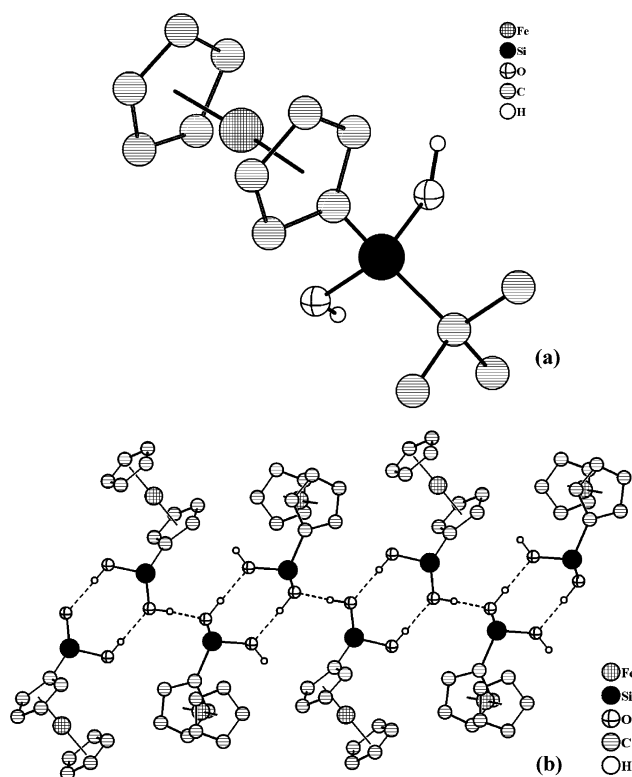


**Figure 36.** (a) Molecular structure of Fe(*c*-Hex)Si(OH)<sub>2</sub> (**163**). (b) Formation of a dimeric structure which further proliferates in a polymeric ribbon-like network due to intermolecular hydrogen bonding.

encountered above. First, an intramolecular hydrogen bonding is in place between two different Si(OH) groups and two *tert*-butoxysiloxy oxygen atoms. This results in a shrinking of the central Si–O–Si angle to 137.7(1)°. Further, propagation of this structure into zigzag polymeric sheets occurs as a result of intermolecular hydrogen bonding, which links the molecules together to form alternate 8- (Si<sub>2</sub>O<sub>4</sub>H<sub>2</sub>) and 12-membered (Si<sub>4</sub>O<sub>6</sub>H<sub>2</sub>) rings. The IR spectrum of **206** shows the presence of broad bands centered at 3438 and 3302 cm<sup>-1</sup> consistent with the hydrogen-bonded structure found in the solid state.<sup>161</sup>

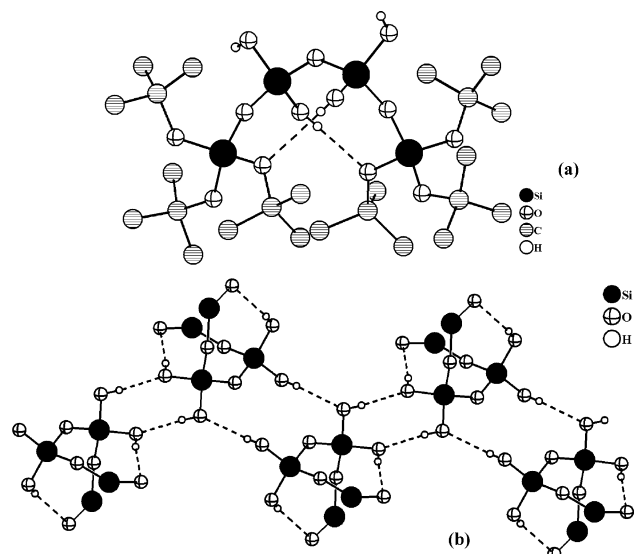


**Figure 37.** (a) Molecular structure of Fe<sub>2</sub>Si(OH)<sub>2</sub> **58**. (b) Formation of a dimeric structure which propagates via a single OH···O intermolecular interactions into the polymeric network.

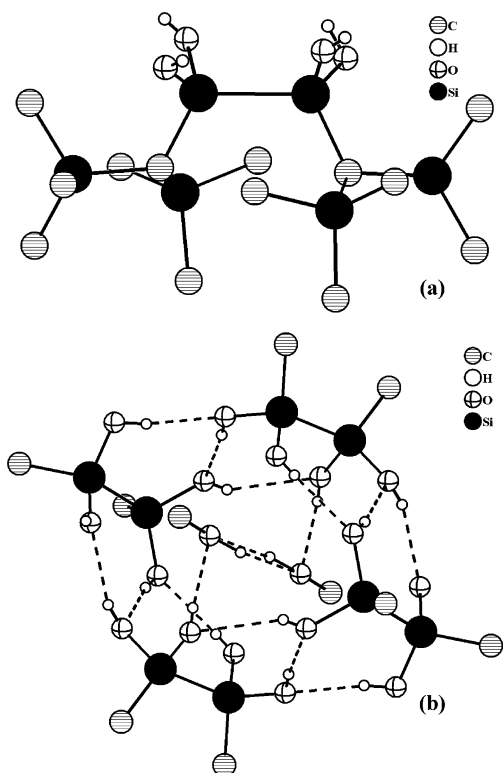


**Figure 38.** (a) Molecular structure of Fe(*t*-Bu)Si(OH)<sub>2</sub> **161**. (b) Formation of a dimeric structure which propagates via a single OH···O intermolecular interaction into the polymeric network.

The tetrahydroxy derivatives [(SiMe<sub>3</sub>)<sub>2</sub>CH}Si(OH)<sub>2</sub>]<sub>2</sub> (**193**) and [{2,6-*i*-Pr<sub>2</sub>-C<sub>6</sub>H<sub>3</sub>-N(SiMe<sub>3</sub>)}Si(OH)<sub>2</sub>]<sub>2</sub>O (**195**) form three-dimensional cage structures as a result of intermolecular hydrogen bonding (Figures 40 and 41). In **193** four molecules are held together by extensive intermolecular hydrogen bonding to form a spherical cage-like architecture (Figure 40). The tetrasilanol **193** crystallizes along with methanol. Accordingly, each tetrameric cage traps two molecules of methanol that are trapped inside the cage by means of intermolecular O–H···O bonds.<sup>112</sup> The tetrasilanol **195** also forms a cage-like structure albeit by participation of three molecules instead of four as in the case of **193**. Of the 12 hydroxyl groups present, 6 are involved in stitching

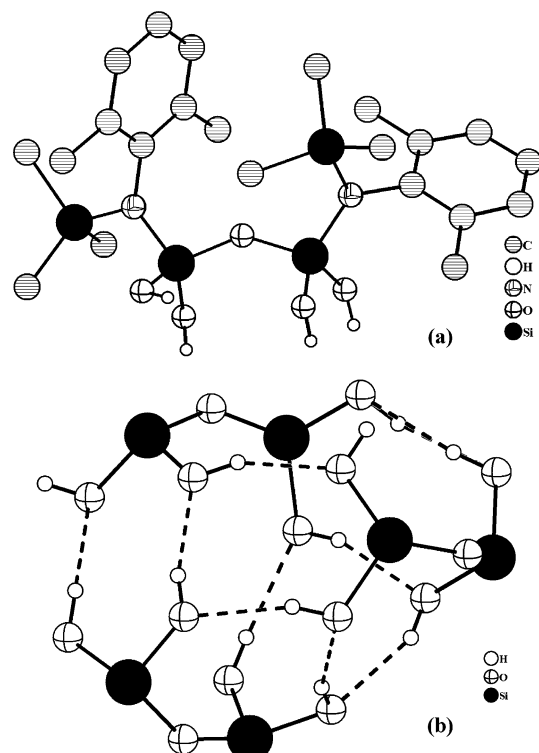


**Figure 39.** (a) DIAMOND figure of the tetrasilanol  $[(t\text{-BuO})_3\text{SiO}\}\text{Si}(\text{OH})_2]_2\text{O}$  (**206**). Two among the four hydroxyl groups are involved in intramolecular hydrogen bonding. (b) Alternate 8- ( $\text{Si}_2\text{O}_4\text{H}_2$ ) and 12- ( $\text{Si}_4\text{O}_6\text{H}_2$ ) membered rings form a zigzag polymeric sheet. The carbon atoms and some of the *tert*-butoxy groups are omitted for clarity.



**Figure 40.** (a) Molecular structure of the tetrahydroxy disilane **193**. (b) Tetrameric cage structure formed as a result of intermolecular hydrogen bonds. Two molecules of methanol are trapped inside the cage by  $\text{OH}\cdots\text{O}$  interactions. The  $\text{SiMe}_3$  groups are omitted for clarity.

the periphery of the cage while 6 more are involved in forming tight intermolecular hydrogen bonding in the interior of the cage (Figure 41). The latter results in shrinking the Si–O–Si angle in each molecule to  $140.7(2)^\circ$ . In the tetrachloro analogue  $[\{2,6\text{-}i\text{-Pr}_2\text{-C}_6\text{H}_3\text{-N}(\text{SiMe}_3)\}\text{SiCl}_2]_2\text{O}$ , which has a monomeric structure, the Si–O–Si angle is  $180^\circ$ , thus attesting



**Figure 41.** (a) Molecular structure of the tetrahydroxy disiloxane **195**. (b) A trimeric cage structure obtained as a result of intermolecular hydrogen bonding. Only the core view is shown for clarity.

to the effect of the intermolecular hydrogen bonding on the structure of **195**.<sup>160</sup>

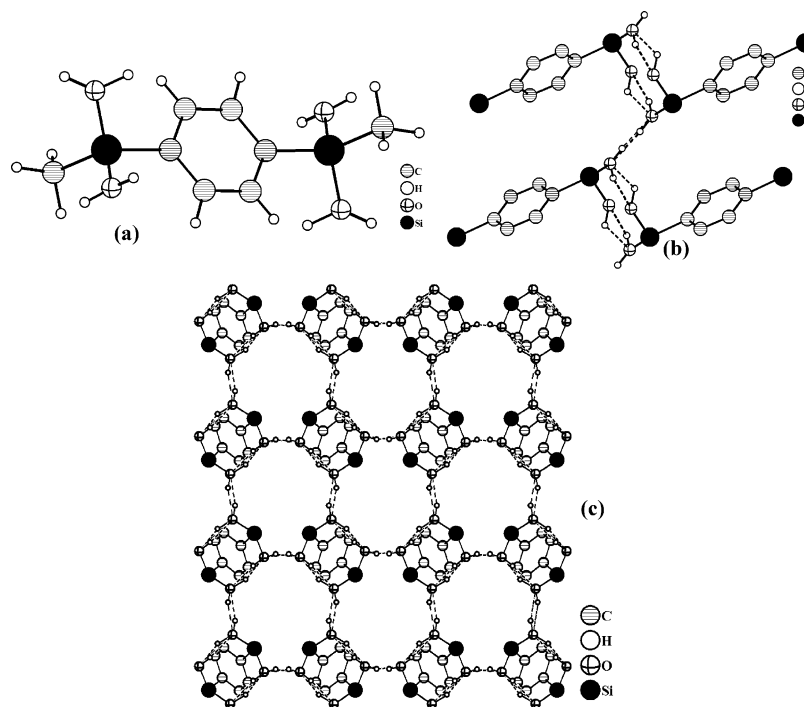
The bis-silanol  $\text{MeSi}(\text{OH})_2\text{-C}_6\text{H}_4\text{-Si}(\text{OH})_2\text{Me}$  (**211**) containing the rigid phenyl spacer group forms a three-dimensional grid in the solid state. The Si–O bond distances in **211** are 1.634(1) and 1.639(5) Å. The IR spectrum of this compound shows a broad band at  $3125\text{ cm}^{-1}$ , indicating the absence of any free Si–OH. Accordingly, an extensive hydrogen-bonded network is found in the solid-state structure of **211**. The hydrogen atoms are disordered in the ratio of 1:1. Both ends of the difunctional molecule are linked with hydrogen bonding (Figure 42b). Repeated addition of the silanol moieties leads to a chainlike structure. Interconnection of such chains mediated by  $\text{O-H}\cdots\text{O}$  bonding leads to formation of a fairly rigid three-dimensional grid-like structure (Figure 42c).<sup>163</sup>

## 7. Silanetriols and Bis(silanetriols) Containing One or Two $\text{Si}(\text{OH})_3$ Units

### 7.1. Synthesis

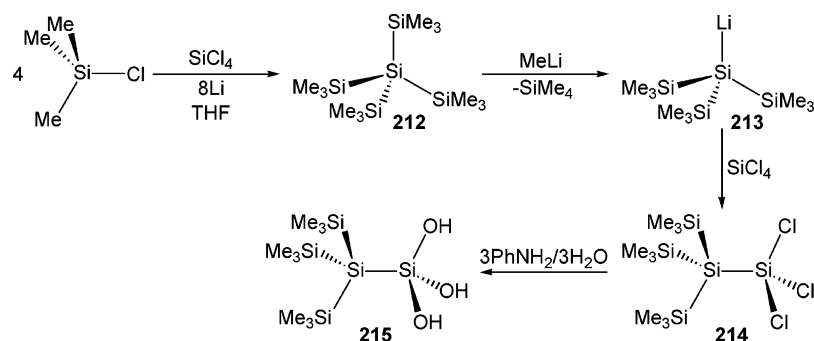
Although compounds containing  $\text{Si}(\text{OH})_3$  units are prone to self-condensation reactions, several such compounds have been prepared and stabilized.<sup>4,10</sup> These include  $\text{PhSi}(\text{OH})_3$ ,<sup>166,167</sup>  $\text{X-C}_6\text{H}_4\text{-Si}(\text{OH})_3$  ( $\text{X} = p\text{-NMe}_2, p\text{-OMe}, p\text{-Me}, m\text{-Me}, m\text{-Cl}, m\text{-CF}_3$ ),<sup>168–170</sup>  $\text{OMe}(\text{CH}_2\text{CH}_2\text{O})_n\text{CH}_2\text{Si}(\text{OH})_3$  ( $n = 1–3, 6, 7$ ),<sup>171</sup>  $(t\text{-BuO})_3\text{SiOSi}(\text{OH})_3$ ,<sup>41</sup>  $(\text{Me}_3\text{Si})_3\text{ESi}(\text{OH})_3$  ( $\text{E} = \text{C}, \text{Si}$ ),<sup>172,173</sup>  $(\text{PhMe}_2\text{Si})_3\text{CSi}(\text{OH})_3$ ,<sup>4</sup>  $c\text{-C}_6\text{H}_{11}\text{Si}(\text{OH})_3$ ,<sup>174,175</sup>  $\text{OsCl}(\text{CO})\text{-}(\text{PPh}_3)_2\text{Si}(\text{OH})_3$ ,<sup>176</sup> etc. Phenyl and substituted phenyl silanetriols have been prepared by hydrolysis of the





**Figure 42.** (a) Molecular structure of the bis-silanediol **211**. (b) Relative disposition of the individual molecules forming the hydrogen-bonded chains. (c) Formation of a three-dimensional grid-like structure as a result of OH $\cdots$ O hydrogen bonding.

#### Scheme 56



corresponding methoxides. By using a similar strategy the cyclohexylsilanetriol has been prepared.<sup>166,168–170</sup> It must be mentioned that  $\text{PhSi}(\text{OH})_3$  has also been prepared by Takiguchi by hydrolysis of phenylsilicontrichloride using ether as the solvent and in the presence of aniline.<sup>167</sup> The preparation of  $(\text{Me}_3\text{Si})_3\text{SiSi}(\text{OH})_3$  is accomplished by a synthetic strategy as shown in Scheme 56. Reaction of  $\text{Me}_3\text{SiCl}$  with lithium followed by silicon tetrachloride affords the pentasilicon derivative  $\text{Si}(\text{SiMe}_3)_4$  (**212**). Reaction of the latter with methyllithium generates the reactive silyllithium derivative  $(\text{SiMe}_3)_3\text{SiLi}$  (**213**), which upon reaction with  $\text{SiCl}_4$  affords the silicon trichloride,  $(\text{Me}_3\text{Si})_3\text{SiSiCl}_3$  (**214**). Hydrolysis of  $(\text{Me}_3\text{Si})_3\text{SiSiCl}_3$  (**214**) by moist diethyl ether affords  $(\text{Me}_3\text{Si})_3\text{SiSi}(\text{OH})_3$  (**215**).<sup>173</sup>

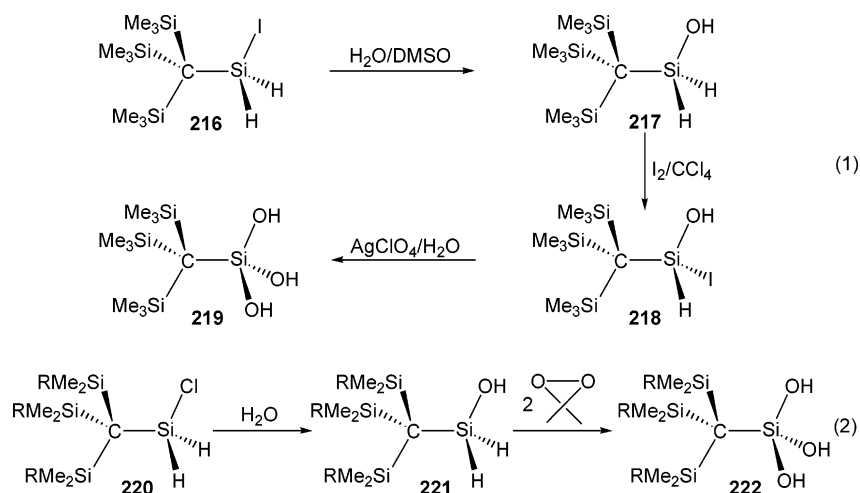
However, the analogous carbon derivative  $(\text{Me}_3\text{Si})_3\text{CSiCl}_3$  is very sluggish in its reactivity. For example, it does not undergo reaction even with refluxing methanol.<sup>7</sup> In view of this poor reactivity, an alternative synthetic procedure has been adopted to prepare  $(\text{Me}_3\text{Si})_3\text{CSi}(\text{OH})_3$  (**219**) (Scheme 57). Thus, the iodo derivative  $(\text{Me}_3\text{Si})_3\text{CSi}(\text{I})\text{H}_2$  (**216**) is chosen as a convenient precursor. Hydrolysis of **216** affords

the monosilanol  $(\text{Me}_3\text{Si})_3\text{CSi}(\text{OH})\text{H}_2$  (**217**). One of the Si–H bonds in **217** can be converted into a Si–I bond by treatment with  $\text{I}_2$  in carbon tetrachloride to afford the compound  $(\text{Me}_3\text{Si})_3\text{CSi}(\text{I})(\text{OH})(\text{H})$  (**218**). The latter on treatment with silver perchlorate followed by hydrolysis affords the silanetriol  $(\text{Me}_3\text{Si})_3\text{CSi}(\text{OH})_3$  (**219**) (eq 1, Scheme 51).<sup>172</sup> The sterically encumbered silane  $(\text{RMe}_2\text{Si})_3\text{CSi}(\text{Cl})\text{H}_2$  (**220**) is converted into the silanetriol  $(\text{RMe}_2\text{Si})_3\text{CSi}(\text{OH})_3$  (**222**) by a two-step process. The first step of the reaction involves hydrolysis of **220** to the monosilanol  $(\text{RMe}_2\text{Si})_3\text{CSi}(\text{OH})\text{H}_2$  (**221**). Oxygen insertion into the Si–H bonds of **221** by dimethyldioxirane leads to formation of the silanetriol **222** (eq 2, Scheme 51).<sup>4,7,8</sup>

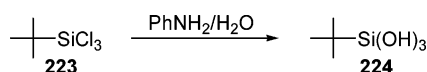
Recent emphasis on synthesis in silanetriols has been on their stability and lipophilicity. In many instances it has been found advantageous to use sterically hindered substituents on silicon, which minimizes the tendency for self-condensation reactions and consequently increases the stability and shelf lives of the silanetriols.<sup>7,8</sup>

The simplest of the sterically hindered substituent containing silanetriol can be prepared by hydrolysis of  $t\text{-BuSiCl}_3$  (**223**) to  $t\text{-BuSi}(\text{OH})_3$  (**224**) in the pres-

## Scheme 57



## Scheme 58

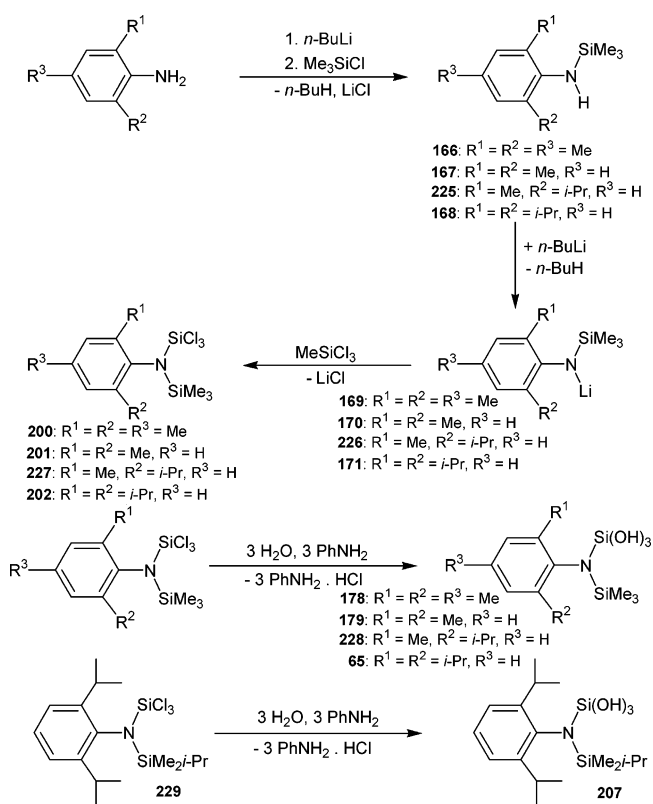


ence of aniline using diethyl ether as the solvent (Scheme 58).<sup>177</sup> It is noted here that this procedure was first used by Takiguchi for preparation of  $\text{PhSi}(\text{OH})_3$ .<sup>167</sup>

Roesky and co-workers pioneered the synthesis of a series of air-stable and lipophilic N-bonded silanetriols.<sup>10,178</sup> The synthetic strategy involves the use of a sterically hindered aromatic amine as the starting material. Typically the amines used included 2,6-*i*-Pr<sub>2</sub>-C<sub>6</sub>H<sub>3</sub>-NH<sub>2</sub>, 2,6-Me<sub>2</sub>-C<sub>6</sub>H<sub>3</sub>-NH<sub>2</sub>, 2-*i*-Pr-6-Me-C<sub>6</sub>H<sub>3</sub>-NH<sub>2</sub>, and 2,4,6-Me<sub>3</sub>-C<sub>6</sub>H<sub>2</sub>-NH<sub>2</sub>. Deprotonation of the aromatic amine followed by silylation with Me<sub>3</sub>SiCl or Me<sub>2</sub>(*i*-Pr)SiCl affords the silylated aromatic amines ArNHSiMe<sub>3</sub> [Ar = 2,4,6-Me<sub>3</sub>-C<sub>6</sub>H<sub>2</sub> (**166**), 2,6-Me<sub>2</sub>-C<sub>6</sub>H<sub>3</sub> (**167**), 2,6-*i*-Pr<sub>2</sub>-C<sub>6</sub>H<sub>3</sub> (**168**), 2-*i*-Pr-6-Me-C<sub>6</sub>H<sub>3</sub> (**225**)]. Further deprotonation of these silylated amines followed by reaction with silicon tetrachloride affords the N-bonded silicon trichlorides ArN(SiMe<sub>3</sub>)(SiCl<sub>3</sub>) [Ar = 2,4,6-Me<sub>3</sub>-C<sub>6</sub>H<sub>2</sub> (**200**), 2,6-Me<sub>2</sub>-C<sub>6</sub>H<sub>3</sub> (**201**), 2,6-*i*-Pr<sub>2</sub>-C<sub>6</sub>H<sub>3</sub> (**202**), 2-*i*-Pr-6-Me-C<sub>6</sub>H<sub>3</sub> (**227**)] as distillable oils or solids. Hydrolysis of these silicon trichlorides in diethyl ether using aniline affords the N-bonded silanetriols ArN(SiMe<sub>3</sub>)-Si(OH)<sub>3</sub> [Ar = 2,4,6-Me<sub>3</sub>-C<sub>6</sub>H<sub>2</sub> (**179**), 2,6-Me<sub>2</sub>-C<sub>6</sub>H<sub>3</sub> (**178**), 2,6-*i*-Pr<sub>2</sub>-C<sub>6</sub>H<sub>3</sub> (**65**), 2-*i*-Pr-6-Me-C<sub>6</sub>H<sub>3</sub> (**228**)] as air-stable lipophilic white solids (eq 1, Scheme 59).<sup>10</sup> In a similar way hydrolysis of 2,6-*i*-Pr<sub>2</sub>-C<sub>6</sub>H<sub>3</sub>-N(SiMe<sub>2</sub>Pr-*i*)(SiCl<sub>3</sub>) (**229**) affords the silanetriol 2,6-*i*-Pr<sub>2</sub>-C<sub>6</sub>H<sub>3</sub>-N(SiMe<sub>2</sub>Pr-*i*)(Si(OH)<sub>3</sub>) (**207**) (eq 2, Scheme 59).<sup>162</sup> Despite the presence of the Si-N bond, all of these N-bonded silanetriols are quite stable and can be handled in open air. The long shelf lives of many of these silanetriols is a good testimony to the efficacy of the strategy of using the sterically hindered substituents on silicon.

A silanetriol containing a Si-O bond also has been prepared. Thus, reaction of the lithium salt of 2,4,6-*t*-Bu<sub>3</sub>-C<sub>6</sub>H<sub>2</sub>-OH with silicon tetrachloride afforded the O-bonded silicon trichloride 2,4,6-*t*-Bu<sub>3</sub>-C<sub>6</sub>H<sub>2</sub>-OSiCl<sub>3</sub> (**230**). Hydrolysis of this material afforded the O-bonded silanetriol 2,4,6-*t*-Bu<sub>3</sub>-C<sub>6</sub>H<sub>2</sub>-OSi(OH)<sub>3</sub>

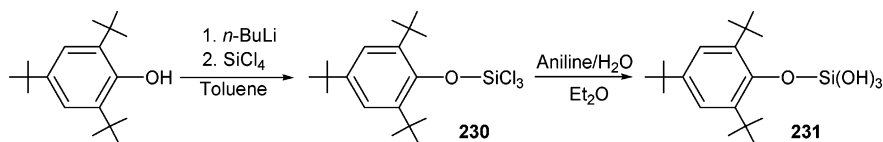
## Scheme 59



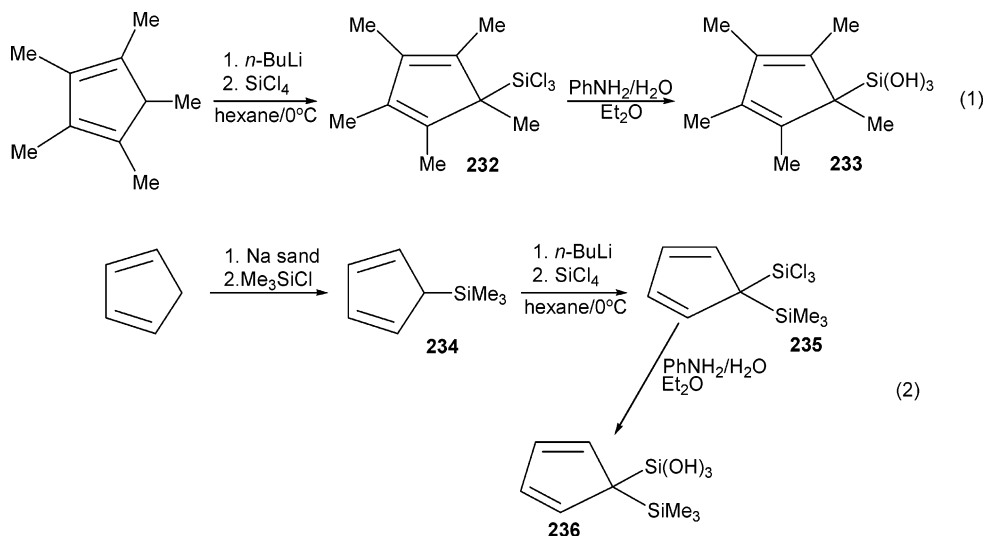
(**231**). However, this compound has not been found to be very stable (Scheme 60).<sup>178</sup>

(Pentamethylcyclopentadienyl)silanetriol ( $\eta^1\text{-Cp}^*$ )-Si(OH)<sub>3</sub> has been synthesized by utilizing a multistep procedure as shown in Scheme 61. Deprotonation of Cp\*H with *n*-BuLi followed by reaction with SiCl<sub>4</sub> affords the ( $\eta^1\text{-Cp}^*$ )SiCl<sub>3</sub> (**232**), which is hydrolyzed in the presence of aniline to afford ( $\eta^1\text{-Cp}^*$ )Si(OH)<sub>3</sub> (**233**) (eq 1, Scheme 52) as an amorphous solid that is soluble in a variety of organic solvents such as diethyl ether, THF, or acetone but poorly soluble in solvents such as toluene, chloroform, or hexane.<sup>179</sup> Further, although ( $\eta^1\text{-Cp}^*$ )Si(OH)<sub>3</sub> (**233**) is stable below 0 °C, it has been found to decompose slowly at room temperature even in the solid state. A slightly less sterically hindered cyclopentadienyl ligand containing silanetriol (5-(trimethylsilyl)cyclopenta-1,3-

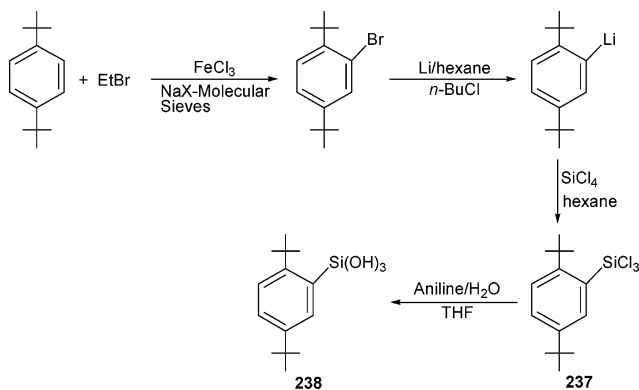
## Scheme 60



## Scheme 61



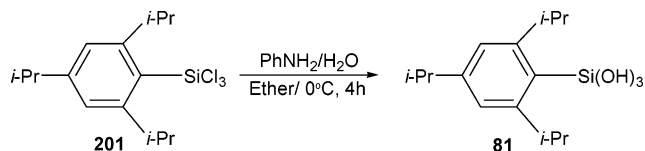
## Scheme 62



dien-5-yl)silanetriol,  $[\eta^1\text{-C}_5\text{H}_4(\text{SiMe}_3)]\text{Si}(\text{OH})_3$  (**236**) was also prepared. This was accomplished by first deprotonating cyclopentadiene with sodium followed by reaction with trimethylsilyl chloride to afford  $\text{C}_5\text{H}_5\text{SiMe}_3$  (**234**). Deprotonation of the trimethylsilyl-cyclopentadiene **234** and subsequent reaction with  $\text{SiCl}_4$  affords  $[\eta^1\text{-C}_5\text{H}_4(\text{SiMe}_3)]\text{SiCl}_3$  (**235**) as a colorless distillable oil. Hydrolysis of this compound in the presence of aniline affords the silanetriol  $\eta^1\text{-C}_5\text{H}_4\text{-}(\text{SiMe}_3)(\text{Si}(\text{OH})_3)$  (**236**) as a colorless solid which is soluble in solvents such as diethyl ether, THF, acetone, and acetonitrile but insoluble in aliphatic and aromatic solvents (eq 2, Scheme 52).<sup>180</sup> Exposure of  $\eta^1\text{-C}_5\text{H}_4(\text{SiMe}_3)(\text{Si}(\text{OH})_3)$  (**236**) to air has been found to cause slow decomposition. Using a similar procedure to that described above, 2,5-di-*tert*-butylphenylsilanetriol **238** has also been synthesized (Scheme 62).<sup>181</sup> A more sterically hindered silanetriol (**81**) from its trichloride (**201**) has been prepared by the aniline–water-mediated hydrolysis in a similar manner.<sup>113</sup>

Silanetriols containing Si–M bonds have been prepared by reaction of the corresponding trihydrides

## Scheme 63

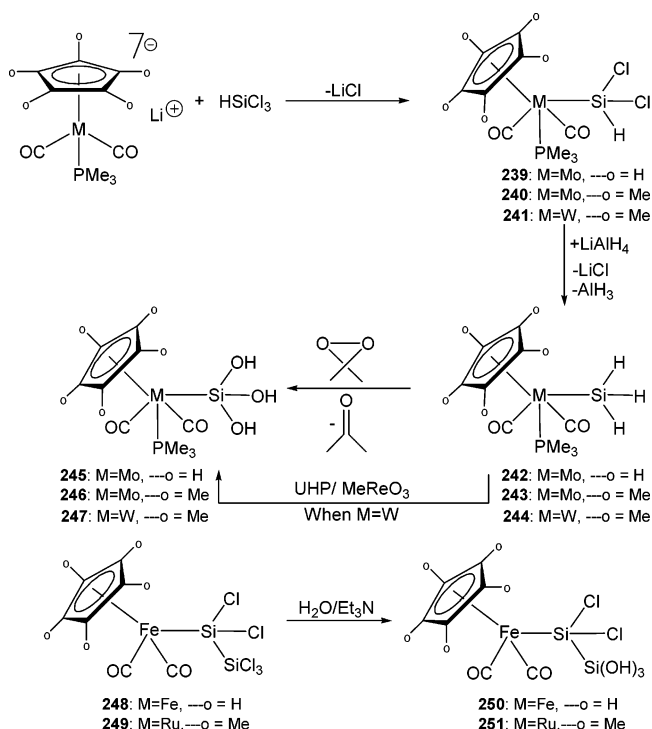


with dioxiranes. Reaction of  $(\eta^5\text{-Cp})\text{Mo}(\text{PMe}_3)(\text{CO})_2\text{-}(\text{SiH}_3)$  (**242**) or  $(\eta^5\text{-Cp}^*)\text{M}(\text{PMe}_3)(\text{CO})_2\text{SiH}_3$  [M = Mo (**243**) or W (**244**)] with dimethyldioxirane at  $-78^\circ\text{C}$  in toluene leads to isolation of the corresponding metal-bound silanetriols  $(\eta^5\text{-Cp})\text{Mo}(\text{PMe}_3)(\text{CO})_2\text{Si}(\text{OH})_3$  (**245**) or  $(\eta^5\text{-Cp}^*)\text{M}(\text{PMe}_3)(\text{CO})_2\text{Si}(\text{OH})_3$  [M = Mo (**246**) or W (**247**)] as beige to yellow crystalline powders (Scheme 64).<sup>182</sup> It has been shown that such silanetriols containing Si–M bonds can also be prepared by catalytic oxidation involving UHP/ $\text{MeReO}_3$ .<sup>76</sup> A remarkable regioselectivity has been observed in the hydrolysis of siliconchlorides. Thus, it has been shown that hydrolysis of  $(\eta^5\text{-Cp})\text{Fe}(\text{CO})_2\text{-SiCl}_2(\text{SiH}_3)$  (**187**) in the presence of triethylamine leads to formation of  $(\eta^5\text{-Cp})\text{Fe}(\text{CO})_2\text{Si}(\text{OH})_2(\text{SiH}_3)$  (**189**). In this case the M– $\text{SiCl}_2$  group is converted to the M– $\text{Si}(\text{OH})_2$  group during hydrolysis. If, however, the hydrolysis is carried out on  $(\eta^5\text{-Cp})\text{Fe}(\text{CO})_2\text{-SiCl}_2(\text{SiCl}_3)$  (**248**) or  $(\eta^5\text{-Cp}^*)\text{Ru}(\text{CO})_2\text{Si}(\text{Cl})_2(\text{SiCl}_3)$  (**249**), the M– $\text{SiCl}_2$  unit remains intact and only the Si– $\text{SiCl}_3$  group gets converted to the  $\text{Si}(\text{OH})_3$  group to afford the silanetriols  $(\eta^5\text{-Cp})\text{Fe}(\text{CO})_2\text{SiCl}_2(\text{Si}(\text{OH})_3)$  (**250**) or  $(\eta^5\text{-Cp}^*)\text{Ru}(\text{CO})_2\text{SiCl}_2(\text{Si}(\text{OH})_3)$  (**251**).<sup>159</sup>

A cobalt-cluster-bound silanetriol,  $\text{Co}_3(\text{CO})_9\text{CSi}(\text{OH})_3$  (**253**), has been prepared by hydrolysis of the corresponding silicontrichloride  $\text{Co}_3(\text{CO})_9\text{CSiCl}_3$  (**252**) (Scheme 65).<sup>183</sup>

Although synthesis of this silanetriol was reported in an earlier procedure,<sup>23</sup> the structure of the compound and its catalytic activity toward hydroformylation of olefins were reported only recently.<sup>183</sup>

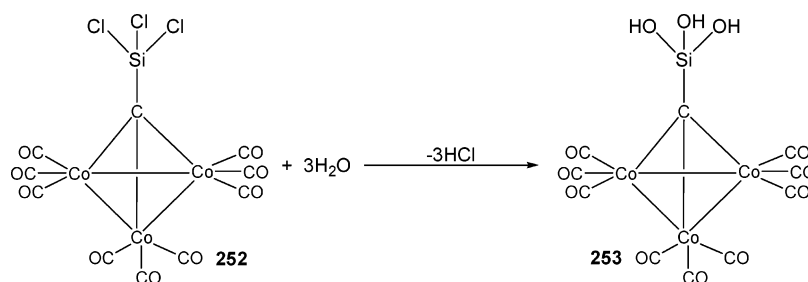
Scheme 64



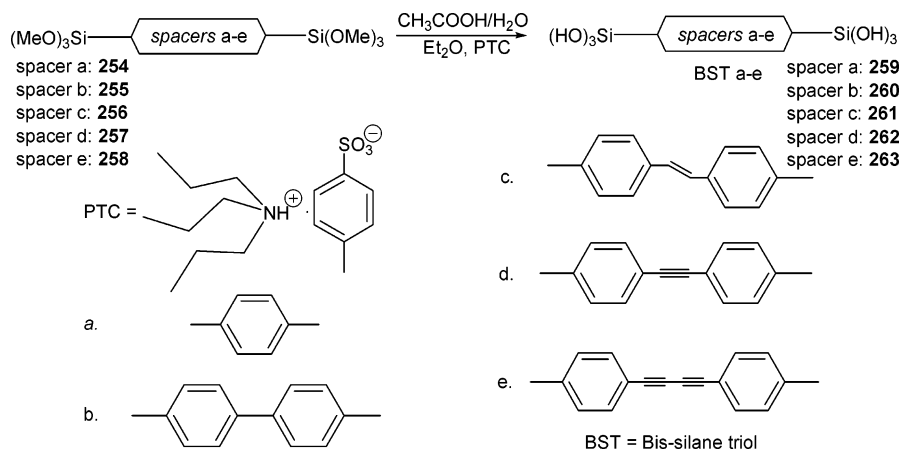
Bis-silanetriols (**259–263**) where the two  $Si(OH)_3$  units are linked by a series of aromatic spacer groups have been prepared by hydrolysis of the corresponding alkoxides (**254–258**). This hydrolysis is carried out in biphasic conditions (ether/water) using AcOH and a phase-transfer catalyst (triethylammonium *p*-toluenesulfonate salt) (Scheme 66).<sup>184,185</sup>

Many of the bis(silanetriols) are insoluble in solvents such as methanol, ethanol, 2-propanol, THF,

Scheme 65



Scheme 66



acetone, diethyl ether, and acetonitrile. However, they were found to be quite soluble in DMSO.

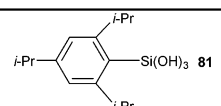
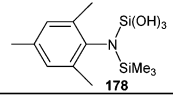
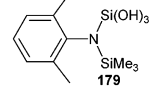
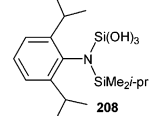
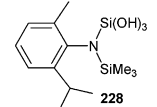
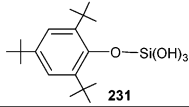
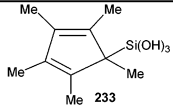
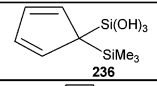

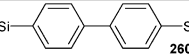
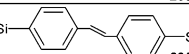
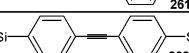
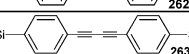
## 7.2. $^{29}Si$ NMR

$^{29}Si$  NMR data for the silanetriols are given in Table 9. Since a minimum of three oxygens are always present in the coordination environment of the silicon in this group of compounds, the chemical shift for  $-Si(OH)_3$  is always at a lower frequency reflecting the fact that silicons are highly shielded. The O-bonded silanetriol (2,4,6-*t*-Bu<sub>3</sub>-C<sub>6</sub>H<sub>2</sub>-O)Si(OH)<sub>3</sub> (**231**) containing a O<sub>4</sub> coordination environment is the most upfield shifted with a chemical shift of  $-83.6$  ppm (entry 6, Table 9).<sup>178</sup> The chemical shifts in the N-bonded silanetriols ArN(SiMe<sub>3</sub>)Si(OH)<sub>3</sub> (**178**, **179**, and **228**) and 2,6-*i*-Pr<sub>2</sub>-C<sub>6</sub>H<sub>3</sub>-N(SiMe<sub>2</sub>Pr-*i*)Si(OH)<sub>3</sub> (**207**)<sup>162</sup> are also considerably upfield and occur between  $-65.3$  and  $-72.3$  ppm (entries 2–5, Table 9). In other silanetriols such as ( $\eta^1$ -Cp\*)Si(OH)<sub>3</sub> (**233**),<sup>179</sup> TipSi(OH)<sub>3</sub> (**81**) (Tip = triisopropylphenyl), and the bis-silanetriol Si(OH)<sub>3</sub>-C<sub>6</sub>H<sub>4</sub>-Si(OH)<sub>3</sub> (**259**), the chemical shifts occur at  $-48.7$ ,  $-52.0$ , and  $-54.3$  ppm, respectively.<sup>185</sup> Interestingly, in the trimethylsilylcyclopentadienylsilanetriol ( $\eta^1$ -Cp)(SiMe<sub>3</sub>)Si(OH)<sub>3</sub> (**236**) although the coordination environment around silicon is CO<sub>3</sub>, an anomalous chemical shift of  $-72.3$  ppm is seen (entry 8, Table 9).<sup>180</sup> The overall trends in the chemical shifts of the silanetriols can be summarized in the order of increasing shielding at the silicon as C-bonded < N-bonded < O-bonded.

## 7.3. X-ray Crystal Structures of Silanetriols

X-ray crystal structural data for silanetriols are summarized in Table 10. In the metal-bound silanetriol OsCl(CO)(PPh<sub>3</sub>)<sub>2</sub>Si(OH)<sub>3</sub> a monomeric structure

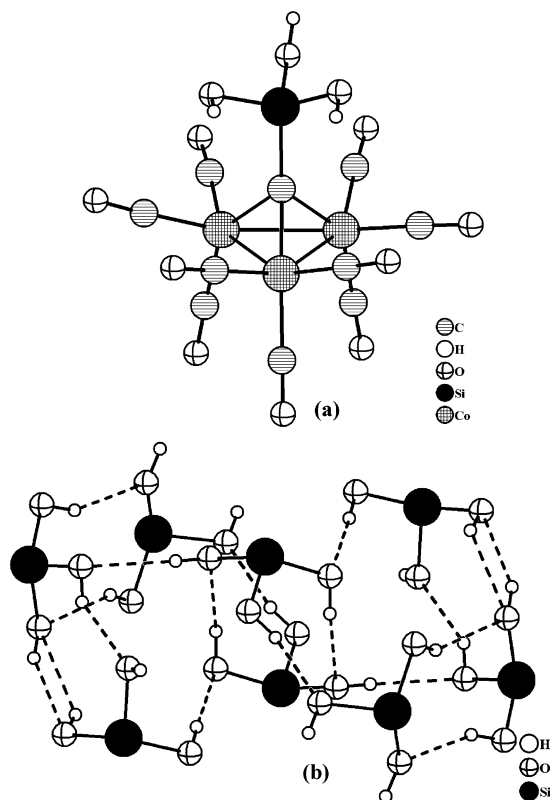
**Table 9.**  $^{29}\text{Si}$  NMR Data for Compounds Containing One or Two  $\text{Si}(\text{OH})_3$  Groups

S.No.	Compound	Coordination Environment around Silicon	$^{29}\text{Si}$ NMR (ppm)	Ref.
1	 <b>81</b>	$\text{CO}_3$	-52.0	113
2	 <b>178</b>	$\text{NO}_3$ $\text{NC}_3$	-65.8 7.3	10
3	 <b>179</b>	$\text{NO}_3$ $\text{NC}_3$	-66.2 7.7	10
4	 <b>208</b>	$\text{NO}_3$ $\text{NC}_3$	-72.3 10.8	162
5	 <b>228</b>	$\text{NO}_3$ $\text{NC}_3$	-65.3 7.5	10
6	 <b>231</b>	$\text{O}_4$	-83.6	178
7	 <b>233</b>	$\text{CO}_3$	-48.7	179
8	 <b>236</b>	$\text{C}_4$ $\text{CO}_3$	10.8 -72.3	180
9	 <b>259</b>	$\text{CO}_3$	-54.3	184, 185
10	 <b>260</b>	$\text{CO}_3$	-54.3	184, 185
11	 <b>261</b>	$\text{CO}_3$	-54.3	185
12	 <b>262</b>	$\text{CO}_3$	-55.2	185
13	 <b>263</b>	$\text{CO}_3$	-55.6	185

is found. No intermolecular  $\text{O}-\text{H}\cdots\text{O}$  or  $\text{O}\cdots\text{O}$  contacts have been found in this silanetriol.<sup>176</sup>

The crystal structures of  $c\text{-C}_6\text{H}_{11}\text{Si}(\text{OH})_3$ <sup>175</sup> and  $t\text{-BuSi}(\text{OH})_3$ , which have been discussed in a previous review,<sup>4</sup> show that these molecules arrange themselves in a *double-sheet structure* in a head-to-head and tail-to-tail manner. The alkyl groups and the  $-\text{OH}$  groups form alternating hydrophobic and hydrophilic double sheets. In contrast, hexameric cage structures are found for  $(\text{Me}_3\text{Si})_3\text{CSi}(\text{OH})_3$  and  $(\text{Me}_3\text{Si})_3\text{SiSi}(\text{OH})_3$ .<sup>4,172,173</sup> These polyhedral cages are formed as a result of extensive hydrogen bonding. Hydrogen bonding between the cages is completely absent. Another sterically hindered silanetriol  $(\text{Me}_2\text{PhSi})_3\text{CSi}(\text{OH})_3$  forms a tetrameric structure mediated by intermolecular hydrogen bonding.<sup>4</sup>

The cobalt-cluster-linked silanetriol  $\{\text{Co}(\text{CO})_3\}_3\text{CSi}(\text{OH})_3$  forms an octameric cage structure (Figure 43). Two types of  $\text{Si}-\text{O}$  bond distances are found, viz., 1.626(1) and 1.641(9) Å. An intricate intermolecular  $\text{O}-\text{H}\cdots\text{O}$  hydrogen bonding is formed in this com-

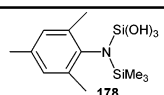
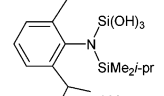
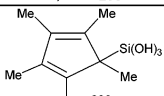
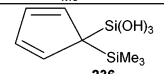
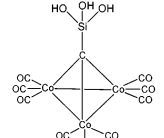



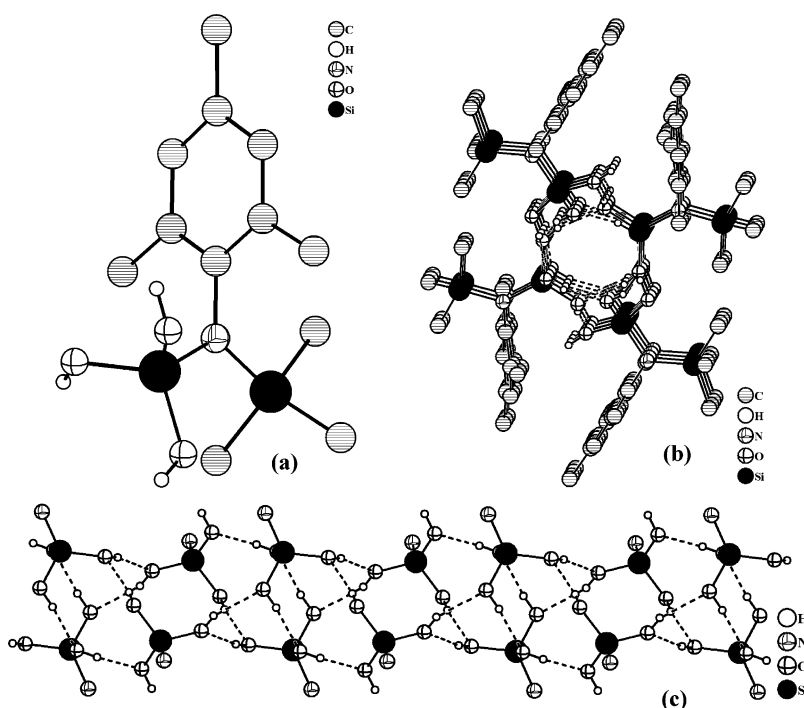
**Figure 43.** (a) Molecular structure of the cobalt cluster-linked silanetriol  $[\text{Co}_3(\text{CO})_9]\text{CSi}(\text{OH})_3$  (**253**). (b) Formation of an octameric cluster as a result of intricate  $\text{OH}\cdots\text{O}$  hydrogen bonds. The  $\text{Co}_3(\text{CO})_9$  units are omitted for clarity.

ound, resulting in the formation of a hydrogen-bonded cluster comprised of eight silicon atoms. The octameric cluster is formed as a result of two symmetry-related tetrameric units being joined together by hydrogen bonding (Figure 43). One of the  $\text{H}\cdots\text{O}$  distances found in these hydrogen bonds is slightly longer (2.410(1) Å), while the other is quite normal (2.055(8) Å). This is reflected in the  $\text{O}\cdots\text{O}$  contacts as well (2.808(1) and 3.173(2) Å, respectively). Also, two types of  $\text{O}-\text{H}\cdots\text{O}$  bond angles are found: a smaller angle of 138.32(4)° and a larger angle of 167.31(7)°, respectively.<sup>183</sup>

In the N-bonded silanetriols, two X-ray crystal structures are known. Thus, 2,4,6- $\text{Me}_3\text{C}_6\text{H}_2\text{N}(\text{SiMe})_3\text{Si}(\text{OH})_3$  (**178**) forms a polymeric tubular network (Figure 44) through extensive inter- and intramolecular hydrogen bonding. The molecules in this compound form linear columns which are arranged in a tubular manner. A perpendicular view along this hydrogen-bonded array shows the presence of a hydrophobic exterior and a hydrophilic interior. The  $\text{O}\cdots\text{O}$  contacts (2.618(2) and 2.819(2) Å) that occur as a result of intermolecular hydrogen bonding indicate the formation of strong hydrogen bonding. Infrared spectra of this compound as a KBr pellet, Nujol mull, or in carbontetrachloride solution (in various concentrations) reveal the presence of a major broad band at  $3400\text{ cm}^{-1}$  and a band of lesser intensity at  $3592\text{ cm}^{-1}$ . The former is due to the stretching frequency of the hydrogen-bonded OH, while the latter is due to the free hydroxyl groups.<sup>10</sup> An increase in the steric bulk in the silanetriol 2,6-

Table 10. X-ray Structural Data for Compounds Containing One or More than One Si(OH)<sub>3</sub> Group

S.No.	Compound	Hydrogen bonding parameters				Structural Summary	Ref.
		Si-OH (Å)	OH...O (Å)	O...O (Å)	O-H...O (°)		
1	 178	1.612(2)- 1.644(2)	1.918(3)- 2.057(3)	2.618(2)- 2.819(2)	149.10(3)- 169.23(1)	Tubular network	10
2	 208	1.619(3)- 1.634(3)	1.902(6)- 2.376(8)	2.700(9)- 3.041(9)	130.56(3)- 163.73(3)	Tetrameric structure	162
3	 233	1.627(2)- 1.630(2)	1.863(1) - 2.143(1)	2.650(4)- 2.760(6)	130.05(2)- 164.66(3)	Two-dimensional layered structure	179
4	 236	1.625(1)- 1.634(1)	1.916(1) - 1.977(1)	2.694(2) - 2.787(1)	153.16(2)- 173.57(3)	Tubular network	180
5	 253	1.626(1)- 1.641(9)	2.410(1)- 2.055(8)	2.808(1)- 3.173(2)	138.32(4)- 167.31(7)	Octameric structure	183
6	 259	1.591(1)- 1.680(1)	-	2.588(1)- 2.825(3)	-	Three-dimensional pillared structure	184

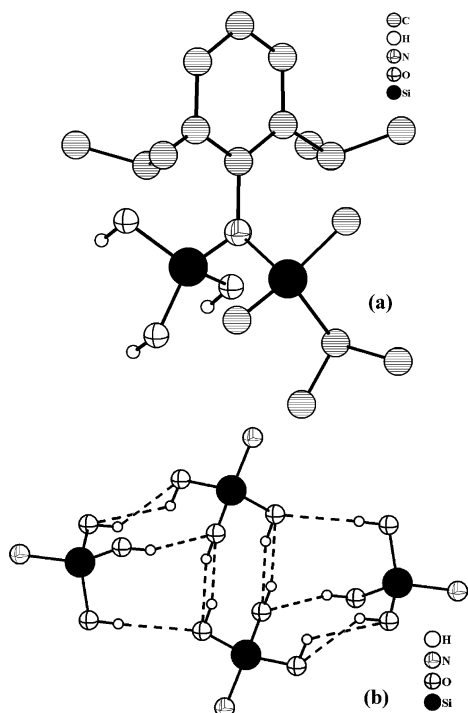


**Figure 44.** (a) DIAMOND picture of the N-bonded silanetriol 2,4,6-Me<sub>3</sub>-C<sub>6</sub>H<sub>2</sub>-N(SiMe<sub>3</sub>)Si(OH)<sub>3</sub> (**178**). (b) Formation of a tubular array consisting of a hydrophobic exterior and hydrophilic interior. (c) View of the tubular network formed as a result of inter- and intramolecular hydrogen bonds.

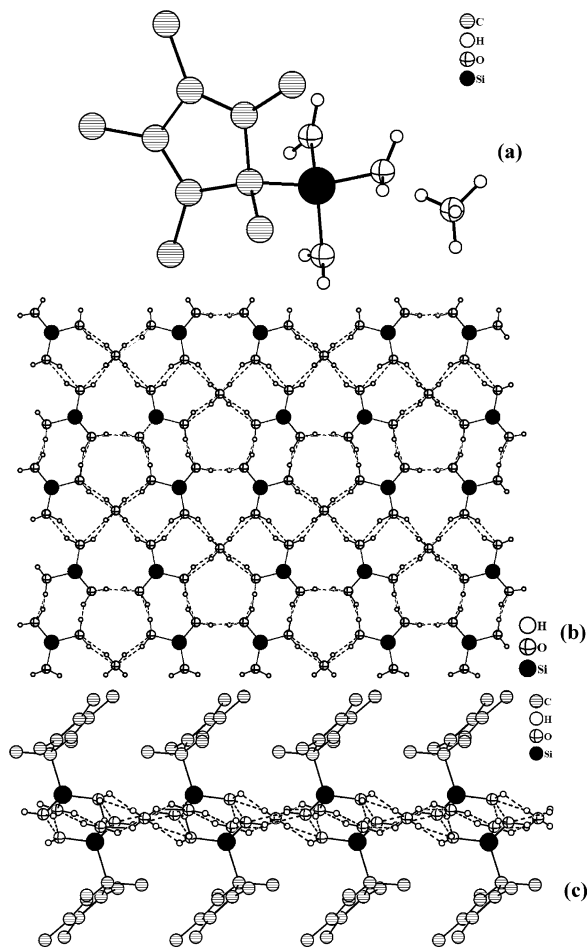
*i*-Pr<sub>2</sub>-C<sub>6</sub>H<sub>3</sub>-N(SiMe<sub>2</sub>Pr-*i*)Si(OH)<sub>3</sub> (**207**) causes the formation of a tetrameric structure (Figure 45). In this structural arrangement a central dimeric structure is formed which contains two O<sub>2</sub>H<sub>2</sub> rings. Either side of this dimer is further hydrogen bonded to one molecule of the triol, generating the tetrameric agglomerate.<sup>162</sup> It is interesting to note that as in the case of the N-bonded silanediols where a subtle increase in steric bulk causes the solid-state structure to change from a polymeric sheet to a hexameric cluster, in the case of N-bonded silanetriols a some-

what similar trend is seen also. However, more examples are required to verify this trend.

( $\eta^1$ -Cp\*)Si(OH)<sub>3</sub> crystallizes as its hemihydrate. It forms a two-dimensional layered structure (Figure 46). The organic Cp\* groups are arranged in a nearly parallel manner in the periphery of the sheet, while the hydrophilic Si(OH)<sub>3</sub> groups along with the water of crystallization form the inner core of the sheet structure.<sup>179</sup> The X-ray crystal structure of ( $\eta^1$ -Cp)-Si(OH)<sub>3</sub> is analogous to that of the N-bonded silanetriol ArN(SiMe<sub>3</sub>)Si(OH)<sub>3</sub> (Ar = 2,4,6-Me<sub>3</sub>C<sub>6</sub>H<sub>2</sub>).



**Figure 45.** (a) X-ray crystal structure of the N-bonded silanetriol 2,6-*i*-Pr<sub>2</sub>-C<sub>6</sub>H<sub>3</sub>-N(SiMe<sub>2</sub>*i*-Pr)Si(OH)<sub>3</sub> (207). (b) Formation of a tetrameric structure as a result of intermolecular hydrogen bonding.



**Figure 46.** (a) Crystal structure of (η<sup>1</sup>-Cp\*)Si(OH)<sub>3</sub>·0.5H<sub>2</sub>O (233). (b) Formation of a layered network as a result of hydrogen bonding among the silanetriol and the water molecules. (c) Parallel arrangement of the Cp\* rings above and below the planar hydrogen-bonded network.

Thus, hydrogen-bonded columns form a tubular network. A perpendicular view of this network shows a hollow hydrophilic core surrounded by the hydrophobic exterior (Figure 47).<sup>180</sup>

Although single crystals of the bis-silanetriol Si(OH)<sub>3</sub>-C<sub>6</sub>H<sub>4</sub>-Si(OH)<sub>3</sub> (259) could not be obtained, its structure was determined from its powder diffraction data by the use of the Rietveld method.<sup>184</sup> Two types of Si-O distances (1.591(1) and 1.680(1) Å) are found. Although the hydrogens could not be located based on the intermolecular O···O contacts, it is observed that this compound forms a three-dimensional pillared structure (Figure 48). The key feature of the hydrogen bonding is that every oxygen atom is involved in a bifurcated hydrogen bonding. The structure of this compound is comprised of interconnected layered sheets. Each layer is built as a result of hydrogen bonding between the Si(OH)<sub>3</sub> units. This results in a hydrophilic region. The hydrophobic region of the layer contains the phenyl spacer group. The layers are interconnected by O-H···O hydrogen bonds. The cumulative effect of these interactions is the formation of a 3D pillared structure where the phenyl spacer groups act as pillars between the hydrophilic sheet segments.<sup>184</sup>

## 8. Emerging Applications of Silanols

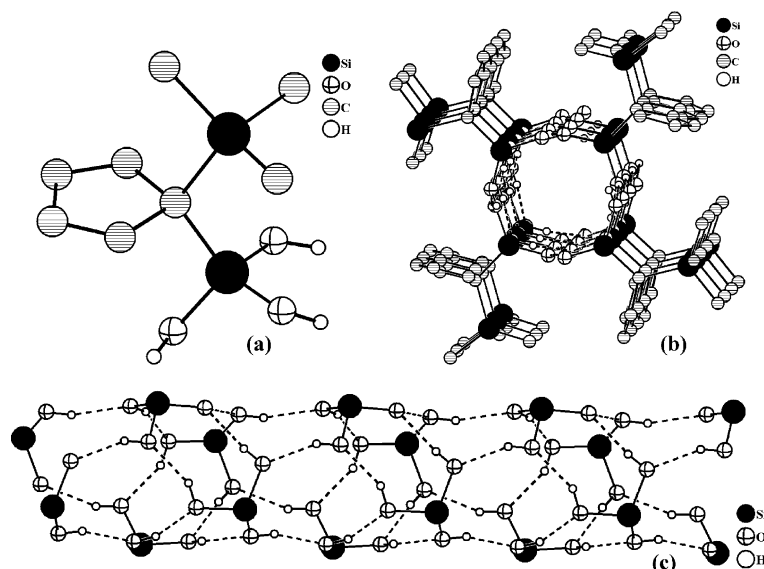
### 8.1. Metallasiloxanes

Although the focus of this review is the synthesis and structures of silanols, some of the emerging applications of these compounds are presented briefly. This is not a comprehensive treatment, and a few examples are chosen to illustrate the diverse new applications of silanols.

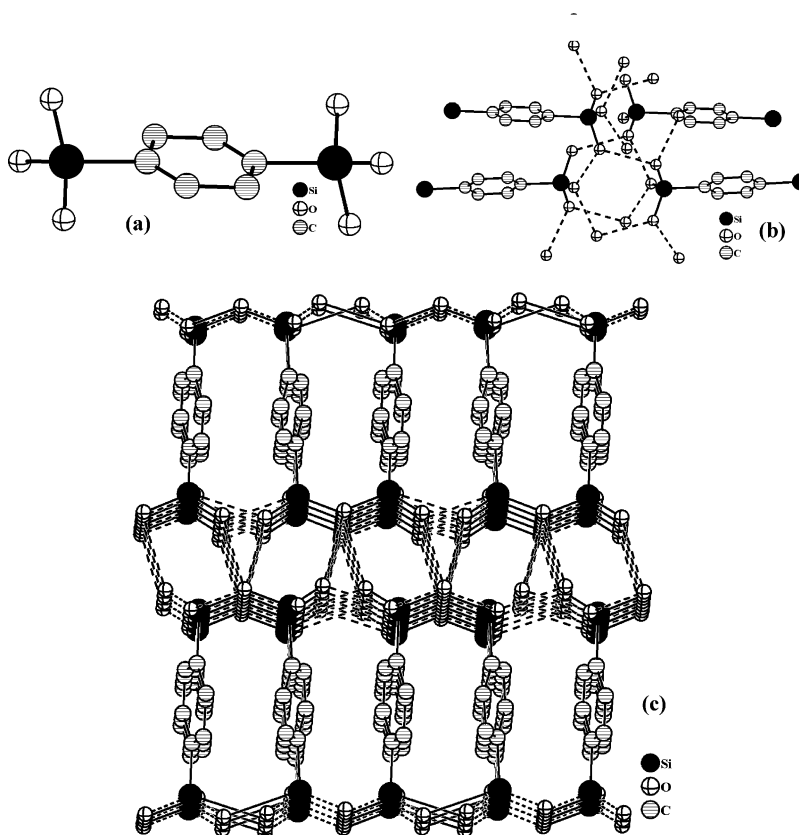
Traditionally silanols have been used as synthons for the construction of metallasiloxanes. This aspect has been the theme of many recent review articles.<sup>81,100,101,186–188</sup> Suffice it to say that the reactions of silanols with metal halides, metal alkyls, metal amides, metal alkoxides, or metal hydrides can lead to formation of a Si-O-M bond. Depending on the reaction conditions and the type of silanol used, products ranging from acyclic architectures to complex three-dimensional cage structures are readily realized. Mention has already been made on the utility of incompletely condensed silsesquioxane silanols.<sup>100,126</sup> The reactivity of N-bonded silanetriols is also a case in point in exemplifying the multitude of metallasiloxanes that can be obtained from a single synthon. Some representative examples of cyclic and cage products obtained in reactions of N-bonded silanetriols are shown in Schemes 67 and 68.<sup>109,189–196,178</sup>

### 8.2. Ceramic Applications

There have been various attempts to design silanols that would lead to the formation of metallasiloxanes which themselves can be used as single-source precursors for ceramics. Tilley and co-workers used the tris(*tert*-butoxy)silanol (*t*-BuO)<sub>3</sub>SiOH (TBSH) to a large extent and the bis(*tert*-butoxy)silanediol (*t*-BuO)<sub>2</sub>Si(OH)<sub>2</sub> (BBSH) to some extent for this purpose.<sup>197–204</sup>



**Figure 47.** (a) Molecular structure of  $(\eta^1\text{-Cp})(\text{SiMe}_3)\text{Si}(\text{OH})_3$  (**236**). (b) Formation of the hollow hydrophilic core and a hydrophobic exterior as a result of  $\text{OH}\cdots\text{O}$  hydrogen bonding. (c) Inner view of the tubular network formed.



**Figure 48.** (a) Molecular structure of the bis-silanetriol (**259**). (b) Various hydrogen-bonding interactions of a single molecule of **259** with its neighbors. (c) Double-layered arrangement of the bis-silanetriol molecules forming a three-dimensional pillared structure.

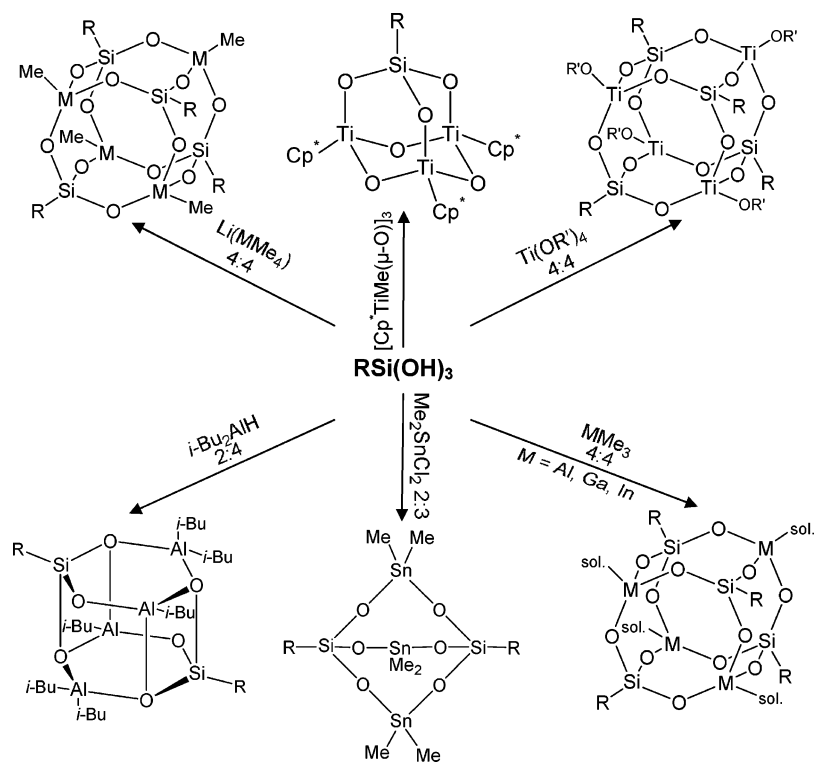
Reaction of dialkylzinc  $\text{ZnMe}_2$  with TBSH occurs in either a 1:2 or 1:1 stoichiometric ratio at  $-40^\circ\text{C}$  in toluene (eqs 1 and 2, Scheme 69). Elimination of methane leads to formation of the corresponding zinc siloxides **264** and **265**. Thus, in the 1:2 reaction both methyl groups are eliminated and the product obtained is  $\text{Zn}(\text{OSi}(\text{OR})_3)_2$  ( $\text{R} = t\text{-Bu}$ ; **264**) (eq 1, Scheme 69).<sup>197</sup>

This product is an asymmetric dimer in the solid state. The 1:1 reaction also leads to formation of a

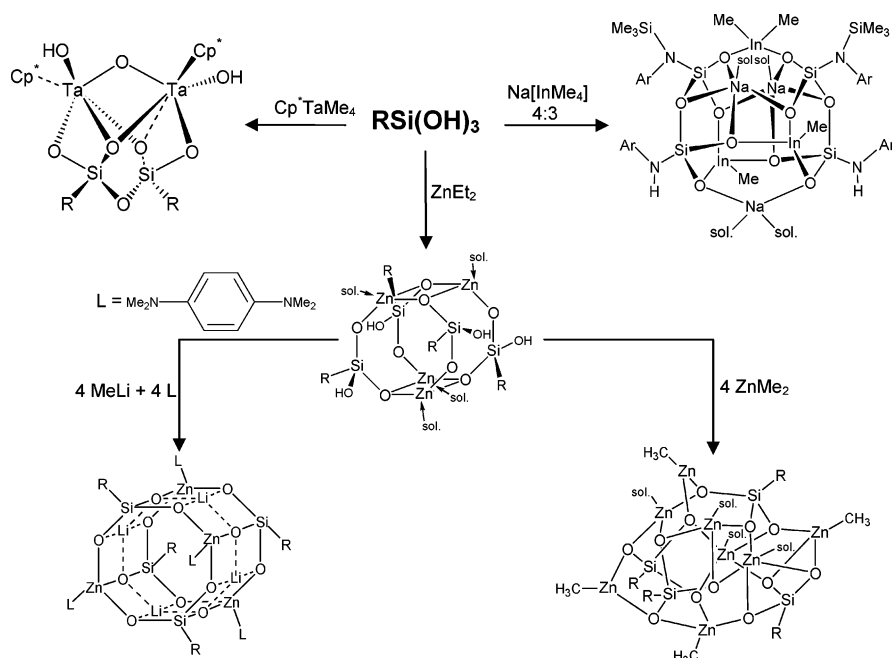
dimeric compound  $[\text{MeZn}\{\mu\text{-OSi}(\text{OR})_3\}]_2$  (**265**) (eq 2, Scheme 69). In contrast, reaction of  $\text{ZnMe}_2$  with the silanediol BBSH leads to the formation of a medium molecular weight polymer  $[\text{ZnOSi}(\text{OR})_2\text{O}]_n$  (**266**) (eq 3, Scheme 69).<sup>197</sup> All three zinc siloxides can be decomposed at relatively low temperatures. Thus, thermolysis of  $[\text{ZnOSi}(\text{OR})_2\text{O}]_n$  (**266**) leads to its complete conversion to a ceramic of composition  $\text{Zn}_2\text{-SiO}_4\cdot\text{SiO}_2$ . This low-temperature decomposition is facilitated by elimination of the *tert*-butyl groups as



Scheme 67



Scheme 68

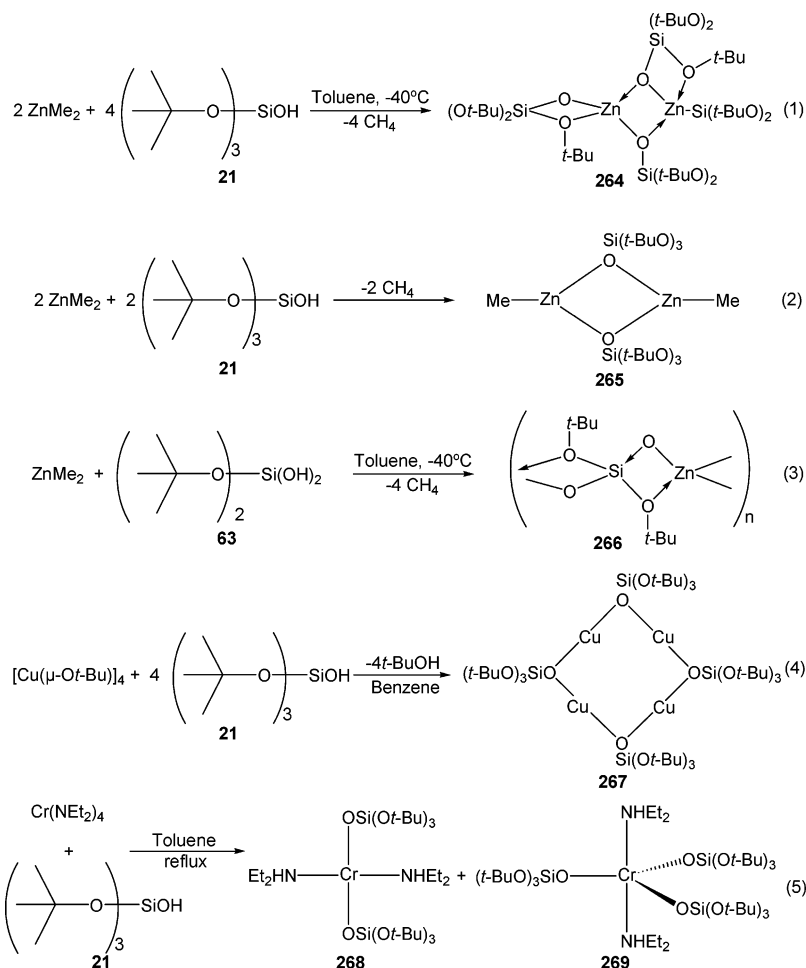


isobutene. The other products that are eliminated include *tert*-butyl alcohol and water. In the decomposition of  $[\text{Zn}(\text{OSi}(\text{OR})_3)_2]_2$  (**264**), similar decomposition products are formed. In addition, elimination of TBSH is also noticed. The most important feature of these thermolytic conversions is that (a) these are low-temperature processes, (b) the final ceramic obtained in each case is carbon and hydrogen free, and (c) the ceramic is also free of ZnO. For example, sol-gel processes to produce the above ceramic lead also to formation of ZnO. Using the above procedure it has also been shown that manganese-doped  $\text{Zn}_2\text{-SiO}_4\cdot\text{SiO}_2$  phosphors could be prepared which show

phosphorescent bands at 535 and 605 nm. The former is dependent on the extent of manganese doping.<sup>197</sup>

Reaction of copper(I) *tert*-butoxide  $[\text{Cu}(\text{OR})_4]$  ( $\text{R} = t\text{-Bu}$ ) with TBSH leads to formation of copper siloxide,  $[\text{CuOSi}(\text{OR})_3]_4$  (**267**) (eq 4, Scheme 69). The byproduct in this reaction is *tert*-butyl alcohol. Although the X-ray crystal structure of  $[\text{CuOSi}(\text{OR})_3]_4$  (**267**) could not be determined, the structure of its analogue  $[\text{CuOSi}(\text{Ph})(\text{OR})_2]_4$  shows that its structure is comprised of a planar  $\text{Cu}_4\text{O}_4$  ring with noninteracting oxygen-bridged copper(I) centers. The thermolysis of  $[\text{CuOSi}(\text{OR})_3]_4$  ( $\text{R} = t\text{-Bu}$ ) in argon leads to a material that has been identified to contain Cu-

## Scheme 69



(0) and  $\text{Cu}_2\text{O}$  nanoparticles dispersed in silica. In contrast, thermolysis in oxygen atmosphere leads to generation of a material that contains  $\text{CuO}$  nanoparticles dispersed in silica. The volatility of  $[\text{CuOSi}(\text{OR})_3]_4$  allowed formation of thin films containing  $\text{Cu/Si}$  in a ratio of 1:0.85 with varying thickness (200 nm to 6  $\mu\text{m}$ ).<sup>198</sup>

Reaction of the chromium amide  $\text{Cr}(\text{NEt}_2)_4$  with TBSH in refluxing toluene leads to formation of green (Cr(II)) and purple (Cr(III)) complexes in a 1:8 ratio. The green complex  $\text{Cr}(\text{OSi}(\text{OR})_3)_2(\text{NHEt}_2)_2$  (**268**) is square planar with a trans geometry (eq 5, Scheme 69). The purple compound is the pentacoordinate trigonal bipyramidal complex  $\text{Cr}(\text{OSi}(\text{OR})_3)_3(\text{NHEt}_2)_2$  (**269**). The equatorial positions in the trigonal bipyramidal structure are occupied by the bulky siloxy ligands.<sup>199</sup>

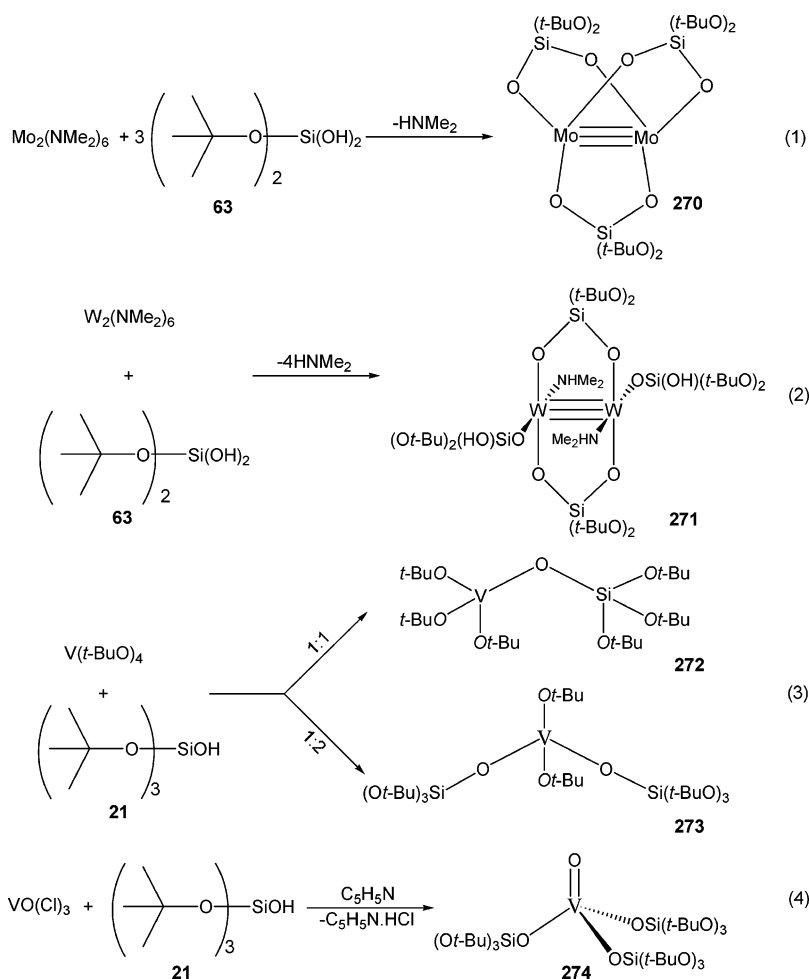
Reaction of  $\text{Mo}_2(\text{NMe}_2)_6$  with BBSH in *n*-pentane at room temperature occurs to afford  $\text{Mo}_2[\text{O}_2\text{Si}(\text{OR})_2]_3$  (**270**) (eq 1, Scheme 70). The silanediol binds the molybdenum in a chelating mode. Complete elimination of dimethylamine is also noticed in this reaction. In the analogous reaction with  $\text{W}_2(\text{NMe}_2)_6$ , the product obtained  $[\text{W}_2(\text{NHMe})_2(\text{O}_2\text{Si}(\text{OR})_2)_2(\text{OSi}(\text{OH})(\text{O}t\text{-Bu})_2)_2]$  (**271**) contains both chelating and monocoordinate silanediol moieties. The structure of compound **271** is of the A-frame type with the two dimethylamine groups completing the coordination around tungsten. Compound **270** can be thermolyzed at 550  $^\circ\text{C}$  to afford a ceramic material with an approximate

composition of  $\text{Mo}_2\text{Si}_3\text{O}_{10}$ . At 1200  $^\circ\text{C}$  a final, nearly carbon-free, ceramic with a composition of  $\text{Mo}_{0.5}\text{Si}_3\text{O}_{6.5}$  is formed via the loss of  $\text{MoO}_3$ . On the other hand, pyrolysis of **271** at 1200  $^\circ\text{C}$  affords a crystalline ceramic with composition  $\text{W}_{2.2}\text{Si}_4\text{O}_{13}$ . This has been shown by XRD analysis to contain crystalline  $\text{W}$  and  $\text{WO}_2$ .<sup>200</sup>

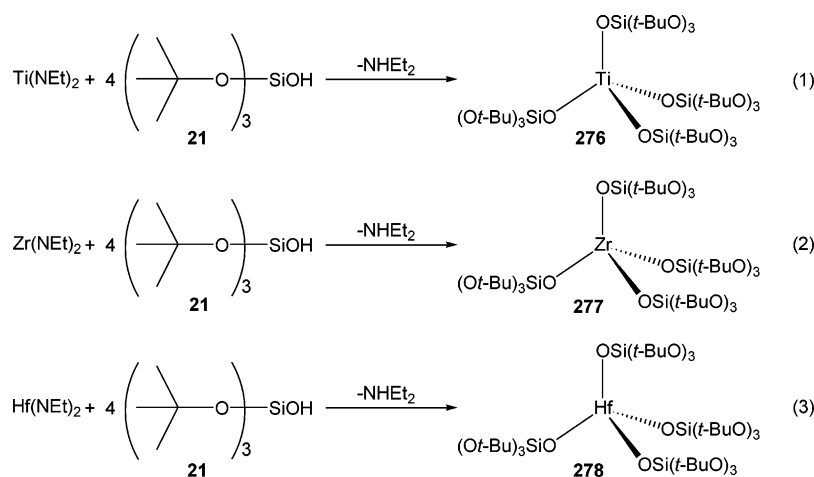
Reaction of  $\text{V}(\text{O}t\text{-Bu})_4$  with TBSH in 1:1 or 1:2 stoichiometry leads to formation of  $(\text{O}t\text{-Bu})_3\text{V}\{\text{OSi}(\text{O}t\text{-Bu})_3\}$  (**272**) and  $(\text{O}t\text{-Bu})_2\text{V}\{\text{OSi}(\text{O}t\text{-Bu})_3\}_2$  (**273**) (eq 3, Scheme 70).<sup>201</sup> On the other hand, reaction of  $\text{V}(\text{O})\text{Cl}_3$  with TBSH in the presence of pyridine leads to formation of  $\text{V}(\text{O})\{\text{OSi}(\text{O}t\text{-Bu})_3\}_3$  (**274**) (eq 4, Scheme 70).<sup>202</sup> Compounds **272** and **273** can be decomposed both in the solid state and in solution to afford materials with compositions  $\text{VO}_{2.5}\cdot\text{SiO}_2$  and  $\text{VO}_{2.5}\cdot 2\text{SiO}_2$ , respectively. The solution thermolysis was carried out in *n*-octane solutions at 180  $^\circ\text{C}$ . The latter method produces dark brown gels which upon air-drying afforded V/Si/O-containing xerogels. Similarly, decomposition of **274** in *n*-octane leads to formation of a green gel which upon air-drying affords a xerogel with a surface area of 320  $\text{m}^2 \text{g}^{-1}$ . The calcined xerogel prepared from **274** was found to be as effective as  $\text{V}_2\text{O}_5$  in the oxidative dehydrogenation of propane to propene.<sup>202</sup>

Tetrakis siloxides of titanium, zirconium, and hafnium (**276**–**278**) were prepared by reactions of the corresponding diethylamides with TBSH (eqs 1–3, Scheme 71). The titanium derivative  $\text{Ti}[\text{OSi}(\text{OR})_3]_4$

Scheme 70



Scheme 71



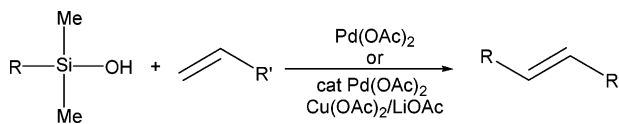
(R = *t*-Bu) (**276**) is readily converted to homogeneous  $\text{TiO}_2 \cdot 4\text{SiO}_2$  material both by a solid state as well as a solution thermolysis.<sup>203</sup> The latter yields a xerogel and possesses a high surface area of  $552 \text{ m}^2 \text{ g}^{-1}$ . Compound **276** has been found to be a homogeneous catalyst for the selective epoxidation of cyclohexene to cyclohexene oxide.<sup>203</sup> Supporting **276** on silica affords an even better catalyst for the epoxidation reaction. Similarly, the siloxides **277** and **278** have been shown to be excellent single-source precursors for the preparation of homogeneous ceramics with composition  $\text{MO}_2 \cdot 4\text{SiO}_2$  (M = Zr, Hf). In these com-

pounds it has been demonstrated also that solution thermolysis leads to high surface area xerogels.<sup>204</sup>

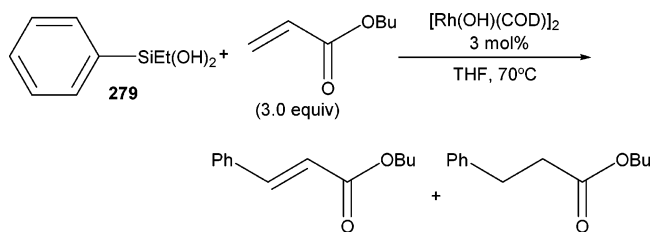
### 8.3. Cross-Coupling Reactions

Organosilanols (monosilanols, silanediols, and silanetriols) are finding new applications in organic synthesis.<sup>205</sup> Thus, the silanetriol [tris(tricarbonylcobaltio)methylene]silanetriol,  $[\text{Co}_3(\text{CO})_9]\text{CSi}(\text{OH})_3$ , has been tested for the hydroformylation of 1-hexene. In a biphasic system high conversions (97–98%) and high chemoselectivities were observed.<sup>183</sup>

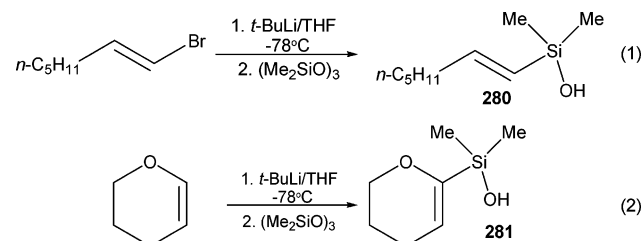
## Scheme 72



## Scheme 73



## Scheme 74



Mori and co-workers initially showed that aryl and alkenyl silanols underwent Mizoroki–Heck-type reaction with an olefin (Scheme 72).<sup>206</sup>

More recently this group has shown that organosilanediods can be used in a hydroxorhodium complex-catalyzed C–C bond-forming reaction with  $\alpha,\beta$ -unsaturated carbonyl compounds (Scheme 73).

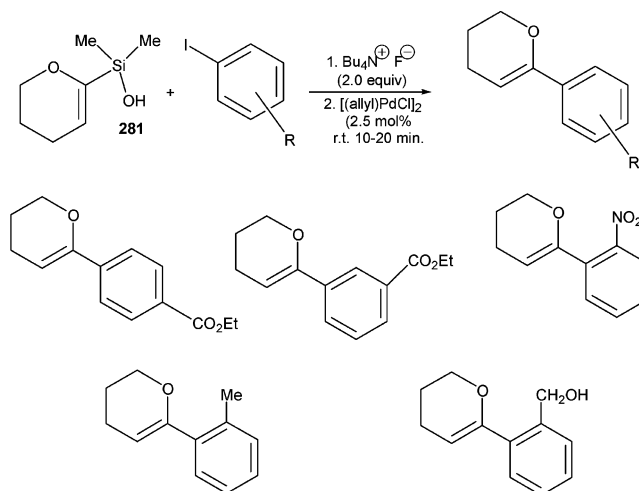
Thus, reaction of ethyl phenyl silanediol with *n*-butyl acrylate catalyzed by 3 mol % of [Rh(OH)(COD)]<sub>2</sub> afforded *n*-butyl-3-phenyl acrylate in 81% yield with a minor amount of the conjugate adduct. However, the yield of the conjugate adduct can be dramatically increased by conducting the reaction in THF/water instead of THF. Silanediods are the best substrates for this reaction. Thus, although the reaction proceeds with the monosilanol (4-Me C<sub>6</sub>H<sub>4</sub>)-SiMe<sub>2</sub>OH, the yield of the product is low. Other  $\alpha,\beta$ -unsaturated carbonyl compounds that were successfully used for this reaction are CH<sub>2</sub>=CHCO<sub>2</sub>Et, CH<sub>2</sub>=CHCO<sub>2</sub>Me, CH<sub>2</sub>=CH–CO<sub>2</sub>CH<sub>2</sub>CF<sub>3</sub>, CH<sub>2</sub>=CHCO<sub>2</sub>*t*-Bu, CH<sub>2</sub>=CHCONMe<sub>2</sub>, and CH<sub>2</sub>=CHCONH*t*-Bu.<sup>207</sup>

Organosilanediods have also been used in cross-coupling reactions. Alkenyl silanols such as **280** and **281** that could be synthesized by the procedure shown in Scheme 74 were employed as substrates.<sup>205</sup>

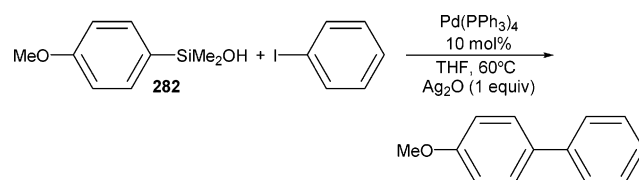
Such silanols were used in palladium-catalyzed, fluoride-promoted, cross-coupling reactions with aryl iodides (Scheme 75).<sup>205</sup> Recently this reaction was used in silver-oxide-promoted conditions (Scheme 76).<sup>208</sup>

It was found that cross-coupling reaction of iodobenzenes occurs effectively in the presence of Ag<sub>2</sub>O. A number of substituted iodobenzenes could be used. Silanediods and -triols were found to be even better substrates; lower reaction times are required. Indeed, even crude silanediods and -triols were found to be adequate (Scheme 77).<sup>209</sup>

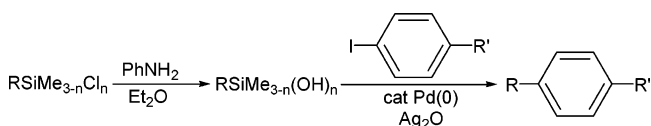
## Scheme 75



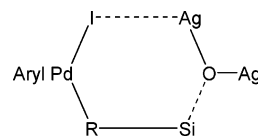
## Scheme 76



## Scheme 77



## Chart 10



The role of Ag<sub>2</sub>O appears to be 2-fold. (1) It acts as a nucleophilic activator of the silanols which also facilitates the transfer of an organic group on silicon to palladium. (2) In view of the iodophilicity of silver, Ag<sub>2</sub>O also appears to interact with the arylpalladium iodide complex which is formed as a result of the oxidative addition of the aryl iodide with palladium.<sup>209</sup> Powder X-ray diffraction reveals the formation of AgI. These cumulative interactions of Ag<sub>2</sub>O with silanol and Ar–Pd–I are shown in Chart 10.

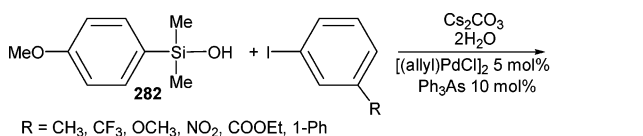
The palladium-catalyzed cross-coupling of aryl silanols with aryl iodides and aryl bromides (in the presence of cesium carbonate) furnished various biaryl products in high yields.<sup>210</sup>

In the place of Ag<sub>2</sub>O, cesium carbonate has also been found to be an activator. Thus, the palladium (allyl palladium complex) catalyzed cross-coupling of arylsilanols with aryl iodides and aryl bromides were found to be promoted by cesium carbonate to afford biaryl products in high yields (Scheme 78).<sup>210</sup>

## 8.4. Protease Inhibitors

Specifically designed silanediods<sup>211–213</sup> have been recently investigated as metalloprotease inhibitors.

Scheme 78



Scheme 79

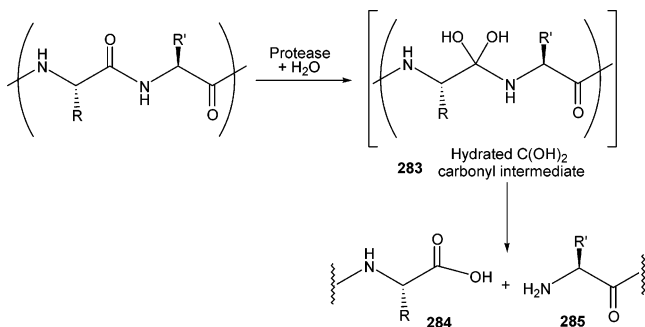
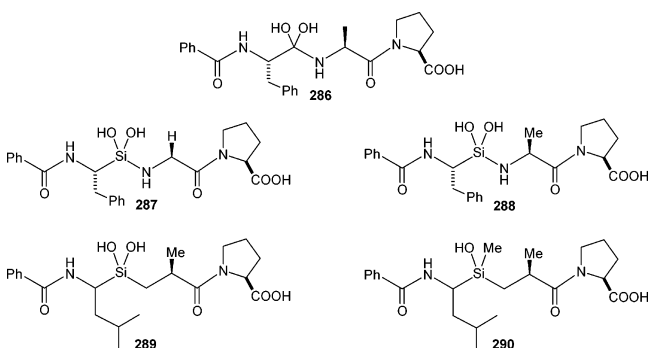


Chart 11

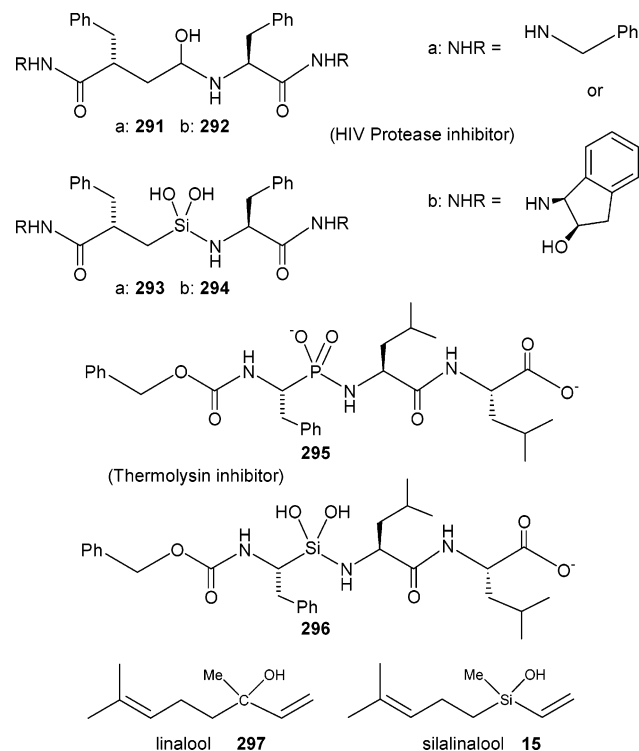


The idea of utilizing a silanediol for this purpose stems from the recognition that the Si(OH)<sub>2</sub> group can emulate an unstable C(OH)<sub>2</sub> group. The latter are the hydrated intermediates involved in the protease-mediated hydrolysis of peptides.<sup>214</sup> Metalloproteases and aspartic proteases catalyze the addition of water to an amide to generate unstable geminal C(OH)<sub>2</sub> intermediates of the type **283** which decompose into the amide and carboxylic acid (Scheme 79).

One of the possibilities for the design of a protease inhibitor is a nonhydrolyzable isostere of the tetrahedral carbonyl intermediate **283**. Such transition-state analogues have potential applications in drug design.<sup>215,216</sup> Recently silanol and silanediol peptide analogues have been synthesized and evaluated as inhibitors of angiotensin-converting enzyme (ACE).<sup>211,214</sup>

ACE is a zinc-containing metalloprotease and generates angiotensin II, which raises blood pressure. Almqvist's ketone inhibitor **286** (Chart 11) is an excellent ACE inhibitor. Silanediol analogues of **286** have been synthesized and shown to be quite effective ACE inhibitors (**287**, **288**). Also, silanediol tripeptide mimics (**289**, **290**) have been found to inhibit ACE quite well. In contrast, the monosilanol (**290**) has been found to be a poor inhibitor. It has been suggested that the high activity of silanediols stems

Chart 12



from their capability to chelate to the zinc active site in ACE.<sup>214</sup>

Similar approaches are also being used for the design and testing of silicon-based inhibitors of the HIV protease<sup>217</sup> and thermolysin<sup>218</sup> (Chart 12). Thus, compounds **291** and **292** have been known as HIV protease inhibitors. The silanediol analogues **293** and **294** have been synthesized. Interestingly, the enzyme inhibition activity of bioisostere **293** is as good as the carbon derivative **291**.

Similar approaches have also been used to synthesize a silicon-based thermolysin inhibitor. Thermolysin is a typical and well-studied metalloprotease that contains zinc(II) in its active site. The Globelny/Bartlett phosphinate **295** is an excellent inhibitor of thermolysin even at nanomolar concentrations. A silanediol analogue **296** has been synthesized. Its inhibition activity toward thermolysin has been found to be quite affective.<sup>218</sup>

The pheromone (*S*)-linalool is an attractant to the males of the solitary bee species *Colletes cunicularius* (*Hymenoptera: Colletidae*). A silicon bioisostere of **297** has been synthesized, and its enantiomers were separated using chiral chromatographic procedures. Electroantennographic studies reveal that both enantiomers of **15** are well perceived.<sup>68</sup>

## 9. Summary and Outlook

Silanols have come a long way since the initial observations of Rochow on the instability of Me<sub>2</sub>Si(OH)<sub>2</sub> toward self-condensation. As detailed in this article, various types of stable silanols are now known. Stable molecular compounds containing Si-OH, Si-(OH)<sub>2</sub>, and Si-(OH)<sub>3</sub> units have been synthesized and structurally characterized. The structural diversity of silanols is also quite amazing. The

special features of the silanols which render them good Brønsted acids as well as bases allow these molecules to organize themselves into a multitude of structural forms. While the exact reasons for the preference of particular structural type are not yet completely clear, some of the influencing parameters including remote substituents on silicon are being understood. Indeed, the structural diversity of silanols in the solid state by itself will drive the synthesis of a number of new silanols. Apart from this, silanols have been found to be useful in various applications. They are useful synthons for the assembly of metallasiloxanes. It is now possible by a careful choice of an appropriate silanol and a metal substrate to design and assemble specific metallasiloxanes of interest. While some of these have found applications in catalysis, others have been used as single-source precursors for material synthesis. It is clear that this theme of using silanols as precursors for assembling homo- and heterometallic siloxanes will flourish. Many new applications are emerging. As outlined in this article, silanols have found utility as reagents in organic synthesis as well as bioisosteres for enzymes and pheromones. This area is quite nascent, and clearly more exciting developments are in the future. Thus, in summary, silanols will continue to interest chemists of various hues in years to come.

## 10. Acknowledgment

We are thankful to the Department of Science and Technology and the Council of Scientific and Industrial Research, New Delhi, India, for financial support. We thank Mr. K. Gopal, Indian Institute of Technology—Kanpur, for the design of the cover art.

## 11. References

- Greenwood, N. N.; Earnshaw, A. *Chemistry of the Elements*; Pergamon Press: Oxford, 1984.
- Tréguer, P.; Nelson, D. M.; Van Bennekom, A. J.; DeMaster, D. J.; Leynaert, A.; Quéguiner, B. *Science* **1995**, *268*, 375.
- Tacke, R. *Angew. Chem., Int. Ed.* **1999**, *38*, 3015.
- Lickiss, P. D. *Adv. Inorg. Chem.* **1995**, *42*, 147.
- Lickiss, P. D. *The Chemistry of Organic Silicon Compounds*; Rappoport, Z., Apeloig, Y., Eds.; John Wiley: Chichester, 2001; Vol. III, p 695.
- Rochow, E. G. *Silicon and Silicones*; Springer: Berlin, Heidelberg, 1987.
- Lickiss, P. D. *Organosilicon Chemistry III from Molecules to Materials*; Auner, N., Weis, J., Eds.; VCH: Weinheim, 1998; p 369.
- Murugavel, R.; Voigt, A.; Walawalker, M. G.; Roesky, H. W. *Organosilicon Chemistry III from Molecules to Materials*; Auner, N., Weis, J., Eds.; VCH: Weinheim, 1998; p 376.
- Duffaut, N.; Calas, R.; Macé, J. *Bull. Chem. Soc. Fr.* **1959**, 1971.
- Murugavel, R.; Chandrasekhar, V.; Voigt, A.; Roesky, H. W.; Schmidt, H.-G.; Noltemeyer, M. *Organometallics* **1995**, *14*, 5298.
- (a) Adam, W.; Mello, R.; Curci, R. *Angew. Chem., Int. Ed.* **1990**, *29*, 890. (b) Minisci, F.; Recupero, F.; Punta, C.; Guidarini, C.; Fontana, F.; Pedulli, G. F. *Synlett* **2002**, 1173. (c) Mori, K.; Tano, M.; Mizugaki, T.; Ebitani, K.; Kaneda, K. *New J. Chem.* **2002**, *26*, 1536.
- Badger, R. M.; Bauer, S. H. *J. Chem. Phys.* **1937**, *5*, 839.
- Popowski, E.; Schott, G.; Kelling, H. Z. *Anorg. Allg. Chem.* **1972**, *391*, 137.
- Hampton, J. F.; Laceyfield, C. W.; Hyde, J. F. *Inorg. Chem.* **1965**, *4*, 1659.
- Brook, A. G.; Pannell, K. H. *J. Organomet. Chem.* **1967**, *8*, 179.
- Pedde, G. J.; Woznow, R. J.; McGeachin, S. G. *J. Organomet. Chem.* **1969**, *17*, 331.
- Nillius, O.; Kriegsmann, H. *Spectrochim. Acta* **1970**, *26A*, 121.
- Jarvie, A. W.; Holt, A.; Thompson, J. *J. Organomet. Chem.* **1968**, *11*, 623.
- Beckmann, J.; Dakternieks, D.; Duthie, A.; Larchin, M. L.; Tiekink, E. R. T. *Appl. Organomet. Chem.* **2003**, *17*, 52.
- Holdt, H. J.; Popowski, E.; Kelling, H. Z. *Anorg. Allg. Chem.* **1984**, *519*, 233.
- Chojnowski, J.; Chrzczonowicz, S. *Bull. Acad. Pol. Sci., Ser. Sci. Chim.* **1965**, *13*, 143.
- Chandrasekhar, V.; Nagendran, S.; Butcher, R. J. *Organometallics* **1999**, *18*, 4488.
- Seyferth, D.; Nivert, C. L. *J. Am. Chem. Soc.* **1977**, *99*, 5209.
- Bassindale, A. R.; Taylor, P. G. *The Chemistry of Organic Silicon Compounds*; Patai, S., Rappoport, Z., Eds.; John Wiley: Chichester, 1989; Vol. I, p 809.
- West, R.; Baney, R. H. *J. Am. Chem. Soc.* **1959**, *81*, 6145.
- Sommer, L. H.; Pietrusza, E. W.; Whitmore, F. C. *J. Am. Chem. Soc.* **1946**, *68*, 2282.
- Rutz, W.; Lange, D.; Kelling, H. Z. *Anorg. Allg. Chem.* **1985**, *528*, 98.
- Sauer, R. O. *J. Am. Chem. Soc.* **1944**, *66*, 1707.
- Corey, E. J.; Mehrotra, M. M.; Khan, A. U. *J. Am. Chem. Soc.* **1986**, *108*, 2472.
- Nagai, Y.; Honda, K.; Migita, T. *J. Organomet. Chem.* **1967**, *8*, 372.
- Dexheimer, E. M.; Spialter, L.; Smithson, L. D. *J. Organomet. Chem.* **1975**, *102*, 21.
- Weidenbruch, M.; Peter, W.; Pierrard, C. *Angew. Chem., Int. Ed.* **1976**, *15*, 43.
- Barton, T. J.; Tulley, C. R. *J. Org. Chem.* **1978**, *43*, 3649.
- Holdt, H.-J.; Schott, G.; Popowski, E.; Kelling, H. Z. *Chem.* **1983**, *23*, 252.
- Ouellette, R. J.; Marks, D. L. *J. Organomet. Chem.* **1968**, *11*, 407.
- Spialter, L.; Pazdernik, L.; Bernstein, S.; Swansiger, W. A.; Buell, G. R.; Freeburger, M. E. *J. Am. Chem. Soc.* **1971**, *93*, 5682.
- Eaborn, C. *Organosilicon Compounds*; Butterworth: London, 1960.
- Puff, H.; Braun, K.; Reuter, H. *J. Organomet. Chem.* **1991**, *409*, 119.
- Bourne, S. A.; Nassimbeni, L. R.; Weber, E.; Skobridis, K. *J. Org. Chem.* **1992**, *57*, 2438.
- Backer, H. J.; Klasens, H. A. *Recl. Trav. Chim.* **1942**, *61*, 500.
- Abe, Y.; Kijima, I. *Bull. Chem. Soc. Jpn.* **1969**, *42*, 1118.
- Wojnowski, W. Z. *Anorg. Allg. Chem.* **1974**, *403*, 186.
- Schott, G.; Engelbrecht, L.; Holdt, H. J. Z. *Anorg. Allg. Chem.* **1979**, *459*, 177.
- Popowski, E.; Holst, N.; Kelling, H. Z. *Anorg. Allg. Chem.* **1982**, *494*, 166.
- Patterson, W. J.; McManus, S. P.; Pittman, C. U., Jr. *Macromol. Synth.* **1977**, *6*, 99.
- Boksányi, L.; Liardon, O.; Kováts, E. Sv. *Helv. Chim. Acta* **1976**, *59*, 717.
- Eaborn, C. *J. Chem. Soc.* **1952**, 2840.
- Damrauer, R. *J. Organomet. Chem.* **1981**, *216*, C1.
- El-Kaddar, Y. Y.; Eaborn, C.; Lickiss, P. D. *J. Organomet. Chem.* **1993**, *460*, 7.
- Al-Shali, S. A.; Eaborn, C.; Fatah, F. A.; Najim, S. T. *Chem. Commun.* **1984**, 318.
- Graalmann, O.; Klingebiel, U. *J. Organomet. Chem.* **1984**, *275*, C1.
- Graalmann, O.; Klingebiel, U.; Clegg, W.; Haase, M.; Sheldrick, G. M. *Angew. Chem., Int. Ed. Engl.* **1984**, *23*, 891.
- Voss, P.; Meinicke, C.; Popowski, E.; Kelling, H. J. *Prakt. Chem.* **1978**, *320*, 34.
- Schütte, S.; Freire-Erdbrügger, C.; Klingebiel, U.; Sheldrick, G. M. *Phosphorus Sulfur Silicon Relat. Elem.* **1993**, *78*, 75.
- Chu, H.-K.; Cross, R. P.; Crossan, D. I. *J. Organomet. Chem.* **1992**, *425*, 9.
- Eaborn, C.; Reed, D. E. *J. Chem. Soc., Perkin Trans. 2* **1985**, 1687.
- Merker, R. L.; Scott, M. J. *J. Polym. Sci., Part A* **1964**, *2*, 15.
- Sommer, L. H.; Korte, W. D.; Frye, C. L. *J. Am. Chem. Soc.* **1972**, *94*, 3463.
- Aiube, Z. H.; Buttrus, N. H.; Eaborn, C.; Hitchcock, P. B.; Zora, J. A. *J. Organomet. Chem.* **1985**, *292*, 177.
- Al-Juaid, S. S.; Al-Nasr, A. K.; Ahmad, K. A.; Eaborn, C.; Hitchcock, P. B. *Chem. Commun.* **1991**, 1482.
- Malisch, W.; Schmitzer, S.; Kaupp, G.; Hindahl, K.; Käß, H.; Wachtler, U. *Organosilicon Chemistry from Molecules to Materials*; Auner, N., Weis, J., Eds.; VCH: Weinheim, 1994; p 185.
- Raez, J.; Zhang, Y.; Cao, L.; Petrov, S.; Erlacher, K.; Wiesner, U.; Manners, I.; Winnik, M. A. *J. Am. Chem. Soc.* **2003**, *125*, 6010.
- Sollott, G. P.; Peterson, W. R. *J. Am. Chem. Soc.* **1967**, *89*, 6783.
- Manners, I. *Chem. Commun.* **1999**, 857.
- MacLachlan, M. J.; Zheng, J.; Thieme, K.; Lough, A. J.; Manners, I.; Mordas, C.; LeSuer, R.; Geiger, W. E.; Liable-Sands, L. M.; Rheingold, A. L. *Polyhedron* **2000**, *19*, 275.
- Jia, W.-L.; Liu, Q.-D.; Song, D. T.; Wang, S. *Organometallics* **2003**, *22*, 321.

- (67) Bassindale, A. R.; Parker, D. J.; Taylor, P. G.; Auner, N.; Herrschaft, B. *Chem. Commun.* **2000**, 565.
- (68) Tacke, R.; Schmid, T.; Hofmann, M.; Tolasch, T.; Francke, W. *Organometallics* **2003**, *22*, 370.
- (69) Harrison, P. G. *J. Organomet. Chem.* **1997**, *542*, 141.
- (70) Lugmair, C. G.; Fujidala, K. L.; Tilley, T. D. *Chem. Mater.* **2002**, *14*, 888.
- (71) Brinker, C. J. *J. Non-Cryst. Solids* **1988**, *100*, 31.
- (72) Beckmann, J.; Dakternieks, D.; Tiekink, E. R. T. *J. Organomet. Chem.* **2002**, *648*, 188.
- (73) (a) Malisch, W.; Hofmann, M.; Nieger, M.; Schöller, W. W.; Sundermann, A. *Eur. J. Inorg. Chem.* **2002**, 3242. (b) Hofmann, M.; Malisch, W.; Hupfer, H.; Nieger, M. *Z. Naturforsch.* **2003**, *58b*, 36.
- (74) Möller, S.; Fey, O.; Malisch, W.; Seelbach, W. *J. Organomet. Chem.* **1996**, *507*, 239.
- (75) Malisch, W.; Jehle, H.; Mitchel, C.; Adam, W. *J. Organomet. Chem.* **1998**, *566*, 259.
- (76) Malisch, W.; Vögler, M.; Schumacher, D.; Nieger, M. *Organometallics* **2002**, *21*, 2891.
- (77) (a) Goikhman, R.; Aizenberg, M.; Kraatz, H.-B.; Milstein, D. *J. Am. Chem. Soc.* **1995**, *117*, 5865. (b) Goikhman, R.; Aizenberg, M.; Shimon, L. J. W.; Milstein, D. *Organometallics* **2003**, *22*, 4020. (c) Goikhman, R.; Aizenberg, M.; Shimon, L. J. W.; Milstein, D. *J. Am. Chem. Soc.* **1996**, *118*, 10894.
- (78) (a) Lucenti, E.; Roberto, D.; Roveda, C.; Ugo, R.; Sironi, A. *Organometallics* **2000**, *19*, 1051. (b) D'Alfonso, G.; Formaggio, V.; Roberto, D.; Ugo, R.; Lucenti, E.; Carlucci, L. *Organometallics* **2003**, *22*, 3271.
- (79) Beckmann, J.; Jurkschat, K.; Schürmann, M. *J. Organomet. Chem.* **2000**, *602*, 170.
- (80) Harris, G. I. *J. Chem. Soc.* **1963**, 5978.
- (81) King, L.; Sullivan, A. C. *Coord. Chem. Rev.* **1999**, *189*, 19.
- (82) Lickiss, P. D.; Redhouse, A. D.; Thompson, R. J.; Stanczyk, W. A.; Rozga, K. *J. Organomet. Chem.* **1993**, *453*, 13.
- (83) Polishchuk, A. P.; Antipin, M. Yu.; Timofeeva, T. V.; Makarova, N. N.; Golovina, N. A.; Struchkov, Yu. T. *Sov. Phys.-Cryst. (Engl. Transl.)* **1991**, *36*, 50.
- (84) Polishchuk, A. P.; Makarova, N. N.; Antipin, M. Yu.; Timofeeva, T. V.; Kravers, M. A.; Struchkov, Yu. T. *Sov. Phys.-Cryst. (Engl. Transl.)* **1990**, *35*, 258.
- (85) Clegg, W. *Acta Crystallogr., Sect. C: Cryst. Struct. Commun.* **1983**, *C39*, 901.
- (86) Mazzah, A.; Haudi-Mazzah, A.; Noltemeyer, M.; Roesky, H. W. *Z. Anorg. Allg. Chem.* **1991**, *604*, 93.
- (87) Khananashvili, L. M.; Vardosanidze, Ts. N.; Griunova, G. V.; Shklover, V. E.; Struchkov, Yu. T.; Markarashvili, E. G.; Tsutsunava, M. Sh. *Izv. Akad. Nauk Gruz. SSR, Ser. Khim.* **1984**, *10*, 262.
- (88) Chogovadze, T. V.; Nogaideli, A. I.; Khananashvili, L. M.; Nakaidze, L. I.; Tskhovrebashvili, V. S.; Gusev, A. I.; Nesterov, D. U. *Proc. Acad. Sci. USSR* **1979**, *246*, 281.
- (89) Graalman, O.; Klingebiel, U.; Clegg, W.; Haase, M.; Sheldrick, G. M. *Chem. Ber.* **1984**, *117*, 2988.
- (90) Behbehani, H.; Brisdon, B. J.; Mahon, M. F.; Molloy, K. C.; Mazhar, M. *J. Organomet. Chem.* **1993**, *463*, 41.
- (91) Chen, B.; Xie, Z.; Wang, J. *Jiegou Huaxue* **1984**, *3*, 113; *Chem. Abstr.* **1984**, *103*, 62901y.
- (92) Ovchinnikov, Y. E.; Shklover, V. E.; Struchkov, Yu. T.; Dement'ev, V. V.; Frunze, T. M.; Antipova, B. A. *J. Organomet. Chem.* **1987**, *335*, 157.
- (93) Leites, L. A.; Yadritseva, T. S.; Dement'ev, V. V.; Antipova, B. A.; Frunze, T. M.; Zhdanov, A. A. *Organomet. Chem. USSR (Engl. Transl.)* **1989**, *2*, 537.
- (94) Buttrus, N. H.; Eaborn, C.; Hitchcock, P. B.; Lickiss, P. D.; Taylor, A. D. *J. Organomet. Chem.* **1986**, *309*, 25.
- (95) Kakudo, M.; Kasai, N.; Watase, T. *J. Chem. Phys.* **1953**, *21*, 1894.
- (96) Aigbirhio, F. I.; Al-Juaid, S. S.; Eaborn, C.; Habtemariam, A.; Hitchcock, P. B.; Smith, J. D. *J. Organomet. Chem.* **1991**, *405*, 149.
- (97) Alexander, L. E.; Northolt, M. G.; Engmann, R. *J. Phys. Chem.* **1967**, *71*, 4298.
- (98) Ruud, K. A.; Sepeda, J. S.; Tibbals, F. A.; Hrcncir, D. C. *Chem. Commun.* **1991**, 629.
- (99) Al-Juaid, S. S.; Eaborn, C.; Hitchcock, P. B.; Lickiss, P. D. *J. Organomet. Chem.* **1988**, *353*, 297.
- (100) Feher, F. J.; Budzichowski, T. A. *Polyhedron* **1995**, *14*, 3239.
- (101) Lorenz, V.; Fischer, A.; Giessmann, S.; Gilje, J. W.; Gun'ko, Y.; Jacob, K.; Edelman, F. T. *Coord. Chem. Rev.* **2000**, *206–207*, 321.
- (102) Beckmann, J.; Jurkschat, K.; Müller, D.; Rabe, S.; Schürmann, M. *Organometallics* **1999**, *18*, 2326.
- (103) Zeitler, V. A.; Brown, C. A. *J. Am. Chem. Soc.* **1957**, *79*, 4618.
- (104) Lee, M. E.; Cho, H. M.; Kang, D. J.; Lee, J.-S.; Kim, J. H. *Organometallics* **2002**, *21*, 4297.
- (105) MacLachlan, M. J.; Zheng, J.; Lough, A. J.; Manners, I.; Mordas, C.; LeSuer, R.; Geiger, W. E.; Liable-Sands, L. M.; Rheingold, A. L. *Organometallics* **1999**, *18*, 1337.
- (106) Murugavel, R.; Prabusankar, G.; Walawalkar, M. G. *Inorg. Chem.* **2001**, *40*, 1084.
- (107) Siefken, R.; Teichert, M.; Chakraborty, D.; Roesky, H. W. *Organometallics* **1999**, *18*, 2321.
- (108) Montero, M. L.; Usón, I.; Roesky, H. W. *Angew. Chem., Int. Ed. Engl.* **1994**, *33*, 2103.
- (109) Voigt, A.; Murugavel, R.; Montero, M. L.; Wessel, H.; Liu, F.-Q.; Roesky, H. W.; Usón, I.; Albers, T.; Parisini, E. *Angew. Chem., Int. Ed. Engl.* **1997**, *36*, 1001.
- (110) Voigt, A.; Murugavel, R.; Roesky, H. W.; Schmidt, H.-G. *J. Mol. Struct.* **1997**, *436–437*, 49.
- (111) Tacke, R.; Burschka, C.; Heermann, J.; Richter, I.; Wagner, B.; Willeke, R. *Eur. J. Inorg. Chem.* **2001**, 2211.
- (112) (a) Ackerhans, C.; Roesky, H. W.; Labahn, T.; Magull, J. *Organometallics* **2002**, *21*, 3671. (b) Ackerhans, C.; Rake, B.; Krätzner, R.; Müller, P.; Roesky, H. W.; Usón, I. *Eur. J. Inorg. Chem.* **2000**, 827.
- (113) Unno, M.; Tanaka, T.; Matsumoto, H. *J. Organomet. Chem.* **2003**, *686*, 175.
- (114) Klingebiel, U.; Neugebauer, P.; Müller, I.; Noltemeyer, M.; Usón, I. *Eur. J. Inorg. Chem.* **2002**, 717.
- (115) Ishida, S.; Iwamoto, T.; Kabuto, C.; Kira, M. *Nature* **2003**, *421*, 725.
- (116) (a) Coupar, P. I.; Jaffrès, P.-A.; Morris, R. E. *J. Chem. Soc., Dalton Trans.* **1999**, 2183. (b) Jaffrès P.-A.; Morris, R. E. *J. Chem. Soc., Dalton Trans.* **1998**, 2767.
- (117) Shklover, V. E.; Struchkov, Yu. T.; Karpova, I. V.; Odinets, V. A.; Zhdanov, A. A. *J. Struct. Khim. (Engl. Transl.)* **1985**, *26*, 251.
- (118) Ovchinnikov, Y. E.; Zamaev, I. A.; Struchkov, Yu. T.; Astapova, T. V.; Zhdanov, A. A. *Organomet. Chem. USSR (Engl. Transl.)* **1989**, *2*, 452.
- (119) Feher, F. J.; Schwab, J. J.; Soulivong, D.; Ziller, J. E. *Main Group Chem.* **1997**, *2*, 123.
- (120) Voronkov, M. G.; Lavrent'yev, V. I. *Top. Curr. Chem.* **1982**, *102*, 199.
- (121) Schwab, J. J.; Lichtenhan, J. D. *Appl. Organomet. Chem.* **1998**, *12*, 707.
- (122) Vansant, E. F.; van der Voort, P.; Vranken, K. C. *Stud. Surf. Sci. Catal.* **1995**, *93*, 59.
- (123) Morrow, B. A.; Gay, I. D. In *Adsorption on Silica Surfaces*; Papirer, E., Ed.; Marcel Dekker: New York, 2000; p 9.
- (124) Krijnen, S.; Harmsen, R. J.; Abbenhuis, H. C. L.; van Hooff, J. H. C.; Van Santen, R. A. *Chem. Commun.* **1999**, 501.
- (125) Abbenhuis, H. C. L. *Chem. Eur. J.* **2000**, *6*, 25.
- (126) Duchateau, R. *Chem. Rev.* **2002**, *102*, 3525.
- (127) Feher, F. J.; Newman, D. A.; Walzer, J. F. *J. Am. Chem. Soc.* **1989**, *111*, 1741.
- (128) Feher, F. J.; Budzichowski, T. A.; Blanski, R. L.; Weller, K. J.; Ziller, J. W. *Organometallics* **1991**, *10*, 2526.
- (129) Feher, F. J.; Budzichowski, T. A.; Rahimian, K.; Ziller, J. W. *J. Am. Chem. Soc.* **1992**, *114*, 3859.
- (130) Gerritsen, G.; Duchateau, R.; van Santen, R. A.; Yap, G. P. A. *Organometallics* **2003**, *22*, 100.
- (131) Feher, F. J.; Phillips, S. H.; Ziller, J. W. *J. Am. Chem. Soc.* **1997**, *119*, 3397.
- (132) Feher, F. J.; Soulivong, D.; Lewis, G. T. *J. Am. Chem. Soc.* **1997**, *119*, 11323.
- (133) Feher, F. J.; Terroba, R.; Ziller, J. W. *Chem. Commun.* **1999**, 2309.
- (134) Feher, F. J.; Newman, D. A. *J. Am. Chem. Soc.* **1990**, *112*, 1931.
- (135) Abbenhuis, H. C. L.; Burrows, A. D.; Kooijman, H.; Lutz, M.; Palmer, M. T.; van Santen, R. A.; Spek, A. L. *Chem. Commun.* **1998**, 2627.
- (136) Wada, K.; Bundo, M.; Nakabayashi, D.; Itayama, N.; Kondo, T.; Mitsudo, T. *Chem. Lett.* **2000**, 628.
- (137) Arnold, P. L.; Blake, A. J.; Hall, S. N.; Ward, B. D.; Wilson, C. *J. Chem. Soc., Dalton Trans.* **2001**, 488.
- (138) Feher, F. J.; Phillips, S. H.; Ziller, J. W. *Chem. Commun.* **1997**, 829.
- (139) Feher, F. J.; Soulivong, D.; Eklund, A. G. *Chem. Commun.* **1998**, 399.
- (140) Corriu, R. J. P.; Guerin, C. *J. Organomet. Chem.* **1980**, *198*, 231.
- (141) Feher, F. J.; Soulivong, D.; Nguyen, F. *Chem. Commun.* **1998**, 1279.
- (142) Feher, F. J.; Nguyen, F.; Soulivong, D.; Ziller, J. W. *Chem. Commun.* **1999**, 1705.
- (143) (a) Feher, F. J.; Terroba, R.; Ziller, J. W. *Chem. Commun.* **1999**, 2153. (b) Feher, F. J.; Terroba, R.; Jin, R.-Z. *Chem. Commun.* **1999**, 2513.
- (144) Dijkstra, T. W.; Duchateau, R.; van Santen, R. A.; Meetsma, A.; Yap, G. P. A. *J. Am. Chem. Soc.* **2002**, *124*, 9856.
- (145) Morrow, B. A.; McFarlan, A. J. *The Colloid Chemistry of Silica*; Bergna, H. E., Ed.; American Chemical Society: Washington, D.C., 1994; p 183.
- (146) (a) Duchateau, R.; Harmsen, R. J.; Abbenhuis, H. C. L.; van Santen, R. A.; Meetsma, A.; Thiele, S. K.-H.; Kranenburg, M. *Chem. Eur. J.* **1999**, *5*, 3130. (b) Skowronska-Ptasinska, M. D.; Duchateau, R.; van Santen, R. A.; Yap, G. P. A. *Eur. J. Inorg. Chem.* **2001**, 133.

- (147) (a) Hofmann, U.; Endell, K.; Wilm, D. *Angew. Chem.* **1934**, *47*, 539. (b) Vansant, E. F.; Van der voort, P.; Vrancken, K. C. *Characterization and Chemical Modification of the Silica Surface*; Elsevier: Amsterdam, 1995. (c) Zhuravlev, L. T. *Colloids Surf. A* **1993**, *74*, 71.
- (148) (a) Morrow, B. A.; Gay, I. D. *Adsorption on Silica surfaces*; Papirer, E., Ed.; Marcel Dekker Inc.: New York, 2000; p 9. (b) Zhao, X. S.; Lu, G. Q.; Whittaker, A. K.; Millar, G. J.; Zhu, H. Y. *J. Phys. Chem. B* **1997**, *101*, 6525.
- (149) Tomlins, P. E.; Lydon, J. E.; Akrigg, D.; Sheldrick, B. *Acta Crystallogr., Sect. C: Cryst. Struct. Commun.* **1985**, *C41*, 941.
- (150) Kasai, N.; Kakudo, M. *Bull. Chem. Soc. Jpn.* **1954**, *27*, 605.
- (151) Buttrus, N. H.; Eaborn, C.; Hitchcock, P. B.; Sexena, A. K. *J. Organomet. Chem.* **1985**, *284*, 291.
- (152) Schott, G.; Sprung, W. D. *Z. Anorg. Allg. Chem.* **1964**, *333*, 76.
- (153) Harris, G. I. *J. Chem. Soc. B* **1970**, 488.
- (154) Al-Juaid, S. S.; Eaborn, C.; Hitchcock, P. B.; Lickiss, P. D.; Möhrke, A.; Jutzi, P. *J. Organomet. Chem.* **1990**, *384*, 33.
- (155) Simons, R. S.; Galat, K. J.; Rapp, B. J.; Tessier, C. A.; Youngs, W. J. *Organometallics* **2000**, *19*, 5799.
- (156) Reyes-García, E. A.; Cervantes-Lee, F.; Pannell, K. H. *Organometallics* **2001**, *20*, 4734.
- (157) MacLachlan, M. J.; Ginzburg, M.; Zheng, J.; Knöll, O.; Lough, A. J.; Manners, I. *New J. Chem.* **1998**, *22*, 1409.
- (158) Murugavel, R.; Voigt, A.; Chandrasekhar, V.; Roesky, H. W.; Schmidt, H.-G.; Noltemeyer, M. *Chem. Ber.* **1996**, *129*, 391.
- (159) Malisch, W.; Jehle, H.; Möller, S.; Saha-Möller, C.; Adam, W. *Eur. J. Inorg. Chem.* **1998**, 1585.
- (160) Murugavel, R.; Böttcher, P.; Voigt, A.; Walawalkar, M. G.; Roesky, H. W.; Parisini, E.; Teichert, M.; Noltemeyer, M. *Chem. Commun.* **1996**, 2417.
- (161) Rulkens, R.; Coles, M. P.; Tilley, T. D. *J. Chem. Soc., Dalton Trans.* **2000**, 627.
- (162) Klemp, A.; Hatop, H.; Roesky, H. W.; Schmidt, H.-G.; Noltemeyer, M. *Inorg. Chem.* **1999**, *38*, 5832.
- (163) Carré, F.; Cerveau, G.; Corriu, R. J. P.; Dabiens, B. *J. Organomet. Chem.* **2001**, *624*, 354.
- (164) Chandrasekhar, V.; Nagendran, S.; Boomishankar, R.; Butcher, R. J. *Inorg. Chem.* **2001**, *40*, 940.
- (165) MacDonald, J. C.; Whitesides, G. M. *Chem. Rev.* **1994**, *94*, 2383.
- (166) Tyler, L. J. *J. Am. Chem. Soc.* **1955**, *77*, 770.
- (167) Takiguchi, T. *J. Am. Chem. Soc.* **1959**, *81*, 2359.
- (168) Andrianov, K. A.; Zhdanov, A. A. *Zh. Obshch. Khim.* **1957**, *27*, 156.
- (169) Lapkin, I. I.; Povarnitsina, T. N. *Zh. Obshch. Khim.* **1964**, *34*, 1202.
- (170) Michalska, Z.; Lasocki, Z. *Bull. Acad. Polon. Sci. Ser. Sci. Chim.* **1971**, *19*, 757.
- (171) Birchall, J. D.; Carey, J. G.; Howard, A. J. *Nature* **1977**, *266*, 154.
- (172) Damja, R. I.; Eaborn, C. *J. Organomet. Chem.* **1985**, *290*, 267.
- (173) Al-Juaid, S. S.; Buttrus, N. H.; Damja, R. I.; Derouiche, Y.; Eaborn, C.; Hitchcock, P. B.; Lickiss, P. D. *J. Organomet. Chem.* **1989**, *371*, 287.
- (174) Ishida, H.; Koenig, J. L. *J. Polym. Sci., Polym. Phys. Ed.* **1979**, *17*, 1807.
- (175) Ishida, H.; Koenig, J. L.; Gardner, K. C. *J. Chem. Phys.* **1982**, *77*, 5748.
- (176) Rickard, C. E. F.; Roper, W. R.; Salter, D. M.; Wright, L. J. *J. Am. Chem. Soc.* **1992**, *114*, 9682.
- (177) Winkhofer, N.; Roesky, H. W.; Noltemeyer, M.; Robinson, W. T. *Angew. Chem., Int. Ed.* **1992**, *31*, 599.
- (178) Winkhofer, N.; Voigt, A.; Dorn, H.; Roesky, H. W.; Steiner, A.; Stalke, D.; Reller, A. *Angew. Chem., Int. Ed.* **1994**, *33*, 1352.
- (179) Jutzi, P.; Strassburger, G.; Schneider, M.; Stammler, H.-G.; Neumann, B. *Organometallics* **1996**, *15*, 2842.
- (180) Jutzi, P.; Schneider, M.; Stammler, H.-G.; Neumann, B. *Organometallics* **1997**, *16*, 5377.
- (181) Kornev, A. N.; Chesnokova, T. A.; Zhezlova, E. V.; Kurskii, Yu. A.; Makarenko, N. P. *Russ. Chem. Bull.* **1999**, *48*, 1563.
- (182) Malisch, W.; Lankat, R.; Schmitzer, S.; Reising, J. *Inorg. Chem.* **1995**, *34*, 5701.
- (183) Ritter, U.; Winkhofer, N.; Schmidt, H.-G.; Roesky, H. W. *Angew. Chem., Int. Ed.* **1996**, *35*, 524.
- (184) Cerveau, G.; Corriu, R. J. P.; Dabiens, B.; LeBideau, J. *Angew. Chem., Int. Ed.* **2000**, *39*, 4533.
- (185) Cerveau, G.; Chappellet, S.; Corriu, R. J. P.; Dabiens, B.; LeBideau, J. *Organometallics* **2002**, *21*, 1560.
- (186) (a) Murugavel, R.; Voigt, A.; Walawalkar, M. G.; Roesky, H. W. *Chem. Rev.* **1996**, *96*, 2205. (b) Roesky, H. W.; Anantharaman, G.; Chandrasekhar, V.; Jancik, V.; Singh, S. *Chem. Eur. J.* **2004**, *10*, 4106.
- (187) Murugavel, R.; Chandrasekhar, V.; Roesky, H. W. *Acc. Chem. Res.* **1996**, *29*, 183.
- (188) Murugavel, R.; Bhattacharjee, M.; Roesky, H. W. *Appl. Organomet. Chem.* **1999**, *13*, 227.
- (189) Voigt, A.; Murugavel, R.; Parisini, E.; Roesky, H. W. *Angew. Chem., Int. Ed.* **1996**, *35*, 748.
- (190) Chandrasekhar, V.; Murugavel, R.; Voigt, A.; Roesky, H. W.; Schmidt, H.-G.; Noltemeyer, M. *Organometallics* **1996**, *15*, 918.
- (191) Voigt, A.; Murugavel, R.; Roesky, H. W. *Organometallics* **1996**, *15*, 5097.
- (192) Gouzyr, A. I.; Wessel, H.; Barnes, C. E.; Roesky, H. W.; Teichert, M.; Usón, I. *Inorg. Chem.* **1997**, *36*, 3392.
- (193) Voigt, A.; Walawalkar, M. G.; Murugavel, R.; Roesky, H. W.; Parisini, E.; Lubini, P. *Angew. Chem., Int. Ed.* **1997**, *36*, 2203.
- (194) Anantharaman, G.; Roesky, H. W.; Schmidt, H.-G.; Noltemeyer, M.; Pinkas, J. *Inorg. Chem.* **2003**, *42*, 970.
- (195) Anantharaman, G.; Reddy, N. D.; Roesky, H. W.; Magull, J. *Organometallics* **2001**, *20*, 5777.
- (196) Anantharaman, G.; Roesky, H. W.; Magull, J. *Angew. Chem., Int. Ed.* **2002**, *41*, 1226.
- (197) Su, K.; Tilley, T. D.; Sailor, M. J. *J. Am. Chem. Soc.* **1996**, *118*, 3459.
- (198) Terry, K. W.; Lugmair, C. G.; Gantzel, P. K.; Tilley, T. D. *Chem. Mater.* **1996**, *8*, 274.
- (199) Terry, K. W.; Gantzel, P. K.; Tilley, T. D. *Inorg. Chem.* **1993**, *32*, 5402.
- (200) Su, K.; Tilley, T. D. *Chem. Mater.* **1997**, *9*, 588.
- (201) Fujdala, K. L.; Tilley, T. D. *Chem. Mater.* **2002**, *14*, 1376.
- (202) Rulkens, R.; Male, J. L.; Terry, K. W.; Olthof, B.; Khodakov, A.; Bell, A. T.; Iglesia, E.; Tilley, T. D. *Chem. Mater.* **1999**, *11*, 2966.
- (203) Coles, M. P.; Lugmair, C. G.; Terry, K. W.; Tilley, T. D. *Chem. Mater.* **2000**, *12*, 122.
- (204) Terry, K. W.; Lugmair, C. G.; Tilley, T. D. *J. Am. Chem. Soc.* **1997**, *119*, 9745.
- (205) Denmark, S. E.; Sweis, R. F. *Acc. Chem. Res.* **2002**, *35*, 835.
- (206) Hirabayashi, K.; Nishihara, Y.; Mori, A.; Hiyama, T. *Tetrahedron Lett.* **1998**, *39*, 7893.
- (207) Mori, A.; Danda, Y.; Fujii, T.; Hirabayashi, K.; Osakada, K. *J. Am. Chem. Soc.* **2001**, *123*, 10774.
- (208) Hirabayashi, K.; Kawashima, J.; Nishihara, Y.; Mori, A.; Hiyama, T. *Org. Lett.* **1999**, *1*, 299.
- (209) Hirabayashi, K.; Mori, A.; Kawashima, J.; Suguro, M.; Nishihara, Y.; Hiyama, T. *J. Org. Chem.* **2000**, *65*, 5342.
- (210) Denmark, S. E.; Ober, M. H. *Org. Lett.* **2003**, *5*, 1357.
- (211) Sieburth, S. McN.; Nittoli, T.; Mutahi, A. M.; Guo, L. X. *Angew. Chem., Int. Ed.* **1998**, *37*, 812.
- (212) Organ, M. G.; Buon, C.; Decicco, C. P.; Combs, A. P. *Org. Lett.* **2002**, *4*, 2683.
- (213) Glekas, A.; Sieburth, S. McN. *Tetrahedron Lett.* **2001**, *42*, 3799.
- (214) Mutahi, M. W.; Nittoli, T.; Guo, L. X.; Sieburth, S. McN. *J. Am. Chem. Soc.* **2002**, *124*, 7363.
- (215) Leung, D.; Abbenante, G.; Fairlie, D. P. *J. Med. Chem.* **2000**, *43*, 305.
- (216) Ripka, A. S.; Rich, D. H. *Curr. Opin. Chem. Biol.* **1998**, *2*, 441.
- (217) Chen, C.-A.; Sieburth, S. McN.; Glekas, A.; Hewitt, G. W.; Trainor, G. L.; Erickson-Viitanen, S.; Garber, S. S.; Cordova, B.; Jeffrey, S.; Klabe, R. M. *Chem. Biol.* **2001**, *8*, 1161.
- (218) Kim, J.; Glekas, A.; Sieburth, S. McN. *Bioorg. Med. Chem. Lett.* **2002**, *12*, 3625.

CR0306135